Dissertation zur Erlangung des Doktorgrades
der Fakultät für Chemie und Pharmazie
der Ludwig-Maximilians-Universität München

Selective DNA Modification Using the Cu(I)-Catalyzed Alkyne-Azide Cycloaddition

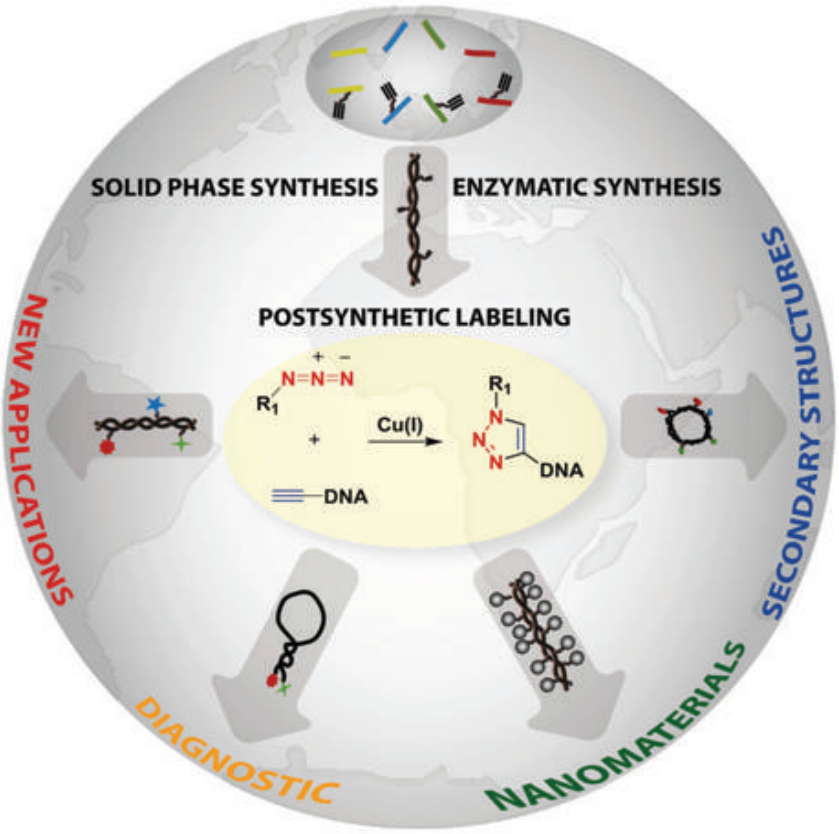

Philipp Mathias Edwin Gramlich
aus
München
2008

Dissertation zur Erlangung des Doktorgrades
der Fakultät für Chemie und Pharmazie
der Ludwig-Maximilians-Universität München

Selective DNA Modification Using the Cu(I)-Catalyzed Alkyne-Azide Cycloaddition

Philipp Mathias Edwin Gramlich
aus
München
2008

Bibliografische Information der Deutschen Nationalbibliothek
Die Deutsche Nationalbibliothek verzeichnet diese Publikation in der Deutschen Nationalbibliografie; detaillierte bibliografische Daten sind im Internet über http://dnb.ddb.de abrufbar.
1. Aufl. - Göttingen : Cuvillier, 2008
Zugl.: München, Univ., Diss., 2008

978-3-86727-730-3

Erklärung

Diese Dissertation wurde im Sinne von § 13 der Promotionordnung vom 29. Januar 1998 von Prof. Dr. Thomas Carell betreut.

Ehrenwörtliche Versicherung

Diese Dissertation wurde selbständig, ohne unerlaubte Hilfe, erarbeitet.

München, am 15. 7. 2008

Philipp Gramlich

Dissertation eingereicht am	
1. Gutachter	Prof. Dr. Thomas Carell
2. Gutachter	Prof. Dr. Thomas Bein
Mündliche Prüfung	15. 7. 2008

Nonnenstieg 8, 37075 Göttingen
Telefon: 0551-54724-0
Telefax: 0551-54724-21
www.cuvillier.de

1. Auflage, 2008
Gedruckt auf säurefreiem Papier

978-3-86727-730-3

To my family

Don´t say sorry, say I do it better next time!

Acknowledgements

I want to thank my PhD supervisor Prof. Thomas Carell for giving me the chance to enter the research life through his group. It would take me ten years to take all the chances he opened up for me and I am happy with the ones I realized.

I am grateful to Prof. Thomas Bein for refereeing this thesis.

Probably the strongest trump card within the Carell group is the high quality of academic staff and the highly cooperative atmosphere. In this context I need to thank the entire group as each and every member helped me at some point. The advent of digital photography impeded a stronger involvement of my person on the beer-table, but nonetheless I greatly enjoyed my time in the group.

I want to thank the predecessors on the click chemistry project, namely Johannes Gierlich and Glenn Burley. Despite all the stress they had while setting up the project, they were always available for my questions and problems. As I am currently working for the start-up company stemming from their work (baseclick GmbH) I can say without exaggeration that my whole life got enriched by their prowess.

Christian Wirges has been my direct labmate for almost three years, during which time I developed great respect for him as a person and a scientist. It was simply fascinating to work with him and he helped me out a few times when all looked like going wrong.

I am very glad to have been a member of the TCFM (Thomas Carell Fancy Materials) subgroup, consisting of the above-mentioned people, Katrin Gutsmiedl, Dave Hammond and Corinna Kaul. It is hard to think about a constellation where one would really fail to meet his aims when the colleagueship is so pronounced. Just to mention an example: I took some DNA strand from Katrin and when I wanted to give back the rest a few days later she did not have a clue what I was talking about as it was so natural for us to share all the material and knowledge.

A great thanks to all the people I shared labspace with. In addition to the people mentioned above I really enjoyed my time working with Christian Trindler, David Kuchen, Antonio Manetto and Simon Warncke. Christian will stay in my memory for being so refreshingly *Nouvelle-Suisse*, Dr. Kuchen for drunken-man-wrestling and being song recipient. After all I shared with Simon Warncke and Antonio Manetto (Anton Handspiel), it feels wrong to acknowledge them with a few words. Including PhD, Simon studied with me for a total of 17 semesters. We have grown to be really good friends in a short amount of time and this never changed. Stay as you are. I was always happy to see Anton, apart from a short, two-year period after the last football world cup. From a very personal viewpoint I feel like moving out of Munich for a while, but his presence in the baseclick GmbH is a strong argument for staying here. Another interesting character from the Carell group to be remembered is Sebastian Hooray-Bareyt, whom I wish all the best for his young family. He often pronounces his "strange-

ness", but I find nothing disturbing about it, after all we´re scientists and new ideas tend to sound strange in the beginning.

The students performing their bachelor theses under my supervision (Dimitra Skakas, Markus Spallek, Alexandra Schmidt and Stefan Schießer) are acknowledged for their hard work and the pleasant time we spent together. Two of them literally needed to be coated with teflon to be able to remove them from the fume hood.

The Cusanuswerk granted me two scholarships over six years for which I am very grateful. The financial support allowed me to focus all my energy on my education and some of the great personalities I could meet there are still a part of my life.

Great thanks to the baseclick GmbH, BASF Venture Capital and all associated people for giving me the exciting opportunity to experience the birth of a new company. Also the support before the exam has to be acknowledged.

Thanks to Sven Weber and Susanne Katzorke for their motivated work on the Litzka Foundation. My midriff would be a lot less trained without you. Sven, I want you to stay Germany´s fattest model. Su, all the health in the world to you and your son.

Last but certainly not least I would like to thank my family, which is about to be expanded by my brother´s wife, Steffi and hopefully many of their children. My brother taught me to speak and this still clings to both our lives: he is now a teacher and I sometimes find it hard to stop speaking. My parents, in addition to always giving me strong support for even the weirdest ideas, are simply the coolest pensioners on the planet.

Publications

[1] Gierlich, J., Burley, G. A., Gramlich, P. M. E., Hammond, D. M., Carell, T. Click Chemistry as a Reliable Method for the High-Density Postsynthetic Functionalization of Alkyne-Modified DNA. *Org. Lett.* **2006**, *8 (17)*, 3639-3642.

[2] Fischler, M., Simon, U., Nir, H., Eichen, Y., Burley, G. A., Gierlich, J., Gramlich, P. M. E., Carell, T. Formation of Bimetallic Ag-Au Nanowires by Metallization of Artificial DNA Duplexes. *Small* **2007**, *3 (6)*, 1049-1055.

[3] Hammond, D. M., Manetto, A., Gierlich, J., Azov, V. A., Gramlich, P. M. E., Burley, G. A., Maul, M., Carell, T. DNA Photography: An Ultrasensitive DNA-Detection Method Based on Photographic Techniques**.** *Angew. Chem. Int. Ed.* **2007**, *46 (22)*, 4184-4187.

[4] Gierlich, J., Gutsmiedl, K., Gramlich, P. M. E., Schmidt, A., Burley, G. A., Carell, T. Synthesis of Highly Modified DNA using a Combination of PCR with Alkyne-bearing Triphosphates and Click Chemistry. *Chem. Eur. J.* **2007**, *13 (34)*, 9486-9494.

[5] Wirges, C. T. M., Gramlich, P. M. E., Gutsmiedl, K., Gierlich, J., Carell, T. Pronounced Effect of DNA Hybridization on Click Reaction Efficiency. *QSAR Comb. Sci.* **2007**, *26 (11-12)*, 1159-1164.

[6] Gramlich, P. M. E., Wirges, C. T. M., Gierlich, J., Carell, T. Synthesis of Modified DNA by PCR with Alkyne-Bearing Purines Followed by a Click Reaction. *Org. Lett.* **2008**, *10 (2)*, 249-251.

[7] Gramlich, P. M. E., Warncke, S., Gierlich, J., Carell, T. Click-Click-Click: Single, Double and Triple Modification of DNA. *Angew. Chem. Int. Ed.* **2008**, *47 (18)*, 3442-3444.

[8] Gramlich, P. M. E., Wirges, C. T., Manetto, A., Carell, T. Postsynthetic DNA Modification via the Copper-Catalyzed Azide-Alkyne Cycloaddition. *Angew. Chem. Int. Ed.* accepted.

Conference presentations

[1] Gramlich, P. M. E., Burley, G. A., Gierlich, J., Hammond, D. M., Wirges, C. T. M., Carell, T. DNA Functionalisation via Click Chemistry *3rd IUPAC-sponsored International Symposium on Macro- and Supramolecular Architectures and Materials (MAM-06): Practical Nano-Chemistry and Novel Approaches.* Poster presentation, Tokyo **2006**.

[2] Gramlich, P. M. E., Burley, G. A., Gierlich, J., Hammond, D. M., Wirges, C. T. M., Carell, T. High Density and Selective Functionalisation of DNA. *Bionanotechnology.* Poster presentation, Cambridge **2007**.

Table of contents

Summary

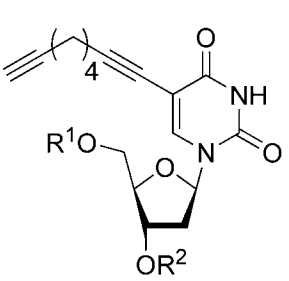

1

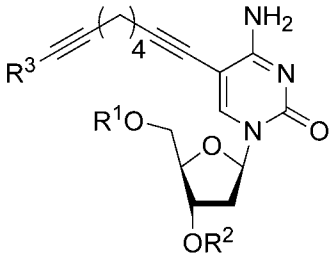

2

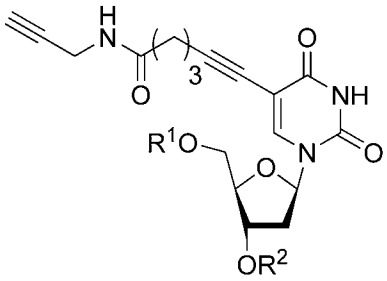

3

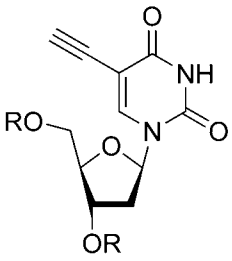

4

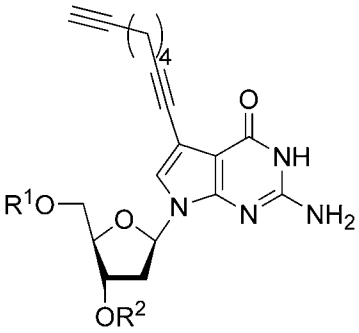

5

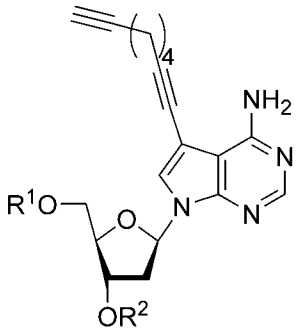

6

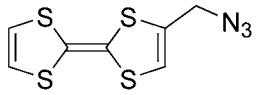

7

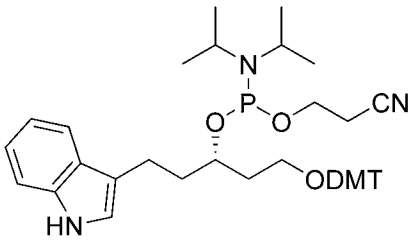

8

The PhD thesis presented herein concludes the academic research in the group of Prof. Carell on the methodology of the postsynthetic functionalization of DNA using the Cu(I) catalyzed Huisgen cycloaddition (termed click reaction). Johannes Gierlich, Dave Hammond and Glenn Burley laid the foundations in that they established the click reaction on DNA as well as the enzymatic incorporation of alkyne-containing triphosphates into PCR products.

After an introductory chapter about click chemistry on DNA in general (Section 1), a study on the efficiency of the click reaction on ssDNA containing up to six consecutive uridine alkynes **1** is reported in Section 2. The synthesis of these alkyne nucleosides could be greatly facilitated by performing the key step, a Sonogashira cross-coupling on 5-iodo-2′-deoxyuridine, with mono-protected octadiyne. Later on, synthesis of the analogous alkyne cytidine **2** was accomplished without the need for protecting groups or synthetic precautions like dry and degassed solvents, as was reported for **1**. The cytidine phosphoramidite was incorporated into synthetic DNA strands, which were used as click substrates in the development of a DNA detection system based on the chemistry of the photographic process (Section 3). The analogous cytidine triphosphate was found to be incorporated into DNA strands via PCR with a better efficiency than the corresponding uridine triphosphate. Therefore the cytidine triphos-

phate was used to build up long alkyne-bearing DNA strands for a click reaction with a sugar azide (Section 4). The sugar moieties were subsequently used to reduce Ag(I) to form uniform silver nanowires on the DNA scaffold. Further enhancement with gold led to bimetallic silver-gold nanowires, whose time-dependent growth was probed by AFM. In order to increase the incorporation rates of our building blocks by PCR even further, alkyne uridine triphosphate **3** with an amide bond in the linker was synthesized (Section 5). To our surprise the triphosphate could not be incorporated by enzymatic means. This study, which contained an in-depth investigation of the incorporation and click functionalization of a whole range of different alkyne triphosphates, concluded with the open question, whether ss- or dsDNA would constitute a more suitable substrate for the click reaction. This question was addressed by creating single- and double-stranded PCR products (using **4**) by enzymatic methods (Section 6). Investigation of the click reaction efficiency of these constructs clearly showed that ssDNA exhibits a higher click reaction conversion than the corresponding dsDNA, which was attributed to steric effects. It could also be clearly shown that the most important factor determining the success of a click reaction is the concentration of the azide used. Successful synthesis of alkyne-bearing purine triphosphates **5** and **6** completed our "alkyne alphabet" and could be used to synthesize a stretch of DNA containing only alkyne-derived nucleobases by primer extension (Section 7). Incorporation of all four canonical alkyne triphosphates into PCR products failed due to the inability of the polymerases to insert a modified triphosphate opposite another modified base on the template strand.

The central issue of this thesis was to introduce multiple *different* labels onto a DNA strand. Therefore a protecting group strategy was devised, in which silyl-protected alkynes were introduced into the DNA strands together with unprotected alkynes (Section 8). Using this methodology, it was possible to attach up to three different labels to an ODN in a facile and highly efficient process involving only simple steps for work-up and purification. This opens up a practical route to multiply modified DNA probes like molecular beacons, which are a particularly expensive type of biomolecular entities. It was attempted to expand this technology of multi-labeling to PCR products (Section 9). Using a TMS-protected alkyne cytidine triphosphate **2** it was possible to achieve a partial selectivity in attaching two different labels on two different nucleobases. Katrin Gutsmiedl is currently continuing the project by employing a TES protecting group strategy, which is expected to yield the desired complete selectivity. This would pave the way for a novel class of readily available, but still highly complex, nanomaterials. The first application of the sequential click chemistry was realized in a collaboration with the group of Prof. Bein (LMU München). A synthetic DNA strand bearing one free and one protected alkyne strand was used to attach a quencher to the DNA, which was subsequently attached to a colloidal mesoporous silica nanoparticle (Section 10). The sequence of this strand can be used to hybridize the complementary DNA strand onto the nanoparticle. Thereby the DNA construct is envisioned to form a lid for the nanoparticle pores for the liberation of encapsulated drug molecules in a defined biological context. The project is currently being continued by Simon Warncke.

The benign conditions of the postsynthetic click reaction allow for the introduction of sensitive and reactive moieties onto DNA. Several groups have already tried to attach the strong π electron donor TTF onto DNA without any success. The ultimate goal of such endeavors is to produce electrically conductive nanowires Using click chemistry, it was possible to attach

TTF **7** onto DNA for the first time (Section 11). Dr. Aline Gegout is currently continuing the project by measuring the UV/Vis and fluorescent properties of the resulting DNA constructs together with π acceptors, which could ultimately be conjugated to DNA by a sequential click chemistry approach.

In a collaboration with the group of Prof. Armitage (Carnegie Mellon University, Pittsburgh), several fluorescent dyes were conjugated to DNA strands with the aim of constructing strongly fluorescent and switchable DNA-based nanotags (Section 12). Initial investigations showed that the covalent attachment of these dyes greatly increased the fluorescent properties of the nanotags. Christian Wirges is continuing the project by synthesizing highly modified DNA three-way junctions.

Section 13 describes a collaboration project not concerned with click chemistry. In order to investigate the electron transfer mechanisms in natural photolyase enzymes, DNA hairpins are to be synthesized, in which the components of this electron transfer reaction (flavin and tryptophan) are kept at defined distances. To this end, a novel indole nucleoside **8** was synthesized in order to act as tryptophan mimetic and was incorporated into DNA test strands. Structural investigations were necessary to prove that the indole moiety, which is bearing an acyclic linker, is indeed situated inside the DNA helix. The work is currently being continued by Stefan Schießer, who also started the project in the context of his bachelor thesis.

General remarks

This PhD thesis has been devised as a compilation of previous publications plus Sections on the unpublished work. Where appropriate, the publication Sections were expanded by results obtained afterwards or remarks which appeared useful. As introduction, a minireview about click chemistry on DNA in general, has been used, followed by seven publications comprising primary research results. Sections 9-13 describe unpublished projects, which are currently being continued by members of the Carell group. Sections 9-12 describe applications of the click chemistry methodology elaborated in the published Sections, while Section 13 contains a research project on DNA-based enzyme model substances for electron transfer studies. The author´s personal contribution to the respective works is commented on in a short paragraph at the end of the sections.

1 Postsynthetic DNA Modification via the Copper-Catalyzed Azide-Alkyne Cycloaddition

This Section is submitted for publication:

P. M. E. Gramlich, C. T. Wirges, A. Manetto, T. Carell, *Angew Chem. Int. Ed.* accepted.

1.1 Abstract

The attachment of labels onto DNA is of utmost importance in many areas of biomedical research. It also proves valuable in the construction of DNA-based functional nanomaterials. Today, the most widespread methods in use for the conjugation of DNA to functional molecules suffer from low conversion efficiencies or the susceptibility of the reactant functional groups to side reactions. The Cu(I)-catalyzed Huisgen cycloaddition (click reaction) has recently been added to the repertoire of DNA labeling methods, allowing the virtually unlimited functionalization of both small synthetic oligonucleotides and large gene fragments with unprecedented efficiency. The click reaction yields the labeled polynucleotides in very high purity after a simple precipitation step. The reviewed technology is currently changing the way of how functionalized DNA strands are generated cost-efficiently in high quality for their application in molecular diagnostics systems and nanotechnological research.

1.2 Introduction

The 1,3-dipolar cycloaddition between azides and alkynes -the Huisgen reaction[1]- has recently found a tremendous number of novel applications (~1000 publications) after the discovery that the reaction can be efficiently catalyzed by Cu(I).[2] This copper-catalyzed form of the reaction (Huisgen-Meldal-Sharpless reaction) is presently the most prominent example of a class of reactions named click reactions. These reactions are, according to Sharpless' definition, characterized by high yields, mild reaction conditions and by the fact that they tolerate a broad range of functional groups. Typically, the reactions require simple or no workup and purification of the product. For reasons of simplicity, the Cu(I)-catalyzed alkyne azide cycloaddition (CuAAC) discussed here will be referred to as click reaction.

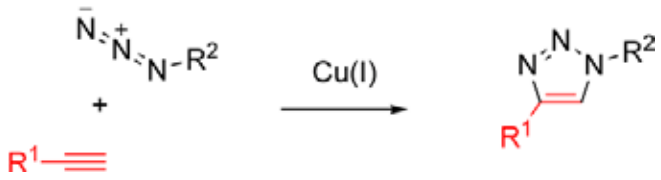

The most important characteristic of the click reaction is its unique bioorthogonality, as both azide and terminal alkyne functional groups are generally not present in natural systems. A wide range of biomolecules has thus been labeled to date, including peptides,[3] proteins,[4] polysaccharides[5] and even an entire virus.[6] The use of this method for DNA modification has been somewhat delayed by the fact that copper ions damage DNA, typically yielding

strand breaks.[7] As these problems have now been overcome by the use of a Cu(I)-stabilizing ligand (TBTA),[8] click chemistry is in an excellent position to take over as the state-of-the-art methodology to label and modify DNA.

In a variety of applications such as molecular diagnostics, DNA needs to bear labels like fluorescent dyes for detection of the DNA molecule. In addition biotin is often attached to DNA to facilitate DNA purification or most recently carbohydrates have been used to functionalize DNA in order to allow selective silver deposition or to set up carbohydrate microarrays. Two general strategies exist for the labeling of oligonucleotides called presynthetic and postsynthetic labeling (Figure 1.1). Presynthetic labeling denotes that the nucleotide monomers already carry the desired label before DNA synthesis, deprotection and purification. Postsynthetic labeling requires the introduction of a small reactive moiety into DNA, which can be coupled to the label later on, after completion of DNA synthesis.

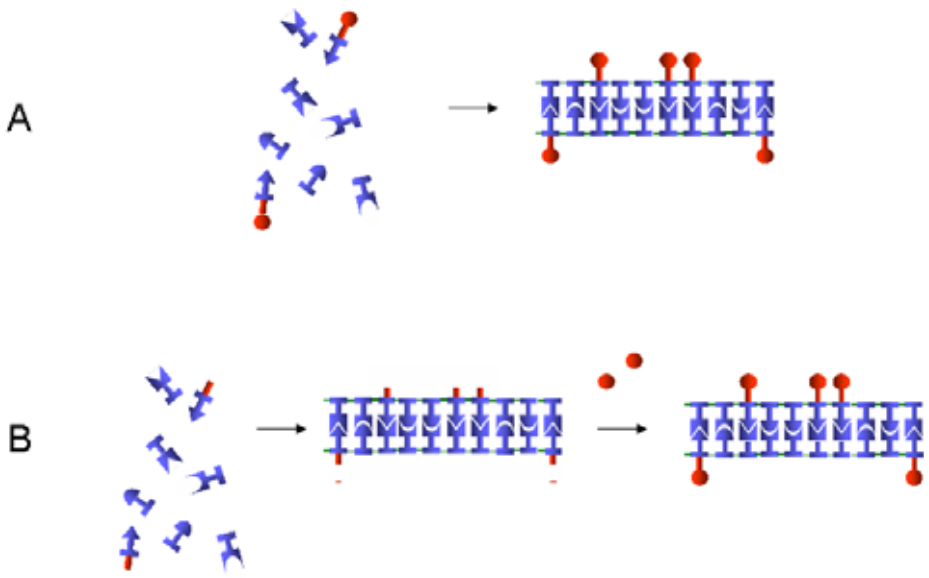

Figure 1.1 Schematic representation for presynthetic (A) and postsynthetic labeling (B).

In the presynthetic strategy (A in Figure 1.1) a phosphoramidite bearing the desired label is synthesized, which needs to be stable enough to survive the harsh conditions employed during solid phase synthesis (acidic, alkaline and oxidative conditions) and deprotection (strongly alkaline conditions) of the DNA strand. Additionally, the P(III) phosphoramidite group, which is susceptible to oxidation to the corresponding P(V) phosphoramidate, needs to be stable in the presence of the label. This method thus excludes the use of labels with reactive functional groups or inherent base or acid-sensitivity. Alternatively, the label can be prepared as the corresponding triphosphate using DNA polymerases to insert the label during primer extension or PCR. This method is limited to those modifications which are accepted as substrates by polymerases and there are often steric limitations.

In the postsynthetic labeling strategy (B in Figure 1.1), a small reactive group is introduced into DNA, which can then be conjugated to the desired functional molecule in a selective manner after DNA synthesis and deprotection. Presently, the most widely utilized method for

postsynthetic labeling is to prepare DNA bearing an amino group (amino modifier), which reacts with an active ester functional group (e.g. NHS) of the desired modification.[9] Sensitive or reactive moieties can be introduced in this way, but the strategy is highly dependent on the selectivity and efficiency of the postsynthetic modification step. This strategy allows for a higher degree of modularity, because changing the label does not require a novel nucleotide synthesis as in the case of presynthetic labeling. However, the low coupling yields and the need for intensive oligonucleotide purification by HPLC after the labeling is limiting this approach making labeled oligonucleotides very expensive compounds. Nucleobases which carry the reactive amino group can also be used as triphosphates for the incorporation into DNA by either primer extension or PCR.[10]

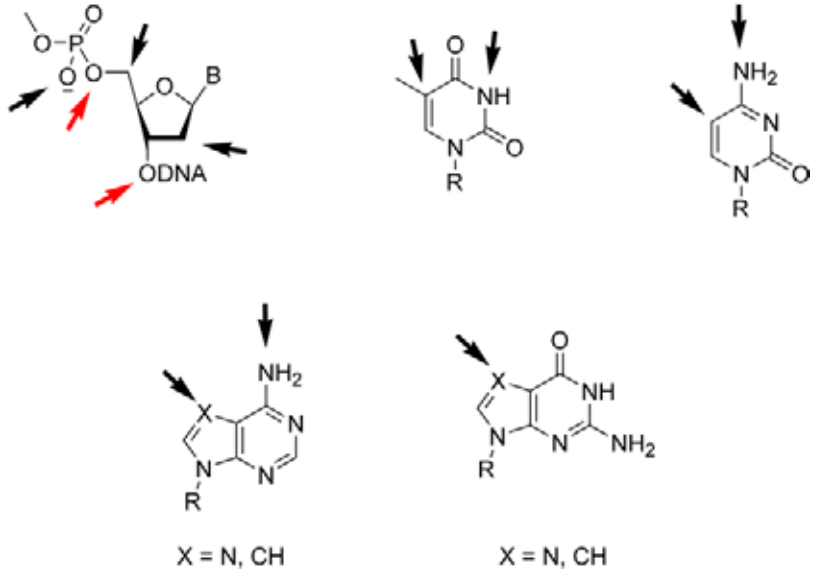

Scheme 1.1 Overview over the different positions that have up to now been used for the attachment of azides or alkynes onto DNA. Red arrows indicate attachment points for terminal modification only.

Click chemistry offers solutions to these issues. The chemistry is clean, high yielding and operates at mild conditions. In order to allow oligonucleotide modification by the click reaction, however, DNA building blocks are required which carry either alkyne or azide functional groups. As depicted in Scheme 1.1, alkyne or azide functionalities have already been attached to many different positions on DNA. In addition a number of non-nucleosidic alkyne/azide DNA modifiers have been prepared.[11, 12] In this minireview we summarize the various approaches to modify oligonucleotides with the click reaction. In Sections 1.2 to 1.6 we describe the click chemistry applications of DNA strands prepared by solid-phase synthesis. In Section 1.7, we summarize click chemistry in combination with enzymatic strategies.

1.3 Preparation of Surface Immobilized DNA with Click Chemistry

The first example of a successful click chemistry modification of DNA[a] used a 5′-alkylamino-modified DNA strand, which was reacted with succinimidyl 5-azidovalerate to display an azide group at the 5′-terminus.[13, 14] Thermal (not Cu(I)-catalyzed) cycloaddition with an alkyne-modified fluorescein furnished the reaction product in excellent yield, but as a regioisomeric mixture of the 1,4- and 1,5-triazoles. These mixtures are typical for the Huisgen cycloaddition without Cu(I) catalysis. The direct incorporation of azides into synthetic DNA strands is intrinsically difficult because the azide group reacts with the P(III) of the phosphoramidite group in a Staudinger reduction.[15] However, the two step procedure for attaching the azide to the DNA strand allowed the subsequent attachment of the DNA to a glass surface for a sequencing by synthesis approach.[16] An alternative approach for the immobilization of DNA on surfaces using click chemistry has employed an alkyne group attached to the 5′-OH of a DNA strand, which reacted with azide modified gold surfaces.[17] Even simpler is the approach of Reinhoudt et al.. This group pressed a polydimethylsiloxane (PDMS) stamp, which was covered with alkyne modified DNA, directly onto an azide-terminated glass slide to achieve the click reaction under pressure without any Cu(I) catalyst added. [12]

1.4 Preparation of DNA-Protein Conjugates with Click Chemistry

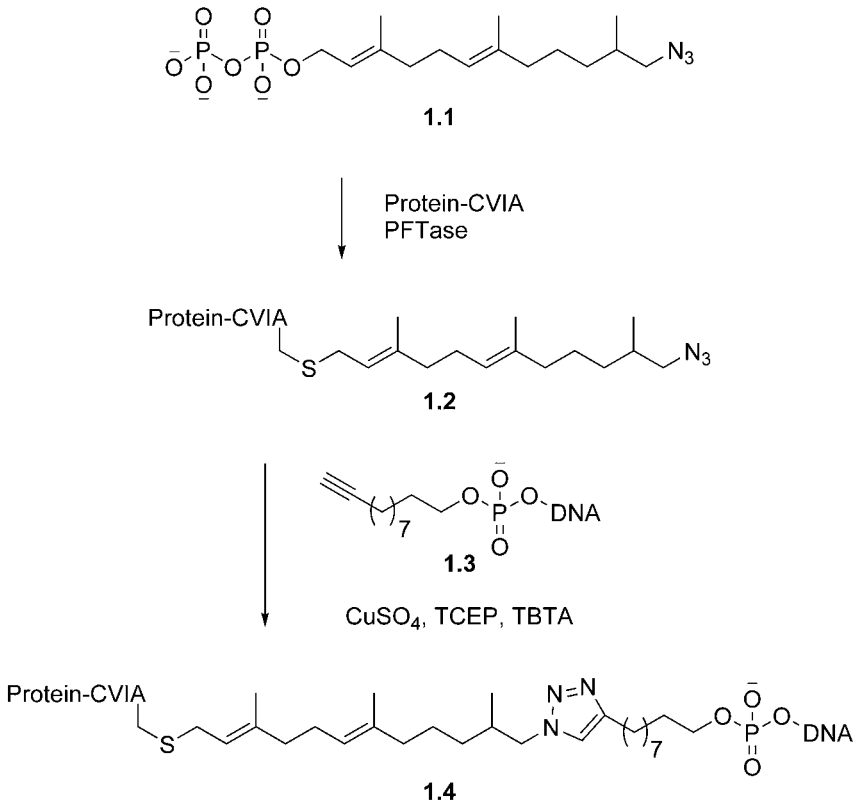

Scheme 1.2 Synthetic strategy for DNA-protein conjugates.

[a] At this point the cycloaddition was performed thermally without Cu(I) catalysis, presumably due to the DNA degrading effect of free Cu(I) species in aqueous solutions. After publication of a Cu(I) stabilizing ligand, which accelerates the click reaction, most of the following work makes use of the Cu(I) catalyzed version of the Huisgen cycloaddition. Nonetheless the work by Ju et al. is seen as the prototypical example of click chemistry on DNA.

Click chemistry has been successfully utilized for the preparation of complex DNA-protein conjugates.[18] Distefano et al. attached the specific tetrapeptide CVIA to green fluorescent protein (GFP). To this tag the authors specifically attached an azide modified isoprenoid diphosphate with the help of the enzyme protein farnesyltransferase (PFTase, Scheme 1.2).[19] The obtained azide bearing protein was then reacted with a single stranded oligonucleotide (ssODN), carrying an alkyne attached to a 5′-terminal phosphate group. In order to test whether the DNA sequence can still be addressed despite the presence of the protein, a counter strand containing a Texas Red label was successfully hybridized to the DNA strand attached to the protein. Using this construct, the group successfully built up nanoscale DNA tetrahedra,[20] which were finally decorated with up to four GFPs. The methodology is currently being exploited for the preparation of protein modified DNA-nanostructures.

1.5 Preparation of Circularized and Branched DNA Structures Using Click Chemistry

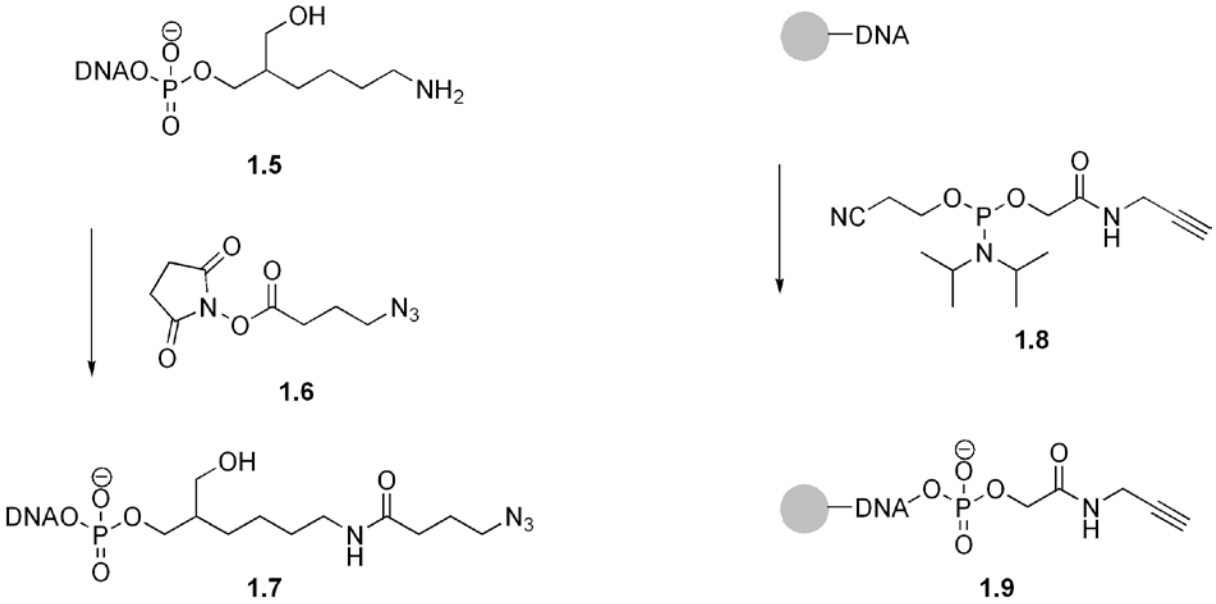

Scheme 1.3 Building blocks for the synthesis of circularized and catenated DNA.

Click chemistry has vastly simplified the synthesis of circularized and catenated DNA structures.[15, 21] Brown et al. have devised a strategy to label a ssODNs with both a 5′-terminal alkyne and a 3′-terminal azide.[22] The azide was generated as described by Ju et al.[13] by coupling of succinimidyl 4-azidobutyrate to an amino linker at the DNA yielding the required 3′-terminal azide (**1.7** in Scheme 1.3). The alkyne group, in contrast, was introduced at the 5′-terminus by terminating the solid phase synthesis with the propargylated phosphoramidite **1.8**. Such a doubly modified DNA strand reacts under high dilution conditions with itself in a click reaction to give a cyclic ssODN. When the complementary ODN, which also carries an azide and an alkyne group, is hybridized to this cyclic ODN, it can in turn also be cyclized to yield a covalently catenated dsDNA. In this reaction, the first ODN templates the click reaction of the second DNA strand which reduces side reactions. The catenated DNA showed a vastly increased resistance to exonuclease degradation.

The exonuclease stability of circularized DNAs was also exploited by Matsuda et al.[23] This group prepared a dsODN which binds to the κB transcription factor as a decoy molecule to inhibit *in vitro* and ex vivo transcription. Then propargyl and azidoethyl linkers on the N3-position of thymidine were introduced. The dangling 5′-azide and 3′-alkyne groups of the dsODN were used to form a circular DNA, which can also be viewed as a double hairpin or dumbbell structure. The internal double stranded binding region of this decoy molecule was not significantly distorted, whereas the thermal stability and the exonuclease stability were strongly increased. The binding affinity to the nuclear factor was shown not to be hampered by the circularization.

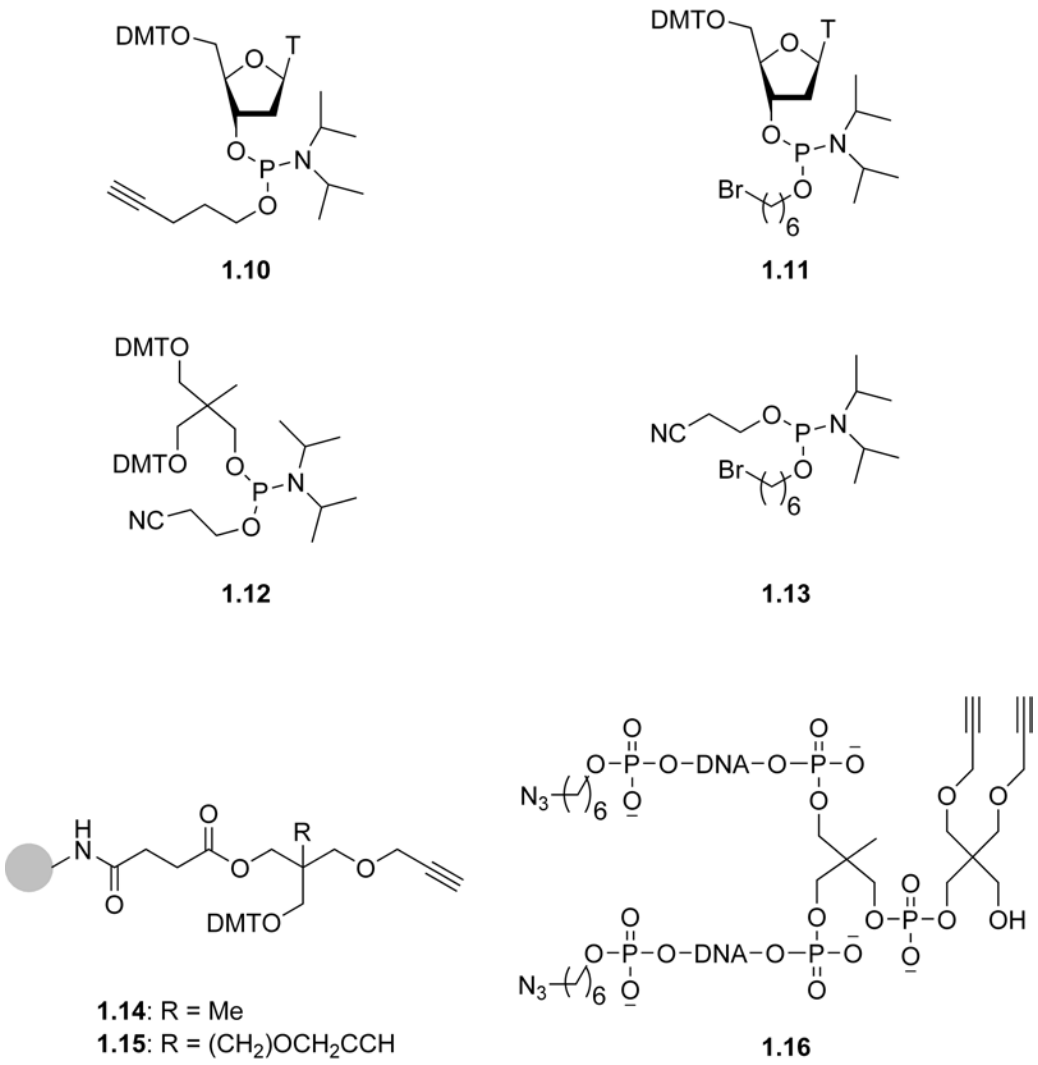

Scheme 1.4 The molecular toolbox for the synthesis of cyclic, branched cyclic and bicyclic DNA introduced by Morvan et al.

A whole range of different DNA structures was made accessible by the work of Morvan et al.[24] Alkynyl and bromoalkyl groups were introduced at the phosphoramidite group of nucleotides **1.10** and **1.11**, respectively, to allow for labeling inside a DNA strand (Scheme 1.4). The bromoalkyl group is stable to standard phosphoramidite coupling procedures and can be used to generate an azide group after the solid phase synthesis by treatment with sodium

azide.[25] Phosphoramidite **1.13** can analogously be used to produce DNAs with an azide label on the 5′-terminus. Universal supports **1.14** and **1.15** can be used to introduce one or two 3′-terminal alkynes. This repertoire of building blocks opens up the access to a wide array of structures like DNA cycles and branched DNA cycles, as it is possible to label each position of a DNA strand with alkynes as well as with azides. Even bicyclic DNAs can be built up by using the double alkyne resin **1.15**. Phosphoramidite **1.12**, bearing two DMT protected alcohols, can be used in the first elongation step to give a branched structure. Terminating the DNA synthesis with the bromoalkyl phosphoramidite **1.13**, one can obtain a structure with two alkynes and two azides (**1.16**), which can be cyclized to give the desired, bicyclic DNA.

1.6 Analytical Applications of Click Modified DNA

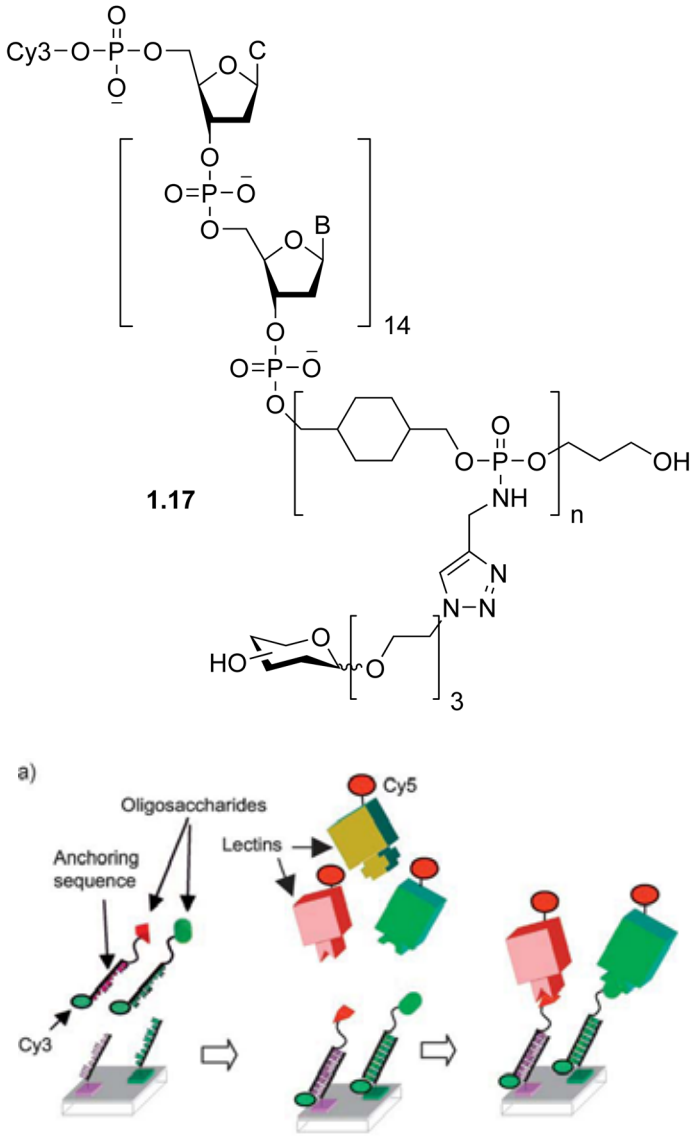

Scheme 1.5 DNA-carbohydrate conjugates (top) and their use in microarrays. Copyright Wiley-VCH Verlag GmbH & Co. KGaA. Reproduced with permission.[26]

Analytical applications of ODNs are vastly extended by the use of click chemistry due to the higher yield and selectivity of the labeling reaction compared with classical methods. E. g. conjugation to very hydrophobic dye structures can be achieved.[27] In addition, the synthesis of highly modified DNAs is possible, opening up a wide array of potential applications.
Morvan et al. synthesized oligonucleotide scaffolds (**1.17** in Scheme 1.5) containing up to ten alkyne groups for the conjugation of galactose[28] and fucose to the DNA strands.[29] In the latter case the binding of the fucose clusters to the fucose-specific bacterial lectin (PA-IIL) was up to 20 times stronger compared to single fucose molecules.
This technology was further developed for the preparation of DNA-based carbohydrate arrays depicted in Scheme 1.5.[26] 3′-Amine oligonucleotides were covalently immobilized onto functionalized glass slides and then hybridized to DNA counter strands such as **1.17** bearing a clicked-on sugar molecule at the 3'-terminus and a Cy3 fluorescence label at the 5'-terminus. The successful hybridization event could be monitored by FRET. The carbohydrate arrays constructed in this way were used to study the interaction with Cy5 labeled lectins. The sensitivity of the method was found to be excellent, with detection limits for lectins between 2 and 20 nM.
Detection of DNA synthesis *in vivo* was recently also accomplished using click chemistry. To this end 5-ethynyl-2′-deoxyuridine **1.21a** (Scheme 1.6) was synthesized and injected into mice or added to a NIH 3T3 cell culture.[30] The structural similarity between the alkyne-uridine **1.21a** and thymidine enabled the polymerase based incorporation of the alkyne base into DNA during the S-phase of the cell cycle. After lysis of the cells the genomic DNA could be directly stained with an azide modified fluorescent dye in order to quantify the rate of DNA synthesis in different tissues. This method was found to be more sensitive and user-friendly than the standard BrdU assay, which requires a time-consuming immunological step involving specific anti-BrdU antibodies.

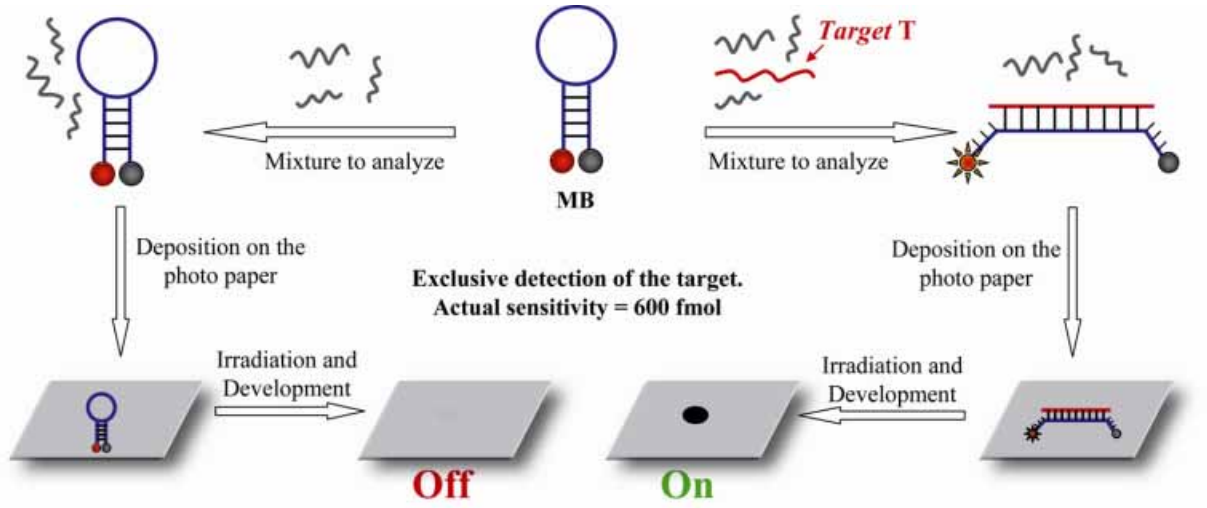

Figure 1.2 Working principle of the molecular beacon based DNA photography. Copyright Wiley-VCH Verlag GmbH & Co. KGaA. Reproduced with permission.[31]

A very simple and sensitive DNA detection method based on the silver halide photographic process was presented by Carell et al.[31] Photographic AgBr emulsions are generally sensitive

up to 520 nm of incident light. Organic dyes are typically added to black and white photopaper to sensitize the photographic films over the whole visible range. The signal enhancement of the photographic development procedure with amplification factors of up to 10^{11} results in sensitivities similar to the polymerase chain reaction (PCR). In this study a photographic film devoid of any sensitizing dyes was treated with DNA (incorporating either **1.18c** or **1.23c**, Scheme 1.6) to which the photographic red light sensitizer (pinacyanol dye azide) was clicked on. After a short irradiation of the film only the parts of the film which contained the spotted on DNA displayed a black spot after the development indicating that the dye present at the DNA selectively sensitized the AgBr crystals in its vicinity. The whole method allowed the detection of DNA by eye up to a detection limit of only 300 amol. In order to furnish a simple experimental setup for the detection system, a molecular beacon (MB) based approach was devised (Figure 1.2). For this, a commercially available molecular beacon with the Cy3/BHQ2 (black hole quencher) FRET couple was used which featured a base sequence characteristic for Yersinia pestis in the loop region. In the closed state of the hairpin, the fluorescence of the Cy3 dye is quenched by BHQ2 and can therefore not sensitize the photographic film. If the characteristic sequence is present in the analysis mixture, it will hybridize to the loop region and open the hairpin, which immediately reactivates Cy3 fluorescence and sensitizing properties. If this solution is now spotted onto the sensitizer-free photographic film, the fluorescing Cy3-labeled DNA allows sensitization of the AgBr crystals during brief irradiation, which enables the eye-based detection of the analyte with a sensitivity limit of 600 fmol.

1.7 Multiple, Sequential Labeling of DNA by Click Chemistry

The attachment of alkynyl side chains to the 5-position of pyrimidines (**1.18-1.23** in Scheme 1.6) or to the 7-position of 7-deazapurines (**1.24** and **1.25** in Scheme 1.6) offers a variety of possibilities for the versatile labeling of DNA. These positions have the advantage that the corresponding alkyne-modified bases are generally well accepted by polymerases for the enyzmatic incorporation into PCR and primer extension products (Section 1.7).[32] Functional molecules attached to these positions of the nucleobases will protrude into the major groove of the B-duplex, which causes in principle only small distortions of the duplex structures required for efficient hybridization with the counter strand. Indeed, such modified DNA strands exhibit only a small increases in melting temperatures compared to natural DNA, showing the small effect of modifications at C5 of pyrimidines and C7 of 7-deazapurines on the duplex.[33, 34] If a high density functionalization of DNA is required, the octadiynyl spacer protruding from these positions into the major group proved to be superior to the short ethynyl linker in **1.21**, possibly because of better steric access. SsODNs with up to six consecutive octadiynyl uridines **1.23c** were synthesized and indeed with this alkyne spacer, quantitative click yields were always detected with a variety of azides (fluorescein, coumarin and galactose).[35]

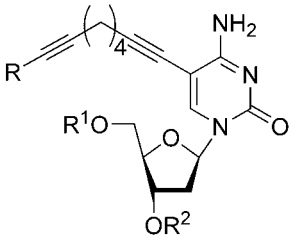

1.18a/b/c: R = H
1.19a/b/c: R = TMS
1.20a/b/c: R = TIPS

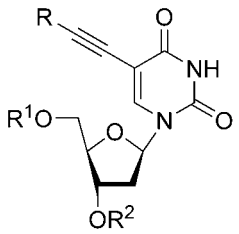

1.21a/b/c: R = H
1.22a/b/c: R = $(CH_2)_2CCH$
1.23a/b/c: R = $(CH_2)_4CCH$

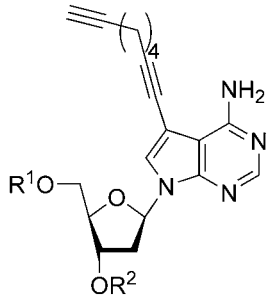

1.24a/b/c

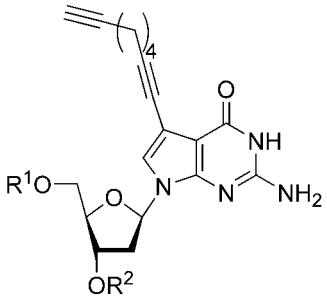

1.25a/b/c

Scheme 1.6 Nucleobase-modified phosphoramidites and triphosphates. **1.18-1.25a**: $R^1 = R^2 = H$; **1.18-1.25b**: $R^1 = P_3O_9^{4-}$, $R^2 = H$; **1.18-1.25c**: R^1 = DMT, $R^2 = P(NiPr_2)[O(CH_2)_2CN]$.

The possibility to prepare a set of different alkyne modified bases was then shown to be the basis for an efficient modification of DNA with different labels. Such multiply modified DNA strands find wide use, e. g. as sophisticated FRET probes in molecular diagnostics applications. To this end, DNA strands containing TMS (**1.19c**) and TIPS (**1.20c**) protected alkyne cytidine analogs were prepared.[36] These two building blocks, together with the alkyne modified uridine analog **1.23c**, were incorporated into DNA strands. Three different click reactions were performed consecutively, first at the free alkyne, then at the TMS protected alkyne after TMS deprotection and finally at the TIPS protected alkyne site after TIPS deprotection. This allowed the introduction of three different labels with unprecedented yield and efficiency. The click modification could even be achieved directly at the resin allowing in principle the derivatization of oligonucleotides using a DNA synthesizer. In many cases, a simple ethanol precipitation was sufficient to purify the labeled oligonucleotides with yields between 60 to 90% observed for the three-step click-deprotect-click reaction sequence in solution.

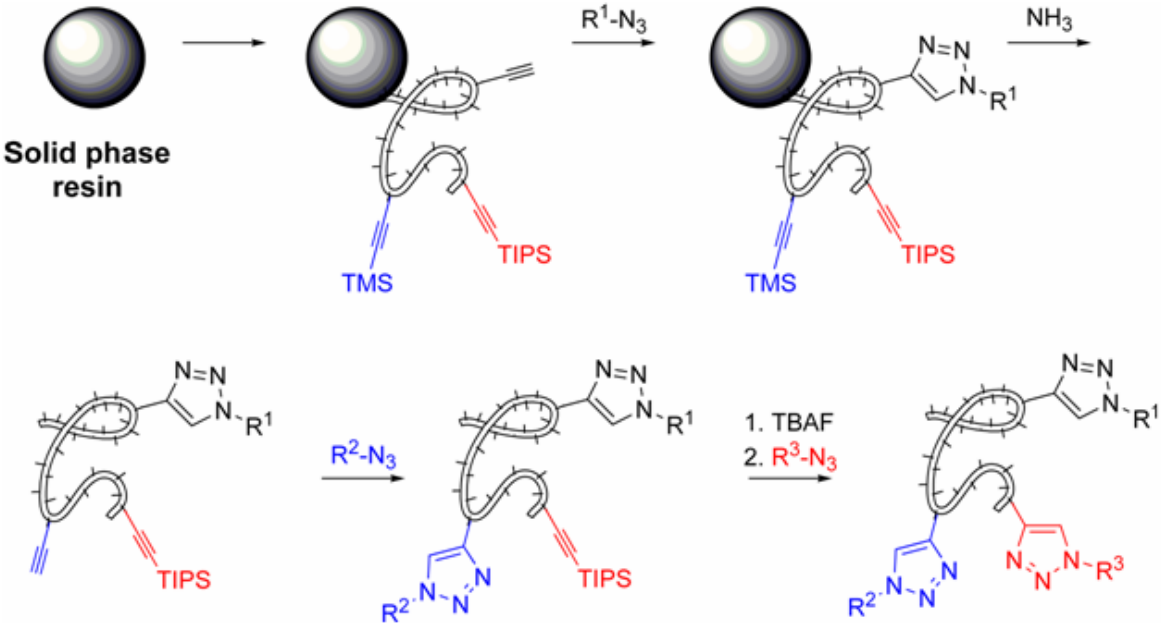

Figure 1.3 Schematic representation of the sequential click chemistry based modification of DNA.

1.8 Enzymatic Incorporation of Alkynes into DNA and Click Based DNA Metallization

The alkyne modified triphosphates **1.18b**-**1.25b** can be efficiently incorporated into PCR products enzymatically. In a screening of different polymerases, Pwo, Deep Vent exo$^-$ and KOD XL polymerases were found to be particularly proficient at incorporating these unnatural nucleotide triphosphates.[33] Indeed even the preparation of 2000mer PCR products with all cytosine bases replaced by the alkyne modified cytosine **1.18b** was reported. With a galactose azide these highly modified DNA amplicons were subsequently converted into sugar coated DNA strands possessing 887 sugar molecules attached to the DNA. Again, the longer and more flexible bisalkyne linkers present in **1.18** and **1.23** were found to lead to higher clicking efficiencies compared to the ethynyl modified base **1.21**. A substitution of all four canonical bases by alkyne bases in a PCR reaction proved unfeasible, showing that the polymerases are not capable of placing an alkyne nucleotide opposite to another alkyne nucleotide. In simple primer extension experiments, however, replacement of all four canonical bases was possible.[37] Most important however, was the observation that the as-modified amplicons can function as templates for normal PCR reactions. Sequencing of these amplicons revealed no mutations showing that the alkyne bases can be used to label PCR products which can then be used for further cloning and PCR experiments.

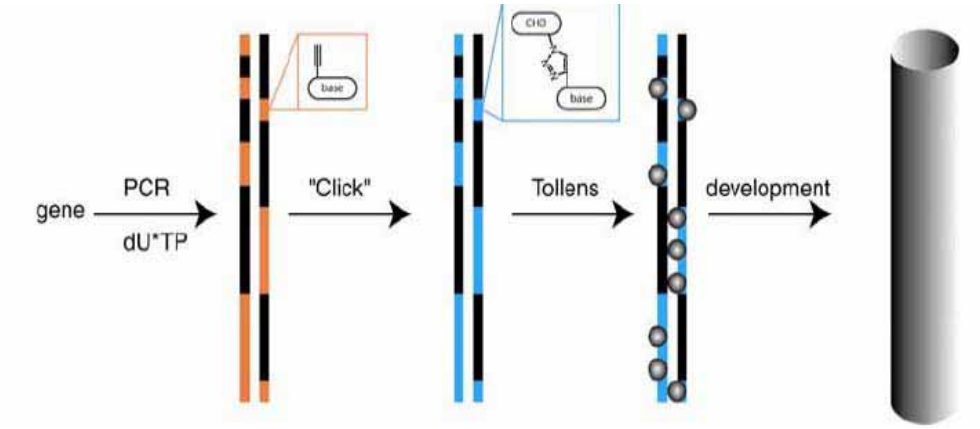

Figure 1.4 Schematic representation of the metal deposition on PCR products.

An interesting application of the sugar coated DNA is the fabrication of metallized DNA strands. (Figure 1.4). Carell et al. prepared 2000mer DNA strands with all natural dT bases replaced by ethynyl uridine **1.21b**.[32] This DNA was subsequently modified with galactose azide using the click reaction. Treatment of the as-prepared DNA with Tollens solution allowed selective deposition of Ag nanoparticles on the DNA which were exposed to a gold enhancer solution in a second step (AuSCN, hydroquinone)[38] to achieve the deposition of gold around the DNA. The resulting gold-DNA nanowires were shown to have an extremely uniform diameter of ≤ 10 nm. Even the time-dependent growth of the gold mantle around the DNA could be studied by AFM on silica and mica (Figure 1.5). Using click chemistry it was recently also possible to deposit size-uniform gold nanoparticles to the backbone of alkyne-containing PCR products. For this purpose the click reaction was performed with a gold nanoparticle that was bound to an azide modified glutathione ligand. Again, the gold nanoparticles exhibited a very uniform distribution along the DNA scaffold.[39]

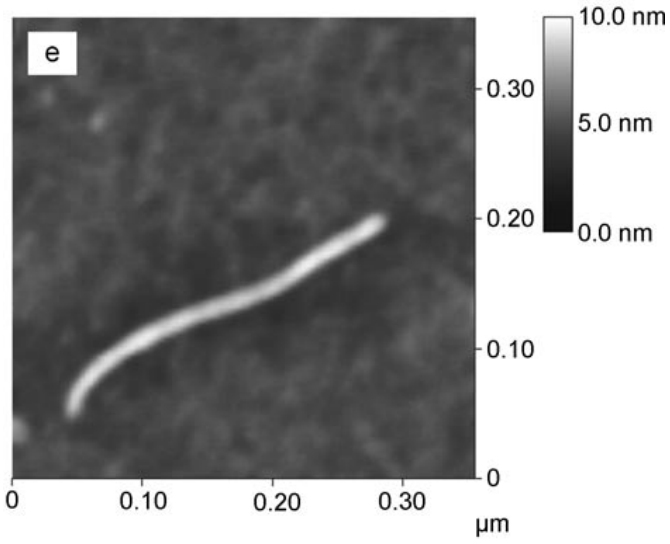

Figure 1.5 AFM pictures of bimetallic silver-gold nanowires deposited on sugar-decorated DNA. Copyright Wiley-VCH Verlag GmbH & Co. KGaA. Reproduced with permission.[38]

Most recently, Rajski et al.[40] developed an ingenious method to label large DNA fragments site selectively using the click reaction based on seminal discoveries of Weinhold an co-workers.[41] This group employed methyltransferases (MTases), which catalyze the transfer of an activated methyl group from the ubiquitous cofactor S-adenosyl-L-methinone (AdoMet or SAM) to adenine or cytosine residues on DNA within specific DNA sequences that range between 2 and 8 base pairs.[42] Similar to Weinhold et al.,[41] the group prepared the novel cofactor **1.26**, which is accepted by the methyltransferase M.TaqI instead of natural SAM. With the novel cofactor, however, not a methyl group but a propargyl modified adenine moiety was transferred to the N6 nitrogen of adenine in the palindromic sequence 5′-AGCT-3′. The resulting DNA is thus selectively labeled with an alkynyl adenine at each AGCT site. The alkyne group was then further functionalized with azides using the Cu(I) catalyzed Huisgen reaction. This method is not restricted by the length of the DNA strand and could thereby lead to the assembly of alkyne labeled genomic DNA with a low density of functionalization.

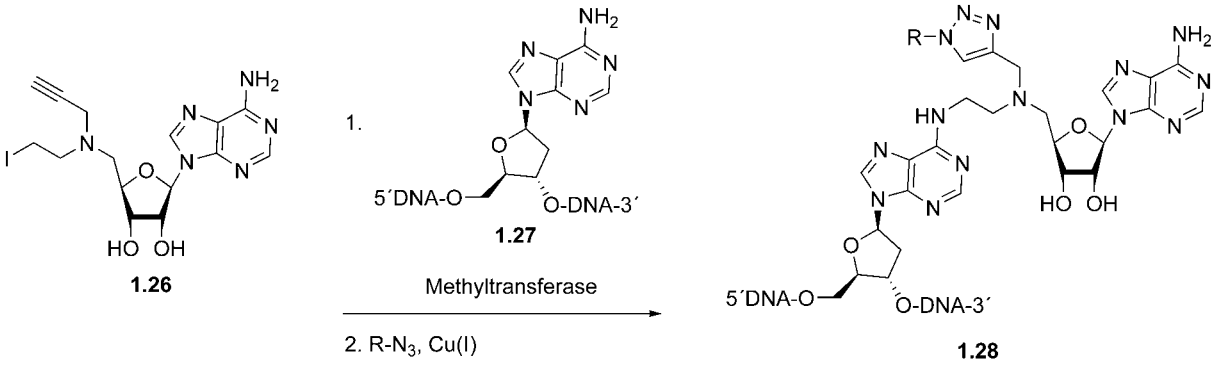

Scheme 1.7 MTase-mediated decoration of DNA with alkyne groups.

1.9 Summary and Outlook

The copper catalyzed azide-alkyne cycloaddition (click reaction) has changed the way of how modified oligonucleotides can be prepared today. It is possible to attach all kinds of labels to small oligonucleotides using alkyne modified phosphoramidites. One, two or even three different labels can be attached either in solution or on solid support. With the help of alkyne modified triphosphates or using the methyltransferase technology one can readily prepare large PCR fragments or genomic DNA containing one or multiple alkyne sites ready for click modification. It is astonishing that many alkyne modified bases are readily accepted by polymerases allowing the full replacement of the canonical bases in an amplicon by alkyne modified bases. The alkyne bearing DNA can be modified using the click reaction in extremely high yields. Many of the click modified oligonucleotides are easily purified using simple ethanol precipitation procedures circumventing time consuming and expensive HPLC purification protocols. The alkyne modified DNA strands can be used as tools for modern molecular diagnostic applications and they can act as building blocks for the construction of functional DNA based nanomaterials ready for the modification with all types of functional molecular entities. For DNA chemists working in the fields of diagnostics, medicine or nanotech-

nology, click chemistry on DNA has vastly broadened the synthesis capabilities paving the way for the preparation of totally new DNA based molecules and nanosystems.

1.10 References

[1] R. Huisgen, *Vol. 1,3-Dipolar Cycloaddition Chemistry*, Wiley, New York, **1984**, pp. 1-176.

[2] C. W. Tornoe, C. Christensen, M. Meldal, *J. Org. Chem.* **2002**, *67*, 3057-3064; V. V. Rostovtsev, L. G. Green, V. V. Fokin, K. B. Sharpless, *Angew. Chem. Int. Ed.* **2002**, *41*, 2596-2599.

[3] V. Aucagne, D. A. Leigh, *Org. Lett.* **2006**, *8*, 4505-4507; H. T. T. Brink, J. T. Meijer, R. V. Geel, M. Damen, D. W. P. M. Löwik, J. C. M. v. Hest, *J. Pept. Sci.* **2006**, *12*, 686 - 692.

[4] A. E. Speers, B. F. Cravett, *Chem. Biol.* **2004**, *11*, 535-546.

[5] T. Liebert, C. Hänsch, T. Heinze, *Macromol. Rapid Commun.* **2006**, *27*, 208-213.

[6] Q. Wang, T. R. Chan, R. Hilgraf, V. V. Fokin, K. B. Sharpless, M. G. Finn, *J. Am. Chem. Soc.* **2003**, *125*, 3192-3193.

[7] C. J. Burrows, J. G. Muller, *Chem. Rev.* **1998**, *98*, 1109-1151; S. Thyagarajan, N. N. Murthy, A. A. N. Sarjeant, K. D. Karlin, S. E. Rokita, *J. Am. Chem. Soc.* **2006**, *128*, 7003-7008.

[8] T. R. Chan, R. Hilgraf, K. B. Sharpless, V. V. Fokin, *Org. Lett.* **2004**, *6*, 2853-2855.

[9] L. M. Smith, S. Fung, M. W. Hunkapiller, T. J. Hunkapiller, L. E. Hood, *Nucleic Acids Res.* **1985**, *13*, 2399-2412.

[10] M. Kuwahara, Y. Takahata, A. Shoji, A. N. Ozaki, H. Ozaki, H. Sawai, *Bioorg. Med. Chem. Lett.* **2003**, *13*, 3735-3738; A. Roychowdhury, H.Illangkoon, C. L. Hendrickson, S. A. Benner, *Org. Lett.* **2004**, *6*, 489-492; M. M. Masud, M. Kuwahara, H. Ozaki, H. Sawai, *Bioorg. Med. Chem.* **2004**, *12*, 1111-1120.

[11] I. Geci, V. V. Filichev, E. B. Pedersen, *Chem. Eur. J.* **2007**, *13*, 6379-6386.

[12] D. I. Rozkiewicz, J. Gierlich, G. A. Burley, K. Gutsmiedl, T. Carell, B. J. Ravoo, D. N. Reinhoudt, *ChemBioChem* **2007**, *8*, 1997-2002.

[13] T. S. Seo, Z. Li, H. Ruparel, J. Ju, *J. Org. Chem.* **2003**, *68*, 609-612.

[14] Z. Li, T. S. Seo, J. Ju, *Tetrahedron Lett.* **2004**, *45*, 3143-3146.

[15] A. M. Jawalekar, N. Meeuwenoord, J. G. O. Cremers, H. S. Overkleeft, G. A. v. d. Marel, F. P. J. T. Rutjes, F. L. v. Delft, *J. Org. Chem.* **2008**, *73*, 287-290.

[16] T. S. Seo, X. Bai, H. Ruparel, Z. Li, N. J. Turro, J. Ju, *Proc. Nat. Acad. Sci. USA* **2004**, *101*, 5488-5493; T. S. Seo, X. Bai, D. H. Kim, Q. Meng, S. Shi, H. Ruparel, Z. Li, N. J. Turro, J. Ju, *Proc. Nat. Acad. Sci. USA* **2005**, *102*, 5926-5931.

[17] N. K. Devaraj, G. P. Miller, W. Ebina, B. Kakaradov, J. P. Collman, E. T. Kool, C. E. D. Chidsey, *J. Am. Chem. Soc.* **2005**, *127*, 8600-8601.

[18] S. Mazzini, F. Garcia-Martin, M. Alvira, A. Avino, B. Manning, F. Albericio, R. Eritja, *Chem. Biodiversity* **2008**, *5*, 209-218; M. Alvira, R. Eritja, *Chem. Biodiversity* **2007**, *4*, 2798-2809; K. Gogoi, M. V. Mane, S. S. Kunte, V. A. Kumar, *Nucl. Acids Res.* **2007**, *35*, e139; M. Humenik, Y. Huang, Y. Wang, M. Sprinzl, *Chembiochem* **2007**, *8*, 1103-1106.

[19] B. P. Duckworth, Y. Chen, J. W. Wollack, Y. Sham, J. D. Mueller, T. A. Taton, M. D. Distefano, *Angew. Chem. Int. Ed.* **2007**, *46*, 8819-8822; B. P. Duckworth, Y. Chen, J. W. Wollack, Y. Sham, J. D. Mueller, T. A. Taton, M. D. Distefano, *Angew. Chem. Int. Ed.* **2007**, *46*, 8819-8822.

[20] R. P. Goodman, I. A. T. Schaap, C. F. Tardin, C. M. Erben, R. M. Berry, C. F. Schmidt, A. J. Turberfield, *Science* **2005**, *310*, 1661-1665.
[21] M. Nakane, S. Ichikawa, A. Matsuda, *Nucl. Acids Symp. Ser.* **2005**, *49*, 189-190.
[22] R. Kumar, A. El-Sagheer, J. Tumpane, P. Lincoln, L. M. Wilhelmson, T. Brown, *J. Am. Chem. Soc.* **2007**, *129*, 6859-6864.
[23] M. Nakane, S. Ichikawa, A. Matsuda, *J. Org. Chem.* **2008**, *73*, 1842-1851.
[24] J. Lietard, A. Meyer, J.-J. Vasseur, F. Morvan, *J. Org. Chem.* **2008**, 191-200; A. Meyer, C. Bouillon, S. Vidal, J.-J. Vasseur, F. Morvan, *Tetrahedron Lett.* **2006**, *47*, 8867-8871.
[25] J. Lietard, A. Meyer, J.-J. Vasseur, F. Morvan, *Tetrahedron Lett.* **2007**, *48*, 8795-8798.
[26] Y. Chevolot, C. Bouillon, S. Vidal, F. Morvan, A. Meyer, J.-P. Cloarec, A. Jochum, J.-P. Praly, J.-J. Vasseur, E. Souteyrand, *Angew. Chem. Int. Ed.* **2007**, *46*, 2398-2402; Y. Chevolot, C. Bouillon, S. Vidal, F. Morvan, A. Meyer, J.-P. Cloarec, A. Jochum, J.-P. Praly, J.-J. Vasseur, E. Souteyrand, *Angew. Chem. Int. Ed.* **2007**, 46, 2398-2402.
[27] A. V. Ustinov, V. V. Dubnyakova, V. A. Korshun, *Tetrahedron* **2008**, *64*, 1467-1473; A. V. Ustinov, V. A. Korshun, *Russ. Chem. Bull.* **2006**, *55*, 1268-1274.
[28] C. Bouillon, A. Meyer, S. Vidal, A. Jochum, Y. Chevolot, J.-P. Cloarec, J.-P. Praly, J.-J. Vasseur, F. Morvan, *J. Org. Chem.* **2006**, *71*, 4700-4701.
[29] F. Morvan, A. Meyer, A. Jochum, C. Sabin, Y. Chevolot, A. Imberty, J.-P. Praly, J.-J. Vasseur, E. Souteyrand, S. Vidal, *Bioconj. Chem.* **2007**, *18*, 1637-1643.
[30] A. Salic, T. J. Mitchison, *Proc. Nat. Acad. Sci. USA* **2008**, *105*, 2415-2420.
[31] D. M. Hammond, A. Manetto, J. Gierlich, V. A. Azov, P. M. E. Gramlich, G. A. Burley, M. Maul, T. Carell, *Angew. Chem. Int. Ed.* **2007**, *46*, 4184-4187.
[32] G. A. Burley, J. Gierlich, M. R. Mofid, S. T. H. Nir, Y. Eichen, T. Carell, *J. Am. Chem. Soc.* **2006**, *128*, 1398-1399.
[33] J. Gierlich, K. Gutsmiedl, P. M. E. Gramlich, A. Schmidt, G. Burley, T. Carell, *Chem. Eur. J.* **2007**, *13*, 9486-9494.
[34] F. Seela, V. R. Sirivolu, *Helv. Chim. Acta* **2007**, *90*, 535-552; F. Seela, V. R. Sirivolu, *Chem. Biodiversity* **2006**, *3*, 509-514; F. Seela, V. R. Sirivolu, P. Chittepu, *Bioconj. Chem.* **2008**, 211-224; F. Seela, V. R. Sirivolu, *Nucleosides, Nucleotides Nucleic acids* **2007**, 597-601; P. Kocalka, N. K. Andersen, F. Jensen, P. Nielsen, *Chembiochem* **2007**, *8*, 2106-2116.
[35] J. Gierlich, G. A. Burley, P. M. E. Gramlich, D. M. Hammond, T. Carell, *Org. Lett.* **2006**, *8*, 3639-3642.
[36] P. M. E. Gramlich, S. Warncke, J. Gierlich, T. Carell, *Angew. Chem. Int. Ed.* **2008**, *47*, 3442-3444.
[37] P. M. E. Gramlich, C. T. Wirges, J. Gierlich, T. Carell, *Org. Lett.* **2008**, *10*, 249-251.
[38] M. Fischler, U. Simon, H. Nir, Y. Eichen, G. A. Burley, J. Gierlich, P. M. E. Gramlich, T. Carell, *Small* **2007**, *3*, 1049-1055.
[39] M. Fischler, A. Sologubenko, J. Mayer, G. Clever, G. Burley, J. Gierlich, T. Carell, U. Simon, *Chem. Commun* **2008**, 169-171.
[40] R. L. Weller, S. R. Rajski, *Org. Lett.* **2005**, *7*, 2141-2144; R. L. Weller, S. R. Rajski, *Chembiochem* **2006**, 243-245.
[41] M. Pignot, C.Siethoff, M.Linscheid, E.Weinhold, *Angew. Chem. Int. Ed.* **1998**, *37*, 2888-2891.
[42] G. Pljevaljcic, F. Schmidt, A. J. Scheidig, R. Lurz, E. Weinhold, *Chembiochem* **2007**, *8*, 1516-1519.

2 Click Chemistry as a Reliable Method for the High-Density Postsynthetic Functionalization of Alkyne-Modified DNA

This Section was published in:

J. Gierlich, G. A. Burley, P. M. E. Gramlich, D. M. Hammond, T. Carell, *Org. Lett.* **2006**, *8*, 3639-3642.

2.1 Abstract

We report the development of the Cu(I)-catalyzed Huisgen cycloaddition (click) reaction for the multiple postsynthetic labeling of alkyne-modified DNA. A series of alkyne-modified oligodeoxyribonucleotides (ODNs) of increasing alkyne density were prepared and the click reaction using various azide labels was investigated. Complete high-density conversion was observed for ODNs containing up to six consecutive alkyne functions. Compatibility of the click conditions with long DNA strands was shown using a PCR product obtained with an alkyne modified primer.

2.2 Introduction

The development of fast, simple and reliable DNA sequencing and detection methods is important for life science research and the diagnosis of pathogenic and genetic disorders.[1, 2] A variety of methods are now available for the sequencing of specific DNA strands or genetic variants thereof.[3] However, protocols that rely on the incorporation and detection of fluorescently tagged nucleoside building blocks have been by far the most sensitive, with single-molecule sensitivity achieved within milliseconds.[4] Unfortunately, the enzymatic replacement of each natural building block with a fluorescently tagged analogue is a challenging exercise, often requiring highly modified protocols.[1, 5] An alternative method is the incorporation of small chemical reporter groups into particular genes that can be further functionalized (termed postsynthetic functionalization).[6] Such a methodology requires a modular protocol in which appropriately modified nucleoside building blocks are incorporated into DNA strands either by an enzymatic process (e.g. PCR) or via solid-phase synthesis. As a second requirement, this post-synthetic functionalization method must be a highly efficient and specific process, resulting in the quantitative conversion of reporter groups into labeled products. Of the handful of chemical motifs that possess the required attributes for use as chemical reporter groups,[6] azides and terminal alkyne functions have been shown to be elegantly suited for biomolecular ligation via the Cu(I)- mediated Huisgen cycloaddition reaction (click chemistry).[7] Indeed, preliminary investigations by our group have demonstrated the power of incorporating reporter group modified nucleosides to direct metal deposition for DNA detection.[8]

2.3 Results and Discussion

We now report the construction of modified oligodeoxyribonucleotides (ODNs) bearing alkyne reporter groups in high density and the development of a click reaction protocol which now enables loading of DNA in high yield with a variety of molecular labels. This two-step process involving the initial chemical or enzymatic incorporation of an alkyne-nucleoside building block and postsynthetic functionalization can be used to decorate DNA for identification or isolation according to the nature of the probe.

Table 2.1 ODN series comprising **2.1** or **2.2**.

ODN-**2.1***	5′-GCG CTG TXC ATT CGC G-3′
ODN-**2.2**	5′-GCG CTG XXC ATT CGC G-3′
ODN-**2.3**	5′-GCG CXG TXC AXT CGC G-3′
ODN-**2.4**	5′-GCG CXX XXX XGT CGC G-3′
ODN-**2.5****	5′-GCG CTG TYC ATT CGC G-3′
ODN-**2.6**	5′-GCG CTG YYC ATT CGC G-3′
ODN-**2.7**	5′-GCG CYG TYC AYT CGC G-3′
ODN-**2.8**	5′-GCG CYY YYY YGT CGC G-3′
ODN-**2.9**	5′-TTA ATT GAA TTC GAT TYG GGC CGG AYT TGT TTC-3′
ODN-**2.10**	5′-GCA GGC YTC AYG CCA GAA TTA CCA GAA G-3′

*X = **2.1**.
Y = **2.2.

To evaluate whether click chemistry[9] would be a useful postsynthetic method for high-density labeling of DNA, the modified uridine nucleosides **2.1** and **2.2** were prepared and incorporated into a series of 16-mer ODNs via their corresponding phosphoramidites. To circumvent potential steric problems with the high-density labeling of ODNs containing the alkyne **2.1**, we also prepared the nucleoside **2.2**. The alkyne function in **2.2** is separated from the uridine base by a flexible spacer. Incorporation of building blocks **2.1** and **2.2** into 16-mer strands via solid-phase DNA synthesis proceeded smoothly albeit with a slight alteration in the phosphoramidite coupling protocol (Table 2.1). The compatibility of the click reaction was then investigated via the coupling of the ODN series in Table 2.1 with azides **2.3**-**2.5**. Azides **2.3**-**2.5** were chosen as they represent a small selection of desirable labels. Azidosugar **2.3** is a semiprotected aldehyde used for selective Ag staining,[8] coumarin azide **2.4** fluoresces only after triazole formation[10] and fluorescein azide **2.5** is a strongly fluorescent molecule used in a variety of biophysical applications.[11]

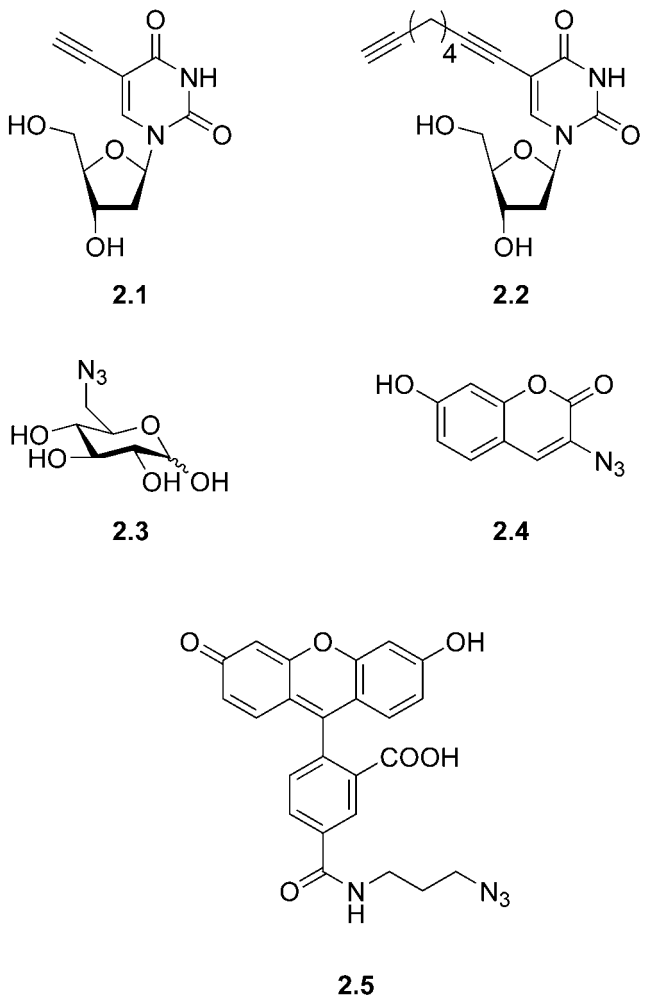

Figure 2.1 Nucleosides and azides used in this study.

In the presence of excess azide, a Cu(I) salt and ODN-**2.1** or ODN-**2.5** (i.e. ODNs comprising one click site), a range of adducts corresponding to strand breaks were observed, suggesting that the original click procedure was not amenable to high-density functionalization of DNA. However, using the Cu(I)-stabilizing ligand (tris(benzyltriazolylmethyl)-amine),[7, 10, 12] full conversion of both ODN-**2.1** and ODN-**2.4** to their respective triazole products was observed using azides **2.3**-**2.5** with no apparent degradation. This finding was consistent with previous results[13] which conclude that the Cu(I)-stabilizing ligand protects biomolecules from unwanted aqueous Cu(I)-mediated chemistry, such as •OH production.[14]

The rigid alkyne series ODN-**2.1**-ODN-**2.4** was then assayed using azides **2.3**-**2.5**. Investigation of the click reaction using the sugar azide **2.3** and ODN-**2.1** revealed complete conversion (Figure 2.1a, ODN-**2.1**, MW = 5082 $[M + Na]^+$) by MALDI-TOF analysis; however, when the alkyne density was increased to two adjacent alkyne click sites (Figure 2.2a, ODN-**2.2**), an additional small amount of the monoclick product (MW = 5110 $[M + Na]^+$) was observed in addition to the fully clicked product (MW = 5297). This result was also consistent with the click reaction between **2.3** and the ODN containing three alkyne functions (ODN-**2.3**) separated by two bases each. A minor amount of the two-clicked adduct (MW = 5320 $[M + Na]^+$) was obtained in addition to the three-clicked adduct (MW = 5508) as the major product. These findings were also supported by the reaction with ODN-**2.4** con-

taining six adjacent alkynes. The major click product then corresponded to only a five-clicked adduct (MW = 5970 $[M + 2Na]^+$) in addition to minor products corresponding to a four- (MW = 5784 $[M + 3Na]^+$) and six- (MW = 6158 $[M + Na]^+$) clicked adduct, respectively. Therefore, it became apparent that the steric shielding of the alkyne by the DNA backbone (ODN-**2.1**- ODN-**2.4**) was contributing to the less than optimal labeling yields. In contrast to the ODN-**2.1**-ODN-**2.4** series, full conversion was observed for ODN-**2.5**, ODN-**2.6**, and ODN-**2.8** containing the flexible alkyne according to MALDI-TOF analysis (Figure 2.2b).

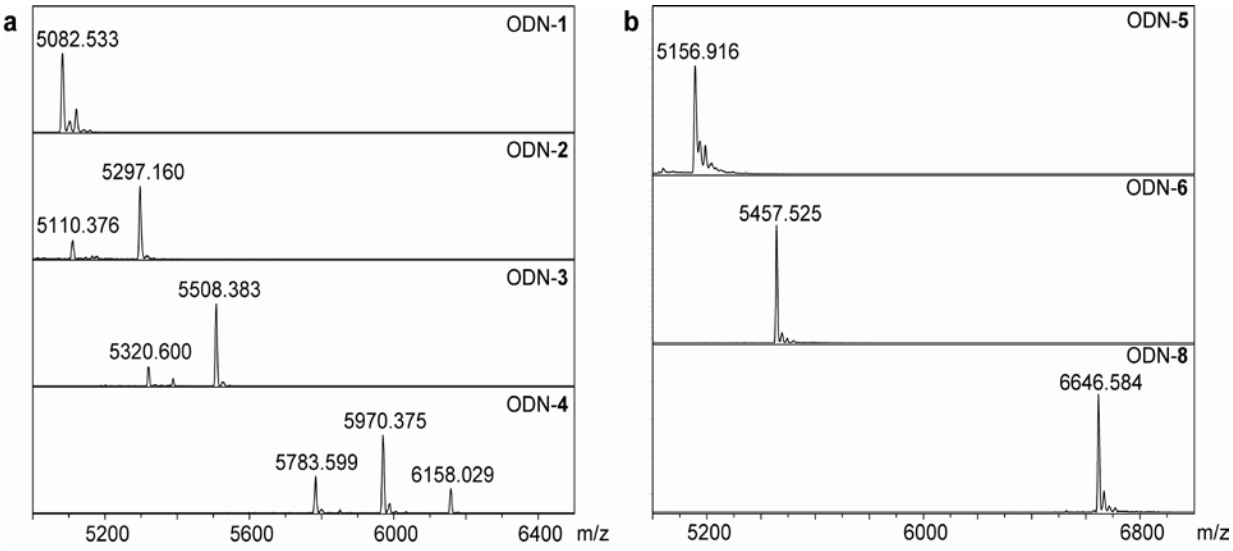

Figure 2.2 MALDI-TOF spectra of: (a) click reaction performed with azide **2.3** and ODNs comprising alkyne **2.1** with one (ODN-**2.1**, MW = 4872), two (ODN-**2.2**, MW = 4882), three (ODN-**2.3**, MW = 4892), and six (ODN-**2.4**, MW = 4902) alkyne functions and (b) click chemistry performed with azide **2.3** and ODNs comprising alkyne **2.2** with one (ODN-**2.5**, MW = 4952), two (ODN-**2.6**, MW = 5042), and six (ODN-**2.8**, MW = 5379) alkyne functions.

Switching to the nonfluorescent coumarin azide **2.4** provided the added benefit of forming a highly fluorescent click product. Both ODN series (ODN-**2.1**-ODN-**2.3** and ODN-**2.5**-ODN-**2.8**) were assayed against azide **2.4** and revealed a clicking scenario similar to that observed for azide **2.3**: the rigid alkyne series (ODN-**2.1**-ODN-**2.3**) produced less than quantitative conversion to the fluorescent click product, whereas the flexible alkyne series (ODN-**2.5**-ODN-**2.8**) produced fully labeled products. With the flexible alkyne spacer nucleoside **2.2**, it is therefore possible to achieve highly reliable, complete high-density functionalization of ODNs.

Gel electrophoresis studies of coumarin-labeled ODN products (ODN-**2.5**-ODN-**2.7**) are depicted in Figure 2.3a.

When click chemistry was performed using the fluorescein azide **2.5**, the resulting products were easily observed by the difference in electrophoretic mobility as a consequence of a much larger increase in molecular weight (Figure 2.3b,c). As expected, in the case of the ODN-**2.1**-ODN-**2.4** series, only partial conversion was observed (Figure 2.3b). For two click sites (lane 2) and three click sites (lane 3), the product mixtures are clearly visible. The click reaction between **2.5** and ODN-**2.4** in particular revealed a range of products (Figure 2.3b, lane 4).

Consistent with previous click studies using the ODN-**2.5**-ODN-**2.8** series, full conversion was observed for all strands by gel electrophoresis (Figure 2.3c). Lanes 5-8 show complete conversion of one, two, three and six click sites.

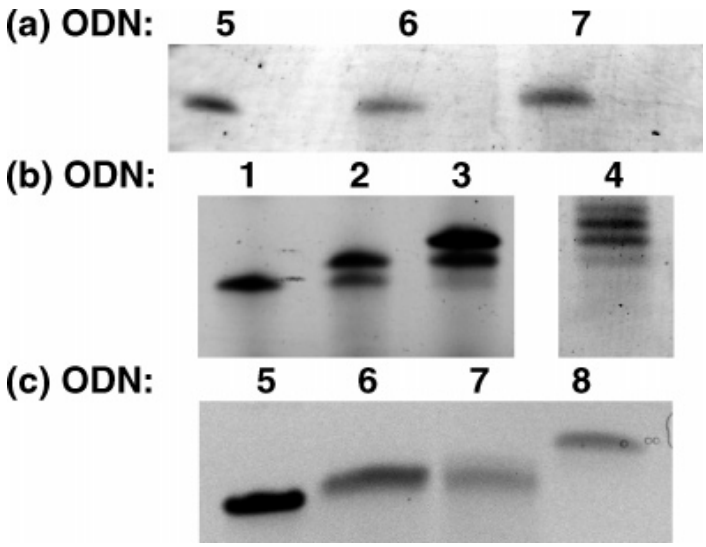

Figure 2.3 Gel electrophoresis of click reactions. (a) Click reactions of ODNs containing **2.2** with coumarin azide **2.4**, detection using a 460 nm cutoff filter. (b) Click reactions of the ODN series containing the nucleoside **2.1** and the fluorescein azide **2.5**. (c) Click reactions of the ODN series containing the nucleoside **2.2** and the fluorescein azide **2.5**.

To investigate whether click chemistry can be utilized to label long DNA fragments for a labeling method based on click chemistry, the PCR primers ODN-**2.9** and ODN-**2.10** containing two click sites were synthesized and subsequently used in a PCR to amplify a range of PCR products from two different plasmid templates. Melting point analysis of ODN-**2.9** revealed no destabilization of the DNA strand due to the two modifications.

The resulting amplicons comprise two alkyne moieties at one end of the double strand. The purified DNA was then treated with azide **2.5** using the CuBr/ligand method.[12] Gel electrophoresis of the reaction product showed only a single band corresponding to a fluorescein labeled click product (Figure 2.4a, lane 2 and Figure 2.4b, lanes 2 and 4). An unmodified DNA fragment treated identically showed no fluorescence (Figure 2.4a, lane 3, Figure 2.4b, lanes 1 and 3). No sign of DNA degradation was observed when staining the gels with SYBR Green II or ethidium bromide in either case. The same results were obtained on PCR fragments up to 2000 base pairs (Section 2.5.3).

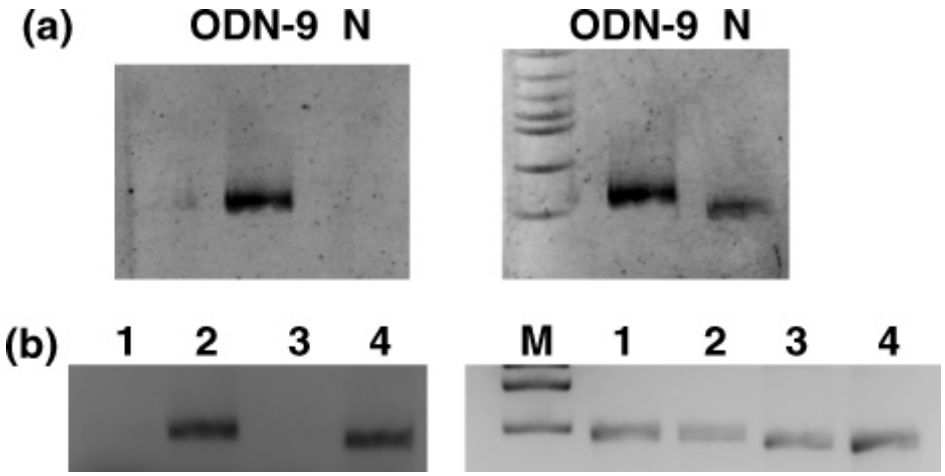

Figure 2.4 Click reactions on the PCR product using fluorescein azide **2.5**. (a) Click on 300 bp PCR fragment comprising ODN-**2.9** (lane 1: 100 bp marker, lane 2: alkyne DNA (primer ODN-**2.9**), lane 3: control with unmodified DNA; N = natural). The right gel is stained with SYBR Green II. (b) Agarose gels of a click on an 800 bp PCR product using ODN-**2.10** (lane 2) and a 900 bp PCR product using ODN-**2.9** (lane 4). Lanes 1 and 3 are controls using unmodified primers. The right gel was run with ethidium bromide.

2.4 Summary and Outlook

In summary, click chemistry is a simple and robust method for the conversion of alkyne-modified DNA into labeled products. Using the alkyne nucleoside **2.2**, the high-density reliable modification of all alkyne sites can be achieved. The method can even be employed to modify long DNA fragments obtained by PCR without DNA cleavage. Efforts are now underway to investigate the utility of click chemistry in the functionalization of specific genes of several hundred to several thousand base pairs in length.

2.5 Experimental Section

2.5.1 Synthesis

The azides **2.3**,[15] **2.4**[10] and **2.5**[7, 16] were prepared according to literature procedures.

The preparation of nucleoside **2.1** and its phosphoramidite **2.6** (Scheme 2.1) have been reported elsewhere.[17]

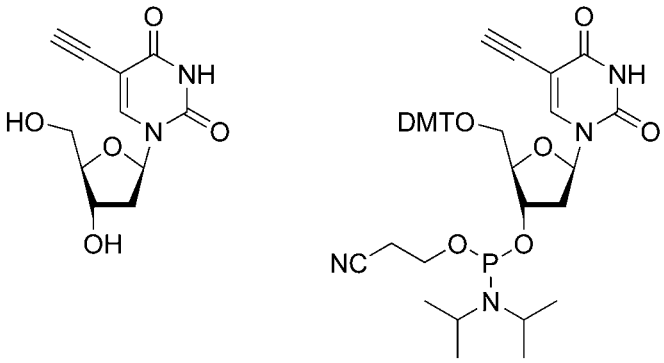

2.1 **2.6**

Scheme 2.1 Uridine building blocks **2.1** and **2.6**.

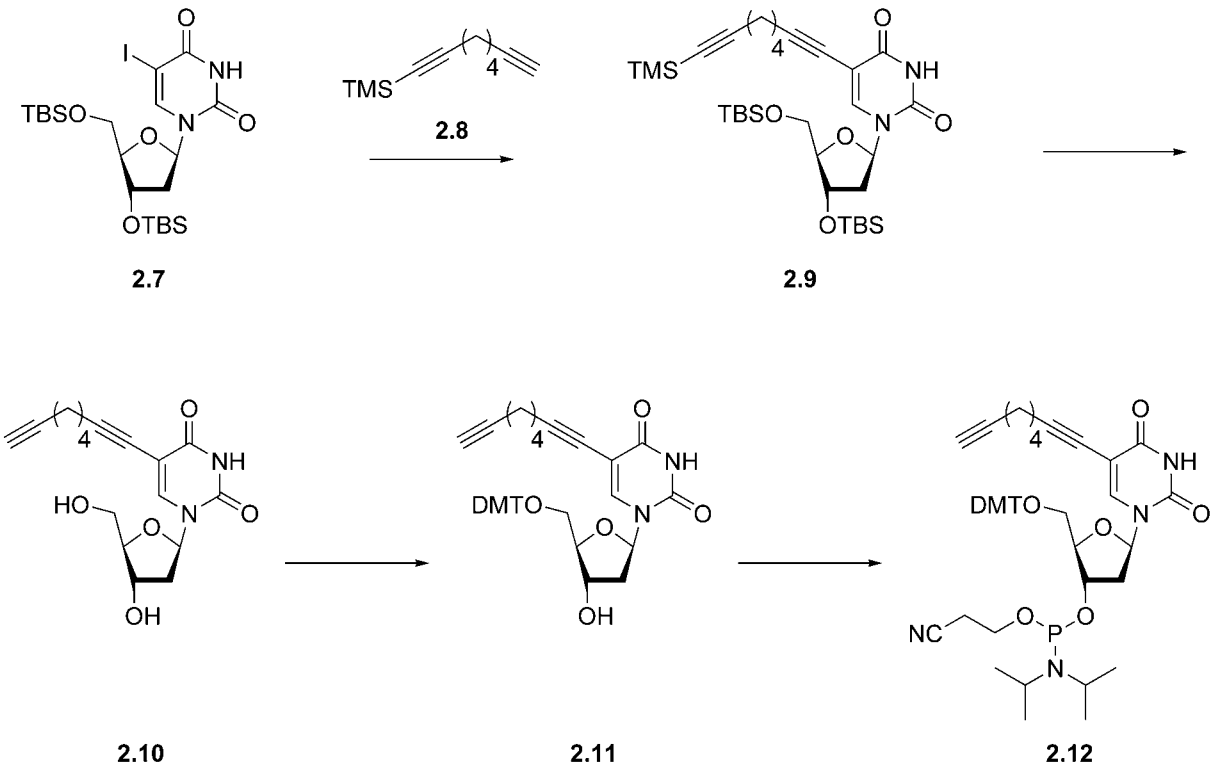

Scheme 2.2 Synthesis of uridine phosphoramidite **2.12**.

5-(8-Trimethylsilyl-octa-1,7-diynyl)-3′,5′-di-*O*-(*tert*-butyldimethylsilyl)-2'-deoxyuridine (**2.9**)

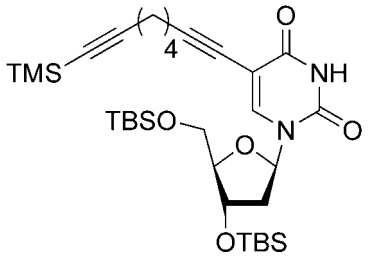

To a thoroughly degassed solution of **2.7** (2.70 g, 4.26 mmol), $PdCl_2(PPh_3)_2$ (0.299 g, 0.426 mmol) and CuI (0.161 g, 0.852 mmol) in dry DMF (3 mL) was added degassed DIPEA (3.9 mL, 21 mmol) and the reaction mixture stirred at r. t. for 10 min. A degassed solution of trimethylsilyl-1,7-octadiyne **2.8** (0.908 g, 5.54 mmol) in dry DMF (1 mL) was added drop-wise to the reaction mixture over 1 h. After complete addition, the reaction mixture was stirred at r. t. over night. After concentration *in vacuo*, the crude mixture was diluted with EtOAc (200 mL) and the organic layer was washed with brine (3 × 50 mL) followed by water (50 mL). The organic layer was dried ($MgSO_4$), filtered and concentrated *in vacuo*. Flash column chromatography (EtOAc/*i*Hex 1:9) provided **2.4** (2.63 g, 92%) as a pale yellow foam. ^{1}H-NMR (600 MHz, $CDCl_3$): δ = -0.06 (s, 3H, $OSiCH_3$), -0.05 (s, 3H, $OSiCH_3$), -0.00 (s, 12H, $OSiCH_3$, $Si(CH_3)_3$), 0.01 (s, 3H, $OSiCH_3$), 0.76 (s, 9H, $C(CH_3)_3$), 0.80 (s, 9H, $C(CH_3)_3$), 1.51 (m, 4H, CH_2), 1.89 (m, 1H, CH_2), 2.11 (t, 2H, J = 6.5 Hz, C≡ CCH_2), 2.16 (m, 1H, $C_{2'}H$), 2.19 (m, 1H, $C_{2'}H$), 2.26 (t, 2H, J = 6.5 Hz, C≡ CCH_2), 3.63 (dd, 1H, J = 9.8, 1.4 Hz, $C_{5'}H$), 3.76 (dd, 1H, J = 9.8, 1.4 Hz, $C_{5'}H$), 3.82 (d, 1H, J = 1.4 Hz, $C_{4'}H$), 6.16 (t, 1H, J = 6.8 Hz, $C_{1'}H$), 7.8 (s, 1H, C_6H), 9.64 (s, 1H, NH). ^{13}C-NMR (150 MHz, $CDCl_3$): δ = -5.7 ($SiCH_3$), -5.5 ($SiCH_3$), -5.0 ($SiCH_3$), -4.8 ($SiCH_3$), 0.0 ($Si(CH_3)_3$), 17.8 ($SiC(CH_3)_3$), 18.2 ($SiC(CH_3)_3$), 19.0 (-CH_2-), 19.2 (-CH_2-), 25.6 ($SiC(CH_3)_3$), 25.9 ($SiC(CH_3)_3$), 27.4 (C≡ C-CH_2-), 27.9 (C≡ C-CH_2-), 41.7 ($C_{2'}$), 62.9 ($C_{5'}$), 71.6 (C≡ C), 72.0 ($C_{3'}$), 84.4 (C≡ C), 85.4 ($C_{1'}$), 88.0 ($C_{4'}$), 94.2 (C≡ C), 100.6 (C_5), 106.8 (C≡ C), 141.3 (C-6), 149.4 (C_2), 162.1 (C_4). HRMS (ESI) calcd. for $C_{32}H_{56}N_2NaO_5Si_3^+$: 655.3389 $[M+Na]^+$, found: 655.3400.

5-(Octa-1,7-diynyl)-2'-deoxyuridine (**2.10**)

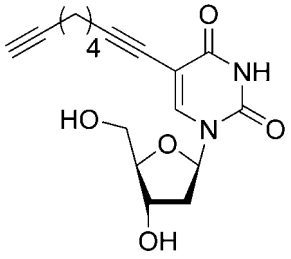

To a cooled solution (0 °C) of **2.9** (2.10 g, 3.40 mmol) in dry THF (5 mL) was added TBAF (1.0 M in THF, 10.9 mL, 10.9 mmol) under a nitrogen atmosphere. The reaction mixture was

stirred for 3 h, quenched with glacial acetic acid (1.0 mL) and concentrated *in vacuo*. Column chromatography (flash silica) eluting with 10% MeOH in EtOAc afforded **2.10** (1.18 g, 85%) as a colorless oil.
^{1}H-NMR (400 MHz, d_6-DMSO): δ = 1.57 (m, 4H, CH_2CH$_2$), 2.11 (m, 2H, $C_{2'}$H), 2.19 (m, 2H, C≡ CCH$_2$), 2.38 (m, 2H, C≡ CCH$_2$), 2.75 (m, 1H, C≡ CH), 3.55-3.65 (m, 2H, $C_{5'}$H), 3.78 (dd, 1H, *J* = 6.6, 3.5 Hz, $C_{4'}$H), 4.23 (m, 1H, $C_{3'}$H), 5.06 (t, 1H, *J* = 4.8 Hz, OH), 5.22 (d, 1H, *J* = 4.0 Hz, OH), 6.10 (t, 1H, *J* = 6.5 Hz, $C_{1'}$H), 8.10 (s, 1H, C_6H), 11.3 (sbr, 1H, NH). ^{13}C-NMR (100 MHz, d_6-DMSO): δ = 17.1 (C≡ C-*C*H$_2$CH$_2$), 18.2 (C≡ C-*C*H$_2$CH$_2$), 27.0 (C≡ C-CH$_2$*C*H$_2$), 27.1 (C≡ C-CH$_2$*C*H$_2$), 39.9 ($C_{2'}$), 60.9 ($C_{5'}$), 70.1 ($C_{3'}$), 71.2 (C≡ *C*-H), 72.9 (C≡ C), 84.1 ($C_{1'}$), 84.5 ($C_{4'}$), 87.4 (C≡ C), 92.8 (C≡ C), 98.9 (C_5), 142.6 (C_6), 149.4 (C_2), 161.6 (C_4). HRMS (ESI) calcd. for $C_{17}H_{19}N_2O_5^-$: 331.1299 [M- H]$^-$, found: 331.1295.

5-(Octa-1,7-diynyl)-5´-*O*-(4,4´-dimethoxytrityl)-2'-deoxyuridine (**2.11**)

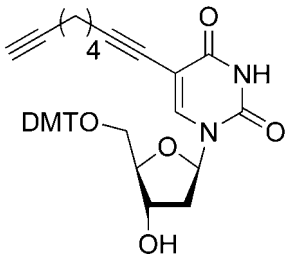

To a solution (0 °C) of **2.10** (1.58 g, 4.97 mmol) in dry pyridine (5 mL) was added DMAP (cat), followed by 4,4'-dimethoxytriphenylmethyl chloride (1.85 g, 5.47 mmol) under a nitrogen atmosphere and the reaction mixture was stirred over night. After concentration *in vacuo*, the crude mixture was diluted with EtOAc (200 mL) and the organic layer was washed with brine (3 x 50 mL) followed by water (50 mL). The organic layer was dried ($MgSO_4$), filtered and concentrated *in vacuo*. Flash column chromatography (SiO_2) eluting with a gradient of EtOAc/*i*Hex (+ 1% pyridine) (1:9 → 1:1) provided **2.11** as a pale yellow foam (1.41 g, 46%).
^{1}H-NMR (400 MHz, CD_2Cl_2): δ = 1.42 (m, 4H, CH_2CH$_2$), 1.96 (t, 1H, *J* = 2.5 Hz, C≡ CH), 2.07 (td, 2H, *J* = 6.8, 2.5 Hz, CH_2C≡ CH), 2.15 (td, 2H, *J* = 7.1, 1.6 Hz, CH$_2$C≡ C), 2.28 (m, 1H, $C_{2'}$H), 2.46 (m, 1H, $C_{2'}$H), 3.34 (d, 2H, *J* = 3.3 Hz, $C_{5'}$H), 3.79 (s, 6H, ArOCH$_3$), 4.08 (dd, 1H, *J* = 6.2, 3.3 Hz, $C_{4'}$H), 4.55 (m, 1H, $C_{3'}$H), 6.29 (dd, 1H, *J* = 7.7, 5.8 Hz, $C_{1'}$H), 6.87 (d, 4H, *J* = 8.5 Hz, CH$_{Ar}$), 7.24 (m, 1H, CH$_{Ar}$), 7.31 (m, 2H, CH$_{Ar}$), 7.36 (dd, 4H, *J* = 8.5, 1.9 Hz, CH$_{Ar}$), 7.45 (dd, 2H, *J* = 8.6, 1.5 Hz, CH$_{Ar}$), 7.97 (s, 1H, C_6H). ^{13}C-NMR (150 MHz, CD_2Cl_2): δ = 20.1 (C≡ C-*C*H$_2$CH$_2$), 21.2 (C≡ C-*C*H$_2$CH$_2$), 29.7 (C≡ C-*C*H$_2$-), 30.0 (C≡ C-*C*H$_2$), 45.7 ($C_{2'}$), 59.6 (O-CH$_3$), 67.9 ($C_{5'}$), 72.6 (C≡ *C*-H), 75.6 ($C_{3'}$), 76.5, 88.4, 89.6 ($C_{1'}$), 90.9 ($C_{4'}$), 91.3, 98.6, 105.0, 117.6 (4C), 128.0, 128.2, 131.3 (2C), 132.2, 132.4, 134.3, 134.4, 139.9, 140.0, 140.4, 146.0, 146.2, 149.1, 153.8, 153.9, 163.0, 163.3. HRMS (ESI) calcd. for $C_{38}H_{38}N_2NaO_7^+$: 657.2571 [M+Na]$^+$, found 657.2570.

5-(Octa-1,7-diynyl)-3′-*O*-[(2-cyanoethoxy)(diisopropylamino)-phosphono)]-5′-*O*-(4,4′-dimethoxytrityl)-2'-deoxyuridine (**2.12**)

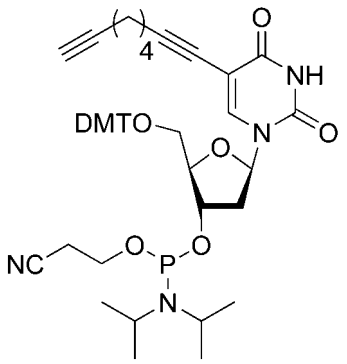

To a solution (0 °C) of **2.11** (0.200 g, 0.32 mmol) in dry DCM (5 mL) was added triisopropyl tetrazolide (0.068 g, 0.40 mmol) followed by 2-cyanoethyl tetraisopropyl phosphoramidite (306 µL, 0.97 mmol) under a nitrogen atmosphere and the reaction mixture was stirred at r. t. for 4 h. After concentration *in vacuo*, the crude mixture was purified by flash column chromatography (SiO_2) eluting with EtOAc/*i*Hex (1:3 + 1% pyridine) to afford **2.12** (0.188 g, 70%) as a white solid.
^{31}P-NMR (81 MHz, CD_2Cl_2): δ = 149.9, 149.6. MS (MALDI-TOF): 857 $[M + Na]^+$.

1-Trimethylsilyl-octa-1,7-diyne (**2.8**)[18]

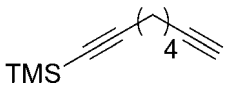

To a solution of 1,7-octadiyne (12.86 mL, 96.9 mmol) in dry THF (150 mL) at -78 °C was added LiHMDS (1 M, 96.9 mL). The solution was stirred for 30 min and TMS-Cl (12.3 mL, 96.9 mmol) was added over 30 min. The solution was warmed to r. t. and stirred for 4 h, quenched with water (100 mL), extracted with Et_2O and washed with 1 M HCl. The organic layer was dried over Na_2SO_4 and the solvent was removed *in vacuo*. The crude product was distilled (bath temp = 120 °C, 4 mbar) to give 7.25 g (40.7 mmol, 42%) of **2.8** as a clear liquid. ^{1}H-NMR (200 MHz, $CDCl_3$): δ = 0.12 (s, 9H, $Si(CH_3)_3$), 1.61 (quin, 4H, *J* = 3.4 Hz, $CH_2CH_2CH_2CH_2$), 1.93 (t, 1H, *J* = 2.7 Hz, C≡ CH), 2.16-2.26 (m, 4H, C≡ CCH_2). HRMS (EI) calcd. for $C_{10}H_{17}Si^-$ $[M-H]^-$: 177.1105, found: 177.1099.

2.5.2 Click Procedure for Short DNA Oligos

Using TCEP

To 25 µL of a 0.5 mM DNA solution (12.5 nmol) in water, 6.25 µL of an azide solution (0.1 N, 625 nmol) and 10 µL of a solution containing Cu(II)-salt ($CuSO_4$) and ligand[19] in a 1:1 ratio in 4:3:1 water/DMSO/*t*BuOH was added (0.05 N, 250 nmol). The mixture was vortexed and as the last component 5 µL of a freshly prepared TCEP solution in water was added (0.1 N, 500 nmol). The solution was shaken at 15 °C over night. The reaction was diluted with water (200 µL) and used for gel electrophoresis without further purification.

Using CuBr

To 25 µL of a 0.5 mM DNA solution (12.5 nmol) in water 6.25 µL of an azide solution (0.1 N, 625 nmol) and 10 µL of a freshly prepared solution containing CuBr and ligand[19] in a 1:1 ratio in 4:3:1 water/DMSO/*t*BuOH was added (0.05 N, 250 nmol). The mixture was vortexed and shaken at 15 °C for 1 h. The reaction was diluted with water (200 µL) and used for the gel without further purification.

2.5.3 PCR Amplification

For PCR amplification two different templates were used. Template **A** is the Gateway expression vector pExp007-polη with the polymerase η gene from Rad30 *S. cervisiea*.[20] Template **B** is the Gateway entry vector pENTR201-FPG with the FPG repair protein gene from *Lactococcus lactis subsp. cremoris*.

Primer 1 ODN-**2.9**
Primer 2 5'-TTA ATT GAA TTC GAT TTG GGC CGG ATT TGT TTC-3'
Primer 3 5'-ATT AAG AAT TCT TTT ATG CTA TCT CTG ATA CCC TTG-3’
Primer 4 5'-TGA TGC CCT TGT ACG CAA CTG-3'
Primer 5 5'-GGA AGA TGT AAC TTG TTT CTT CTG-3'
Primer 6 5'-GGG TTA TTG TCT CAT GAG CG-3'
Primer 7 ODN-**2.10**
Primer 8 5’-GGG GAC AAG TTT GTA CAA AAA AGC AGG CTT CAT GCC AGA GTT ACC AGA AG-3’
Primer 9 5’-GGG GAC CAC TTT GTA CAA GAA AGC TGG GTC TTA TTT TTG CTG ACA GAA TGG G-3’

Table 2.2 Combination of primers used and the length of the resulting PCR product.

Forward Primer	Reverse Primer	Template	PCR product length (bp)
Primer 1	Primer 3	A	305
Primer 2	Primer 3	A	305
Primer 1	Primer 4	A	934
Primer 2	Primer 4	A	934
Primer 1	Primer 5	A	1398
Primer 2	Primer 5	A	1398
Primer 1	Primer 6	A	2149
Primer 2	Primer 6	A	2149
Primer 7	Primer 9	B	800
Primer 8	Primer 9	B	822

PCR conditions

The PCR was run with 0.18 µM of each dNTP, 0.09 µM of each primer, 300 ng of template and 1.25 U Taq Polymerase (Promega) in the reaction buffer provided by the supplier (50 mM KCl, 10 mM Tris-HCl (pH 9.0), 0.1% Triton® X-100, 1.5mM $MgCl_2$). Total volume was 22 µL. For production PCRs the volume of the PCR was doubled keeping all concentrations constant.
Temperature program for 300 bp PCR products : 96 °C for 90 s, then 29 cycles of 94 °C for 10 s, 58 °C (-0.3 °C each cycle) for 15 s, 72 °C for 1 min; then 24 cycles of 95 °C for 10 s, 55 °C for 15 s, 72 °C for 1 min. For the long PCR products the elongation time was increased to 2 min.
The PCR product was purified using QIAquick PCR Purification Kit (QIAGEN) and the concentration determined by UV absorption.

2.5.4 Click on PCR Product

Click on the 300 bp product

To 10 µL DNA solution (1-4 pmol DNA, 10 mM Tris), 10 µL fluorescein azide solution (5 mM, diluted with 10 mM Tris with 5% *t*BuOH from a stock of 0.1 N in DMSO) and 10 µL precomplexed Cu(I) was added (10 mM; 1 mg CuBr (99.99%) dissolved in 700 µL 10 mM ligand[19] in *t*BuOH/DMSO 1:3) The sample was shaken at 37 °C for 2 h. Then formamide buffer was added and the samples analyzed with a 5% PAGE gel. Control experiments showed that the reaction is over in less than 30 min.

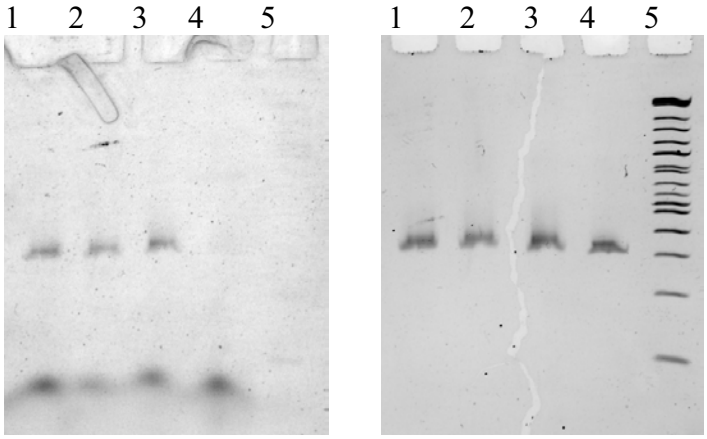

Figure 2.5 Lane 1: 30 min, lane 2: 1 h, lane 3: 2 h, lane 4: 2 h but without CuBr, lane 5: DNA 100 bp ladder (New England Biolabs) The lower spot is due to fluorescein azide in the reaction mixture. On the right side is the same gel stained with SYBR Green II to visualize all DNA fragments.

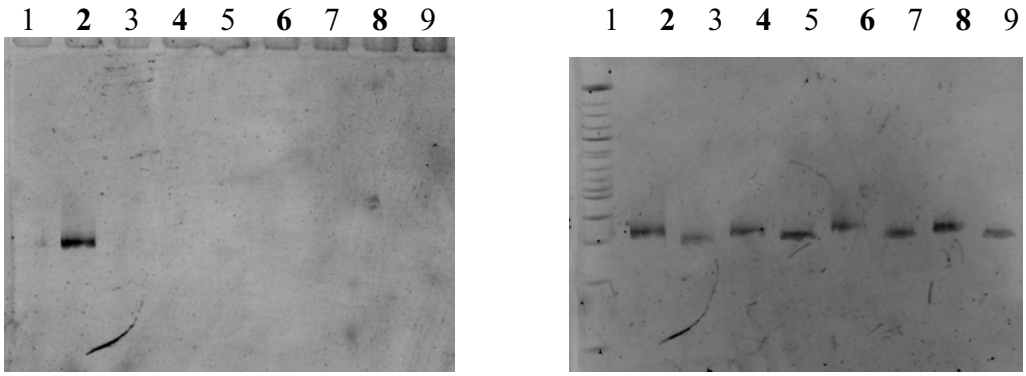

Figure 2.6 Lane 1 is a 2-log DNA ladder (New England Biolabs). Lanes 2,4,6,8 contain alkyne-primer DNA (in bold) with one Biotin on the reverse primer. Lanes 3,5,7,9 contain normal DNA without any modification. The right gel is stained with SYBR Green to visualize all DNA strands. See Table 2.3 for the combinations of reagents for these control experiments.

Table 2.3 Reagent combinations used in Figure 2.6.

lane	2	3	4	5	6	7	8	9
Cu/Lig	+	+	-	-	+	+	-	-
Azide	+	+	+	+	-	-	-	-

Click on the long DNA strands

To 10 µL DNA solution (1-4 pmol DNA, 10 mM Tris), 10 µL fluorescein azide solution (5 mM, diluted with 10 mM Tris with 5% *t*BuOH from a stock of 0.1 N in DMSO) and 10 µL precomplexed Cu(I) was added (10 mM; 1 mg CuBr (99.99%) dissolved in 700 µL 10 mM ligand[19] in *t*BuOH/DMSO 1:3) The sample was shaken at 20 °C for 2 h. Then the reaction mixture was purified using QIAquick PCR Purification Kit (QIAGEN).

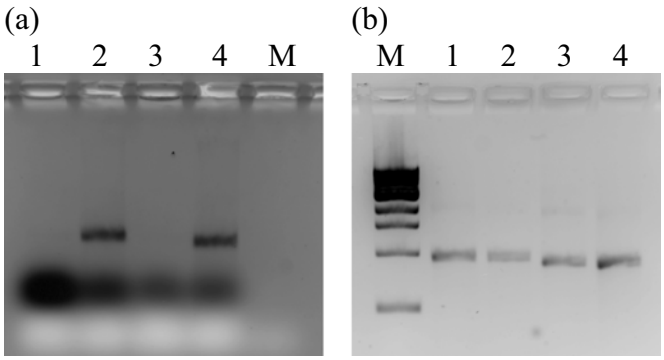

Figure 2.7 2% Agarose gel of the click on PCR products using following primer combinations: lane 1: 2+4, lane 2: 1+4, both with template **A**, lane 3: 8+9, lane 7+9, both with template **B**. (a) Gel without staining using 0.6 pmol DNA per lane (ca. 600 ng). The black spots on the front are free fluorescein azide, the white one bromphenolblue. The picture was taken using 460 epi-illumination with 515 nm cutoff filter. (b) Agarose gel of click samples using the same conditions stained with ethidium bromide using less DNA due to overloading. The picture was taken using 312 nm UV through and 605 nm cutoff filter. As Marker Quick-Load™ 1 kb DNA ladder (New England Biolabs) was used.

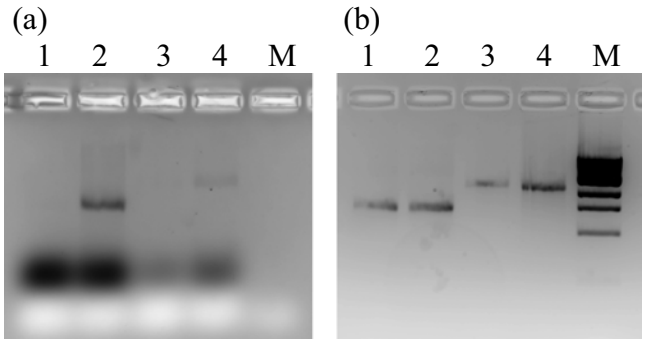

Figure 2.8 2% Agarose gel of the click on PCR products using the following primer combinations: lane 1: 2+5, lane 2: 1+5, lane 3: 2+6, lane 4: 1+6, all with template **A.** All gel conditions are identical to the conditions above.

2.5.5 Melting Point Analysis of ODN-**9**

The melting points were measured using a Cary 100 Bio spectrophotometer. The samples (3 μM DNA, 150 mM NaCl, 10 mM Tris pH 7.4) were cycled five times between 85 °C and 0 °C (0.5 °C/min) starting at 85 °C. The melting points were derived from the average of five measurements at 260 nm corrected by the background absorption.

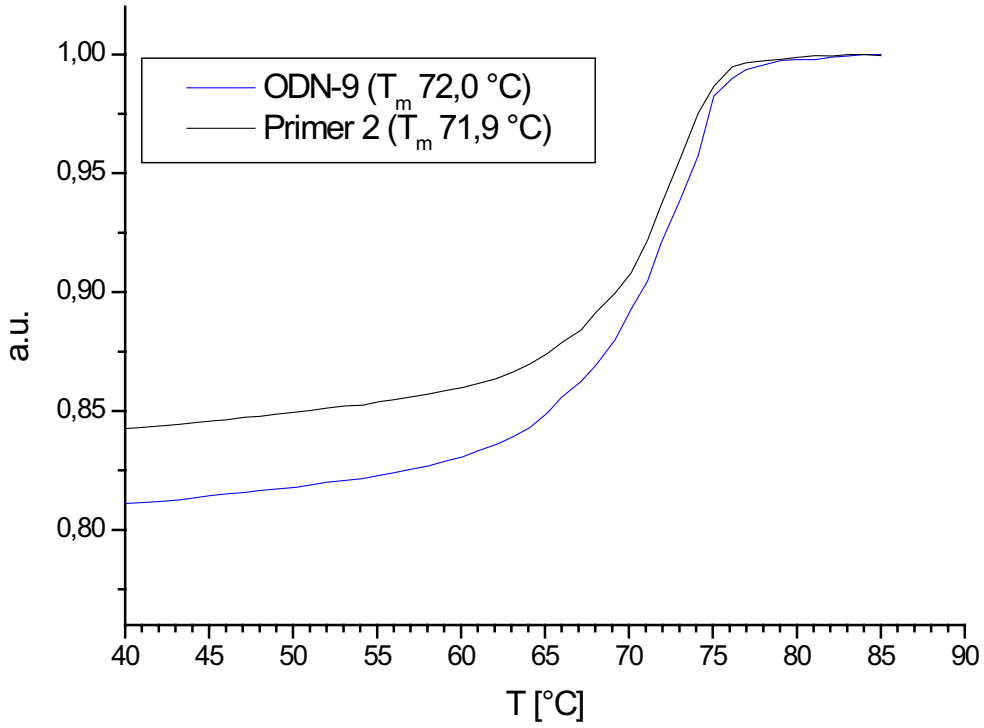

Figure 2.9 Melting point analyses.

2.5.6 MALDI-TOF Spectra of Coumarin Click

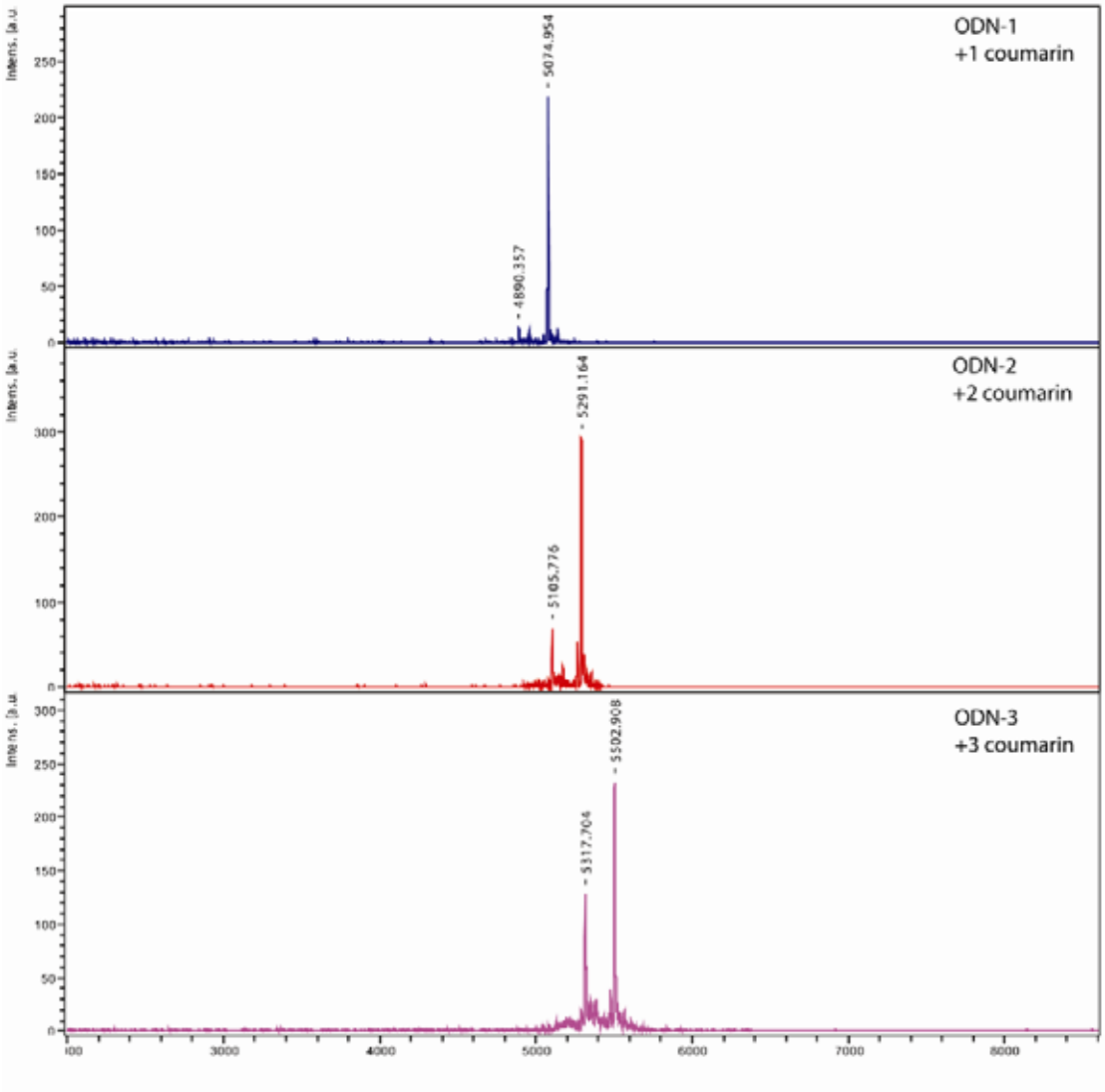

Figure 2.10 MALDI-TOF of series ODN-**2.1** to ODN-**2.3**.

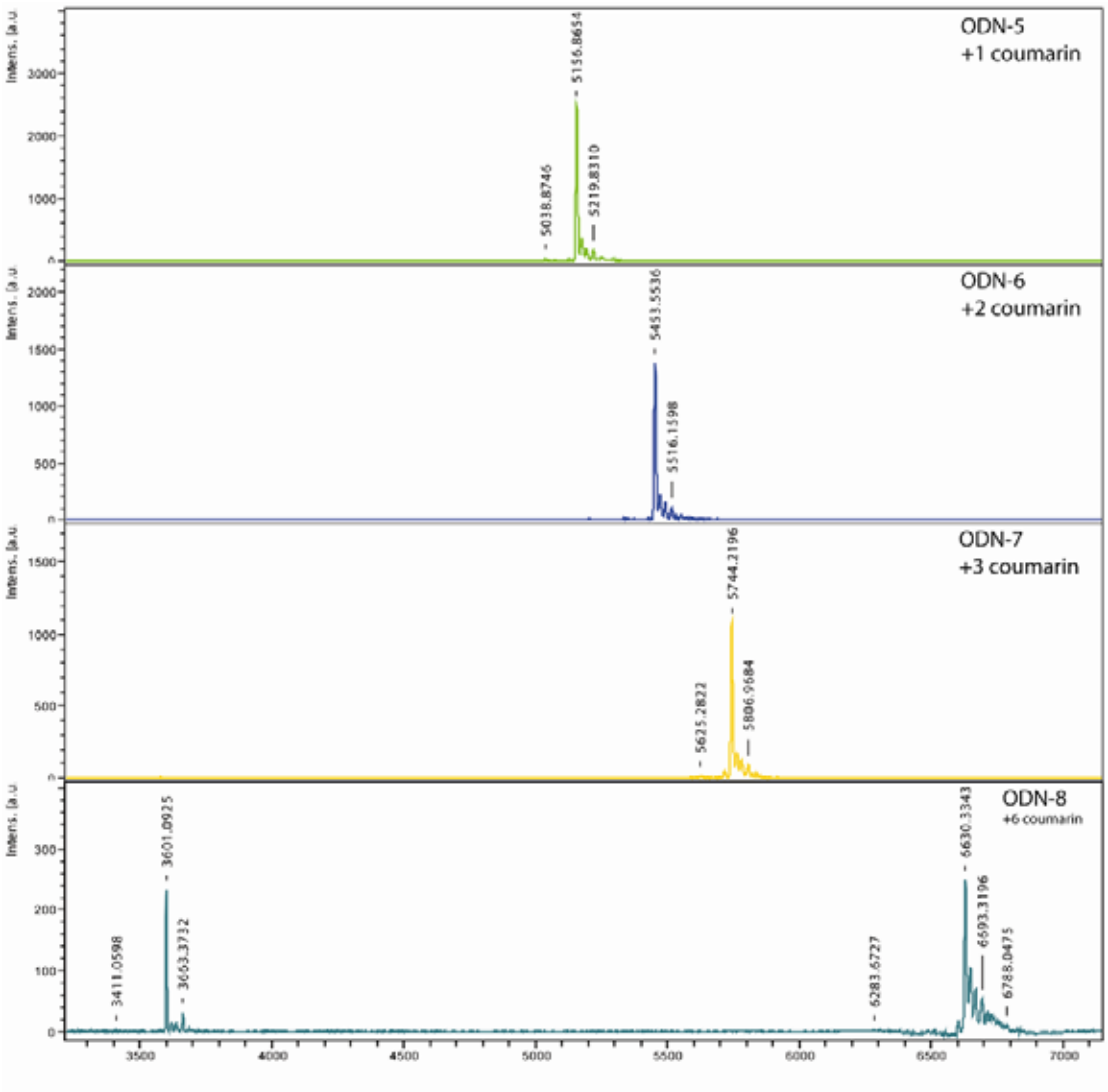

Figure 2.11 MALDI-TOF of series ODN-**2.5** to ODN-**2.8**.

2.6 Author´s Contribution

The author developed the synthesis of an alkyne-bearing cytidine nucleoside. Key step of this synthesis is a Sonogashira cross-coupling of mono-protected octadiyne on 5-iodo-cytidine. This reaction was applied to the synthesis of ***2.2****, thereby greatly facilitating the entire procedure which was shortened by two steps. After publication, it was found out that the use of protecting groups as well as the synthetic precautions (dry and degassed solvents) were not required, leading to an even shorter synthesis.* ***2.2*** *can now be synthesized in gram amounts within just over a week.*

2.7 References

[1] S. Brakmann, S. Lobermann, *Angew. Chem. Int. Ed.* **2001**, *40*, 1427-1429; S. Brakmann, S. Lobermann, *Angew. Chem. Int. Ed.* **2002**, *41*, 3215-3217.
[2] R. M. Twyman, *Curr. Top. Med. Chem.* **2004**, *4*, 1421-1429.
[3] N. L. Rosi, C. A. Mirkin, *Chem. Rev.* **2005**, *105*, 1547-1562.

[4] J. G. Hacia, L. C. Brody, M. S. Chee, S. P. A. Fodor, F. S. Collins, *Nat. Genet.* **1996**, *14*, 441-447.
[5] S. Jäger, M. Famulok, *Angew. Chem. Int. Ed.* **2004**, *43*, 3337-3340; S. Jäger, G. Rasched, H. Kornreich-Leshem, M. Engeser, O. Thum, M. Famulok, *J. Am. Chem. Soc.* **2005**, *127*, 15071-15082.
[6] J. A. Prescher, C. R. Bertozzi, *Nat. Chem. Biol.* **2005**, *1*, 13-21.
[7] Q. Wang, T. R. Chan, R. Hilgraf, V. V. Fokin, K. B. Sharpless, M. G. Finn, *J. Am. Chem. Soc.* **2003**, *125*, 3192-3193.
[8] G. A. Burley, J. Gierlich, M. R. Mofid, S. T. H. Nir, Y. Eichen, T. Carell, *J. Am. Chem. Soc.* **2006**, *128*, 1398-1399.
[9] H. C. Kolb, M. G. Finn, K. B. Sharpless, *Angew. Chem. Int. Ed.* **2001**, *40*, 2004-2021; V. V. Rostovtsev, L. G. Green, V. V. Fokin, K. B. Sharpless, *Angew. Chem. Int. Ed.* **2002**, *41*, 2596-2599.
[10] K. Sivakumar, F. Xie, B. M. Cash, S. Long, H. N. Barnhill, Q. Wang, *Org. Lett.* **2004**, *6*, 4603-4606.
[11] T. S. Seo, Z. Li, H. Ruparel, J. Ju, *J. Org. Chem.* **2003**, *68*, 609-612.
[12] K. E. Beatty, F. Xie, Q. Wang, D. A. Tirrell, *J. Am. Chem. Soc.* **2005**, *127*, 14150-14151; A. J. Link, M. K. S. Vink, D. A. Tirrell, *J. Am. Chem. Soc.* **2004**, *126*, 10598-10602; A. J. Link, D. A. Tirrell, *J. Am. Chem. Soc.* **2003**, *125*, 11164-11165.
[13] N. K. Devaraj, G. P. Miller, W. Ebina, B. Kakaradov, J. P. Collman, E. T. Kool, C. E. D. Chidsey, *J. Am. Chem. Soc.* **2005**, *127*, 8600-8601; R. L. Weller, S. R. Rajski, *Org. Lett.* **2005**, *7*, 2141-2144.
[14] C. J. Burrows, J. G. Muller, *Chem. Rev.* **1998**, *98*, 1109-1151.
[15] F. Moris-Varas, X.-H. Qian, C.-H. Wong, *J. Am. Chem. Soc.* **1996**, *118*, 7647-7652.
[16] M. Adamczyk, J. R. Fishpaugh, K. J. Heuser, *Bioconjugate Chem.* **1997**, *8*, 253-255.
[17] P. J. Barr, A. S. Jones, P. Serafinowski, R. T. Walker, *J. Chem. Soc., Perkin Trans. 1* **1978**, *10*, 1263-1267; D. Graham, J. A. Parkinson, T. Brown, *J. Chem. Soc., Perkin Trans. 1* **1998**, *6*, 1131-1138.
[18] B. M. Trost, M. T. Rudd, *Org. Lett.* **2003**, *5*, 4599 - 4602.
[19] T. R. Chan, R. Hilgraf, K. B. Sharpless, V. V. Fokin, *Org. Lett.* **2004**, *6*, 2853-2855.
[20] M. Ober, H. Müller, C. Pieck, J. Gierlich, T. Carell, *J. Am. Chem. Soc.* **2005**, *125*, 18143-18149.

3 DNA Photography: An Ultrasensitive DNA-Detection Method Based on Photographic Techniques

This Section was published in:

D. M. Hammond, A. Manetto, J. Gierlich, V. A. Azov, P. M. E. Gramlich, G. A. Burley, M. Maul and T. Carell, *Angew. Chem. Int. Ed.* **2007**, *46*, 4184-4187.

3.1 Introduction

The ability to manipulate and analyze the genetic information of all organisms along with the discovery that small RNA strands control critical cellular functions has given rise to the development of new, sophisticated methods for the ultrasensitive detection of DNA and RNA.[1] In the postgenomic era, it is believed that such techniques will revolutionize the diagnosis of genetically encoded diseases such as cancer. In fact, the development of more-personalized medicine is critically linked to the development of reliable ultrasensitive DNA detection methods in combination with novel methods that allow isolation of the gene of interest (analyte) from biological samples. The method reported herein provides a simple solution to the first part of the problem. Although the polymerase chain reaction (PCR) is predominantly used for DNA detection, new methods for the highly sensitive detection of DNA and RNA are constantly being developed. Most recently, for example, Mirkin and co-workers, Willner and co-workers, and Heeger and co-workers have reported the utilization of nanoparticles, aptamers, or novel electrochemical setups to detect DNA with sensitivity limits in the range of pico- and femtomoles.[1-3] Even sensitivities in the zeptomolar regime (≈ 10 copies in 30 μL) have been reported.[4] All these methods require sophisticated technology, which limits their widespread use. We report herein a simple and efficient method for DNA detection in the femto- to attomole (10^{-18} mol) range based on the amplification process provided by black and white photography (Figure 3.1).

In the black and white photographic process, a few photons captured by a light-sensitive AgBr-crystal-containing layer (film or photopaper) induce the formation of an Ag_n nucleus as a latent image center. In the subsequent development process, this Ag_n cluster (for $n > 3$) catalyzes the reduction of the entire AgBr crystal to Ag(0), which stains the photopaper black.[5] To date, the detection of analytes based on silver deposition has been performed with Ag and Au clusters followed by Ag deposition from solution and not through photopaper.[6] The solution process is limited to amplification factors of about 10^5. Herein, we report the application of the standard and inexpensive AgBr-crystal-based photographic process for the detection of labeled biomolecules. This process can provide, in principle, amplification factors of 10^{11},[5] which are similar to standard PCR reactions.

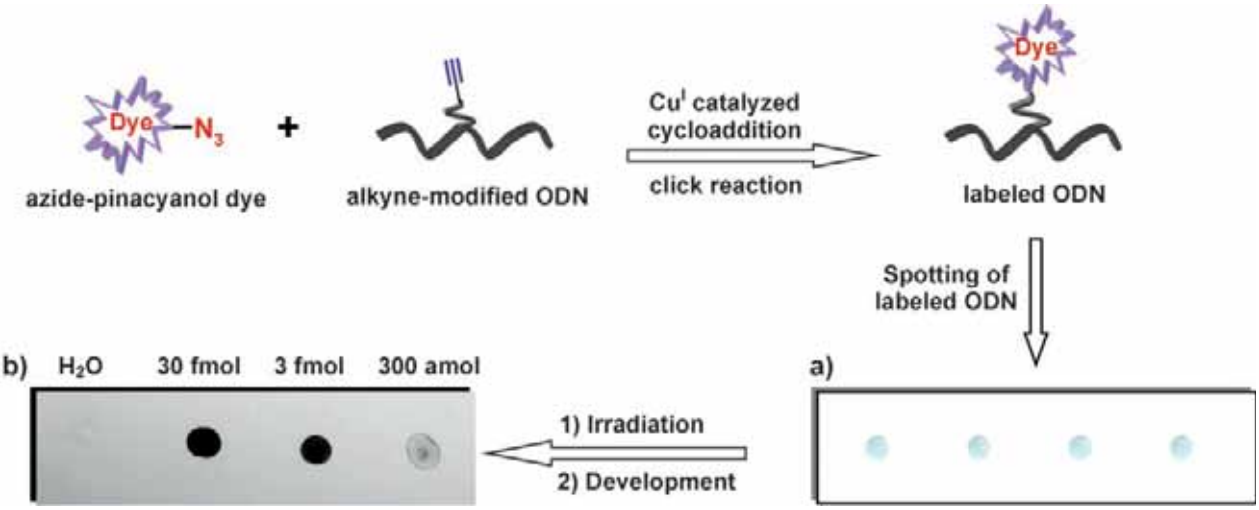

Figure 3.1 DNA detection using the methods of black and white photography. a) Commercial photopaper loaded with different concentrations of the labeled ODN (graphical representation). b) Photopaper after irradiation and development (scanner reproduction). Visual detection of the labeled ODN at three different concentrations; 1 µL spotted (× 4).

3.2 Results and Discussion

We recently reported the ability to modify oligonucleotides with the help of copper(I)-catalyzed azide/alkyne cycloaddition (click chemistry).[7, 8] To link DNA detection to the photographic process, we aimed to couple DNA to special dyes, so-called spectral photographic sensitizers. These dyes are used in the black and white photographic process to sensitize the AgBr emulsion present in the photopaper to light of wavelengths above 520 nm, where AgBr does not absorb light.

To investigate the sensitivity limits of the method, we initially explored one of the most widespread photosensitizers used in black and white photography, the pinacyanol dye, which is modified as azide **3.9**. This dye has the advantage that it strongly adsorbs to AgBr crystals providing an efficient energy/electron transfer to the AgBr crystals. The synthesis of the dye azide and the structure of the 2'-deoxycytidine alkyne **3.10**[9] and 2'-deoxyuridine alkyne **3.11**,[8] building blocks needed for the click reaction, are shown in Scheme 3.1.

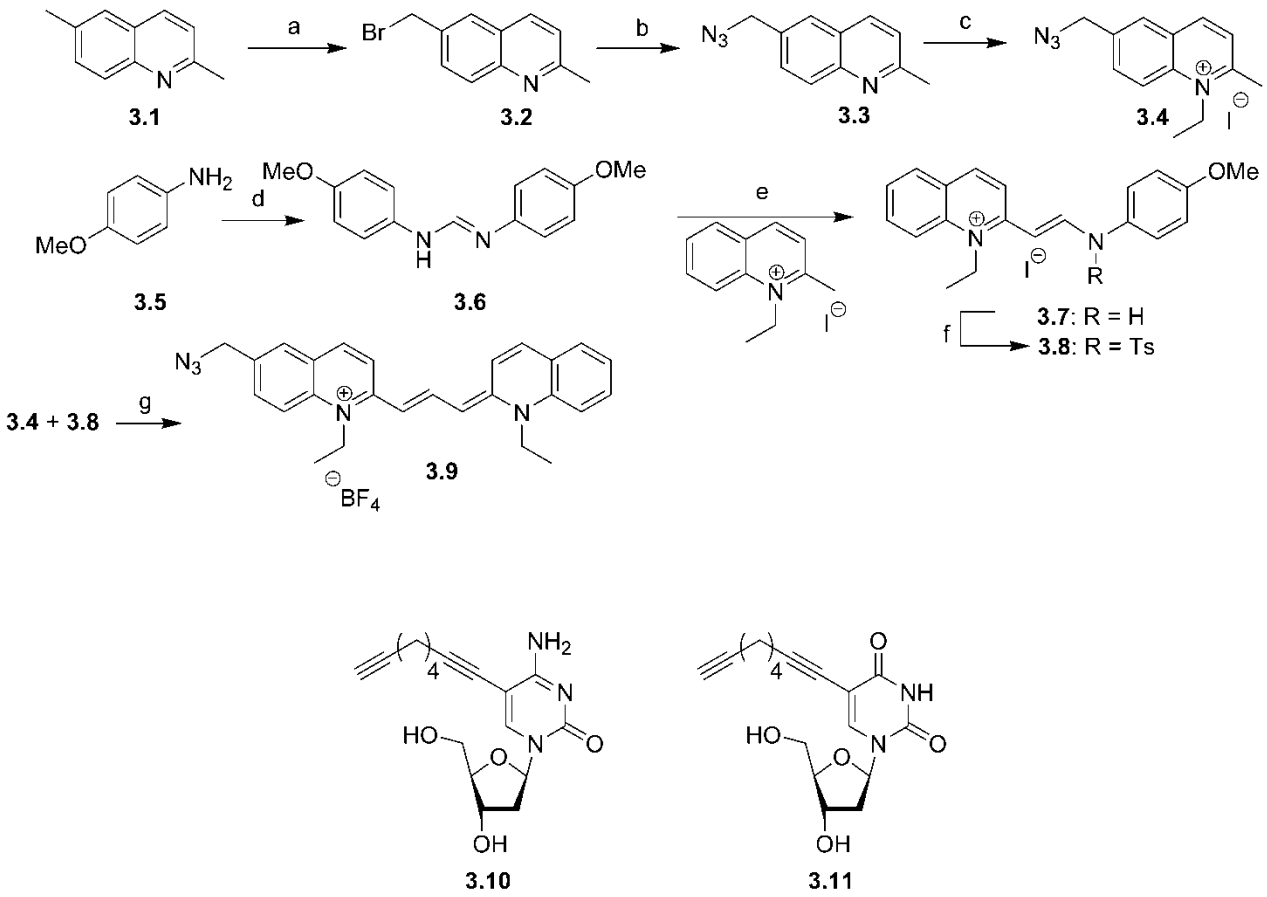

Scheme 3.1 a) NBS, benzoyl peroxide, CCl_4, reflux, 47%, b) NaN_3, DMF, 97%, c) EtI, MeCN, 70% (based on recovered starting material), d) triethyl *ortho*-formate, 140 °C, 55%, e) triethyl *ortho*-formate, BuOH, reflux, 91%, f) TsCl, DIPEA, CH_2Cl_2, 70%, g) 1) **3.4**, DIPEA, pyridine, 2) Dowex 1x8–200, NH_4BF_4, 47%. DIPEA = *N*,*N*-diisopropylethylamine, DMF = *N*,*N*-dimethylformamide, Ts = toluene-4-sulfonyl.

Commercially available 2,6-dimethylquinoline (**3.1**) was first brominated by using *N*-bromosuccinimide (NBS) to give the monobrominated compound **3.2**.[10] Nucleophilic displacement of bromide by using sodium azide afforded the azido derivative **3.3**, which was subsequently alkylated with ethyl iodide to give the quinolinium salt **3.4**. In a parallel synthesis, *p*-methoxyaniline was condensed with triethylformate, yielding amidine **3.6**. This was then reacted with 1-ethyl-2-methylquinolinium iodide to give the hemicyanine dye **3.7**, which was subsequently tosylated and coupled with intermediate **3.4** to give the target azido cyanine **3.9**. We next prepared three oligodeoxyribonucleotides (ODNs) containing various alkyne-modified nucleotides as shown in Table 3.1. We incorporated the 5-alkynyl-2'-dC **3.10** (dC = deoxycytidine)[9] into ODN-**3.1** and ODN-**3.2** and the 5-alkynyl-2'-dU **3.11** (dU = deoxyuridine)[8] in ODN-**3.3** through their corresponding phosphoramidites.

In the presence of a Cu(I) salt and a Cu(I)-stabilizing ligand,[11] the cycloaddition between azide **3.9** and the three alkyne-modified oligonucleotides proceeded quantitatively, as evidenced by MALDI-TOF analysis; this proves that the click reaction is amenable to both the cytidine- and uridine-containing ODNs. The oligonucleotides were subsequently precipitated from ethanol for purification. Owing to the high yield of the click reaction, this simple precipitation step was sufficient to fully separate the ODNs from any excess dye azide as proven by

the clean HPLC traces and MALDI-TOF spectra obtained from the precipitated ODN compounds.

Table 3.1 Alkyne-modified ODNs used to click **3.9** onto DNA.[a]

	ODN Sequences
ODN-**3.1**	5′-GCGCTTACXTGTCGCG-3′
ODN-**3.2**	5′- GCGCTTAXXTGTCGCG -3′
ODN-**3.3**	5′-TTA ATT GAA TTC GAT TYG GGC CGG AYT TGT TTC-3′

[a] X = 5-alkynyl-2'-dC, **3.10**; Y = 5-alkynyl-2'-dU, **3.11**.

To test our hypothesis of detecting dye-modified ODNs through a photographic process, we simply spotted 1 µL of a 10 µM solution of either ODN-**3.1**, -**3.2**, or -**3.3** onto commercially available photopaper, which is sensitive only to UV and blue light, under darkroom conditions. The used photopaper contained no red-light spectral sensitizer, which makes it insensitive to light with wavelengths above 520 nm. We then illuminated the photopaper for typically less than 30 s with light, $\lambda > 570$ nm, and subsequently developed the photopaper by using commercially available development reagents (see Section 3.4.7). All ODNs induced under these conditions led to deep black spots of 2-3 mm diameter on the photopaper. In contrast, control oligonucleotides, which contained no dye molecules, gave no spot at all (data not shown), showing that dye-modified ODNs can be selectively detected by using this method. For the control ODNs, only a faint spot was detected at very high concentrations of greater than 50 mM (50 nmol, see Section 3.4.8).

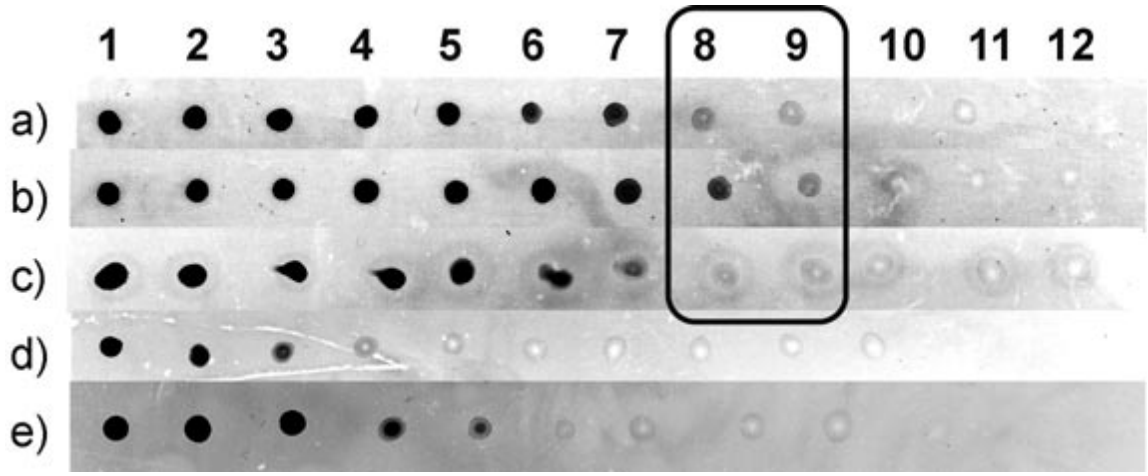

Figure 3.2 Photostrips with sensitizer-modified ODNs. a) ODN-**3.1**, b) ODN-**3.2**, c) ODN-**3.3**, d) Cy5-ODN, e) Cy3-ODN. Amounts of DNA in H_2O (1 µL was spotted): 1: 10 pmol, 2: 1 pmol, 3: 300 fmol, 4: 100 fmol, 5: 30 fmol, 6: 10 fmol, 7: 3 fmol, 8: 1 fmol, 9: 300 amol, 10: 100 amol, 11: 30 amol, 12: H_2O. The black box indicates the detection limit.

We next studied the sensitivity of the method, the results of which are shown in Figure 3.2a–c. When we spotted, irradiated, and then developed a dilution series of dye-modified DNA samples onto the photopaper, we could see that all ODNs with one (ODN-**3.1**) or two (ODN-**3.2** and ODN-**3.3**) pinacyanol dyes displayed a sensitivity of down to 300 attomoles. By using this

method, the detection is purely based on visual inspection of the developed photopaper. Hybridization of ODN-**3** to its counter strand revealed a higher detection limit of 30 femtomoles. To determine if a labeled ODN can be detected in a mixture with other DNA fragments, we used a primer labeled with two dye molecules and generated a 300-bp dsDNA fragment, which was than digested with restriction enzymes. This mixture too provided a positive black spot (see Section 3.4.8). The whole photographic procedure, including spotting of the DNA onto the paper, irradiation, development, and visual inspection, typically took less than 20 min. The photopaper can of course be loaded with multiple samples to create an inexpensive, time-saving, and easy-to-use photographic assay array.

With the direct detection of 300 attomoles, this method is in a sensitivity range that rivals most other non-PCR-based methods whilst having the advantage that no equipment other than a standard photographic darkroom setup is needed. Because the sensitivity limit of 300 attomoles was reached with standard photopaper, we can envision that a special paper tuned for diagnostic purposes will be able to further improve the sensitivity.

To investigate if the method is applicable for the detection of ODNs containing other fluorophores that are currently in use for DNA labeling, we also spotted Cy5- and Cy3-modified DNA onto the photopaper (Figure 3.2d,e). As expected, these ODNs were also detected but the sensitivity was strongly reduced (100 fmol), proving that the dyes developed for photographic purposes provide a significant advantage. The result, however, that typical dye-labeled ODNs can be detected allowed us to set up an initial experiment to clarify if the method would be suitable for the detection of health-threatening pathogens. We set the goal of detecting a short DNA sequence encoding a small part of the 16S rRNA gene (rRNA = ribosomal RNA) from the bacterium *Yersinia pestis*.[12] The commercially available DNA hairpin (molecular beacon, **MB**)[13] with a 5'-Cy3 fluorophore and a BHQ2 fluorescence quencher at the 3'-end was purchased to see whether the fluorescence on–off property of the MB could be exploited for detection based on the photographic process. The loop region was designed to be complementary to the DNA sequence of the rRNA gene with the underlined sequence forming the stem region of the **MB** (5'-Cy3-CGCTGCCCCTTGAGGCGTGGCTGCAGCG-BHQ2-3'; Figure 3.3). In the absence of the specific *Y. pestis* gene (5'-AGCCACGCCTCAAGGG-3'), the **MB** is in the closed state in which the fluorescence is quenched owing to the close proximity to the BHQ2 quencher.[14] Spotting of the non-fluorescing **MB** at a high concentration (1 μL of a 1μM solution) onto the photopaper followed by irradiation and development gave only a faint spot as expected (Figure 3.3b, spot 3), showing that BHQ-2 can inhibit sensitization of the photographic emulsion by the Cy3 dye. The faint staining is the result of residual fluorescence of the quenched molecular beacon, showing again the impressive sensitivity of the method. If we add a mixture of various DNA strands to this hairpin solution, among them the *Y. pestis* DNA sequence, the **MB** opens up, thereby separating the fluorophore from the quencher and enabling it to sensitize the AgBr crystals in the photopaper. Indeed, when we spotted this mixture (1 μL of a 1 μM solution) onto the photopaper, irradiated, and developed the strip, a thick black spot was clearly visible (Figure 3.3b, spot 4).

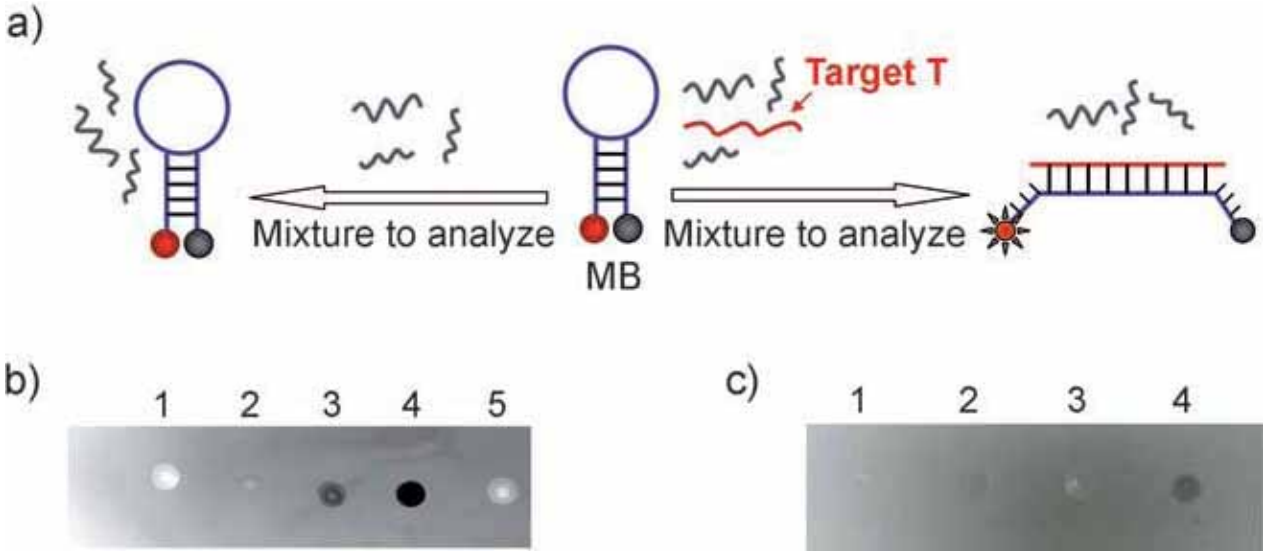

Figure 3.3 a) The MB concept used to detect the *Y. pestis* gene. The beacon opens up in the presence of the target, which increases the fluorescence and hence the ability of the beacon to sensitize the photopaper. Scanner reproductions of two photographic experiments with the positive black spots in b4 and c4. A volume of 1 μL of target-DNA solution in buffer solution was spotted. b) Spots 1 and 5: buffer solution (5 mM Tris-HCl pH 8, 5 mM KCl, 0.5 mM $MgCl_2$, Tris = tris(hydroxymethyl)aminomethane), spot 2: 10 μM **T**, spot 3: 1 μM **MB**, spot 4: 1 μM **MB** and 10 μM **T**. c) Spot 1: buffer solution (5 mM Tris-HCl pH 8, 0.5 mM $MgCl_2$), spot 2: 0.1 μM **MB**, spot 3: 0.6 μM **T**, and spot 4: 0.1 μM **MB** and 0.6 μM (600 fmol) **T**.

We finally investigated the detection limit of this commercially available Cy3-labeled **MB**. As shown in Figure 3.3c, we could detect the presence of the *Y. pestis* gene with the naked eye down to 600 fmol (spot 4) even if we added additional genomic DNA to the solution (see Section 3.4.10).

3.3 Summary and Outlook

In summary, we have identified a novel yet simple technique for the detection of DNA to a detection limit of 300 attomoles by merely spotting sample solutions onto nonsensitized photopaper, irradiating for a few seconds, and developing the image in a standard photographic developing solution. We applied this method for the direct detection of 600 femtomoles of a selected target, which was associated with the disease of plague, by using hybridization probes (MBs). Detection is performed purely by visual inspection without the need for expensive fluorescence detectors or scintillation counters. Optimization of the photopaper, investigation of other photographic dyes, and the development of methods that allow the efficient isolation of the to-be-detected DNA from biological samples are problems that now need to be tackled.

3.4 Experimental Section

3.4.1 Synthesis of Azide-Modified Cyanine Dye **3.9**

Compounds **3.2**,[10] **3.6**[15] and **3.7**[16] were prepared according to established literature procedures. All spectroscopic data were in accordance with the literature.

6-(Azidomethyl)-2-methylquinoline (**3.3**)

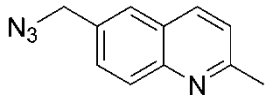

3.2 (1.95 g, 8.21 mmol) and NaN_3 (2.13 g, 32.8 mmol) were dissolved in DMF (40 mL) and stirred in the absence of light over night. The reaction was evaporated to dryness and purified by column chromatography, eluting with 5% EtOAc in DCM. The product was isolated as a yellow syrup (1.59 g, 97%).
^{1}H-NMR (400 MHz, $CDCl_3$): δ = 2.75 (s, 3H, CH_3), 4.52 (s, 2H, CH_2N_3), 7.30 (d, 1H, *J* = 8.4 Hz, C_3H), 7.62 (dd, 1H, *J* = 8.8, 2.0 Hz, C_7H), 7.71 (d, 1H, *J* = 1.8 Hz, C_5H), 8.01 (d, 1H, *J* = 8.6 Hz, C_4H), 8.05 (d, 1H, *J* = 8.2 Hz, C_8H). ^{13}C-NMR (100 MHz, $CDCl_3$): δ = 25.3, 54.6, 122.5, 126.3, 126.6, 129.3, 129.4, 132.8, 136.1, 147.5, 159.5. IR (KBr disc, cm^{-1}): ν(N_3) 2100 *s*. HRMS (EI) calcd. for $C_{11}H_{10}N_4^+$: 198.2280, found 198.0898 [M^+].

6-(Azidomethyl)-1-ethyl-2-methylquinolinium iodide (**3.4**)[17]

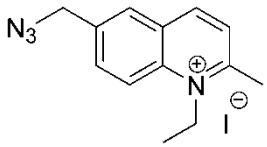

3.3 (1.32 g, 6.66 mmol) was dissolved in dry MeCN (40 mL), ethyl iodide (6.7 mL, 83.2 mmol) added and the reaction was heated to reflux for 28 h. After reduction of the reaction volume by rotary evaporation under vacuum, Et_2O (120 mL) was added dropwise, yielding the product as a yellow precipitate which was filtered off and dried (1.07 g, 70% based on recovered starting material).
^{1}H-NMR (400 MHz, d_6-DMSO): δ = 1.51 (t, 3H, *J* = 7.4 Hz, CH_2CH_3) 3.10 (s, 3H, CH_3), 4.84 (s, 2H, CH_2N_3), 4.97 (q, 2H, *J* = 7.2 Hz, CH_2CH_3), 8.10 (d, 1H, *J* = 8.8 Hz, C_3H), 8.17 (dd, 1H, *J* =9.2, 2.0 Hz, C_7H), 8.36 (d, 1H, *J* = 1.8 Hz, C_5H), 8.63 (d, 1H, *J* = 9.2 Hz, C_4H), 9.08 (d, 1H, *J* = 8.4 Hz, C_8H ^{13}C-NMR (100 MHz, d_6-DMSO): δ = 13.9, 22.7, 47.8, 52.8, 119.9, 126.5, 128.7, 129.4, 135.5, 137.6, 138.1, 145.9, 161.0. IR (KBr disc, cm^{-1}): ν(N_3) 2101 *s*; Anal. calcd for $C_{13}H_{15}IN_4$: C: 44.08%; H: 4.27%; N: 15.82%. Found: C: 44.16%; H: 4.15%; N: 15.74%. MS (MALDI-TOF): calcd. for $C_{13}H_{15}N_4$: 354.1899, found 354.0815 [M^+].

1-Ethyl-2-{(*E*)-2-[(4-methoxyphenyl)(*p*-toluenesulfonyl)amino]vinyl}quinolinium iodide (**3.8**)[18]

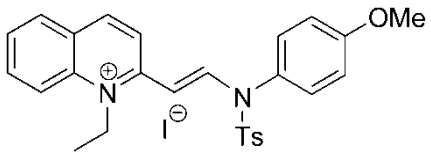

3.7 (0.43 g, 1 mmol) and *p*-toluenesulfonyl chloride (0.20 g, 1.04 mmol) were dissolved in DCM, DIPEA (0.17 mL, 1.04 mmol) was added and the reaction stirred over night. The solvent was removed *in vacuo* and the residue purified by column chromatography, eluting with a gradient of MeOH in $CHCl_3$ (2-10 %). The product was isolated as a green solid (430 mg, 70%).

R_f (DCM/EtOAc 20:1): 0.56. ^{1}H-NMR (400 MHz, CD_3OD): $\delta = 1.66$ (t, 3H, J = 7.2 Hz, CH_2CH_3), 2.35 (s, 3H, Tol-CH_3), 3.69 (s, 3H, OCH_3), 5.18 (q, 2H, J = 7.2 Hz, CH_2CH_3), 6.73 (d, 2H, J = 8.8 Hz, CH), 6.94 (d, 2H, J = 8.8 Hz), 7.24 (d, 2H, J = 8 Hz, CH), 7.52 (d, 2H, J = 8.4 Hz, CH), 7.98 (t, 1H, J = 8 Hz, CH), 8.05 (d, 1H, J = 8.8 Hz, CH), 8.23 (dt, 1H, J = 1.6, 7.2 Hz, CH), 8.34 (dd, 1H, J = 1.2, 8.4 Hz, CH), 8.56 (d, 1H, J = 9.2 Hz), 8.98 (1H, d, J = 8.4 Hz). ^{13}C-NMR (600 MHz, CD_3OD): δ = 13.4, 20.2, 54.6, 54.6, 103.4, 103.4, 104.9, 113.9, 118.9, 124.5, 125.7, 127.1, 129.2, 129.2, 129.5, 130.1, 130.8, 135.6, 136.7, 143.5, 145.5, 157.8. MS (ESI): calcd. for $C_{27}H_{27}N_2O_3S^+$: 459.1737, found 459.1718 [M^+].

6-Azidomethyl-1-ethyl-2-[(1*E*,3*E*)-3-(1-ethylquinolin-2(1*H*)-ylidene)prop-1-en-1-yl]quinolinium iodide (6-Azidomethyl-1,1'-diethylpinacyanol iodide) (**3.9**)

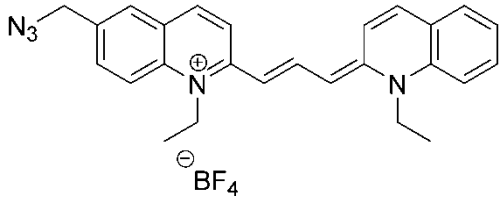

3.8 (0.16 g, 0.28 mmol) and **3.3** (88 mg, 0.25 mmol) were dissolved in pyridine (2 mL) and DIPEA (0.2 mL) added. The solution quickly turned dark blue and a precipitate formed. The reaction was heated to 100 °C for 30 min, cooled to r. t. and evaporated to dryness. The residue was dissolved in $CHCl_3$/MeOH (1:2, 20 mL) and treated with excess KI. Excess $CHCl_3$ was then added to precipitate unreacted KI. The mixture was filtered and the filtrate evaporated to dryness. Purification by silica gel chromatography, eluting with a gradient of MeOH in $CHCl_3$ (10-15%) isolated the product (impure) as a dark red solid. Trituration with diethyl ether (10 mL) afforded pure product (62 mg, 47%). The product was converted to the BF_4^- using Dowex 1x8-200 resin, pre-treated with NH_4BF_4.

R_f ($CHCl_3$/MeOH 9:1): 0.53. ^{1}H-NMR (400 MHz, d_6-DMSO): $\delta = 1.42$ (t, 6H, J = 7.2 Hz, CH_2CH_3), 4.45 (q, 4H, J = 7.2 Hz, CH_2CH_3), 4.58 (s, 2H, CH_2N_3), 6.57 (app t, 2H, J = 8 Hz),

7.46 (t, 2H, *J* = 7.6 Hz), 7.70-7.78 (m, 2H), 7.83 (dd, 1H, *J* = 2.0, 12.4 Hz), 7.86-7.91 (m, 2H), 7.99 (d, 1H, *J* = 9.6 Hz), 8.00 (d, 1H, *J* = 9.6 Hz), 8.29 (d, 1H, *J* = 5.6 Hz), 8.32 (d, 1H, *J* = 5.2 Hz), 8.70 (t, 1H, *J* = 12.4 Hz). ^{13}C-NMR (100 MHz, d_6-DMSO): δ = 12.8, 12.9, 43.3, 43.4, 53.1, 105.7, 106.2, 116.5, 120.4, 121.0, 125.0, 125.2, 125.4, 128.8, 129.6, 132.7, 132.8, 132.9, 135.5, 136.2, 138.7, 138.9, 147.9, 152.1, 152.5. IR (KBr disc, cm^{-1}): ν(N_3) 2093*s*. MS (MALDI-TOF): calcd. for $C_{26}H_{26}N_5$: 408.5264, found 408.0282 [M^+].

3.4.2 Click Procedure for Short DNA Oligos

To 100 µL of a 0.23 mM DNA solution (23 nmol) in water were added 230 µL of a dye azide solution (0.5 mM, 1150 nmol) and 10 µL of a freshly prepared solution containing CuBr and Cu(I) stabilizing ligand[11] in a 1:1 ratio in 4:3:1 H_2O : DMSO : ^{t}BuOH (0.05 N, 250 nmol). The mixture was vortexed and shaken at 37 °C for 2 d. The solvent was removed by SpeedVac and the residue dissolved in 100 µL of a 0.3 M NaOAc solution. 900 µL of EtOH (95%) were added and the tube inverted three times before being cooled to -80 °C for 1 h. The resulting suspension was centrifuged at 13.4 x10^3 rpm for 4 min and re-cooled to -80 °C for 1 h. Following a second centrifugation (13.4 x10^3 rpm for 4 min), the supernatant was decanted off and the residue washed with 500 µL portions of ethanol until the washes remained colourless. The residue was taken up in 100 µL H_2O and analyzed by MALDI-TOF and analytical reversed phase HPLC.

HPLC analysis
A gradient of 0-50% 0.1 M $HNEt_3^+OAc^-$ in H_2O → 0.1 M $HNEt_3^+OAc^-$ in 20:80 H_2O: MeCN over 45 min at a flow rate of 0.5 mL/min was used on a Nucleosil 120-3 C18 column. ODN-**3.1** shows a retention time of 24.1 min, and the corresponding single-click product appears at 27.8 min. ODN-**3.2** shows a retention time of 27.4 min, with the corresponding double-click product appearing at 32.9 min. ODN-**3.3** shows a retention time of 26.3 min, whilst the product with 2 dyes clicked on shows a retention time of 34 min. 3D analysis of these product peaks shows UV spectra with maxima at 257, 557 and 616 nm, the latter two corresponding to the dye absorbances.

The following ODNs were purchased from Metabion:
5'-Cy5-GCG CTG TTC ATT CGC G-Cy5-3'
5'-Cy3-GCG CTG TTC ATT CGC G-3'
and used without further purification in the photography experiments.

3.4.3 MALDI-TOF Spectra of Click Reactions on ODN **3.1-3.3**

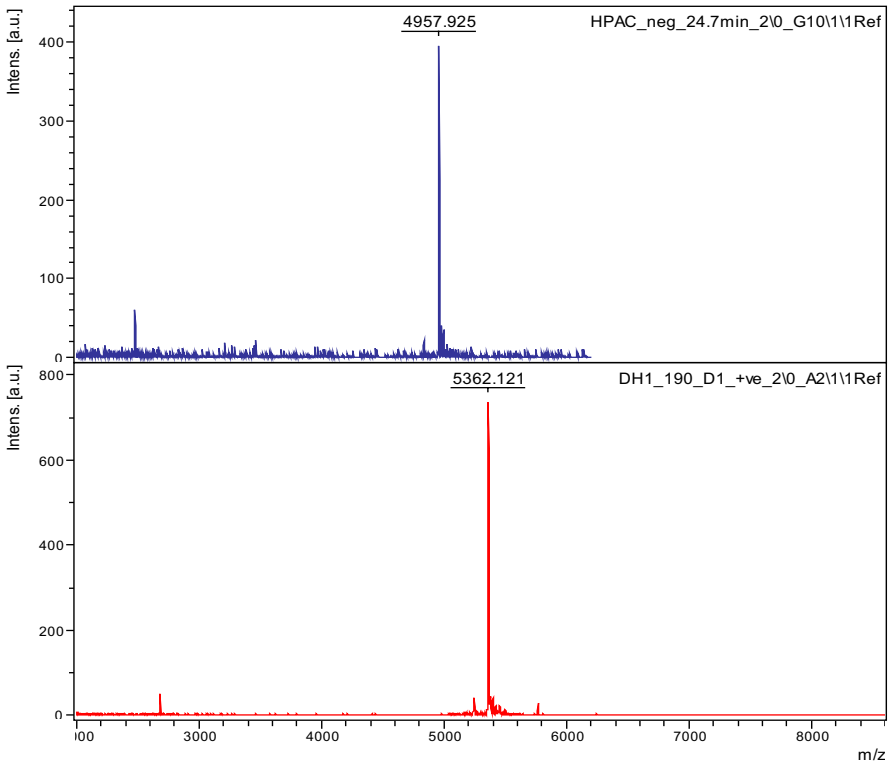

Figure 3.4 ODN-**3.1**.

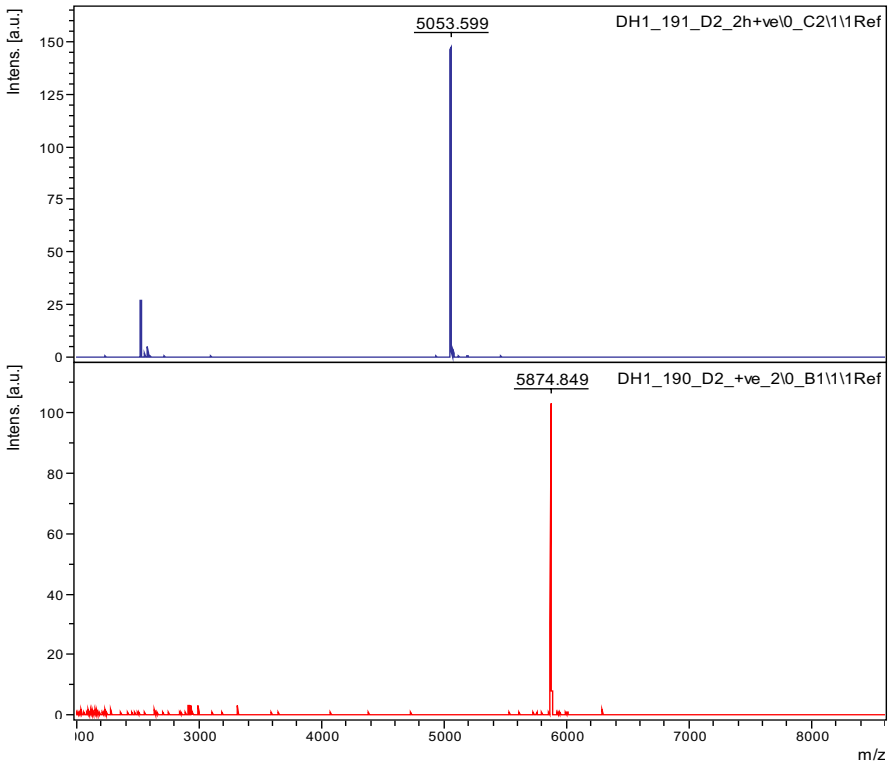

Figure 3.5 ODN-**3.2**.

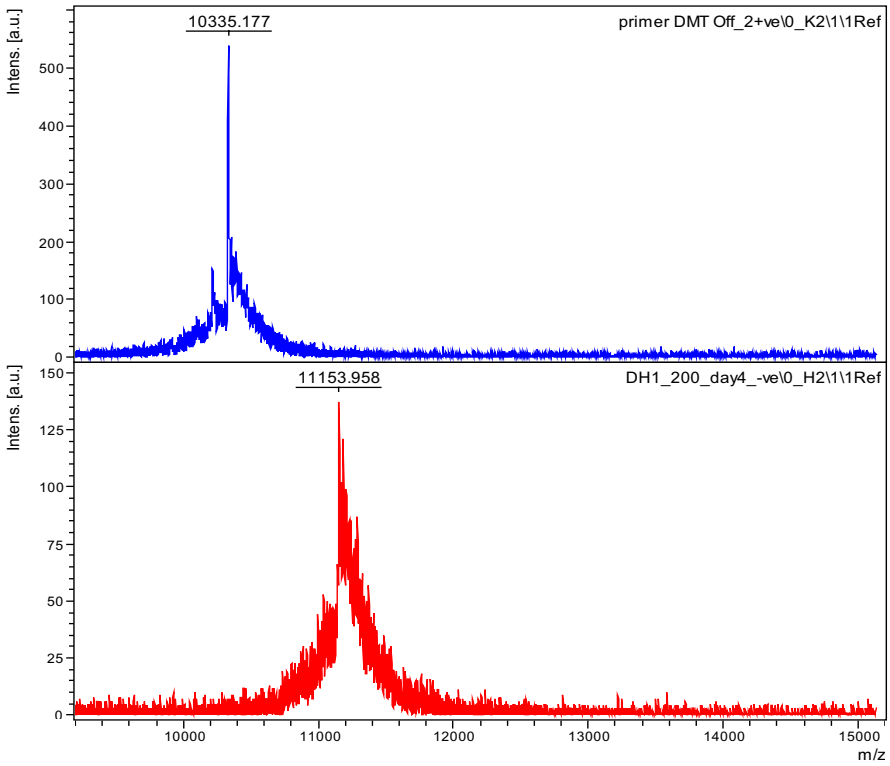

Figure 3.6 ODN-**3.3**.

3.4.4 PCR Conditions

The sequence of the longer ODN-**3.3** was chosen as it is also the sequence of the 5'-primer for a 300 bp fragment from the polymerase η gene from Rad30 *S. cervisiae*. (in vector pExp007-pol η).[19, 20] Using ODN-**3.3** with two cyanine dyes clicked on as a primer, PCR amplification of this gene yielded full-length products. However, when this 300 bp DNA was tested on the photopaper, no DNA could be detected, even at amounts of 1 pmol, which was clearly visible in the ODN series. This is consistent with the results obtained for the duplex DNA earlier. We then identified a restriction site within this gene for the enzyme Rsa I (5'-GTAC-3') which would result in a 60 bp fragment containing the two cyanine dyes.[21] To this end, a concentration series of this sensitizer-labeled 300mer was made up in NEBuffer 2,[3] the restriction reaction carried out on each concentration and the crude solution spotted onto photopaper following enzyme inactivation. Although the sensitivity was poor (1 pmol limit), we assume that this is due to the high salt concentration of 50 mM NaCl in the restriction reaction buffer, and the fact that a 60 bp fragment is probably not mobile enough to diffuse through the photopaper supercoat.

For PCR amplification the forward primer (ODN-**3.3**) 5'-TTA ATT GAA TTC GAT TYG GGC CGG AYT TGT TTC-3', where Y denotes a dye-modified dU, and the reverse primer 5'-TTT TAT GCT ATC TCT GAT ACC CTT G-3' were used. They amplify a 294 bp fragment from the polymerase η gene from Rad30 *S. cervisiae*. in vector pExp007-poḷ η.[20]

PCR conditions: The PCR was run with 0.18 mM of each dNTP, 0.09 µM of each primer, 200 ng of template and 1.25 U Taq Polymerase (Promega) in the reaction buffer provided by the supplier (50 mM KCl, 10 mM Tris-HCl (pH 9.0), 0.1% Triton® X-100, 1.5 mM $MgCl_2$). Total volume was 44 µL.

Temperature program: 96 °C for 90 s, then 29 cycles of 94 °C for 10 s, 58 °C (-0.3 °C each cycle) for 15 s, 72 °C for 60 s; then 24 cycles of 95 °C for 10 s, 55 °C for 15 s, 72 °C for 60 s.

The PCR product was purified using QIAquick PCR Purification Kit (QIAGEN) and the concentration determined by UV absorption.

3.4.5 Restriction Reaction of Dye-Labeled 300mer

10 µL of each concentration from the dilution series of dye-labeled PCR DNA in NEBuffer 2 were transferred to PCR tubes, and 0.1 µL of Rsa I (New England Biolabs) was added to each. The tubes were incubated at 37 °C for 60 min, before the temperature was increased to 65 °C for 20 min to inactivate the protein. The reaction was then cooled down to 20 °C over 60 min. 1 µL aliquots from each concentration were then spotted onto photopaper and treated as described below.

3.4.6 Preparation of DNA Dilution Series for Photography Experiments

For ODN-**3.1** and ODN-**3.2**, the following concentrations were made up using distilled H_2O: 10, 1 µM, 300, 100, 30, 10, 3, 1 nM, 300, 100, 30 pM.
ODN-**3.3** was annealed to the counter-strand as follows: 50 µL ODN-**3.3** (39 µM in H_2O) was mixed with 22.5 µL of the counter-strand (109 µM in H_2O) and evaporated to dryness by SpeedVac. 98 µL of solvent (H_2O or buffer listed below) was added. The solution was heated to 95 °C for 5 min and then cooled down to 20 °C over 60 min.
For ODN-**3.3** and ODN-**3.3** annealed to the counter-strand, the same concentrations as above were made up using the following solvent systems:

1. distilled H_2O
2. 10 mM NaCl
3. 50 mM NaCl
4. 10 mM Tris-HCl, 10mM NaCl
5. 10 mM Tris-HCl, 50mM NaCl

For long DNA, the end-labeled 300 bp PCR product was dissolved in H_2O or NEBuffer 2 from New England Biolabs (10 mM Tris-HCl, 50 mM NaCl, 10 mM $MgCl_2$, 1 mM DTT, pH 7.9 at 25 °C) in the following concentrations: 1 μM, 300, 100, 30, 10, 3, 1 nM, 300, 100 pM.

3.4.7 General Procedure for Photography Experiments

The following steps were all carried out under darkroom conditions: 1 μL aliquots of each concentration from the same dilution series (or with MB-experiment solutions) were spotted onto black and white photographic paper (Ilfospeed RC Deluxe, Ilford) along with 1 μL of a solution reference. During the spotting procedure the contact between the micropipette tips and the photopaper must be avoided. A custom made tips guide was used in order to avoid this contact and to ease the spotting of up to 96 different samples in a few minutes, when needed. The strips of photopaper spotted with the dilution series or with MBs solutions were then placed in a cupboard and kept in darkness for 20 min or until all of the solution had been absorbed into the emulsion. Alternatively, the strips were placed on a warm surface (< 40 °C) in the dark for 1-3 min for a faster absorption process. One strip was then taken and placed into a filter cassette containing a 570 nm cut-off filter and a 0.5 OD density filter. This was then exposed to a white light source (24 V, 250 W) for 5, 15, 20 or 25 s. The photopaper was then developed, stopped and fixed in standard solutions (Phenisol Developer, 2% AcOH in H_2O and Hypam Fixer from Ilford) according to the manufacturer's instructions (1 min in total), washed with running water for 3-5 min and then finally dried (5-10 min). The last two steps do not need dark conditions.

3.4.8 Photography Test Strips

1. ODN-**3.1** (16mer, 1 dye clicked on) in H_2O: 300 amol limit (Spot 9)

2. ODN-**3.2** (16mer, 2 dyes) in H_2O: 300 amol limit (Spot 9)

3. ODN-**3.3** (33mer, 2 dyes) in H_2O: 3 fmol (Spot 7)

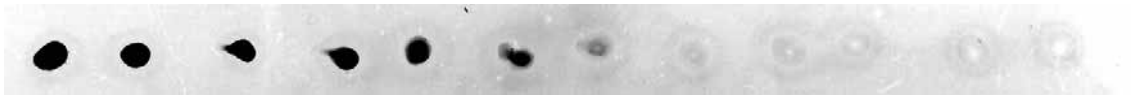

4. ODN-**3.3** in 10 mM NaCl: 100 fmol (Spot 4)

5. ODN-**3.3** in 50 mM NaCl: 100 fmol (Spot 4)

6. ODN-**3.3** in 10 mM Tris, 10 mM NaCl, pH 7.4: 300 fmol (Spot 3)

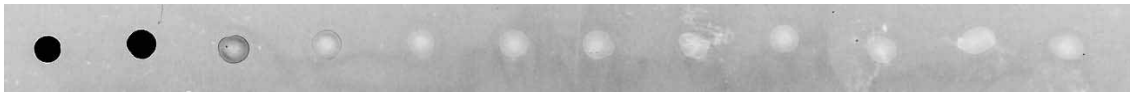

7. ODN-**3.3** in 10 mM Tris, 50 mM NaCl, pH 7.4: 1 pmol (Spot 2)

8. ODN-**3.3** duplex in H_2O: 30 fmol (Spot 5)

9. ODN-**3.3** duplex in 10 mM NaCl: 100 fmol (Spot 4)

10. ODN-**3.3** duplex in 50 mM NaCl: 1 pmol (Spot 2)

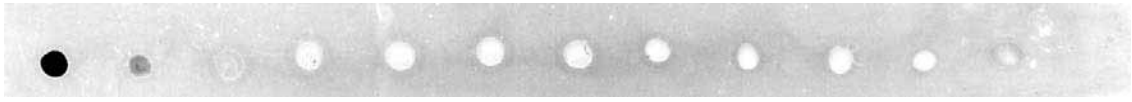

11. ODN-**3.3** duplex in 10 mM Tris, 10 mM NaCl, pH 7.4: 3 fmol (Spot 3)

12. ODN-**3.3** duplex in 10 mM Tris, 50 mM NaCl, pH 7.4: 1 pmol (Spot 2)

13. 5'-Cy5-GCG CTG TTC ATT CGC G-Cy5-3' in H_2O: 300 fmol (Spot 3)

14. 5'-Cy3-GCG CTG TTC ATT CGC G-3' in H_2O: 30 fmol (Spot 5)

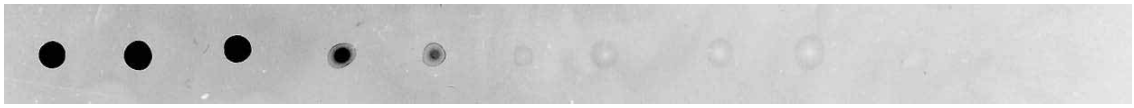

15. 300bp dsDNA (2 dyes on primer) in H_2O: no detection

16. 300bp dsDNA (2 dyes on primer) after restriction reaction with RsaI (gives 60bp fragment) in NEBuffer 2: 1 pmol (Spot 1)

17. Control reaction using natural DNA oligos in H_2O: 50nmol
    A: 5'-GCG ATT CGT TCG C-3'
    B: 5'-CGC GAA TGA ACA GCG C-3'
    C: 5'-GCG ACC GAT TCG C-3'

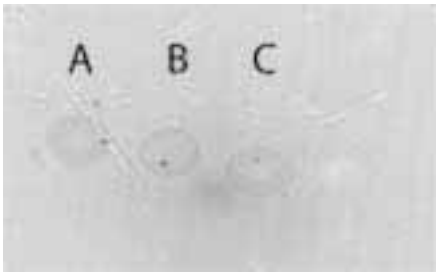

3.4.9 Detection of *Y. Pestis* Target Using MBs and DNA Photography

Materials and Fluorescence measurements

MB (5'-Cy3-CGCTGCCCCTTGAGGCGTGGCTGCAGCG-BHQ2-3') and the target **T** (*Y. pestis* gene, 5'-AGCCACGCCTCAAGGG-3') were purchased from Metabion. Fluorescence measurements of the solutions were performed prior to photographic analysis as control. Fluorescence kinetics and thermal denaturation curves were measured using a JASCO FP 750 spectrometer and fluorescence quartz cuvettes. Two different aqueous solutions were used as buffers: 5 mM Tris-HCl pH 8, 5 mM KCl and 0.5 mM $MgCl_2$ for high concentration assays (i.e. for **MB** 1 μM) and 5 mM Tris-HCl pH 8, 0.5 mM $MgCl_2$ for low concentration assays (i.e. for **MB** 0.2 μM).

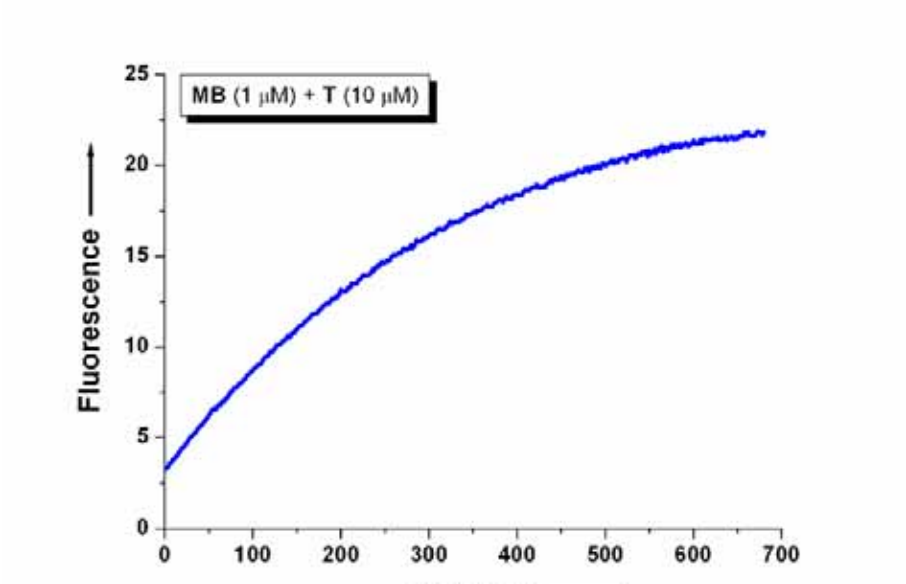

Figure 3.7 Representative fluorescence kinetics measurements (λ_{ex} = 545 nm, λ_{em} = 570 nm) for **MB** 1 μM in 5 mM Tris-HCl pH 8, 5 mM KCl and 0.5 mM $MgCl_2$ a few seconds after the addition of 10 μM of **T**.

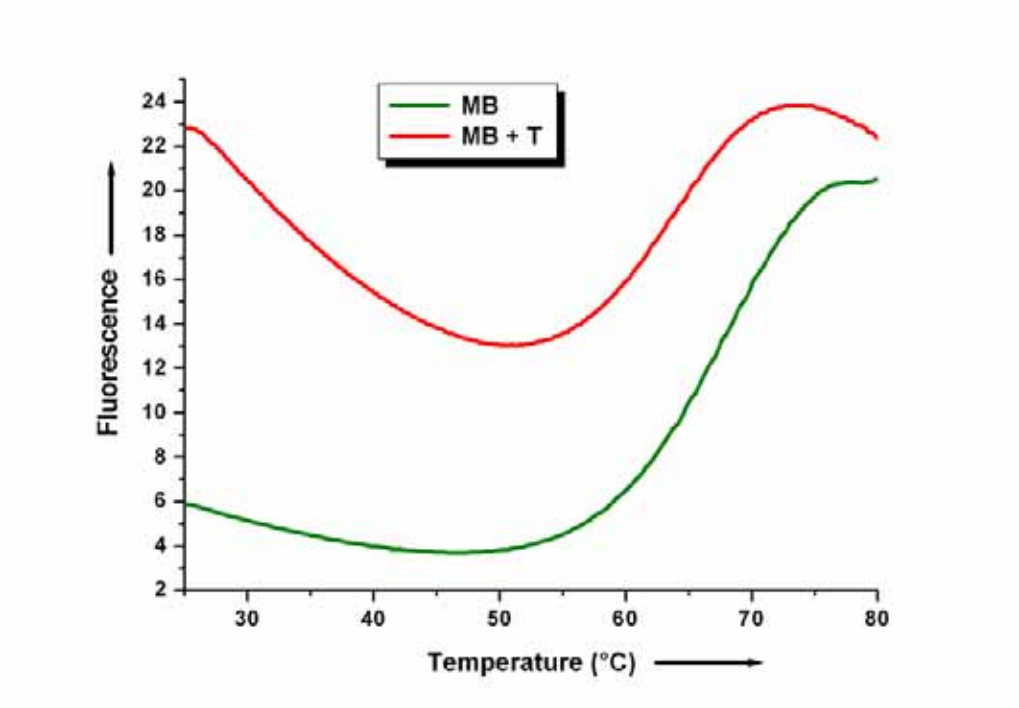

Figure 3.8 Representative fluorescence thermal denaturation measurements (λ_{ex} = 545 nm, λ_{em} = 570 nm). Denaturation curves for **MB** 1 μM in 5 mM Tris-HCl pH 8, 5 mM KCl and 0.5 mM $MgCl_2$ before (in green) and after (in red) the addition of 10 μM of **T**.

Photographic measurements

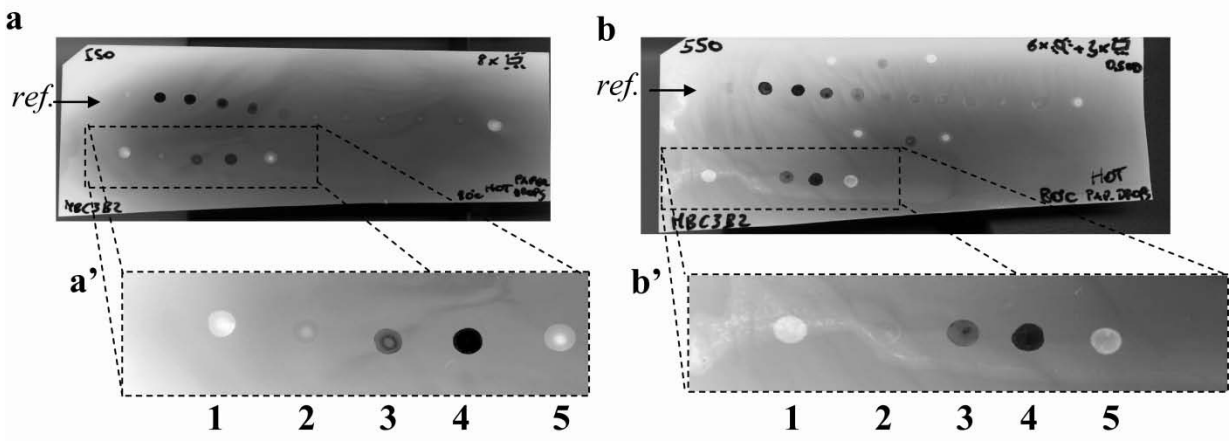

Figure 3.9 Scanner reproduction of two typical MB photo-experiments. In **a** and **b** in the lane *ref.* a Cy3-labeled ODN is spotted in a dilution series from 10 μM to 100 fM. In **a'** and in **b'** the enlargements relative to the MB experiments are reported. Spots (for both **a'** and **b'**) 1 and 5 = buffer (5 mM Tris-HCl pH 8, 5 mM KCl and 0.5 mM $MgCl_2$), spot 2 = 10 μM **T** in buffer, spot 3 = 1 μM **MB** in buffer, spot 4 = **MB** 1 μM plus **T** 10 μM (1:10) in buffer.

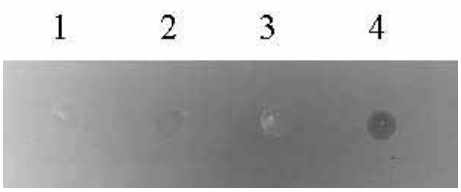

Figure 3.10 Direct detection of 600 fmol of the *Y. pestis* gene (Target **T**). 1 μL of the solutions was spotted. Spot 1 = buffer (5 mM tris-HCl pH 8 and 0.5 mM $MgCl_2$), spot 2 = 0.1 μM **MB** in buffer, spot 3 = 0.6 μM target **T** in buffer, spot 4 = 0.1 μM **MB** plus 0.6 μM **T** (600 fmol of target) in buffer.

3.4.10 Detection of *Y. pestis* Target in Presence of a Complex Mixture

The clear detection of 600 fmol of *Y. Pestis* gene (Target **T**) was achieved in a complex mixture by adding genomic DNA (**gDNA**) to the buffer solution (5 mM Tris-HCl pH 8 and 0.5 mM $MgCl_2$) containing 0.2 μM **MB** and 0.6 μM **T**. The genomic DNA was previously fragmented by sonication. The majority of the resulting fragments ranged from less than 0.5 kb up to 2 kb (more details in "cell line and cell culture" section). The concentration of **gDNA** in the following experiments ranges between 9 and 30 ng/μL. For higher concentrations of **gDNA** false positive signals are detected (Fig. X.16). For a comparison, the concentration of 0.6 μM **T** corresponds to 3 ng/μL of **T** in solution.

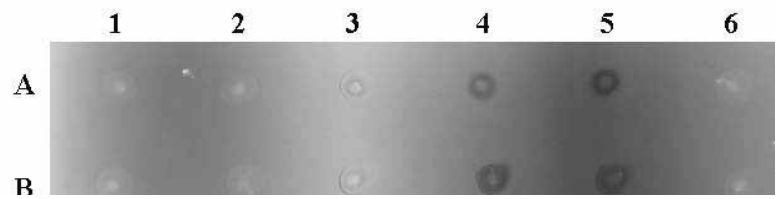

Figure 3.11 Lane **A**: Photopaper loaded with 1 μL of 1) buffer (5 mM Tris-HCl pH 8 and 0.5 mM $MgCl_2$), 2) **T** 0.6 μM in buffer, 3) **MB** 0.2 μM in buffer, 4) and 5) two different batches of **MB** 0.2 μM plus **T** 0.6 μM in buffer, 6) as in spot 1. Lane **B**: The photopaper was loaded with 1 μL of 1) buffer (5 mM Tris-HCl pH 8 and 0.5 mM $MgCl_2$) plus 9 ng/μL of **gDNA**, 2) **T** 0.6 μM plus 9 ng/μL of **gDNA** in buffer, 3) **MB** 0.2 μM plus 9 ng/μL of **gDNA** in buffer, 4) and 5) two different batches of **MB** 0.2 μM plus **T** 0.6 μM plus 9 ng/μL of **gDNA** in buffer, 6) as in spot 1. Irradiation wavelength > 570 nm (cut-off filter), standard development.

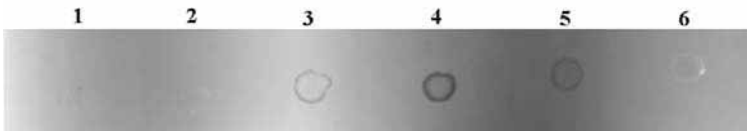

Figure 3.12 Photopaper loaded with 1 μL of 1) buffer (5 mM Tris-HCl pH 8 and 0.5 mM $MgCl_2$) plus 30 ng/μL of **gDNA**, 2) **T** 0.6 μM plus 30 ng/μL of **gDNA** in buffer, 3) **MB** 0.2 μM plus 30 ng/μL of **gDNA** in buffer, 4) and 5) two different batches of **MB** 0.2 μM plus **T** 0.6 μM plus 30 ng/μL of **gDNA** in buffer, 6) as in spot 1. Irradiation wavelength > 570 nm (cut-off filter), standard development.

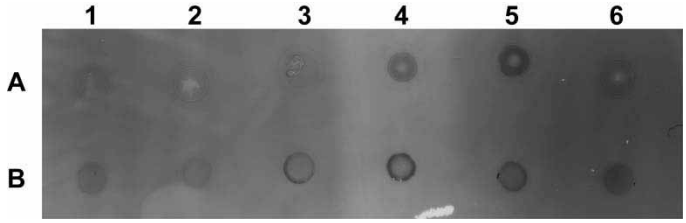

Figure 3.13 Photopaper loaded with 1 μL of (for both lane A and B): 1) buffer (5 mM Tris-HCl pH 8 and 0.5 mM $MgCl_2$) plus **gDNA**, 2) **T** 0.6 μM plus **gDNA** in buffer, 3) **MB** 0.2 μM plus **gDNA** in buffer, 4) and 5) two different batches of **MB** 0.2 μM plus **T** 0.6 μM plus **gDNA** in buffer; 6) as in spot 1. In lane A [**gDNA**] = 50 ng/μL, in lane B [**gDNA**] = 80 ng/μL. Irradiation wavelength > 570 nm (cut-off filter), standard development.

3.4.11 Cell Line and Cell Culture

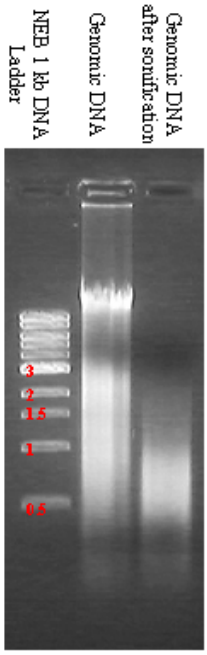

Figure 3.14 1% agarose gel before (lane 2) and after (lane 3) sonication. Stained with ethidium bromide, total amount of genomic DNA per lane: 2.5 µg.

A human colon carcinoma cell line, HCT116, obtained from DSMZ (DSMZ no. ACC 581), was routinely grown in DMEM medium supplemented with 10% fetal bovine serum and antibiotics. Once the cells reached confluence, they were harvested and subjected to genomic DNA isolation. Extraction was carried out using the E.Z.N.A.® Tissue DNA Mini Kit (Peqlab Biotechnologie GmbH). DNA fractions were pooled in a 15 mL Falcon™ Tube and concentrated to approx. 1 µg/µL in a SpeedVac. The genomic DNA was fragmented by sonication. The majority of the resulting fragments ranged from less than 0.5 kb up to 2 kb.

3.5 Author´s Contribution

*Cytidine phosphoramidite **3.10** and ODN-**3.1**-**3.2** were synthesized by the author. IR-absorbing merocyanine dyes were investigated by the author for sensitization of the photographic films, but were found to produce smears on the photopaper and therefore this endeavor was not continued.*

3.6 References

[1] N. L. Rosi, C. A. Mirkin, *Chem. Rev.* **2005**, *105*, 1547-1562.

[2] H. A. Ho, K. Dore, M. Boissinot, M. G. Bergeron, R. M. Tanguay, D. Boudreau, M. Leclerc, *J. Am. Chem. Soc.* **2005**, *127*, 12673 – 12676; J. A. Hansen, R. Mukhopadhyay, J. O. Hansen, K. V. Gothelf, *J. Am. Chem. Soc.* **2006**, *128*, 3860-3861; Y. C. Cao, R. Jin, C. S. Thaxton, C. A. Mirkin, *Talanta* **2005**, *67*, 449-455; Y. Xiao, A. L. Lubin, B. R. Baker, K. W. Plaxco, A. J. Heeger, *Proc. Nat. Acad. Sci. USA* **2006**, *103*, 16677-

16680; T. Niazov, V. Pavlov, Y. Xiao, R. Gill, I.Willner, *Nano Lett.* **2004**, *4*, 1683-1687.

[3] R. Elghanian, J. J. Storhoff, R. C. Mucic, R. L. Letsinger, C. A. Mirkin, *Science* **1997**, *277*, 1078-1081.

[4] J. M. Nam, S. I. Stoeva, C. A. Mirkin, *J. Am. Chem. Soc.* **2004**, *126*, 5932-5933.

[5] T. Tani, *Photographic Sensitivity, Theory and Mechanisms*, OUP, Oxford, **1995**; T. Tani, *Phys. Today* **1989**, 36-41.

[6] T. A. Taton, C. A. Mirkin, R. L. Letsinger, *Science* **2000**, *289*, 1757-1760.

[7] V. V. Rostovtsev, L. G. Green, V. V. Fokin, K. B. Sharpless, *Angew. Chem. Int. Ed.* **2002**, *41*, 2596-2599; H. C. Kolb, M. G. Finn, K. B. Sharpless, *Angew. Chem. Int. Ed.* **2001**, *40*, 2004-2021; C. W. Tornoe, C. Christensen, M. Meldal, *J. Org. Chem.* **2002**, *67*, 3057-3064; G. A. Burley, J. Gierlich, M. R. Mofid, S. T. H. Nir, Y. Eichen, T. Carell, *J. Am. Chem. Soc.* **2006**, *128*, 1398-1399.

[8] J. Gierlich, G. A. Burley, P. M. E. Gramlich, D. M. Hammond, T. Carell, *Org. Lett.* **2006**, *8*, 3639-3642.

[9] M. Fischler, U. Simon, H. Nir, Y. Eichen, G. A. Burley, J. Gierlich, P. M. E. Gramlich, T. Carell, *Small* **2007**, *3*, 1049-1055.

[10] P. Warner, A. J. Barker, A. L. Jackman, K. D. Burrows, N. Roberts, J. A. M. Bishop, B. M. O'Connor, L. R. Hughes, *J. Med. Chem.* **1992**, *35*, 2761 - 2768.

[11] T. R. Chan, R. Hilgraf, K. B. Sharpless, V. V. Fokin, *Org. Lett.* **2004**, *6*, 2853-2855.

[12] G. L. Campbell, D. T. Dennis, in *Harrison´s Principles of Internal Medicine*, 14th ed., McGraw Hill, New York, **1998**, pp. 975-983.

[13] S. Tyagi, F. R. Kramer, *Nat. Biotechnol.* **1996**, *14*, 303-308.

[14] S. A. E. Marras, F. R. Kramer, S. Tyagi, *Nucl. Acids Res.* **200**, *30*, 122e.

[15] A. v. Dormael, J. Jaeken, J. Nys, *Bull. Soc. Chim. Belg.* **1949**, *58*, 477-486.

[16] L. G. S. Brooker, A. L. Sklar, H. W. J. Cressman, G. H. Keyes, L. A. Smith, R. H. Sprague, E. V. Lare, G. V. Zandt, F. L. White, W. W. Williams, *J. Am. Chem. Soc.* **1945**, *67*, 1875 - 1889.

[17] A. C. Pardal, S. S. Ramos, P. F. Santos, L. V. Reis, P. Almeida, *Molecules* **2002**, *7*, 320-330.

[18] Z.-H. Peng, H. J. Geise, X.-F. Zhou, B.-X. Peng, R. Carleer, R. Dommisse, *Liebigs Ann. Chem.* **1997**, 27-33.

[19] R. E. Johnson, S. Prakash, L. Prakash, *Science* **1999**, *283*, 1001-1004.

[20] M. Ober, H. Müller, C. Pieck, J. Gierlich, T. Carell, *J. Am. Chem. Soc.* **2005**, *125*, 18143-18149.

[21] M. Meselson, R. Yuan, J. Heywood, *Annu. Rev. Biochem.* **1972**, *41*, 447-466.

4 Formation of Bimetallic Ag–Au Nanowires by Metallization of Artificial DNA Duplexes

This Section was published in:

M. Fischler, U. Simon, H. Nir, Y. Eichen, G. A. Burley, J. Gierlich, P. M. E. Gramlich, and T. Carell, *Small* **2007**, *3*, 1049-1055.

4.1 Abstract

Uniform bimetallic nanowires, tunable in size, have been grown on artificial DNA templates via a two-step metallization process. Alkyne-modified cytosines were incorporated into 900-base-pair polymerase chain reaction fragments. The alkyne modifications serve as addressable metal-binding sites after conversion to a sugar triazole derivative via click chemistry. Reaction of the Tollens reagent with these sugar-coated DNA duplexes generates Ag(0) metallization centers around the sugar modification sites of the DNA. After a subsequent enhancement step using gold, nanowires ≤ 10 nm in diameter with a homogeneous surface profile were obtained. Furthermore, the advantage of this two-step procedure lies in the high selectivity of the process, due to the exact spatial control of modified DNA base incorporation and hence the confinement of metallization centers at addressable sites. Besides experiments on a membrane as a proof for the selectivity of the method, atomic force microscopy (AFM) studies of the wires produced on Si–SiO_2 surfaces are discussed. Furthermore, we demonstrate time-dependent metallization experiments, monitored by AFM.

4.2 Introduction

The continuous miniaturization of electronic circuitry has reached a level where new, interdisciplinary concepts are required in order to overcome size barriers and costs associated with conventional top-down fabrication processes, such as lithography. DNA, a highly programmable, stable, and readily available template, has become a promising tool in the bottom-up fabrication of such nanoscale electronic building blocks.[1] Due to its molecular recognition properties, modularity, and high flexibility, a variety of complicated geometries can be constructed with this biomolecule.[2] Furthermore, through these aforementioned properties, DNA offers ideal prerequisites for patterned metallization. Pioneering work on DNA metallization was presented in 1998 by Braun et al. who synthesized the first DNA- templated nanowires.[3] This DNA-based wire construct involved initial exchange of the native charge-compensation cations for Ag ions, followed by a metal deposition process and further silver enhancement. These seminal works have been advanced by Keren et al. who in 2004 published the first self-assembling field-effect transistor based on a metallized DNA template.[4] Various other syntheses of metallized DNA strands have been reported,[5] that is, by photoreduction of electrostatically bound Ag ions and chemical reduction of electrostatically bound Pt, Pd, or Cu ions.[6] Another strategy uses the affinity of Pt(II) complexes towards DNA strands and subsequent electroless plating to generate Pt nanowires.[7] All these approaches are based on utilizing the electrostatic and/or the coordinative binding sites of natural DNA. However, these

methods suffer from several drawbacks. Firstly, they are not selective, that is, metal deposition cannot be directed efficiently to a specific DNA strand of interest. Secondly, these methods result in uncontrollable metal deposition, in which the resulting nanowires are often inhomogeneously metallized or the diameter of the wires cannot be accurately controlled. A more selective approach, which overcomes these drawbacks through the enzymatic incorporation of artificial DNA bases, has recently been reported by our groups. The artificial bases are outfitted with reporter groups that act as addressable sites for metal deposition and subsequent addressable nanowire construction.[8]

Herein, we present a method for the selective metallization of artificial DNA duplexes to yield highly uniform and size-tunable nanowires via a two-step metallization process.[4, 9] The artificial DNA strands incorporate a modified cytosine derivative which carries an alkyne group that is an addressable site for further modification. These alkyne functions can be post-synthetically functionalized using an appropriate azide tag via the copper(I)-catalyzed Huisgen 1,3-cycloaddition "click" reaction.[10] We have shown that this reaction proceeds in high yield along DNA strands outfitted with terminal alkyne functions.[8] The rate of metallization can potentially be modulated by clicking on sugar azides of varying sugar densities. The general clicking and metallization procedure is depicted in Figure 4.1.

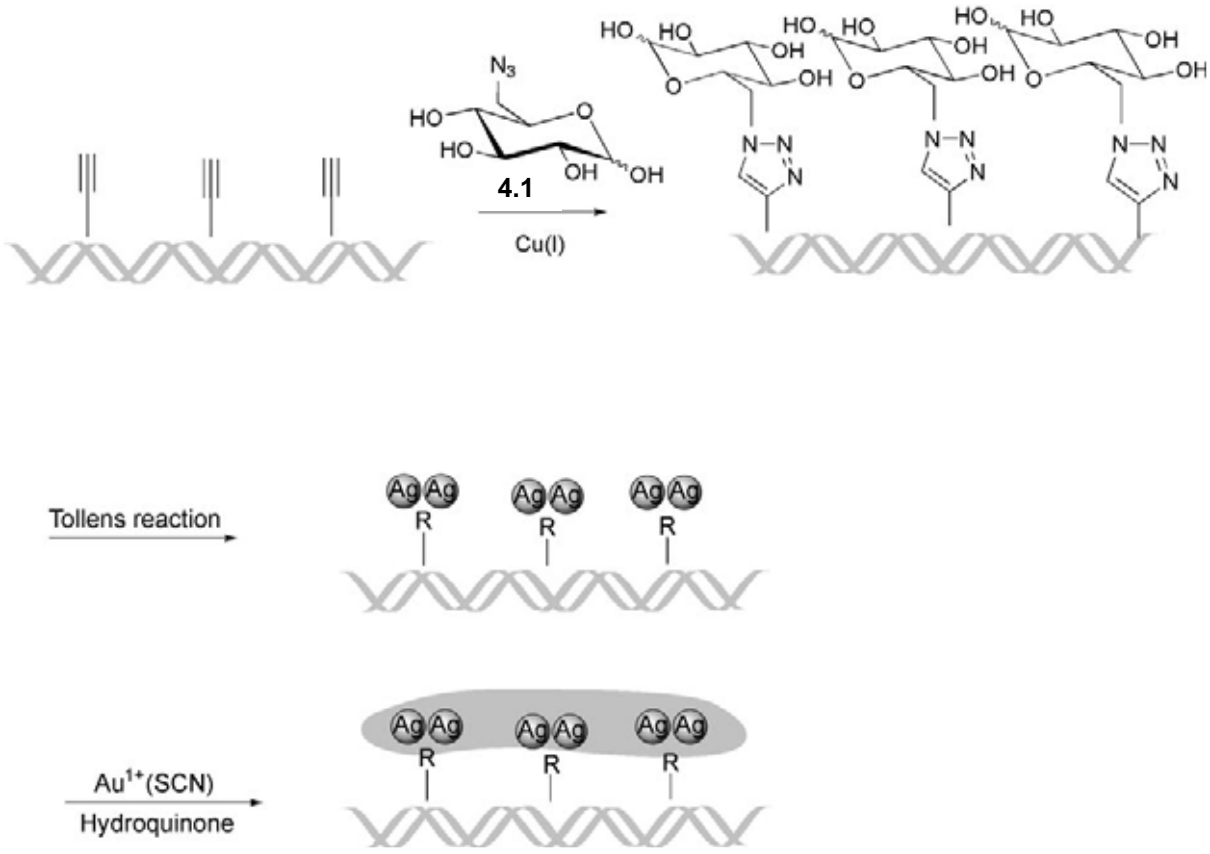

Figure 4.1 General scheme for the metallization procedure.

4.3 Results and Discussion

4.3.1 Synthesis, Sugar-Coating, and Purification of Modified DNA

Recently, we have reported the preparation and incorporation of alkyne-modified uridine nucleosides into DNA strands by both enzymatic and chemical methods.[8] The most accessible site for alkyne modification was found to be the 5-position located on the pyrimidine ring. To extend the possibilities of alkyne incorporation, we surmised that a 5-modified cytosine triphosphate would also be incorporated into DNA strands enzymatically. To assess this hypothesis, we prepared the 2'-deoxycytidine triphosphate (**4.6**), as shown in Scheme 4.1. The alkyne-modified nucleoside (**4.4**) was prepared via Sonogashira coupling of 5-iodo-2'-deoxycytidine (**4.2**) with the monosilylated 1,7-octadiyne (**4.3**), followed by removal of the trimethylsilyl (TMS) group with KOH. Acetyl protection of the 3'-hydroxyl group yielded nucleoside **4.5**, followed by triphosphate formation to yield the desired triphosphate **4.6**.

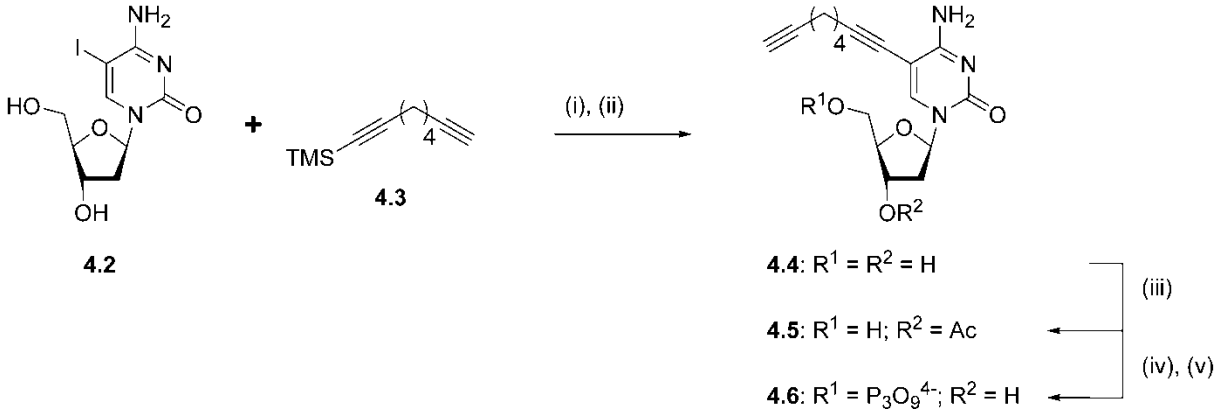

Scheme 4.1 Reagents and conditions: (i) $Pd(PPh_3)_4$, CuI, DMF, 86%; (ii) KOH/THF, 68%; (iii) lipase, vinyl acetate, THF/DMF (1:1), 69%; (iv) 2-chloro-4*H*-1,2,3-dioxaphosphorin-4-one, bis(tri-*N*-butylammonium) pyrophosphate, I_2; (v) NH_3. TMS = trimethylsilyl.

Incorporation of the modified cytidine building block derived from triphosphate **4.6** was effected by polymerase chain reaction (PCR) amplification of a DNA template derived from the Polη gene.[11] Conversion of the alkyne reporter groups into sugar triazole products using the sugar azide **X.1** was achieved via click chemistry. This procedure is simple and facile. An excess of sugar azide was added to the modified DNA solution, followed by an equimolar addition of a CuI–ligand complex.[12] The reaction mixture was then shaken gently for 2 h and purified by conventional ethanol precipitation methods.

4.3.2. Full Metallization of a Sugar-Modified 934-Base-Pair PCR Fragment

As an expedient proof of concept of the selectivity of the metallization of sugar-modified DNA strands, we conducted membrane-blotting experiments using a variety of DNA strands (see Figure 4.2). The membrane was spotted with λ-DNA (I), alkyne-tagged 934-base-pair (934-bp) PCR fragment (II), and sugar-modified alkyne-tagged 934-bp PCR fragment (III) at

the same concentration, and then the membrane was incubated with Tollens solution (see Section 4.5.4) and afterwards rinsed thoroughly with water. No color change was observed for any of the spots at this stage, which indicates that silver deposition ceases after reaction with the sugar molecules. After subsequent gold enhancement, however, spot III turned black whereas the λ-DNA and alkyne-tagged 934-bp PCR fragment did not show any sign of gold deposition. The membrane after silver treatment and gold enhancement is depicted in Figure 4.2.

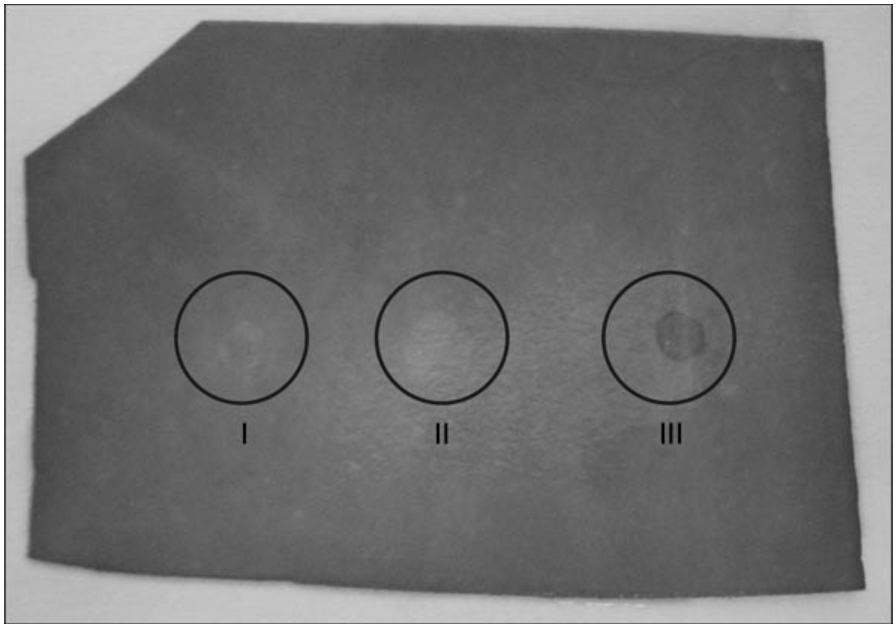

Figure 4.2 Membrane after Tollens reaction and subsequent gold enhancement. Spot I corresponds to λ-DNA, spot II corresponds to alkyne-tagged 900-mer before sugar modification, and spot III corresponds to sugar-coated alkyne-tagged 900-mer (all spots contain approximately the same DNA concentration).

Motivated by these results we conducted metallization experiments of modified DNA strands on surfaces and visualized these constructs using atomic force microscopy (AFM). The DNA was immobilized on mica and Si–SiO_2 surfaces with Mg^{2+} ions. Figure 4.3 depicts the height and phase images of the alkyne-tagged 934-bp PCR fragment on mica before sugar modification (Figure 4.3a–c) and after the sugar-coating process (Figure 4.3d–f). Both the alkyne-tagged and sugar-modified DNA strands show a length of approximately 300 nm, which coincides with the length of a 934-bp DNA fragment. The alkyne-modified duplexes show a height of 1–3 nm under the applied tapping-mode conditions both before and after the click reaction with sugar azide **4.1**. Furthermore, the sugar-coated DNA shows a significantly higher phase shift (approximately 208) than the unmodified duplexes (phase shift value approximately 108), which indicates a change of surface condition that takes place after the sugar-coating process.

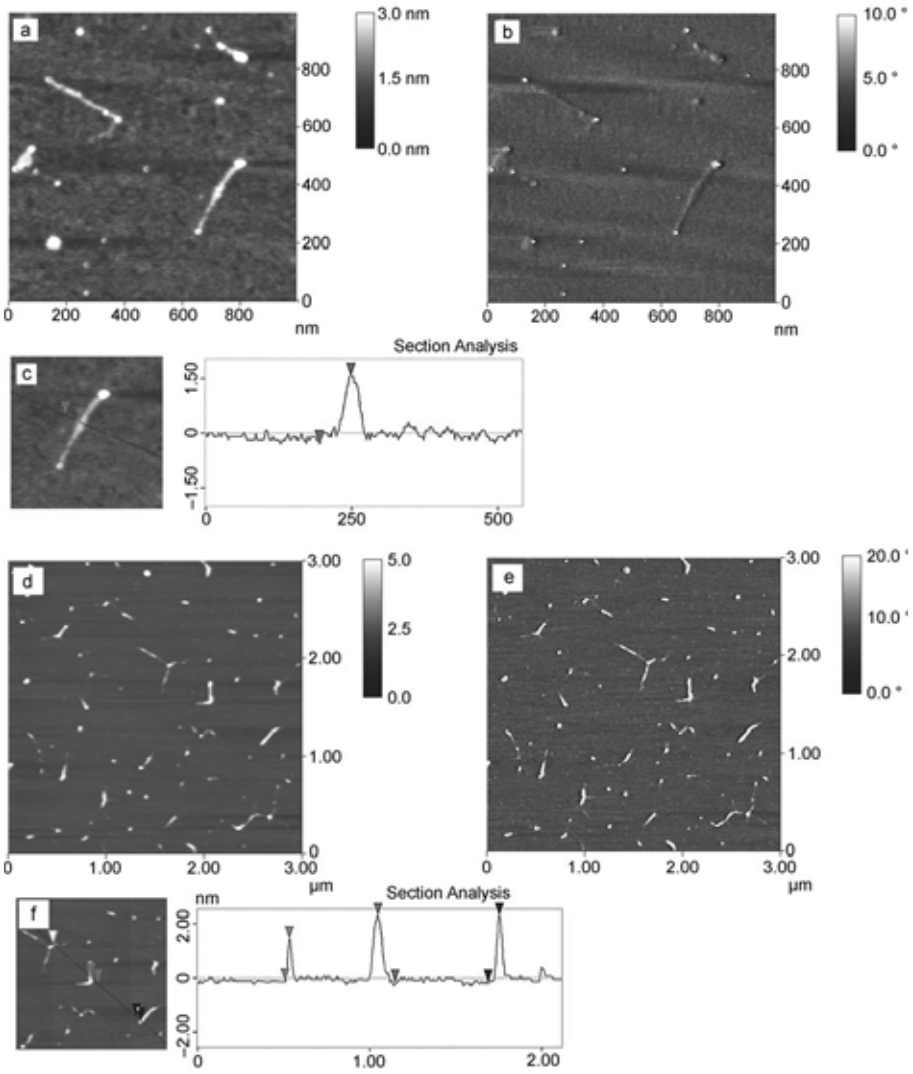

Figure 4.3 AFM images depicting the a) height, b) phase, and c) representative cross section of alkyne-tagged DNA immobilized on mica surfaces, and the d) height, e) phase, and f) representative cross section of sugar-coated alkyne-tagged DNA immobilized on mica surfaces.

For the metallization experiments we used Si–SiO_2 surfaces to avoid side metallization on mica as a consequence of electrostatic interactions of Ag ions with the negatively charged mica surface. The use of Si–SiO_2, however, brings the disadvantage of a less dense coverage of DNA strands over the surface in addition to higher surface roughness, which translates to poorer contrast of the strands in AFM imaging. This can be seen in Figure 4.4a and b, which shows a sugar-modified 934-bp PCR fragment on a Si–SiO_2 surface. For the metallization of the sugar-modified DNA, a drop of Tollens solution was placed on a wafer on which DNA had previously been immobilized. After careful rinsing with water the procedure was repeated with a gold enhancement solution (comprising an Au(I)-SCN complex and hydroquinone) for defined periods of time. After washing and drying, the wafer was analyzed by AFM.

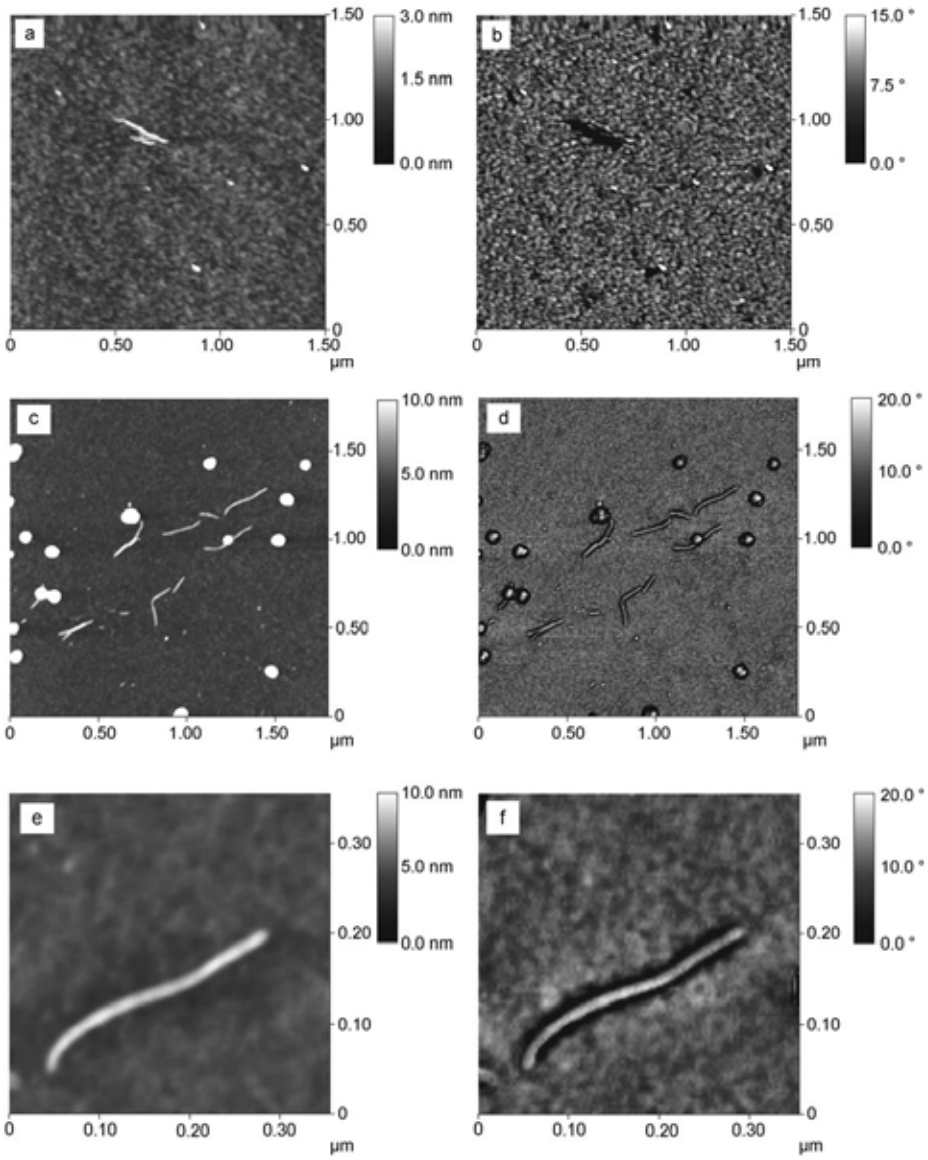

Figure 4.4 AFM images depicting the a) height and b) phase of sugar-coated alkyne-tagged DNA on Si–SiO_2 surfaces, and the c, e) height and d, f) phase of DNA strands after the two-step metallization process. (c) and (d) show an overview; (e) and (f) show zoomed images of a metallized strand.

Figure 4.4c and d shows a characteristic image of the surface after metallization (Tollens treatment: 30 s, gold enhancement 1 min). Nanowires with a height of approximately 8 nm can be found all over the wafer. The length of the objects corresponds to the length of the sugar-modified 900-bp DNA duplexes, which is around 300 nm. The structure of the metallized strands is extremely homogeneous compared to that found in previous works, thus indicating a highly uniform and selective metallization process. Control experiments in which the surface-bound 900-mer was treated with gold enhancement solution without previous Tollens reaction exhibited no metal deposition on the DNA strands.

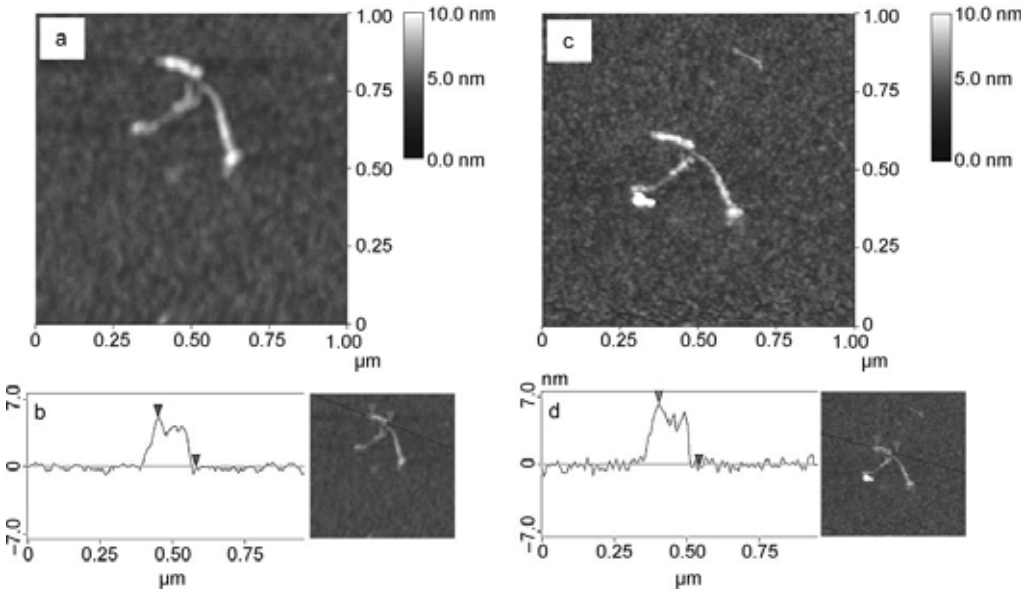

Figure 4.5 AFM images depicting the time-dependent metallization experiment. The same strand is imaged a, b) after Tollens reaction for 30 s and gold enhancement for 30 s and c, d) after gold enhancement for an additional 30 s. Growth of the strand from 5.2 nm in (a, b) to 6.8 nm in (c, d) can be observed. This result is representative for the whole sample.

Time-dependent experiments demonstrate the high degree of control over the diameters of the nanowires. For these experiments we conducted a Tollens reaction on surface-bound DNA strands followed by subsequent steps of gold enhancement for defined time periods. We monitored the growth of the nanowires by AFM imaging on a representative Y-shaped DNA aggregate. This structure was chosen as it could be identified easily due to its characteristic shape after subsequent metallization, washing, and imaging steps. The result is depicted in Figure 4.5. The aggregate shown appears to be inhomogeneously metallized, most likely as a result of partial modification with sugar in the click reaction step or a deficient incubation time with the silver solution. For the observation of time-dependent metal growth we focused on the upper part of the structure that showed a dense metal coverage. Nevertheless, in the upper portion of the DNA aggregate, slow growth of the nanowire was detected during repeated gold enhancement. After 30 s incubation with the gold enhancement solution the nanowire has a height of 5.2 nm. After the second enhancement step of 30 s, the wire shows a profile which is approximately 1.6 nm higher, but as homogeneous.

4.4 Summary and Outlook

In summary, we have demonstrated a method for the generation of homogeneous bimetallic Au–Ag nanowires on DNA templates that carry artificial base pairs with alkyne reporter groups. By reaction with an azide-modified sugar derivative (**4.1**), we were able to coat these strands with metallization-sensitive groups. In a two-step procedure involving the Tollens reagent and subsequent gold enhancement, the DNA template was coated with a homogeneous and dense metal layer to yield wires with a diameter below 10 nm. The metallization time is the size-defining variable, as proven by time-dependent metallization experiments and

AFM studies. The slow growth observed in this investigation allows the fabrication of nanowires with precisely tunable diameters and aspect ratios. To conclude, the present route may serve as a method for the spatially defined and sequence-specific metallization of artificial DNA strands, which could be of great use in the fabrication of nanoscale electrical building blocks.

4.5 Experimental Section

4.5.1 Synthesis

5-(8-Trimethylsilyl-octa-1,7-diynyl)-2'-deoxycytidine

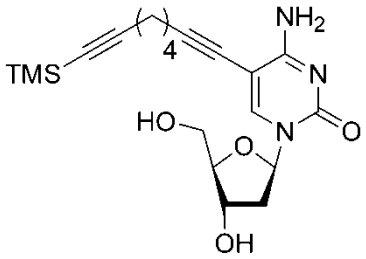

Degassed triethylamine (2.3 mL, 16.5 mmol) was added to a thoroughly degassed solution of **4.2** (1.165 g, 3.30 mmol),[13] $Pd(PPh_3)_4$ (762 mg, 0.66 mmol), and CuI (251 mg, 1.32 mmol) in anhydrous DMF (13 mL). A degassed solution of **4.3** (1.32 mL, 5.94 mmol) in DMF (1 mL) was added to the reaction mixture over 20 min. After complete addition, the reaction mixture was stirred at r. t. over night. The solvent was removed *in vacuo* and the residue was directly applied to a flash column chromatography ($CHCl_3$/MeOH 8:1). The desired product was obtained as a pale yellow powder (1.15 g, 2.85 mmol, 86%).
R_f ($CHCl_3$/MeOH 2:1): 0.73. ^{1}H-NMR (400 MHz, d_6-acetone): δ = 0.11 (s, 9H, $Si(CH_3)_3$), 1.66 (m, 4H, CH_2), 2.19 (ddd, J = 4.6, 4.6, 9.2 Hz, 1H, $C_{2'}H$), 2.27 (t, J = 4.8 Hz, 2H, $C\equiv CCH_2$), 2.33 (ddd, J = 2.4, 4.0, 8.8 Hz, 1H, $C_{2'}H$), 2.46 (t, J = 4.6 Hz, 2H, $C\equiv CCH_2$), 3.74-3.84 (m, 2H, $C_{5'}H$), 3.95 (q, J = 2.1 Hz, 1H, $C_{4'}H$), 4.33 (s, 1H, OH), 4.40 (s, 1H, OH), 4.47 (m, 1H, $C_{3'}H$), 6.22 (t, J = 4.4 Hz, 1H, $C_{1'}H$), 6.34 (s, 1H, NH), 6.94 (s, 1H, NH), 8.19 (s, 1H, C_5H). ^{13}C-NMR (150 MHz, d_6-acetone): δ = 0.0 (3C), 19.3, 19.5, 28.2, 28.3, 41.8, 62.3, 71.5, 72.7, 84.7, 87.3, 88.6, 91.1, 95.7, 107.7, 144.8, 154.4, 165.5. IR (KBr disc, cm^{-1}): ν = 3429 *sbr*, 2947 *m*, 2173 *w*, 1649 *vs*, 1600 *w*, 1508 *s*, 1250 *m*, 1091 *m*, 1057 *m*, 843 *s*, 783 *w*, 760 *w*, 641 *w*. HRMS (ESI): calcd for $C_{20}H_{30}N_3O_4Si$ $[M+H]^+$: 404.2006, found: 404.2004.

5-(Octa-1,7-diynyl)-2'-deoxycytidine (**4.4**)

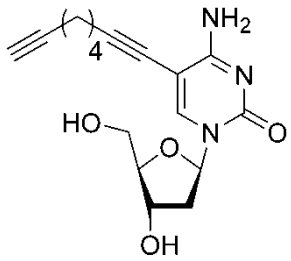

5-(8-Trimethylsilyl-octa-1,7-diynyl)-2'-deoxycytidine (80 mg, 0.20 mmol) was dissolved in THF (3 mL) and KOH (3 M in MeOH, 0.20 mL) was added. The solution was stirred for 3 d at r. t. The solvent was removed *in vacuo* and the residue was directly applied to a flash column chromatography ($CHCl_3$/MeOH 8:1). The product was collected as a white powder (35 mg, 0.11 mmol, 68%).
R_f ($CHCl_3$/MeOH 4:1): 0.33. ^{1}H-NMR (600 MHz, CD_3OD): δ = 1.69 (m, 4H, CH_2), 2.14 (dt, *J* = 6.8, 13.8 Hz, 1H, $C_{2'}H$), 2.23 (m, 3H, H-C≡ C-CH_2), 2.37 (ddd, *J* = 4.2, 6.3, 13.8 Hz, 1H, $C_{2'}H$), 2.47 (t, *J* = 6.9 Hz, 2H, CH_2), 3.73 (dd, *J* = 3.6, 12.1 Hz, 1H, $C_{5'}H$), 3.82 (dd, *J* = 3.1, 12.1 Hz, 1H, $C_{5'}H$), 3.94 (q, *J* = 3.6 Hz, 1H, $C_{4'}H$), 4.36 (dt, *J* = 3.9, 6.0 Hz, 1H, $C_{3'}H$), 6.21 (t, *J* = 6.6 Hz, 1H, $C_{1'}H$), 8.24 (s, 1H, C_5H). ^{13}C-NMR (600 MHz, CD_3OD): δ = 18.6, 19.8, 28.7, 28.9, 42.4, 62.5, 69.8, 71.8, 72.3, 84.7, 87.9, 89.0, 93.6, 97.1, 145.0, 156.8, 166.6. IR (KBr disc, cm^{-1}): 3395 *s*, 3298 *w*, 2936 *w*, 1638 *vs*, 1506 *s*, 1417 *m*, 1306 *m*, 1262 *w*, 1201 *w*, 1100 *s*, 1065 *m*, 996 *w*, 942 *w*, 782 *m*, 646 *mbr*. HRMS (ESI): calcd for $C_{17}H_{22}N_3O_4^+$ $[M+H]^+$: 332.1610; found: 332.1607.

5-(Octa-1,7-diynyl)-3'-*O*-acetyl-2'-deoxycytidine (**4.5**)

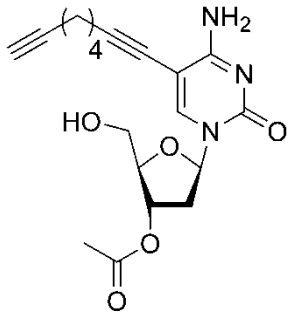

Compound **4.4** (150 mg, 0.45 mmol), lipase (200 mg), and vinyl acetate (94 µL, 1.02 mmol) were suspended in dry THF/DMF (11:1, 11 mL) and heated to 60 °C for 41 h. The suspension was filtered and the filtrate adsorbed onto silica. Flash chromatography ($CHCl_3$/MeOH 10:1) yielded 5-(octa-1,7-diynyl)-2'-deoxy-3'-*O*-acetylcytidine (116 mg, 0.31 mmol, 69%) as a white solid.
R_f ($CHCl_3$/MeOH 4:1): 0.58. ^{1}H-NMR (400 MHz, d_6-acetone): δ = 1.59-1.74 (m, 4H, CH_2), 2.06 (s, 3H, OAc), 2.23 (dt, *J* = 2.4, 6.8 Hz, 2H, H_2CC≡ CH), 2.30–2.44 (m, 2H, $C_{2'}H$), 2.36 (t, *J* = 2.6 Hz, 1H, HC≡ C), 2.46 (t, *J* = 6.8 Hz, 2H, H_2CC≡ C-Ar), 3.83 (d, *J* = 2.8 Hz, 2H, $C_{5'}H$), 4.10 (dt, *J* = 2.0, 3.0 Hz, 1H, $C_{4'}H$), 4.60 (s, 1H, $C_{5'}OH$), 5.33 (td, *J* = 1.0, 6.2 Hz, 1H, $C_{3'}H$), 6.24 (dd, *J* = 5.7, 8.4 Hz, 1H, $C_{1'}H$), 6.49 (s, 1H, NH), 7.34 (s, 1H, NH), 8.18 (s, 1H, C_6H). ^{13}C-NMR (100 MHz, d_6-acetone): δ = 19.2, 20.5, 22.0, 29.3, 29.4, 40.0, 63.6, 71.2, 73.6, 77.0, 85.6, 87.4, 88.6, 97.2, 145.9, 154.7, 171.8, 207.3, 211.0. HRMS (ESI): calcd. for $C_{19}H_{23}ClN_3O_5^-$ $[M+Cl]^-$: 408.1326; found: 408.1348.

5-(Octa-1,7-diynyl)- 5'-*O*-triphosphate-2'-deoxycytidine (**4.6**)[14]

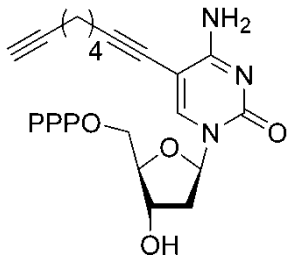

Compound **4.5** (107 mg, 0.29 mmol) was dissolved in dry pyridine and co-evaporated to dryness three times. Molecular sieves (4 Å), dry pyridine (0.6 mL), and dry DMF (2.4 mL) were added and the solution was left standing over night. A solution of 2-chloro-4*H*-1,2,3-dioxaphosphorin-4-one (1 M) in anhydrous dioxane (315 µL, left standing over night over molecular sieves, 4 Å) was injected into the well-stirred solution of the nucleoside. After 10 min a solution of bis(tri-*N*-butylammonium) pyrophosphate (0.5 M) in anhydrous DMF (0.87 mL) and tri-*N*-butylamine (0.29 mL, left standing over night over molecular sieves, 4 Å) was quickly injected. A solution of 1% iodine in pyridine/water (98:2, v/v; 6 mL, 0.47 mmol) was then added. After 15 min excess iodine was destroyed by adding a few drops of a 5% aqueous solution of $NaHSO_3$ and the reaction solution was evaporated to dryness. The residue was dissolved in water (30 mL). After standing at r. t. for 30 min, concentrated NH_3 (90 mL) was added. After 1 h the solution was evaporated to dryness, and the residue was dissolved in water and purified by reversed-phase HPLC. The separation was performed using $HNEt_3$/OAc buffers (0.1 M; buffer A: H_2O, buffer B: MeCN/H_2O 4:1). The flow rate was 15 mL min^{-1} with a linear gradient from 100% buffer A to 50% buffer A in 45 min. The product was eluted at 24.9 min.
^{1}H-NMR (200 MHz, D_2O): δ = 1.45-1.58 (m, 4H, CH_2), 2.02–2.38 (m, 7H, $H_2CC{\equiv}CH$, $H_2CC{\equiv}C$-Ar, 2 × $C_{2'}H$), 3.98–4.10 (m, 3H, $C_{4'}H$, $C_{5'}H$), 4.37-4.48 (m, 1H, $C_{3'}H$), 6.06 (t, *J* = 6.4 Hz, 1H, $C_{1'}H$), 7.86 (s, 1H, C_6H). ^{31}P-NMR (80 MHz, D_2O): δ = -22.1 (t, *J* = 19.4 Hz, 1P, -β), -10.7 (d, *J* = 11.4 Hz, 1P, -α), -10.2 (d, *J* = 18.8 Hz, 1P, -γ). MS (MALDI-TOF): 571.9 $[M+H]^+$.

4.5.2 PCR Amplification

The vector pExp007-Polη with the polymerase η gene from Rad30 *Saccharomyces cerevisiae* was used as template with the primers 5'-TTA ATT GAA TTC GAT TTG GGC CGG ATT TGT TTC-3' and 5'-TGA TGC CCT TGT ACG CAA CTG-3', which amplify a 934-bp fragment of the Polη gene.[11]

PCR conditions

The PCR was run with a final concentration of 0.2 mM of each deoxynucleoside triphosphate (dNTP), 0.3 mM of each primer, 400 ng of template, and 2 U Pwo Polymerase (Roche) in the

reaction buffer provided by the supplier. The total volume was 50 µL. Temperature programming was performed on an Eppendorf personal cycler: 95 °C for 2 min, then nine cycles at 95 °C for 15 s, 58 °C (-1.0 °C each cycle) for 30 s, and 72 °C for 45 s; then 30 cycles at 95 °C for 15 s, 57 °C for 30 s, and 72 °C for 45 s. The PCR product was purified using a QIAquick PCR purification kit (QIAGEN).

4.5.3 Immobilization of DNA on Mica and Silica Surfaces

Mica: The mica samples were dipped into a solution containing MgOAc (4 mM) and rinsed with H_2O. A DNA concentration of 40-60 ng mL^{-1} was used in the following procedures. DNA solution (2 mL) was added to the substrate and absorbed with a filter paper for 5 min. The mica substrates were rinsed with H_2O and dried in a N_2 stream.
Si–SiO_2: DNA solution (5 mL) in Tris buffer was mixed with MgOAc (1 mL, 4 mM) solution and added to the silica surface (1 × 1 cm). After 15 min, the drop was absorbed with a filter paper and the substrate was washed by dipping it for 1 s into H_2O. The samples were dried in a N_2 stream.

4.5.4 Metallization

Tollens solution: H_2O (8 mL), $AgNO_3$ solution (5 mL, 0.5 M), and NaOH solution (1 mL, 3.0 M) were mixed thoroughly. The precipitate dissolved after addition of NH_3 solution (2.2 mL, 12.5%) to yield a clear and colorless solution.
Gold enhancement: A solution of KSCN (0.5 mL, 60 mg mL^{-1}) was mixed with a solution of $KAuCl_4$ (0.5 mL, 23 mg mL^{-1}). The mixture was centrifuged at 2000 rpm for 1 min and the orange precipitate was separated from the supernatant. The precipitate was dissolved in phosphate buffer (8 mL, 0.05 M, pH 5) and added to a solution of hydroquinone (250 mL, 5.5 mg mL^{-1}) immediately before the metallization process.

Metallization on the membrane

A drop of DNA (approximately 20 ng) was added to a nylon blotting membrane. After UV crosslinking the membrane was soaked with diluted Tollens solution (1:10) for 25 min and washed carefully in H_2O for 30 min to avoid metallization through silver residues from the solution. The membrane was then incubated in a gold enhancement solution.

Metallization on surfaces

After DNA immobilization on Si–SiO_2 wafers, a 10 µL drop of freshly prepared Tollens solution was placed on the wafer and rinsed twice with H_2O (10 mL) after the desired metallization time. The wafer was dried and this procedure was repeated with gold enhancement solution (10 µL). The immersion time determined the diameter of the wires; 30 s of gold enhancement in the above-mentioned concentrations yielded wires approximately 5–6 nm in diameter.

4.5.5 AFM Conditions

AFM images were recorded with a Digital Instruments Dimension 3000 microscope in the tapping mode with silicon cantilevers (Olympus OMCL-C160TS, resonance frequency 300 Hz, tip diameter ≤10 nm). The images were recorded with a scan rate of typically 1.0 Hz.

4.6 Author´s Contribution

The author developed the synthesis of cytidine triphosphate ***4.6****, which was used throughout this study.*

4.7 References

[1] C. M. Mirkin, *Inorg. Chem.* **2000**, *39*, 2258-2272; J. J. Storhoff, C. A. Mirkin, *Chem. Rev.* **1999**, *99*, 1849-1862; C. M. Niemeyer, *Angew. Chem. Int. Ed.* **2001**, *40*, 4128-4158.

[2] N. Seeman, *Nature* **2003**, *421*, 427-431; C. Lin, Y. Liu, S. Rinker, H. Yan, *ChemPhysChem* **2006**, *7*, 1641-1647.

[3] E. Braun, Y. Eichen, U. Silvan, G. Ben-Yoseph, *Nature* **1998**, *391*, 775-778; Y. Eichen, E. Braun, U. Sivan, G. Ben-Yoseph, *Acta Polym.* **1998**, *49*, 663-670.

[4] K. Keren, R. Berman, E. Buchstab, U. Sivan, E. Braun, *Science* **2003**, *302*, 1380-1382; K. Keren, M. Krueger, R. Gilad, G. Ben-Yoseph, U. Sivan, E. Braun, *Science* **2002**, *297*, 72-75.

[5] J. Richter, *Physica E* **2003**, *16*, 157-173.

[6] L. Berti, A. Allesandrini, P. Facci, *J. Am. Chem. Soc.* **2005**, *127*, 11216-11217; J. Richter, M. Mertig, W. Pompe, I. Mönch, H. Schackert, *Appl. Phys. Lett.* **2001**, *78*, 536-538; R. Stoltenberg, A. Wooley, *Biomed. Microdevices* **2004**, *6*, 105-111; J. Richter, R. Seidel, R. Kirsch, M. Mertig, W. Pompe, J. Plaschke, H. K. Schackert, *Adv. Mater.* **2000**, *12*, 507-510.

[7] E. W. Ford, O. Harnack, A. Yasuda, J. M. Wessels, *Adv. Mater.* **2001**, *13*, 1793-1797; M. Mertig, L. C. Ciacchi, R. Seidel, W. Pompe, A. D. Vita, *Nano Lett.* **2002**, *2*, 841-844.

[8] G. A. Burley, J. Gierlich, M. R. Mofid, S. T. H. Nir, Y. Eichen, T. Carell, *J. Am. Chem. Soc.* **2006**, *128*, 1398-1399; J. Gierlich, G. A. Burley, P. M. E. Gramlich, D. M. Hammond, T. Carell, *Org. Lett.* **2006**, *8*, 3639-3642.

[9] Y. Eichen, U. Sivan, E. Braun*, Vol. PCT WO0025136*, **1999**.

[10] V. V. Rostovtsev, L. G. Green, V. V. Fokin, K. B. Sharpless, *Angew. Chem. Int. Ed.* **2002**, *41*, 2596-2599.

[11] R. E. Johnson, S. Prakash, L. Prakash, *Science* **1999**, *283*, 1001-1004; U. Hubscher, G. Maga, S. Spadari, *Annu. Rev. Biochem.* **2002**, *71*, 133-163.

[12] T. R. Chan, R. Hilgraf, K. B. Sharpless, V. V. Fokin, *Org. Lett.* **2004**, *6*, 2853-2855.

[13] C. H. Hwang, J. S. Park, J. H. Won, J. N. Kim, E. K. Ryu, *Arch. Pharm. Res.* **1992**, *15*, 69-72.

[14] J. Ludwig, F. Eckstein, *J. Org. Chem.* **1989**, *54*, 631-635.

5 Synthesis of Highly Modified DNA Using a Combination of PCR with Alkyne-Bearing Triphosphates and Click Chemistry

This Section was published in:

J. Gierlich, K. Gutsmiedl, P. M. E. Gramlich, A. Schmidt, G. A. Burley, T. Carell, *Chem. Eur. J.* **2007**, *13*, 9486-9494.

5.1 Abstract

We report the combination of "click chemistry" with PCR by using alkyne-modified triphosphates for efficient and homogeneous labeling of DNA. A series of modified PCR products of different lengths (300, 900 and 2000 base pairs) were prepared by using a variety of alkyne- and azide-containing triphosphates and different polymerases. After intensive screening of real-time PCR methods, protocols were developed that allow the amplification of genes by using these modified triphosphates with similar efficiency to that of standard PCR. The click reaction on the highly modified PCR fragments provided conversion rates above 90% and resulted in the functionalization of hundreds of alkynes on large DNA fragments with superb selectivity and efficiency.

5.2 Introduction

The DNA molecule is currently of outstanding interest for the synthesis of self-assembling nanoarchitectures.[1] The primary sequence and secondary structure of DNA are also used as a general marker in many diagnostic applications. In both areas, the functionalization of DNA is of paramount importance. In nanotechnology, the preparation of functional nanostructures requires the addition of functions such as magnetic properties[2, 3] or electrical conductivity[2, 4] to the DNA molecule, whereas the modification of DNA with fluorophores or other functions, like reducing groups to enable Ag staining of DNA, is highly desirable for diagnostic applications.[5] One efficient method for the functionalization of long DNA strands is achieved through PCR amplification with unnatural triphosphates carrying the desired function.[6-9] This methodology has received significant attention, especially for the synthesis of highly functionalized aptamers.[8-10] Unfortunately, the type of modification accepted by the PCR enzymes is limited and it is frequently unpredictable which modifications will finally be tolerated.[7, 9, 11, 12] We have therefore started to develop a generally applicable method for the dense functionalization of DNA in a highly reliable and flexible way. Recently we used a protocol in which DNA strands are modified by using the Cu(I)-catalyzed version of the azide–alkyne cycloaddition reaction[13] ("click" reaction[14]), which was discovered by the groups of Meldal[15] and Sharpless[16] and is now used in many different areas.[17] From the two possible isomer products of the cycloaddition, the 1,4-adduct is exclusively formed under these conditions. The reaction has been used successfully on DNA strands with both single[18] and multiple alkyne or azide functions.[5, 19] In order to generate large and highly modified DNA strands, an alkyne-modified triphosphate was used in the PCR, for example, 5-modified deoxyuridine triphosphate (dU*TP) instead of the natural thymidine triphosphate (TTP). The

densely alkyne-modified DNA obtained was subsequently further derivatized by means of the click reaction, as depicted in Scheme 5.1.[5, 19]

Recently we described the functionalization of DNA with azides such as **5.1**, which allowed us to direct silver deposition towards alkyne-modified DNA strands through the Tollens reaction.[5, 20] The protocol enables specific Ag staining of alkyne-labeled DNA. This is of great interest because Ag staining can be more sensitive than fluorescence labeling, while no expensive fluorescence detector is required to visualize the analytical result. Herein we report an investigation of the efficiency of the click reaction on long and complex DNA strands. We describe how the PCR followed by the click reaction depends on the DNA length and sequence and on the kind of triphosphate used. A detailed overview of how the various alkyne-modified triphosphates influence the PCR is given. In order to determine the most efficient PCR conditions, we report the utilization of real-time PCR (RT-PCR) as a facile screening method. Furthermore, UV/Vis and CD data revealing the secondary-structure characteristics of the resulting densely modified DNA duplexes are presented.

5.3 Results and Discussion

5.3.1 Synthesis of 5-Modified Pyrimidine Triphosphates

In order to determine the parameters which govern the efficient incorporation of alkyne-modified triphosphates into DNA by PCR, we prepared and screened the incorporation of a set of 5-alkyne- or 5-azide-modified pyrimidine triphosphates, **5.2**-**5.6**, depicted in Scheme 5.2. The syntheses of the previously undescribed compounds **5.3**, **5.5**, and **5.6** are based on Sonogashira coupling of an appropriate 5-iodopyrimidine nucleoside with an appropriate terminal alkyne, followed by the conversion of the free bases into the corresponding triphosphates, as shown in Scheme 5.3. The synthesis of compounds **5.2**[21] and **5.4**[20] has been described previously.

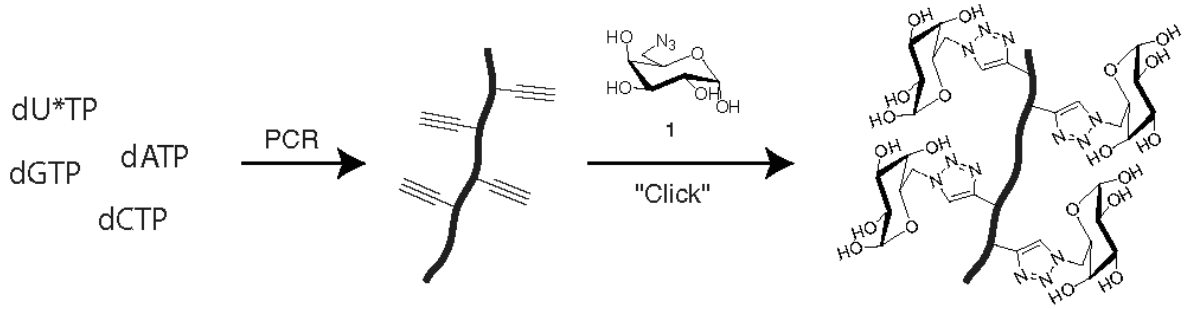

Scheme 5.1 Schematic depiction of the postsynthetic functionalization of DNA strands by using click chemistry. dATP: deoxyadenosine triphosphate, dCTP: deoxycytidine triphosphate, dGTP: deoxyguanosine triphosphate, dU*TP: alkyne triphosphate.

Triphosphate **5.3** was prepared from the known monomer **5.7** (Scheme 5.3).[19] The amide-containing triphosphate **5.5** was synthesized by coupling the acid-modified uridine **5.8** with propargylamine. The synthesis of compound **5.6** begins with the hydrogenation of the triple bond in **5.10**. The azide is introduced by mesylation and subsequent nucleophilic substitution

(see Section 5.5.1). The 5-modified pyrimidine triphosphates possess either free alkynes (**5.2**-**5.5**) or a free azide (**5.6**) to allow direct functionalization through the click reaction. Triphosphate **5.2** features a terminal alkyne in direct conjugation with the uridine nucleobase. In the uridine- or cytidine-based triphosphates **5.3**–**5.5**,the terminal alkyne function is situated remotely from the base, with the rationale being that a remote alkyne would result in higher click yields due to reduced steric hindrance.[19]

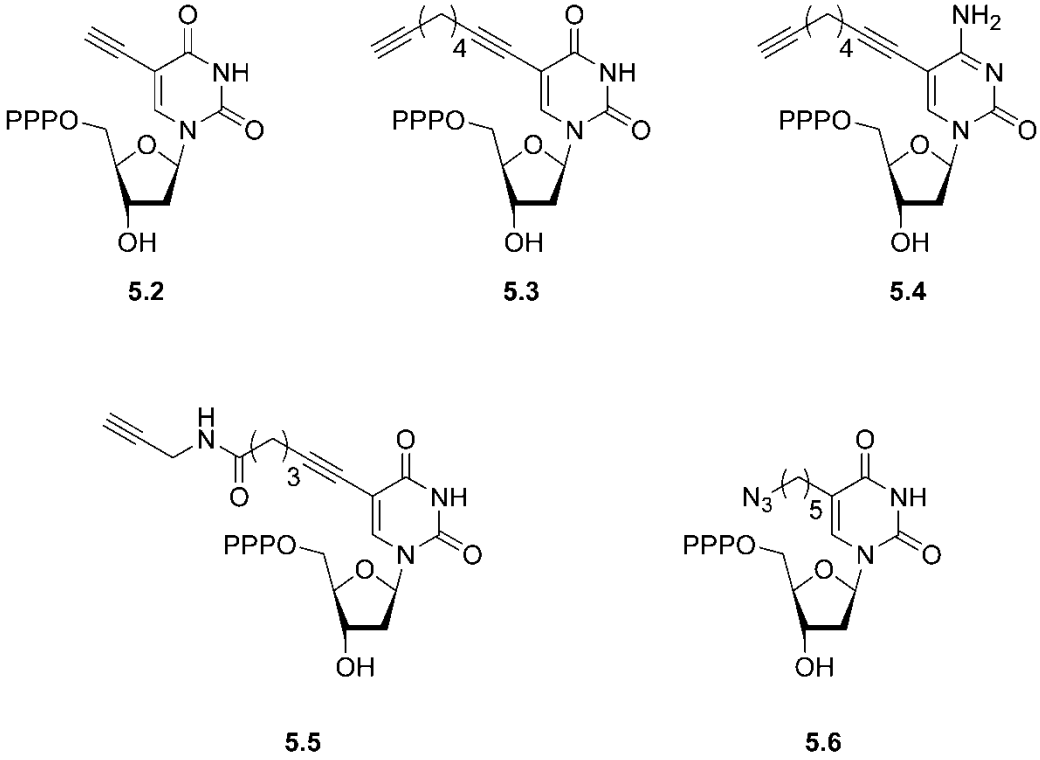

5.2 **5.3** **5.4**

5.5 **5.6**

Scheme 5.2 5-Modified pyrimidine triphosphates used in this study.

Triphosphates **5.3**–**5.5** possess an internal alkyne in direct conjugation with the pyrimidine ring, in addition to the terminal alkyne function. Based on previous studies, which had shown that an extended conjugation can facilitate polymerase incorporation, we hoped that these alkynes would also improve the acceptance of our building blocks by polymerases in the PCR.[8, 11] In order to investigate whether we could reverse the click reaction, we also investigated the incorporation of azide **5.6** into a DNA strand instead of an alkyne. However, in order to create a stable azide-modified triphosphate, we were forced to utilize a saturated carbon chain to link the azide function to the nucleobase in order to avoid a thermally induced intramolecular cycloaddition reaction between the azide and the internal alkyne resulting in a triazole product.[22] Such saturated linkers, however, are known to be somewhat troublesome substrates for polymerases.[11, 23]

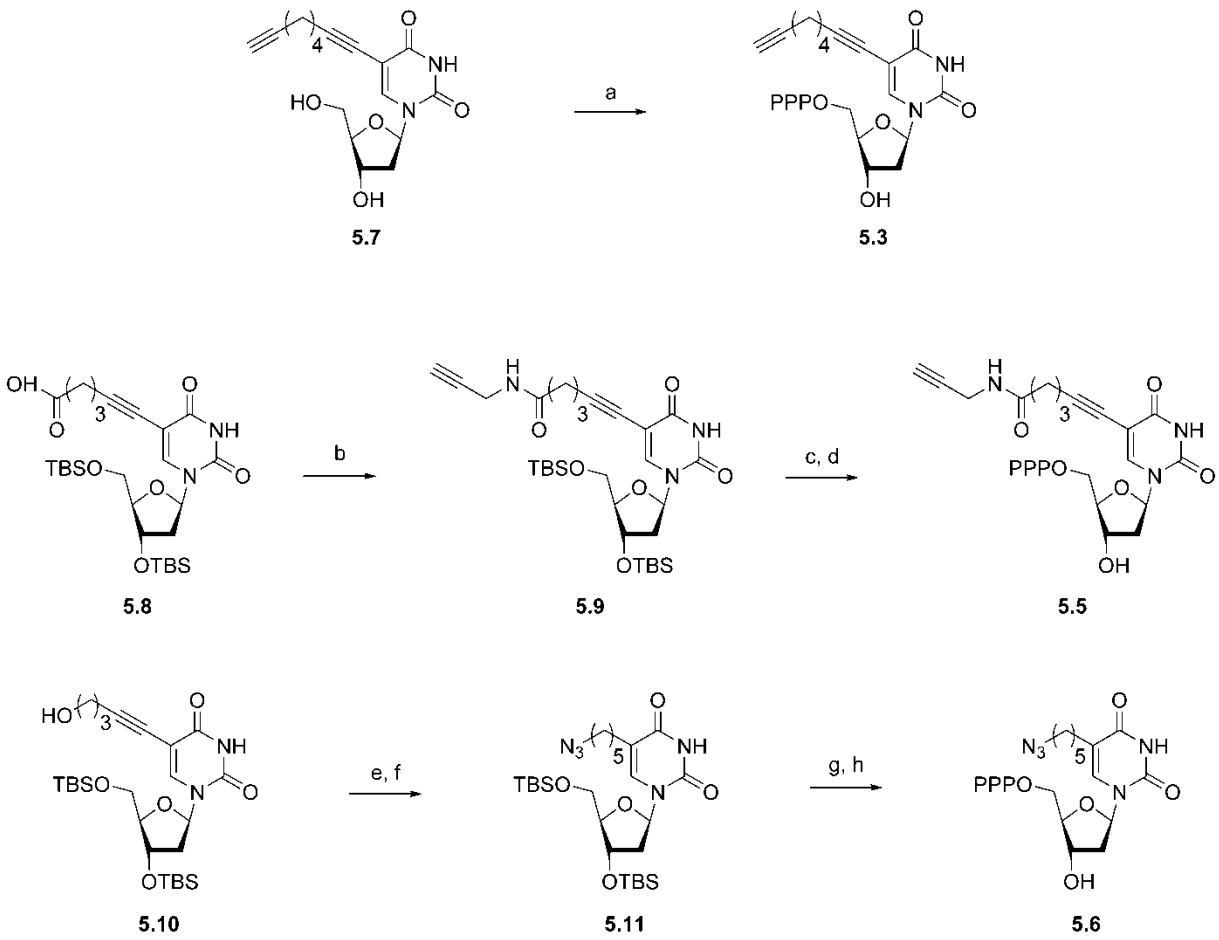

Scheme 5.3 Syntheses of the triphosphates **5.3**, **5.5**, and **5.6**: a) 1) $POCl_3$, proton sponge, 2) tributylammonium pyrophosphate, 3) TEAB, b) HOBT, HBTU, HATU, propargylamine, DCM, 75%, c) TBAF, pyridine, 72%, d) 1) $POCl_3$, proton sponge, 2) tributylammonium pyrophosphate, 3) TEAB, e) Pd/C, H_2, 73%, f) 1) MsCl, DIEA, DCM, 2) NaN_3, DMF, 82%, g) TBAF, THF, 91%, h) 1) $POCl_3$, proton sponge, 2) tributylammonium pyrophosphate, 3) TEAB. TEAB: tetraethylammonium bromide, HOBT: 1-hydroxy-1*H*-benzotriazole, HBTU: *O*-(benzotriazol-1-yl)-*N*,*N*,*N*',*N*'-tetramethyluronium hexafluorophosphate, HATU: *N*,*N*,*N*',*N*'-Tetramethyl-*O*-(7-azabenzotriazol-1-yl)uronium hexafluorophosphate.

5.3.2 Primer Extension Studies

To explore the acceptance of the triphosphates by different polymerases, we initially performed primer extension studies with a range of polymerases, including the family A polymerase from *Thermus aquaticus* (Taq) and the family B polymerases from *Pyrococcus woesi* (Pwo), *Thermococcus litoralis* (Deep Vent exo$^-$) and *Thermococcus kodakaraensis* (KOD XL), which is a mixture of the natural form and an exo$^-$ mutant. The original assay developed by Held and Benner was utilized. This uses different templates of increasing difficulty (**T1**–**T3**).[23] While for **T1** only the incorporation of one modified uridine is needed, **T2** and **T3** demand the polymerase to incorporate two or more consecutive modifications. The sequences of the 5'-fluorescein-labeled primer **P** and the three different templates **T1**–**T3** are listed in Table 5.1. The primer extensions were conducted at 72 °C with a reaction time of only 10 minutes.

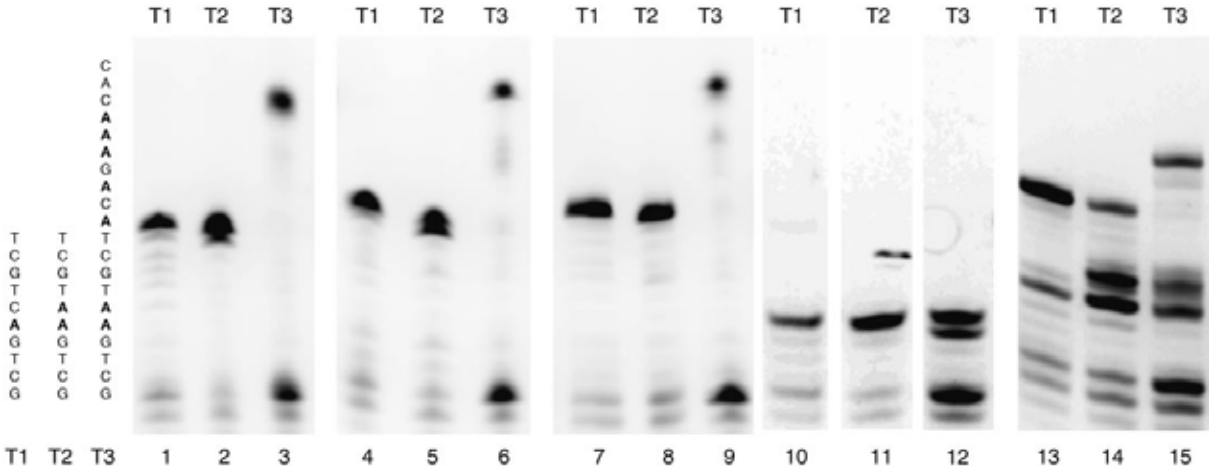

Figure 5.1 Primer extension with Pwo polymerase. Lanes 1–3: dATP, dCTP, dGTP, **5.2**, lanes 4-6: dATP, dCTP, dGTP, **5.3**, lanes 7-9: dATP, **5.4**, dGTP, **5.3**, lanes 10-12: dATP, dCTP, dGTP, **5.5**, lanes 13-15: dATP, dCTP, dGTP, **5.6**.

Figure 5.1 summarizes the results obtained with the most successful polymerase Pwo, which has full exonuclease activity. The experiments with the triphosphates **5.2**-**5.6** revealed efficient incorporation of **5.2**-**5.4**, while only inefficient incorporation of the triphosphates **5.5** and **5.6** was observed (Section 5.5.2).

To our surprise, triphosphate **5.5** was not accepted as a substrate by the polymerases tested. This is difficult to explain because other triphosphates containing an amide bond, albeit in a different direction, and a triple bond adjacent to the base, were efficiently accepted.[8, 11] In the case of triphosphate **5.6**, the inefficient incorporation can most likely be attributed to the saturation of the carbon chain directly attached to the pyrimidine ring because similar results were obtained with other 5-modified pyrimidine triphosphates with saturated carbon linkers.[23] Sawai and co-workers recently reported the efficient incorporation of 5-modified triphosphates bearing an α-methylamide function by using the KOD polymerase (see reference[9] and references cited therein). With our substrate, KOD XL produced only small amounts of full-length extension product with **5.6**. Figure 5.1 shows the results for **5.6** with the Pwo polymerase, which stops at the double-incorporation site and is not able to elongate over the triple-incorporation site of **T3**. The incorporation of **5.2**-**5.4** also occurred with all of the other polymerases tested, a result indicating that these triphosphates should also be substrates for PCR (see Section 5.5.3).

Table 5.1 Sequences of the primer and the templates used in the primer extension experiments. The bold **A** marks the position where the polymerase has to insert a modified dU*TP.

P	3′-CATGGGCCAAGCTTCTTCGG-Fl-5’[a]
T1	5′-TCGTC**A**GTCGGTACCCGGTTCGAAGAAGCC-3’
T2	5′-TCGT**AA**GTCGGTACCCGGTTCGAAGAAGCC-3’
T3	5′-C**A**C**AAA**G**A**C**A**TCGT**AA**TGCGGTACCCGGTTCGAAGAAGCC-3’

[a] Fl: fluorescein.

5.3.3 RT-PCR Investigations

Incorporation of modified triphosphates into long DNA strands through PCR is known to be a rather empirical process. In order to facilitate the finding of the correct conditions, we performed a combinatorial screening of variables such as the cycling time, annealing temperature, chemical additives and substrate concentrations. To this end an RT-PCR assay with SYBR Green II as a fluorescent intercalator was utilized. We first investigated the polymerases Pwo, Deep Vent exo$^-$, KOD XL and Taq for their ability to amplify a 300-base-pair fragment from the Polη gene. In the experiments either dTTP or dCTP, depending on the type of modified base investigated, was fully replaced by either **5.2**, **5.3** or **5.4**. The expected PCR product contains 154 deoxythymidines and 104 deoxycytidines, which are exchanged during the PCR into modified dTTP or dCTP, respectively.

Poor amplification was observed in the presence of the triphosphates **5.2** and **5.4** with the family A polymerase Taq. The polymerase failed completely to amplify a product with triphosphate **5.3**. By contrast, full-length amplicons were produced in high yield with all of the triphosphates **5.2-5.4** if one of the family B polymerases, Pwo, Deep Vent exo$^-$ or KOD XL was employed. This is fully consistent with previous studies by Held and Benner[23] and by Sawai and coworkers,[9] who reported that family B polymerases have a broader substrate acceptance than the members of family A. In agreement with the primer extension studies, we could not, under any circumstances, observe PCR product in the presence of the triphosphates **5.5** and **5.6**.

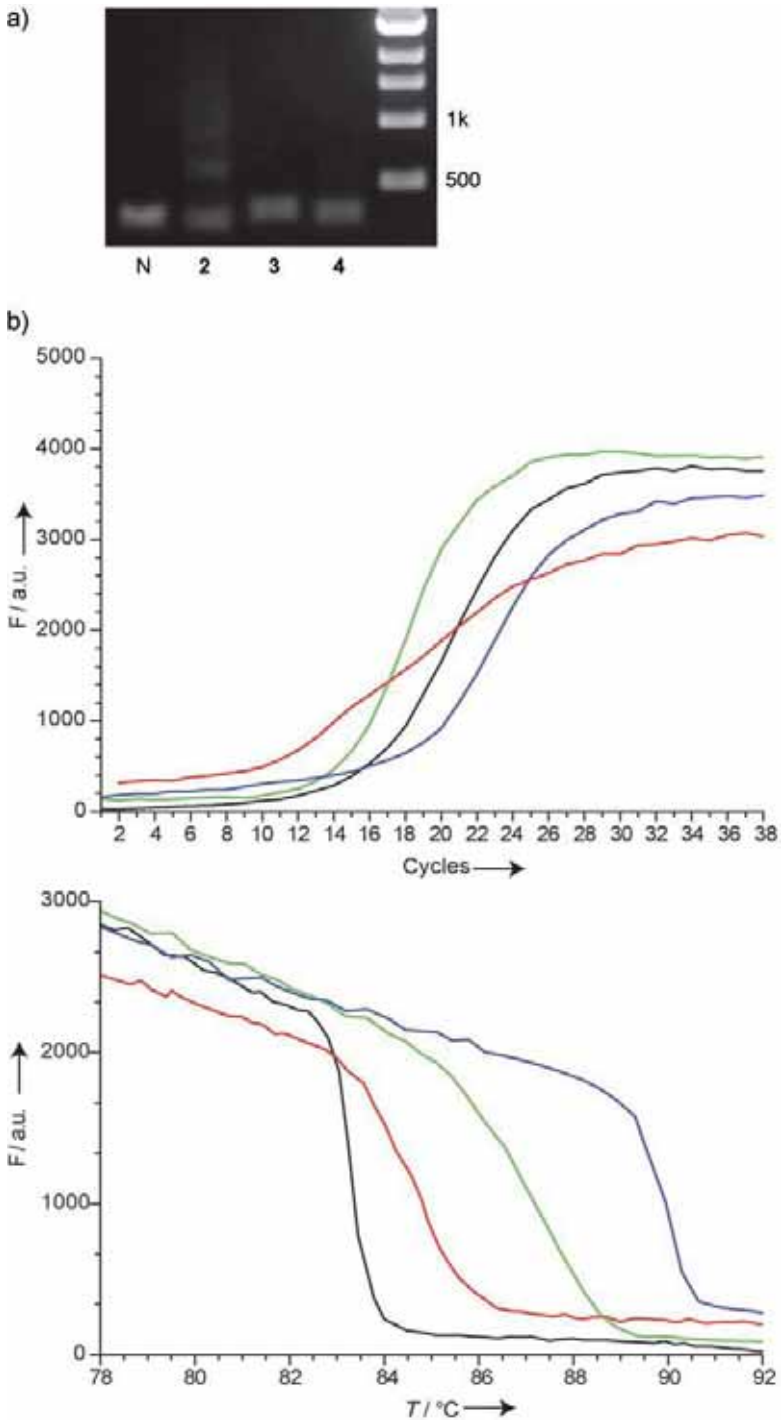

Figure 5.2 Incorporation of modified triphosphates **5.2**-**5.4** into a 300-base-pair fragment by using Pwo for RT-PCR. a) Agarose gels of PCR fragments derived from a 300-base-pair template: lane 1: dATP, dCTP, dGTP, TTP, lane 2: dATP, dCTP, dGTP, **5.2**, lane 3: dATP, dCTP, dGTP, **5.3**, lane 4: dATP, **5.4**, dGTP, TTP, lane 5: DNA ladder. b) Corresponding RT-PCR profiles (top) and melting curves (bottom) of the PCR with Pwo. PCR300·**5.2**-**5.4** (**5.2**: —, **5.3**: —, **5.4**: —) and PCR300·**N** (c) are the products with incorporated triphosphates **5.2**-**5.4** or with only natural triphosphates, respectively.

The Pwo polymerase produced amplicons of the highest quality compared with all other family B polymerases tested (Figure 5.2a). The PCR product PCR300·**5.3** exhibits a slightly re-

duced mobility on the gel. Figure 5.2b shows the fluorescence curves obtained from the RT-PCR study with Pwo polymerase. All of the triphosphates, except **5.3**, provided a typical PCR profile. The slower increase of the PCR signal for **5.3** could indicate a slower incorporation of this triphosphate compared to that of the others. Similar effects were observed with the Deep Vent exo$^-$ polymerase. The slightly less effective incorporation of triphosphate **5.3** may be of importance if longer and/or more demanding templates require amplification (see below). In order to ensure the amplicons created by Pwo possess the correct base sequence, we used the alkyne-containing amplicons as templates for a second PCR with all four natural triphosphates present. These back-amplified amplicons were subsequently sequenced. To our surprise, we detected no sequence errors, which indicates that the incorporation of triphosphates **5.2-5.4** proceeds with high fidelity. Restriction assays with different restriction enzymes revealed that the modifications can, in some cases, inhibit these enzymes (Section 5.5.5).

Table 5.2 Melting temperatures [°C] of PCR300 amplicons as a function of polymerase buffer.

PCR product	Pwo (T_m [°C])	Deep Vent exo$^-$ (T_m [°C])
PCR300·**5.2**	87	85
PCR300·**5.3**	85	82
PCR300·**5.4**	91	88
PCR300·**N**	83	81

Investigation of RT-PCR fluorescence melting curves shows that incorporation of the modified triphosphates **5.2**-**5.4** increased the melting point of the PCR product (Table 5.2). PCR300·**5.4** shows the largest stabilization ($\approx$ 8 °C increase) when compared with a natural control. Intriguingly, PCR300·**5.3** amplicons are destabilized ($\approx$ 6-7 °C decrease) relative to PCR300·**5.4** amplicons, despite having the same bisalkyne addend. The increased linker length of triphosphate **5.3** compared to **5.2** seems to lower the melting point by around 2 °C.
Encouraged by the successful incorporation of triphosphates **5.2**-**5.4**, we next investigated the PCR amplification of longer DNA fragments with 900 base pairs. The investigated PCR product now comprises 551 exchangeable thymidines and 352 exchangeable cytidines (for the RT-PCR traces, see Section 5.5.3). In general, we observed that longer templates were more difficult to produce and careful balancing of the PCR additives and cycling temperatures was required. Besides an elongation of the PCR cycle time, we increased the denaturing temperature to 99 °C and 4% dimethylsulfoxide (DMSO) was added to decrease the melting temperature of all DNA hybrids formed during the PCR. In the presence of triphosphates **5.2** and **5.4**, efficient PCR amplification of the 900-base-pair template could be achieved (Figure 5.3a). Only KOD XL polymerase was able to generate full-length amplicons with triphosphate **5.3**. Again, these amplicons show slightly reduced mobility.

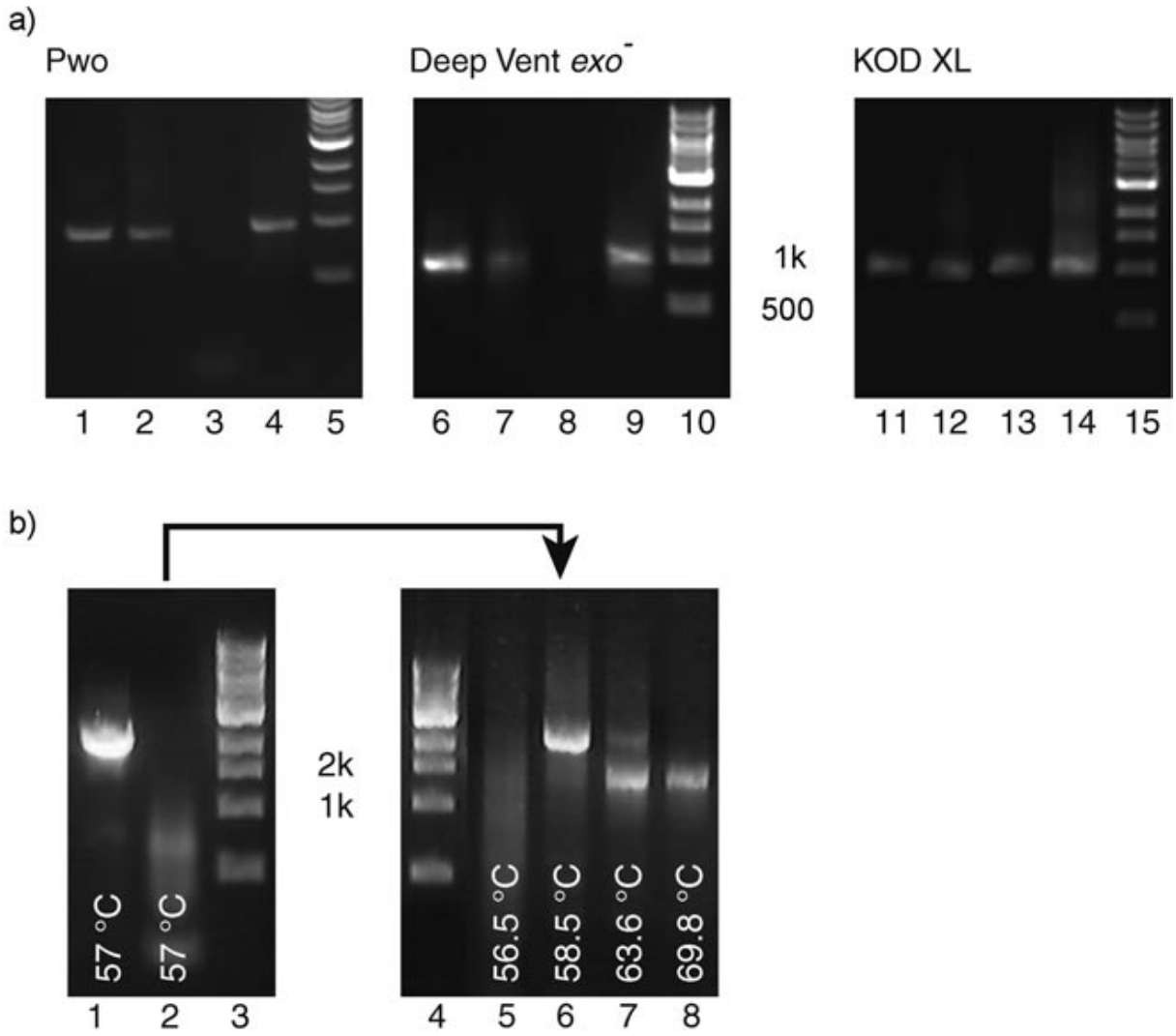

Figure 5.3 a) Incorporation of modified triphosphates **5.2**-**5.4** into a 900-base-pair fragment by using PCR. Agarose gels of the PCR products with the different polymerases: Lanes 1,6,11: dATP, dCTP, dGTP, TTP, lanes 2, 7, 12: dATP, dCTP, dGTP, **5.2**, lanes 3, 8, 13: dATP, dCTP, dGTP, **5.3**, lanes 4, 9, 14: dATP, **5.4**, dGTP, TTP, lanes 5, 10, 15: DNA ladder. b) PCR with a 2000-base-pair fragment. Screening of the annealing temperature for the production of PCR2000·**5.4** with Pwo: comparison between natural (lane 1) and modified (lane 2) triphosphates at a 57 °C annealing temperature, lanes 5-8: screening of different annealing temperatures, lanes 3, 4: DNA ladder.

Encouraged by these results, we investigated the incorporation of modified triphosphates into DNA strands of 2000 base pairs in length, which comprise 887 exchangeable cytidines (see Section 5.5.3). These studies were only performed with the triphosphate **5.4**, which had given the best results thus far. Careful optimization of the PCR protocol was required. Figure 5.3b depicts the results obtained with different annealing temperatures. With a temperature of 57 °C, a PCR product was obtained with natural triphosphates, but only unspecific products were obtained when dCTP was replaced by the modified triphosphate **5.4**. To reduce the unspecific binding of the primer, 4% DMSO was added and the denaturing temperature was set to 99 °C. An annealing temperature screen showed that the correct product was only formed in a small range of temperatures at around 58.5 °C. At higher temperatures, shorter amplicons

were synthesized. In the final protocol, an annealing temperature of 59.3 °C was used, which allowed us to create a 2000-base-pair PCR product with 887 alkynes attached to the modified cytidines.

5.3.4 UV/Vis and CD Spectroscopy of the Modified PCR Amplicons

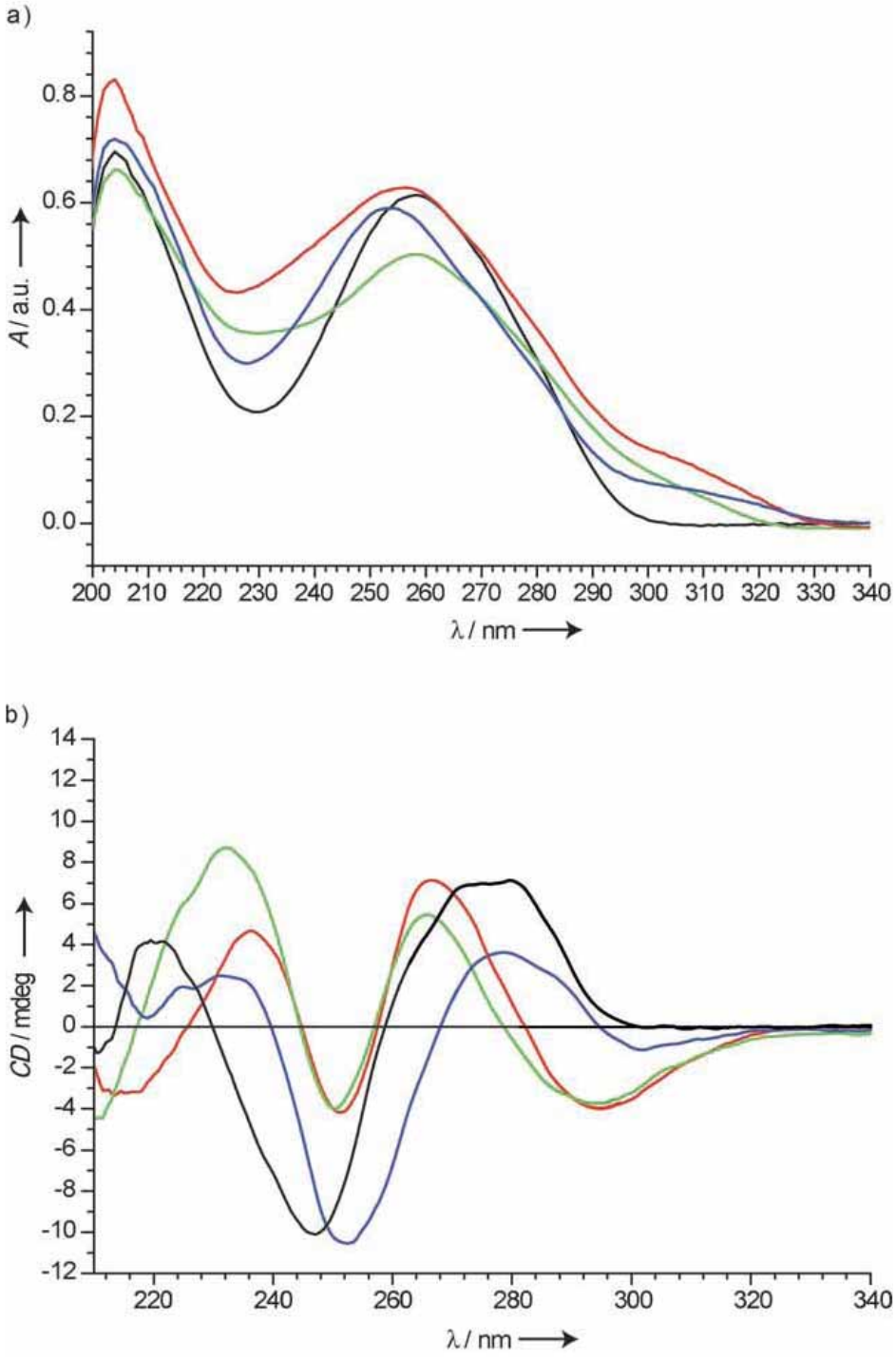

Figure 5.4 a) UV/Vis and b) CD spectra of the 300-base-pair PCR amplicons PCR300·**5.2** (—), PCR300 ·**5.3** (—), and PCR300·**5.4** (—). The spectra of the control amplicon PCR300·**N** (c) are shown in black.

The incorporation of modified triphosphates **5.2**-**5.4** influences the UV spectra of the resulting PCR amplicons as a consequence of the increased π conjugation of the pyrimidine ring due to the presence of the alkyne group. This results in new absorbances in the 300-320 nm region (Figure 5.4a). The UV-absorption spectra feature a small hypsochromic shift of about 5-10 nm for the 260 nm band. The CD spectra reveal an overall B-type secondary structure for all of the generated DNA amplicons (Figure 5.4b). The CD spectra of PCR300·**N** and PCR300·**5.4** show positive maxima between 230-250 nm and 270-290 nm and minima in the 250-260 nm region. Interestingly, the CD spectra of the modified amplicons feature an additional minimum between 280-300 nm due to the additional absorbance in this region.

5.3.5 Analysis of the Click Efficiency

As the alkynes present anchor groups onto which we intended to click various functional molecules, we next investigated the efficiency of the click reaction on DNA strands with hundreds of alkynes. For this investigation, we first performed the click reaction on the amplicons and subsequently digested the obtained DNA products by using a mixture of DNA degrading enzymes (*Penicillium citrinum* nuclease P1, calf spleen phosphodiesterase II, alkaline phosphatase, and *Crotalus adamanteus* snake venom phosphodiesterase I). The mixture of nucleotides obtained was subsequently analyzed by using HPLC-MS/MS. For the investigation we used the shorter PCR300·**5.2**-**5.4** amplicons and the large PCR2000·**5.4** amplicon as examples and the sugar azide **5.1** as the clicking partner. The reaction was conducted by using a copper(I)-stabilizing ligand[24] and CuBr. After a reaction time of 2 h, the DNA was purified by ethanol precipitation.

The results are depicted in Figure 5.5. Enzymatic digests of the amplicons before the reaction provide four peaks corresponding to the monomers of the triphosphates used for the PCR, plus a small amount of inosine which is formed due to deamination of dA under the reaction conditions. Analysis of the amplicons after the click reaction gave clean chromatograms for all of the modified amplicons.

In addition, HPLC analysis of the enzymatic digestion of the products arising from PCR300·**5.2** and PCR300·**5.3** revealed a surprisingly high clicking efficiency of ≥ 95%, according to integration of the residual starting material peaks (22.2 min for PCR300·**5.2**, 42.5 min for PCR300·**5.3**, Figure 5.5a) relative to the product peaks (23.2 min and 24.0 min for PCR300·**5.2,** 30.6 min and 31.2 min for 300·**5.3**, Figure 5.5b) at the diagnostic wavelength of 310 nm for 5-modified pyrimidines (see the UV spectra of the monomers in Section 5.5.6). An even higher efficiency was observed with the construct PCR300·**5.4**. Here, no alkyne starting nucleoside could be detected after the click reaction. The double peaks obtained for the clicked-on sugar nucleosides arise because of the rapid anomerization of the sugar moiety. This was confirmed by HPLC-MS/MS measurements, which showed the same expected molecular weight for both peaks (Section 5.5.8). The same almost-quantitative conversion was also observed for the click reaction with the PCR2000·**5.4** construct containing 887 alkyne modifications. They all were converted into the corresponding product, a result showing the amazing efficiency of the click reaction. To the best of our knowledge, the simultaneous high-yielding modification of more than 800 reaction sites in a single process is unprecedented in the literature.

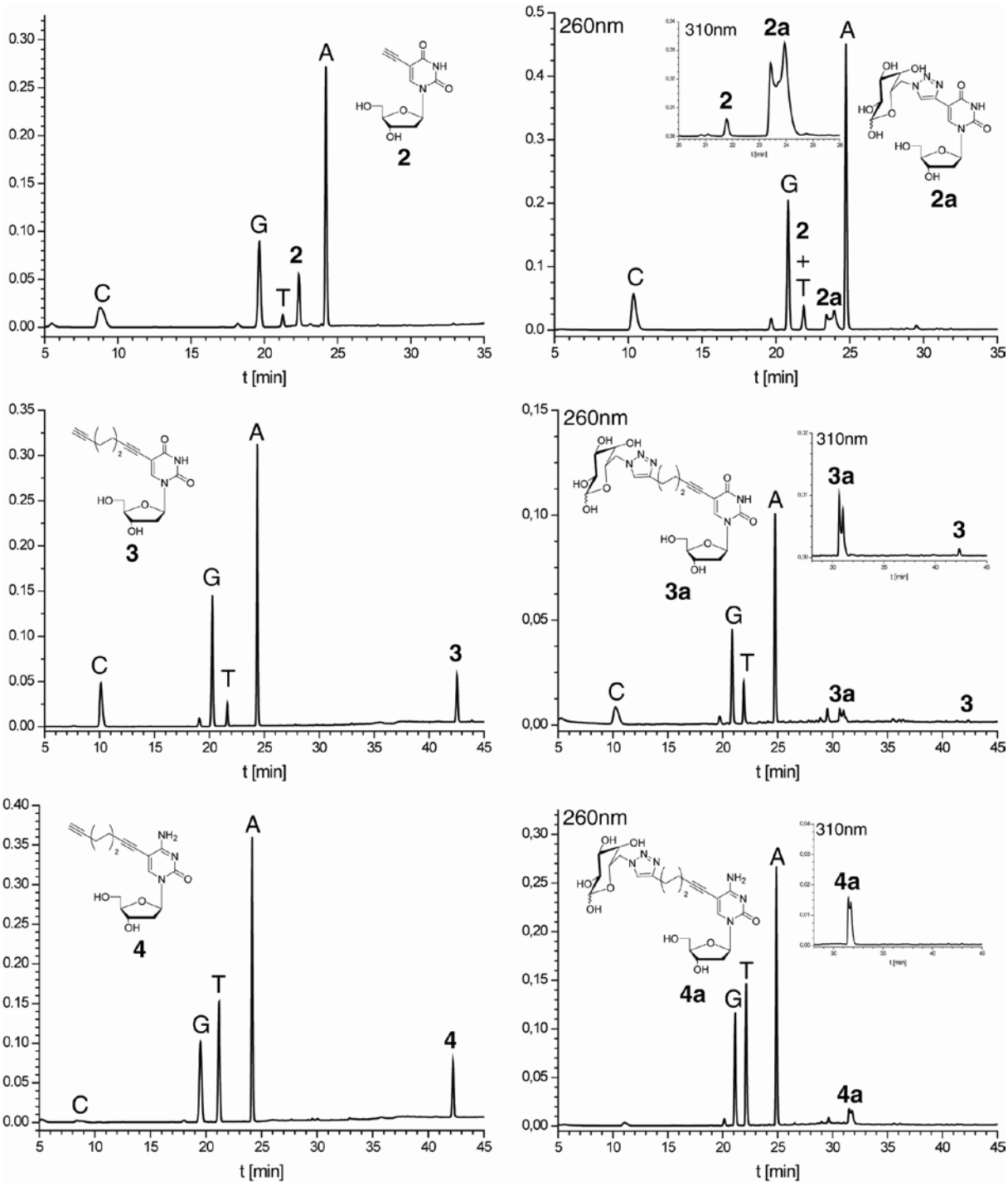

Figure 5.5 HPLC chromatograms of the enzymatic digests of PCR products a) PCR300·**5.2**, b) PCR300·**5.3**, and c) PCR300·**5.4** before (left) and after (right) the click reaction with **5.1** to form the corresponding products **5.2-5.4a**. (In the chromatogram for **5.2a**, the starting material **5.2** lies under the thymidine peak.) The insets show the HPLC traces at 310 nm. * Marks the peaks assigned to inosin, which is formed due to deamination during the assay. dA: deoxyadenosine, dC: deoxycytidine, dG: deoxyguanosine, T: thymidine.

5.4 Summary and Outlook

The incorporation of the different triphosphates **5.2-5.6** confirms the overall trends also observed in other studies. An extended π system improves the acceptance of a triphosphate by a DNA polymerase. The failed incorporation of **5.6** shows that a small modification of the structure of the monomer can induce massive incorporation problems. The reason for this is still not clear and will require more extensive investigation. The stability of the PCR products obtained with the triphosphates **5.2**-**5.4** gives more insight into how they influence the DNA strand structure. All of the alkyne modifications stabilize the DNA with respect to the natural bases. The alkyne content of PCR300 is around 52% (153 alkyne base pairs) for the thymidines and 35% (104 alkyne base pairs) for the cytidines. Consequently, there are about 1.5 times more alkyne base pairs in PCR300·**5.2**/**5.3** than in PCR300·**5.4**. The destabilization of PCR300·**5.3** by about 3 °C compared to PCR300·**5.2** can be attributed to the increased steric clash of the longer alkyl chains in the major groove and the exclusion of water interactions in the major groove.[25] Although PCR300·**5.4** contains the same alkyl modifications, it is more stable than PCR300·**5.3**, possibly because of the decreased density of modifications and the increased stabilization induced by alkyne cytidines compared to alkyne thymidines.[26] Since the same trends are observed in the 900-base-pair series, the stability differences seem to be a general property of PCR products with similar base composition (Section 5.5.3). The increased thermal stability of the modified DNA seems to be the problem when the PCR reaction with triphosphate **5.4** is used for longer PCR products,while the higher density or the sequence of the template seems to be the problem for triphosphate **5.3**.

The differences observed in the CD spectra of PCR300·**N** and PCR300·**5.2**-**5.4** can most likely be attributed to slightly altered base stacking as a consequence of the presence of the alkyne modifications in the 5-position of the pyrimidine nucleobases. The absorptions of the bases at around 300 nm cause an additional CD anomaly. Similar effects were observed by Famulok and co-workers[8] and by He and Seela[27] for either shorter or synthetic DNA strands. Due to the length of the PCR products measured in this study, the unmodified primer regions should not influence the result. What can be deduced from the spectra with reasonable confidence is that the modified DNA still has a B-like conformation. Since the spectra of the longer PCR products are almost identical to the PCR300 series, the measured effects seem to be averaged properties of PCR products with a similar base composition (Section 5.5.6).

The unusually high clicking efficiency observed for PCR300·**5.2** was unexpected considering the less than optimal yields observed in our previous oligonucleotide study.[19] One could speculate that this deviation is a consequence of the secondary structures of the two systems. In the short oligonucleotide series, we utilized single-stranded 16-mers, whereas double-stranded PCR fragments were used for the click reaction in this study. The single-stranded oligonucleotides have greater flexibility and may adopt a variety of secondary structures in solution. This, in turn, might sequester certain alkyne groups. This would be less likely in a PCR fragment where the alkyne functions are pointing out of the major groove in a rather stiff double-helix environment.

An additional explanation of this observed result may be the density of alkyne modifications found in the primary sequence of the PCR fragments. Our preliminary oligonucleotide study revealed that consecutive stretches of truncated alkyne functions decreased the clicking effi-

ciency markedly, yet the primary sequence of PCR300 only contains six consecutive stretches of three thymidines and three consecutive stretches of four thymidines. Thus, the DNA templates used in this study are less demanding, although they are much longer.

The analysis of the products showed that the click conditions used do not induce any DNA damage, for example, no oxidized DNA bases like 8-oxo-dG were found in the enzymatic digest. Only when the reaction mixtures were heated or when they were concentrated at higher temperatures, minor side products were observed. As concluded from the mass spectrometry data, it is most likely that oxidized triazole species are only formed, if at all, through oxidation of the copper triazole species arising during the click reaction (Section 5.5.8).

This study establishes that PCR in combination with the click reaction provides a modular tool for the synthesis of highly modified DNA strands. The optimization of the PCR conditions shows that the stability of the resulting strands may require the design of special PCR programs. In the template series used, the incorporation of 5-modified cytidine triphosphates was found to be more efficient than that of 5-modified uridine triphosphates. The reason for this observation is not yet clear. Polymerases of the B family, like Pwo and KOD XL, are highly superior compared to the other polymerases tested when efficient incorporation of the modified triphosphates is desired. The click reaction is an extremely facile, simple, and efficient (yields of > 90% up to quantitative) method to convert the introduced alkynes, even on long DNA strands containing hundreds of modifications, into the click product of choice. The combination of PCR and the copper(I)-catalyzed reaction of alkynes with azides is a perfect and powerful marriage if the synthesis of highly modified oligonucleotides is desired. The influence of the single or double strand on the click reaction, especially for alkyne **2**, will be the subject of further studies.

5.5 Experimental Section

The synthesis of azide **5.1** has been reported before.[5]

5.5.1 Synthesis

Triphosphate **5.2**[21] and **5.4**[20] were synthesized according to literature procedures.

5-(Octa-1,7-diynyl)- 5'-*O*-triphosphate-2'-deoxyuridine (**5.3**)

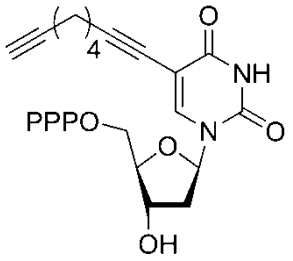

To a cooled solution (0° C) of **5.7**[19] (100 mg, 0.301 mmol) and 1,8-bis(dimethylamino)naphthalene (proton sponge, 103 mg, 0.652 mmol) in trimethyl phosphate (1.0 mL) was added phosphorous oxychloride (41 µL , 0.45 mmol) dropwise over 10 min under a nitrogen atmosphere. The reaction mixture was stirred for 3 h at 0° C. A solution of tributylammonium pyrophosphate (189 mg, 0.55 mmol) and N(*n*-Bu)$_3$ (0.48 mL) in dry DMF (3 mL) was added to the reaction mixture and stirred for 20 min followed by quenching with triethylammonium bicarbonate (1.0 M, 20 mL, pH 8.5). The reaction mixture was stirred for 2 h and lyophilized over night. RP-HPLC purification (0-50% 0.1 M triethylammonium acetate $\rightarrow$ 20 : 80 H_2O : MeCN with 0.1 M triethylammonium acetate gradient over 45 min at a flow rate of 5 mL min^{-1}) yielded **5.2** (30.2 min) as the triethylammonium salt (8.5 mg pure product isolated, 2%).
^{31}P-NMR (81 MHz, D_2O): δ = -22.4 (t, 1P, *J* = 20.2 Hz, -β), -10.5 (d, 1P, *J* = 20.4 Hz, -α), -9.7 (d, 1P, *J* = 20.1 Hz, -γ). MS (MALDI-TOF): 570.6 $[M + 2 H]^-$.

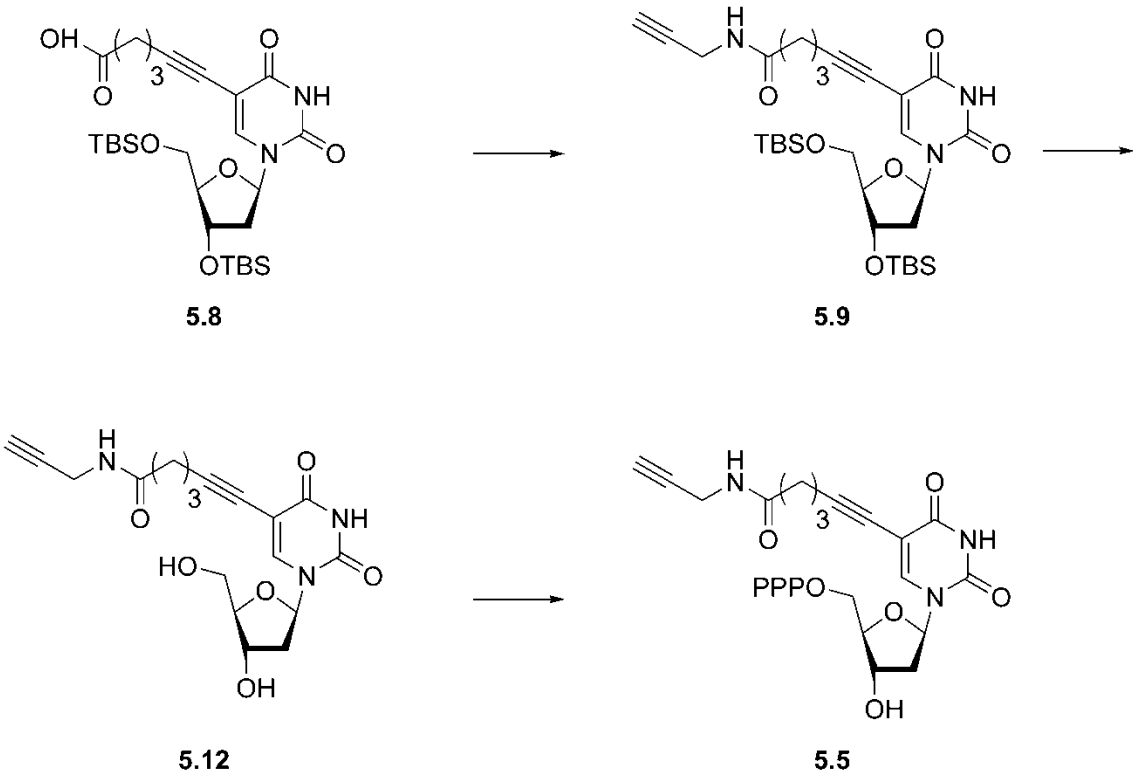

Scheme 5.4 Synthesis of **5.5**.

5-[*N*-(2-Propynyl)-(1-hexyne-6-amide)]-3',5'-di-*O*-(*tert*-butyldimethylsilyl)-2'-deoxyuridine (**5.9**)

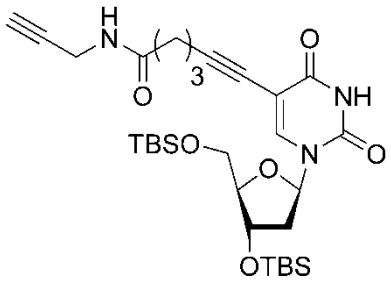

Compound **5.8**[28] (250 mg, 0.441 mmol) was dissolved in dry DCM (11 mL) and cooled to 0 °C. HOBT (149 mg, 1.10 mmol), HBTU (251 mg, 0.662 mmol), HATU (335 mg, 0.882 mmol), DIPEA (0.2 mL, 1.32 mmol) and dry DMF (12 mL) were added and the mixture stirred for 5 min at 0 °C. After the addition of propargyl amine (37 µL, 0.57 mmol), the reaction mixture was allowed to come to r. t. and stirred for additional 2 h. The solvent was removed *in vacuo*, the reaction mixture re-dissolved in DCM (100 mL) and washed twice with H_2O (2 × 100 mL). The combined aqueous phases were extracted again with DCM (100 mL). The combined organic phases were dried over $MgSO_4$, adsorbed onto silica gel and purified by column chromatography (*i*Hex:EtOAc 2:1 → 1:1), providing **5.9** (200 mg, 0.331 mmol, 75%) as a yellow solid.

^{1}H-NMR (600 MHz, $CDCl_3$): δ = 0.07 (s, 3H, CH_3), 0.08 (s, 3H, CH_3), 0.13 (s, 3H, CH_3), 0.14 (s, 3H, CH_3), 0.89 (s, 9H, $C(CH_3)_3$), 0.93 (s, 9H, $C(CH_3)_3$), 1.90 (quin, 2H, *J* = 6.7 Hz,

$CH_2CH_2CH_2$), 2.02 (m, 2H, $C_{2'}H$), 2.16 (t, 1H, J = 2.5 Hz, $HCC{\equiv}CH_2NH$), 2.42 (t, 1H, J = 6.5 Hz, $C(=O)CH_2CH_2$), 2.48 (t, 2H, J = 6.9 Hz, $CH_2CH_2C{\equiv}C$), 3.76 (dd, 1H, J = 11.4, 1.8 Hz, $C_{5'}H$), 3.90 (dd, 1H, J = 11.4, 1.8 Hz, $C_{5'}H$), 3.97-3.95 (m, 1H, $C_{4'}H$), 4.04 (dd, 2H, J = 5.4, 2.5 Hz, $HCCCH_2NH$), 4.39-4.41 (m, 1H, $C_{3'}H$), 6.30 (t, 1H, J = 6.6 Hz, $C_{1'}H$), 7.01 (s, 1H, NHC(=O)), 7.98 (s, 1H, C_6H), 8.94 (s, 1H, NH). ^{13}C-NMR (150 MHz, $CDCl_3$): δ = -5.5 (CH_3), -5.4 (CH_3), -4.9 (CH_3), -4.6 (CH_3), 14.7, 17.5, 18.1 ($CH_2CH_2C{\equiv}C$), 20.8, 23.6, 23.9 ($CH_2CH_2CH_2$), 25.7 (3C, $C(CH_3)_3$), 26.0 (3C, $C(CH_3)_3$), 29.0 ($HC{\equiv}CCH_2NH$), 34.3 ($NHC(=O)CH_2CH_2$), 38.7, 42.1 ($C_{2'}$), 62.9 ($C_{5'}$), 72.2 ($C_{3'}$), 85.7 ($C_{1'}$), 88.4 ($C_{4'}$), 94.6 ($CH_2CH_2C{\equiv}C$), 100.4 (C_5), 141.4 (C_6), 149.0 (C_2), 162.8 (C_4), 172.4 ($C(=O)NHCH_2$). HRMS (ESI): calcd. for $C_{30}H_{51}N_3O_6Si_2^+$: 604.3234 $[M+H]^+$, found 604.3242.

5-[*N*-(2-Propynyl)-(1-hexyne-6-amide)]-2'-deoxyuridine (**5.12**)

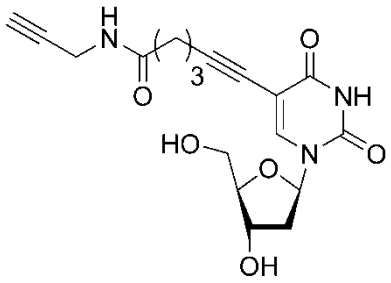

5.9 (180 mg, 0.298 mmol) was dissolved in 2 mL dry pyridine, syringed into a Schlenk flask, evaporated to dryness and re-dissolved in 12 mL dry THF. A solution of TBAF in THF (1 M, 0.66 mL) was added and the mixture stirred at r. t. over night. The reaction mixture was adsorbed onto silica gel and purified by column chromatography (DCM/MeOH 10:1), giving **5.12** (81 mg, 0.216 mmol, 72%) as a yellow oil.
^{1}H-NMR (400 MHz, CD_3OD): δ = 1.87 (quin, 2H, J = 7.1 Hz, $CH_2CH_2CH_2$), 2.20-2.26 (m, 1H, $C_{2'}H$), 2.31 (d, 1H, ^2J = 13.6 Hz, J = 6.4 Hz, J = 3.6 Hz, $C_{2'}H$), 2.38 (t, 2H, J = 7.4 Hz, $CH_2CH_2C{\equiv}C$), 2.44 (t, 2H, J = 6.9 Hz, $C(=O)CH_2CH_2$), 2.57 (t, 1H, J = 2.5 Hz, $CH_2C{\equiv}CH$), 3.75 (dd, 1H, J = 12.0, 3.4 Hz, $C_{5'}H$), 3.83 (dd, 1H, J = 12.0, 3.0 Hz, $C_{5'}H$), 3.92-3.97 (m, 3H, $C_{4'}H$, $CH_2NHC(=O)$), 4.40-4.42 (m, 1H, $C_{3'}H$), 6.25 (t, 1H, J = 6.6 Hz, $C_{1'}H$), 8.26 (s, 1H, C_6-H). ^{13}C-NMR (100 MHz, CD_3OD): δ = 19.6 (CH_2), 24.9 (CH_2), 29.5 (CH_2), 35.6 (CH_2), 41.7 ($C_{2'}$), 59.6, 62.6 ($C_{5'}$), 72.0 ($C_{3'}$), 73.7, 80.7, 87.0 ($C_{1'}$), 89.2 ($C_{4'}$), 94.1 (C_5), 101.0 (CH_2CH_2CC), 144.5 (C_6), 151.3 (C_2), 164.9 (C_4), 175.1 ($CH_2C(=O)NH$). HRMS (ESI) calcd. for $C_{18}H_{22}N_3O_6^+$: 376.1504 $[M+H]^+$, found 376.1506.

5-[*N*-(2-Propynyl)-(1-hexyne-6-amide)]-5′-*O*-triphosphate-2'-deoxyuridine (**5.5**)

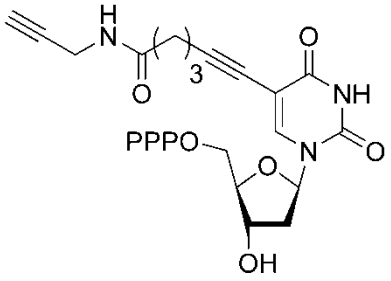

The day before the reaction was run, **5.12** was co-evaporated twice with dry pyridine. Both solutions described below were dried over molecular sieves (4 Å) over night. To a cooled solution (0 °C) of **5.12** (61 mg, 0.16 mmol) and 1,8-bis(dimethylamino)naphthalene (proton sponge, 53 mg, 0.25 mmol) in trimethyl phosphate (1.2 mL) was added phosphorous oxychloride (18 µL, 0.20 mmol) dropwise over 5 min under a nitrogen atmosphere. The reaction mixture was stirred for 3 h at 0° C. A solution of tributylammonium pyrophosphate (161 mg, 0.303 mmol) and 257 µL tributyl amine (1.1 mmol) in dry DMF (2 mL) was added to the reaction mixture and stirred for 10 min followed by quenching with triethylammonium bicarbonate (1.0 M, 23 mL, pH 8.5). The reaction mixture was left standing at r. t. for 2.5 h and lyophilized over night. RP-HPLC purification (0.1 M triethylammonium acetate buffer, A: H_2O, B: H_2O/MeCN 1:4, 0→ 40% B linear gradient over 45 min at a flow rate of 5 mL min^{-1}) yielded **5.5** (24.1 min, 2.0 mg, 3.3 µmol, 2%) as the triethylammonium salt.
^{31}P-NMR (81 MHz, D_2O): δ: -22.5 (t, 1P, J = 20.2 Hz, -β), -11.4 (d, 1P, J = 20.2 Hz, -α), -10.0 (d, 1P, J = 19.8 Hz, -γ). MS (MALDI-TOF): $[M + 4H]^-$ 613.9.

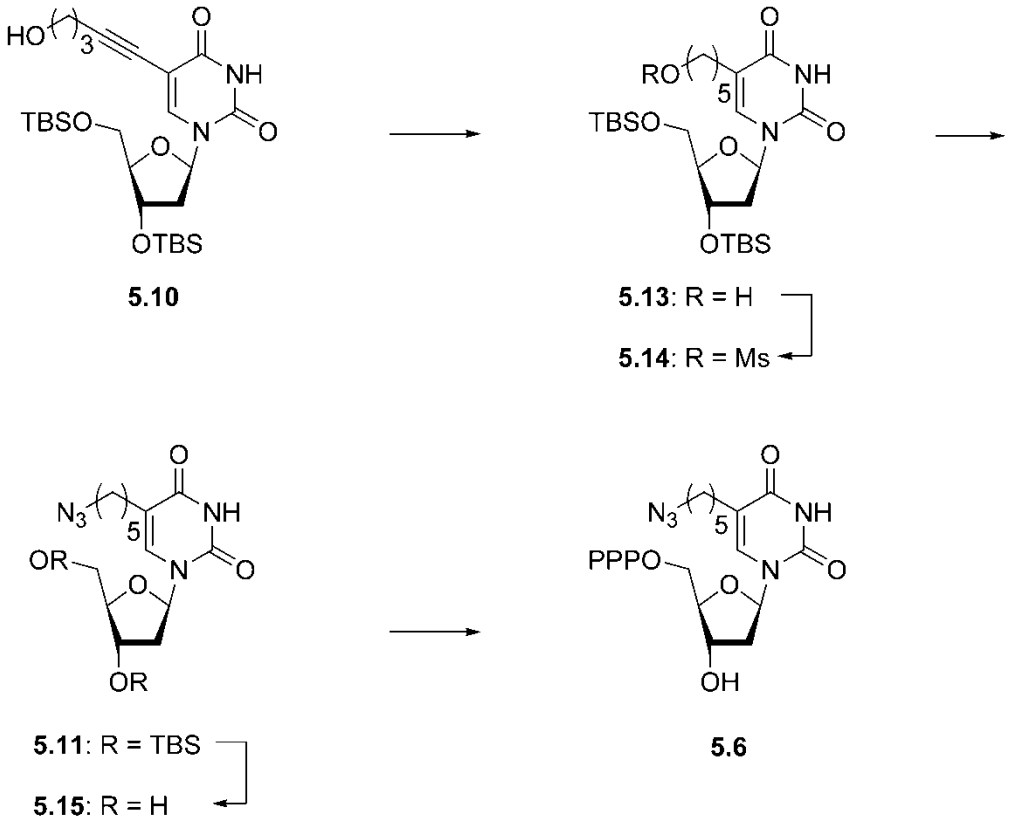

Scheme 5.5 Synthesis of **5.6**.

5-(Pentane-5-ol)-3′,5′-di-*O-tert*-butyldimethylsilyl-2'-deoxyuridine (**5.13**)

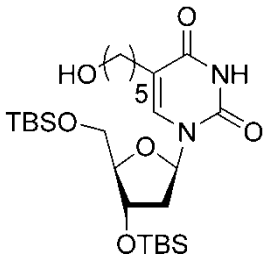

To a solution of **5.10**[5] (0.60 g, 1.12 mmol) in degassed EtOAc/MeOH (1:1, 30 mL) was added 10% Pd/C (0.30 g). The reaction mixture was saturated with H_2 gas and stirred at r. t. over night. The reaction mixture was filtered and concentrated *in vacuo*. Flash column chromatography (SiO_2) eluting with a gradient of *i*Hex → *i*Hex/EtOAc 1:1 provided **5.13** (0.44 g, 73%) as a white solid.
^{1}H-NMR (600 MHz, $CDCl_3$): δ = -0.03 (s, 3H, $OSiCH_3$), -0.05 (s, 3H, $OSiCH_3$), 0.00 (s, 6H, $OSiCH_3$), 0.78 (s, 9H, $C(CH_3)_3$), 0.82 (s, 9H, $C(CH_3)_3$), 1.28 (m, 2H, CH_2), 1.42 (m, 2H, CH_2), 1.48 (m, 2H, CH_2), 1.89 (m, 1H, $C_{2'}H$), 2.18 (m, 4H, $C_{2'}H$, CH_2, CH_2-O*H*), 3.52 (t, 2H, *J* = 6.6 Hz, CH_2), 3.65 (dd, 1H, *J* = 11.3, 2.6 Hz, $C_{5'}H$), 3.76 (dd, 1H, *J* = 11.3, 2.6 Hz, $C_{5'}H$), 3.82 (d, 1H, *J* = 2.6 Hz, $C_{4'}H$), 4.30 (m, 1H, $C_{3'}H$),6.21 (dd, 1H, *J* = 7.9, 5.8 Hz, $C_{1'}H$), 7.30 (s, 1H, C_6H), 9.46 (s, 1H, NH). ^{13}C-NMR (150 MHz, $CDCl_3$): δ = -5.0 ($SiCH_3$), -4.9 ($SiCH_3$), -4.4 ($SiCH_3$), -4.2 ($SiCH_3$), 17.9 (Si*C*$(CH_3)_3$), 18.3 (Si*C*$(CH_3)_3$), 25.3 (-CH_2-), 25.7 (SiC(*C*$H_3)_3$), 25.9 (SiC(*C*$H_3)_3$), 27.2 (-CH_2-), 28.8 (-CH_2-), 32.3 (-CH_2-), 41.2 ($C_{2'}$), 62.5 (-CH_2-), 62.9 ($C_{5'}$), 72.1 ($C_{3'}$), 84.8 ($C_{1'}$), 87.7 ($C_{4'}$), 115.1 (C_5), 135.4 (C_6), 150.3 (C_2), 163.7 (C_4). HRMS (FAB) calcd. for $C_{26}H_{51}N_2O_6Si_2^+$: 543.3280 $[M+H]^+$, found 543.2960.

5-(5-Azidopentane)-3′,5′-di-*O-tert*-butyldimethylsilyl-2'-deoxyuridine (**5.11**)

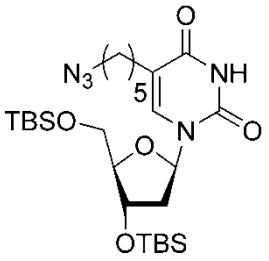

To a cooled solution (0 ° C) of **5.13** (0.43 g, 0.80 mmol) and DIPEA (208 µL, 1.2 mmol) in DCM (10 mL) was added mesityl chloride (74 µL, 1.2 mmol) under a nitrogen atmosphere. The reaction mixture was then allowed to warm to r. t. and stirred for a further 90 min, followed by quenching with brine. The crude mixture was then diluted with DCM (250 mL) and the organic layer was washed with brine (2 x 50 mL) and water (1 x 50 mL). The organic layer was retained, dried ($MgSO_4$) and concentrated *in vacuo*. Flash column chromatography

(SiO_2) eluting with a gradient of *i*Hex → *i*Hex/EtOAc 1:1 provided **5.14** (0.45 g, 91%) as a colorless oil which was used directly in the next step.

To a solution of **5.14 (**0.28 g, 0.45 mmol) in DMF (10 mL) was added NaN_3 (0.15 g, 2.24 mmol) under a nitrogen atmosphere. The reaction mixture was stirred at r. t. over night, followed by dilution with EtOAc (300 mL). The organic layer was washed several times with brine (4 × 50 mL) and water (2 × 50 mL). The organic layer was retained, dried ($MgSO_4$) and concentrated *in vacuo*. Flash column chromatography (SiO_2) eluting with a gradient of *i*Hex → *i*Hex/EtOAc 3:7 provided **5.11** (0.21 g, 82%) as a colorless foam.

^{1}H-NMR (600 MHz, $CDCl_3$): δ = 0.07 (s, 3H, $OSiCH_3$), 0.07 (s, 3H, $OSiCH_3$), 0.10 (s, 6H, $OSiCH_3$), 0.89 (s, 9H, $C(CH_3)_3$), 0.92 (s, 9H, $C(CH_3)_3$), 1.38 (m, 2H, CH_2), 1.54 (m, 2H, CH_2), 1.60 (m, 2H, CH_2), 1.98 (m, 1H, $C_{2'}H$), 2.22 (m, 1H, $C_{2'}H$), 2.30 (m, 2H, CH_2), 3.25 (t, 2H, *J* = 6.9 Hz, CH_2), 3.75 (dd, 1H, *J* = 11.3, 2.6 Hz, $C_{5'}H$), 3.81 (dd, 1H, *J* = 11.3, 2.6 Hz, $C_{5'}H$), 3.91 (d, 1H, *J* = 2.6 Hz, $C_{4'}H$), 4.39 (m, 1H, $C_{3'}H$), 6.31 (dd, 1H, *J* = 8.1, 5.7 Hz, $C_{1'}H$), 7.40 (s, 1H, C_6H), 9.20 (s, 1H, NH). ^{13}C-NMR (150 MHz, $CDCl_3$): δ = -5.4 ($SiCH_3$), -5.4 ($SiCH_3$), -4.8 ($SiCH_3$), -4.7 ($SiCH_3$), 18.0 ($SiC(CH_3)_3$), 18.4 ($SiC(CH_3)_3$), 25.8 ($SiC(CH_3)_3$), 25.9 ($SiC(CH_3)_3$), 26.4 ($-CH_2-$), 27.3 ($-CH_2-$), 28.6 (2C, $-CH_2-$), 41.2 ($C_{2'}$), 51.3 ($-CH_2-$), 63.0 ($C_{5'}$), 72.3 ($C_{3'}$), 84.9 ($C_{1'}$), 87.8 ($C_{4'}$), 114.9 (C_5), 135.5 (C_6), 150.2 (C_2), 163.4 (C_4). IR (KBr, cm^{-1}): 2094. HRMS (FAB): calcd. for $C_{26}H_{50}N_5O_5Si_2^+$: 568.3345 $[M+H]^+$, found 568.3341.

5-(5-Azidopentane)-2'-deoxyuridine (**5.15**)

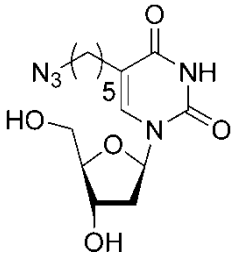

To a cooled solution (0 °C) of **5.11** (0.50 g, 0.88 mmol) in THF (5 mL) was added TBAF (1.0 M, 1.90 mL, 1.90 mmol) under a nitrogen atmosphere. The reaction mixture was stirred for 3 h, quenched with glacial acetic acid (1.0 mL) and concentrated *in vacuo*. Flash column chromatography (SiO_2) eluting with EtOAc/MeOH (10:1) provided **5.15** (0.45 g, 91%) as a colourless oil.

^{1}H-NMR (400 MHz, d_6-acetone): δ = 1.40 (m, 2H, CH_2), 1.52 (m, 3H, $C_{2'}H$, CH_2), 1.59 (m, 2H, CH_2), 2.20 (m, 3H, $C_{2'}H$, CH_2), 3.32 (t, 2H, *J* = 6.9 Hz, CH_2), 3.55 (sbr, 2H, -OH), 3.79 (m, 2H, $C_{5'}H$), 3.92 (q, 1H, *J* = 6.0 Hz, $C_{4'}H$), 4.49 (m, 1H, $C_{3'}H$), 6.31 (t, 1H, *J* = 6.6 Hz, $C_{1'}H$), 7.80 (s, 1H, C_6H), 10.00 (s, 1H, NH). ^{13}C-NMR (150 MHz, d_6-acetone): δ = 28.7 ($-CH_2-$), 29.2 ($-CH_2-$), 30.5 ($-CH_2-$), 31.1 ($-CH_2-$), 43.0 ($C_{2'}$), 53.4 ($-CH_2-$), 62.4 ($C_{5'}$), 74.0 ($C_{3'}$), 87.6 ($C_{1'}$), 90.5 ($C_{4'}$), 116.0 (C_5), 139.1 (C_6), 153.1 (C_2), 166.0 (C_4). IR (KBr, cm^{-1}): 2098.

5-(5-Azidopentane)-5′-*O*-triphosphate-2'-deoxyuridine (**5.15**)

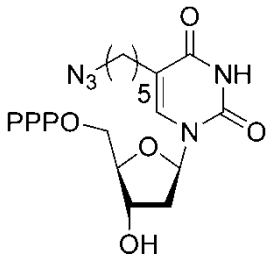

To a cooled solution (0° C) of **5.15** (67 mg, 0.2 mmol) and 1,8-bis(dimethylamino)- naphthalene (proton sponge, 69 mg, 0.32 mmol) in trimethyl phosphate (2 mL) was added phosphorous oxychloride (21.6 µL, 0.23 mmol) dropwise over 5 min under a nitrogen atmosphere. The reaction mixture was stirred for 3 h at 0 °C. A solution of tributylammonium pyrophosphate (352 mg, 1.02 mmol) and 628 µL *n*Bu_3N in dry DMF (5.2 mL) was added to the reaction mixture and stirred for 1 min followed by quenching with triethylammonium bicarbonate (1.0 M, 20 mL, pH 8.5). The reaction mixture was stirred for 2 h and lyophilized over night. RP-HPLC purification (0.1 M triethylammonium acetate buffer, A: H_2O, B: H_2O/MeCN 1:4, 0→ 40% B linear gradient over 45 min at a flow rate of 5 mL min^{-1}) yielded **5.6** (42.2 min) as the triethylammonium salt.
^{31}P-NMR (81 MHz, D_2O): δ = -21.5, -11.0, -7.3. MS (MALDI-TOF): $[M + 2H]^-$ 577.8.

5.5.2 Primer Extension

For primer extension experiments an assay developed by Held *et al.* was used.[23] The sequences of the primer and the three different templates are listed in Table 5.1. For the incorporation of modified thymidines, the templates **T1** to **T3** are of increasing "difficulty" for the polymerase. While **T1** only tests the incorporation of one thymidine or a modified uracil, **T2** and **T3** force the polymerase to incorporate two or more modifications in a row.
The primer extensions were run in a total volume of 20 µL with the final concentrations of 750 nM primer, 900 nM template, 200 µM dNTPs, 1 × PCR buffer of the polymerase tested and 1 U polymerase. The primer and template were hybridized by heating to 95 °C and cooling to 4 °C in half of the volume. The other reagents except the polymerase were added. The extension was started by adding the polymerase and incubating the whole mixture for 10 min at 72 °C. The extension was then quenched with 2 µL EDTA (0.1 M, pH 7.5) and 10 µL gel loading buffer (*Bio-Rad*). From that solution 10 µL were run on a PAGE-Gel.

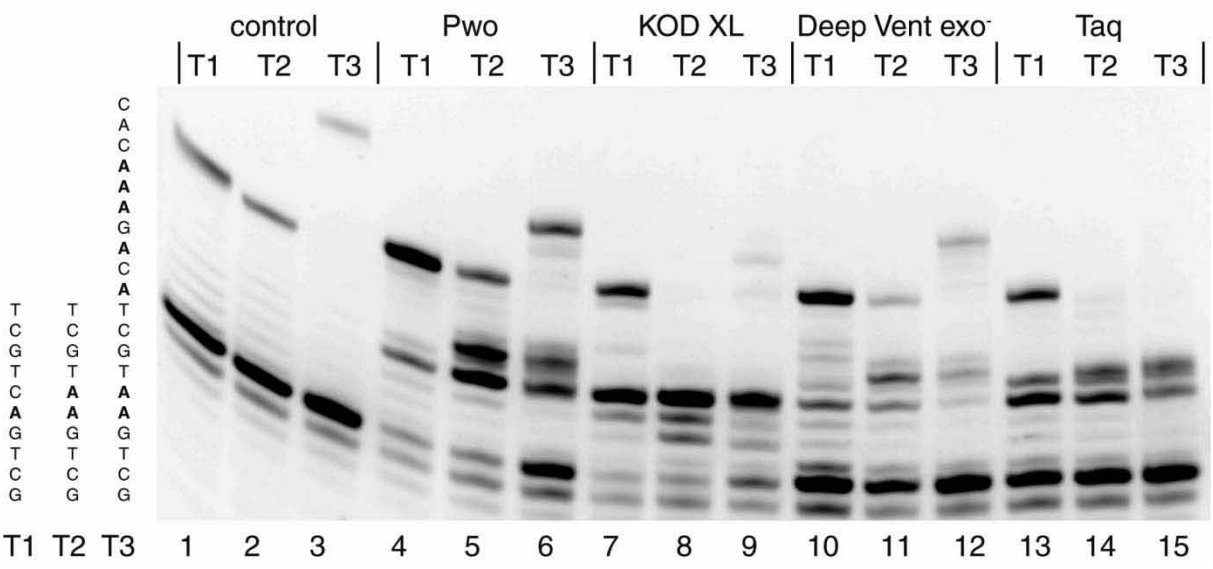

Figure 5.6 Incorporation test of the azide triphosphate **5.6** with different polymerases. Lane 1-3: natural control with Pwo, 4-6: Pwo 7-9: KOD XL, 10-12: Deep Vent exo$^-$, 13-15: Taq.

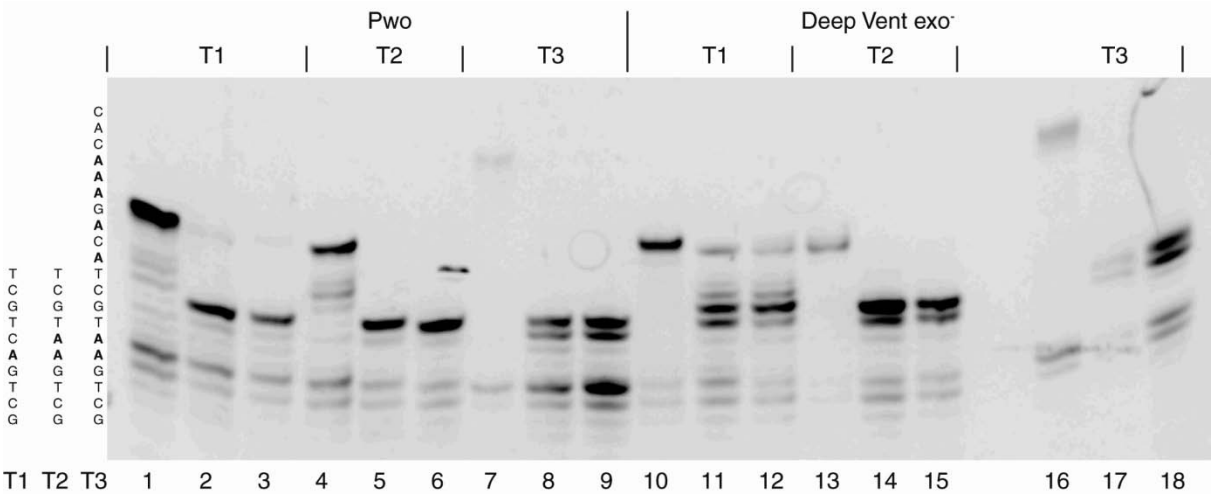

Figure 5.7 Incorporation test of the amide-linked triphosphate **5.5** with different polymerases. Lanes 1,4,7,10,13,16: dATP, dCTP, dGTP, TTP; lanes 2,5,8,11,14,17: dATP, dCTP, dGTP; lanes 3,6,9,12,15,18: dATP, dCTP, dGTP, **5.5**.

5.5.3 PCR Using the Modified Triphosphates

For PCR amplification the same primers and template as in previous studies was used.[19] Template is the Gateway expression vector pExp007-polη with the polymerase η gene from Rad30 *S. cerevisiae.* For all PCR products Primer 1 is the same while the reverse primer is shifted on the vector.

Primer 1 5′-TTA ATT GAA TTC GAT TTG GGC CGG ATT TGT TTC-3′
Primer 2 5′-TTT ATG CTA TCT CTG ATA CCC TTG-3′
Primer 3 5′-TGA TGC CCT TGT ACG CAA CTG-3′
Primer 4 5′-GGG TTA TTG TCT CAT GAG CG-3′

Table 5.3 Combination of primers used and length of the resulting PCR product and the number of exchanged thymidines and 2'-deoxycytidines in the modified PCR product.

Forward Primer	Reverse Primer	PCR product length (exchangeable bases)	Additives	PCR program
Primer 1	Primer 2	294 (T: 153, C: 104)	-	1
Primer 1	Primer 3	934 (T: 551, C: 352)	4 % DMSO	2
Primer 1	Primer 4	2149 (T: 1233, C: 887)	4 % DMSO	3

The PCR reactions were run on an eppendorf realplex^4 (silver block) in a total volume of 25 µL with 0.2 mM dNTPs, 0.3 µM primer, 400 ng template, 1 × PCR buffer and 1 U polymerase. For real time assays 1 µL of a 1:100 dilution of SYBR Green (10.000×; Fluka) in water was added. For **5.2**/Pwo only 0.25 µL were used. For production runs the total volume was doubled. The PCR reactions were purified using the Qiaquick PCR Purification Kit (Qiagen).

In a recent paper utilizing the PCR900•**5.4** PCR product for DNA metallization the PCR was run with PCR program 1.[20] These PCRs were run on an older eppendorf personal thermocycler. When compiling the data for this publication we found that no product was obtained on the "modern" eppendorf realplex machine using the same conditions. Comparing the temperature profiles of both machines we noticed that the older cycler tends to over- or understeer when reaching a set temperature. E. g. in the 15 s of annealing at 95 °C the block temperature reaches almost 98 °C for the first 10 s during the denaturing step. The newer cycler never overshoots the 95 °C during PCR. Since the compositions of the PCRs were identical, it seemed that these small temperature differences inhibited a successful experiment on the eppendorf realplex machine.

Table 5.4 PCR programs used for the different PCR products.

1		2		3	
95 °C, 2 min		95 °C, 2 min		99 °C, 2 min	
9x	95 °C, 15 s 58 °C, 30 s (-1 °C/cycle) 72 °C, 45 s	9x	99 °C, 15 s 58 °C, 30 s (-1 °C /cycle) 72 °C, 30 s	9x	99 °C, 45 s 58 °C, 30 s (-1 °C /cycle) 72 °C, 00 s
30x	95 °C, 15 s 57 °C, 30 s 72 °C, 45 s	30x	95 °C, 15 s 57 °C, 30 s 72 °C, 30 s	30x	99 °C, 45 s 59.3 °C, 30 s 72 °C, 00 s
72 °C, 2 min Hold 4 °C		72 °C, 2 min Hold 4 °C		72 °C, 10 min Hold 4 °C	

300 base pair PCR product (PCR300):

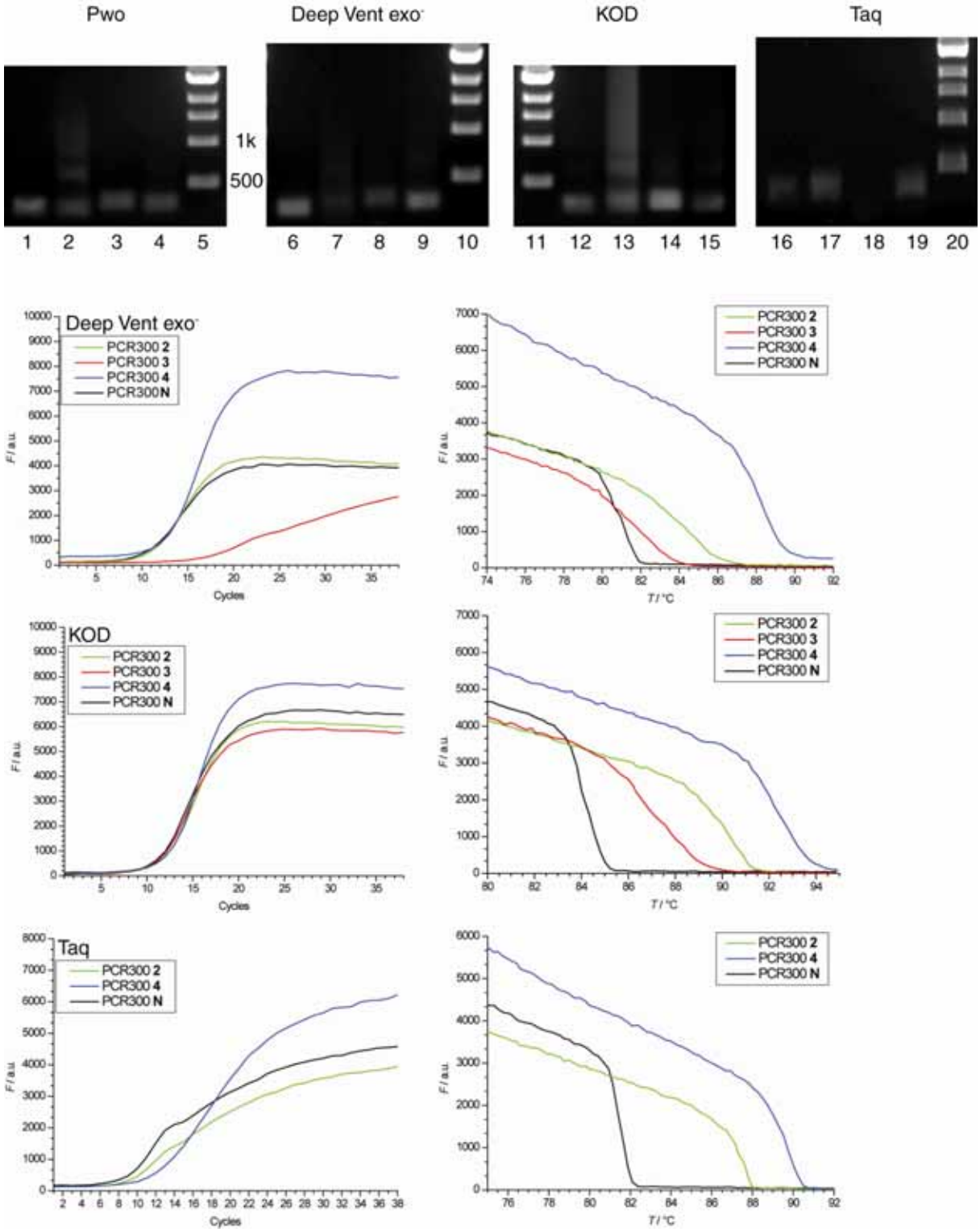

Figure 5.8 Above: agarose gels of the PCR reactions using different polymerases and triphosphates (lanes 1,6,12,16: dATP, dCTP, dGTP, TTP; lanes 2,7,13,17: dATP, dCTP, dGTP, **5.2**; lanes 3,8,14,18: dATP, dCTP, dGTP, **5.3**; lanes 4,9,15,19: dATP, **5.4**, dGTP, dTTP; lanes 5,10,11,20: DNA ladder; below: RT-PCR data and melting point profiles for the 300 base pair PCR product with different polymerases and triphosphates.

900 base pair PCR product (PCR900)

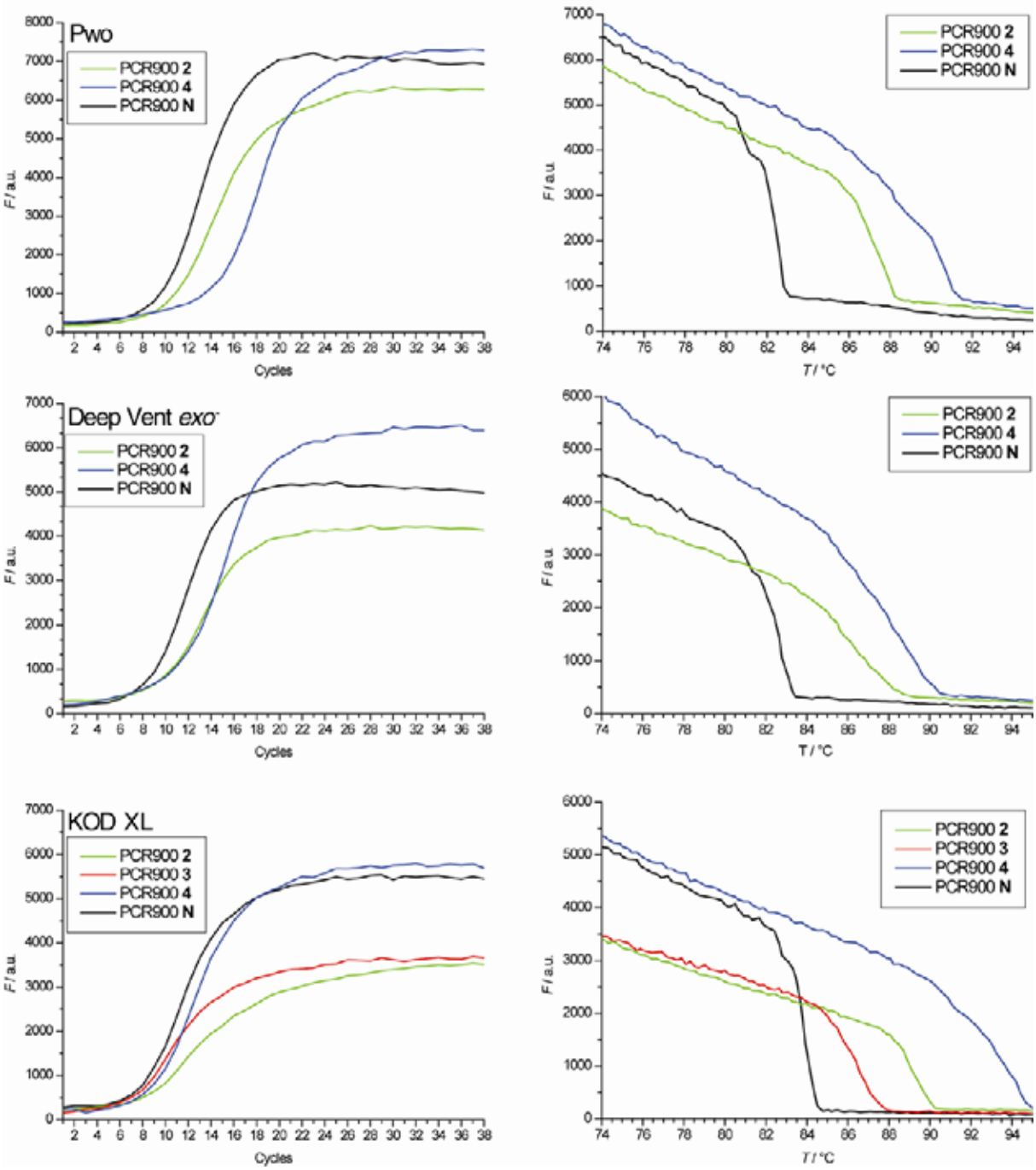

Figure 5.9 RT-PCR data and melting point profiles for the 900 base pair PCR products with different polymerases.

Table 5.5 Melting temperatures of the longer PCR products measured in the PCR-buffer including 4% DMSO.

PCR product	**Melting temperature (˚C)**		
	Pwo	*Deep Vent exo*$^-$	*KOD*
PCR900•**5.2**	87	86	89
PCR900•**5.3**	-	-	86
PCR900•**5.4**	90	89	93
PCR900•**N**	81	82	84

2000 base pair PCR product

(a)

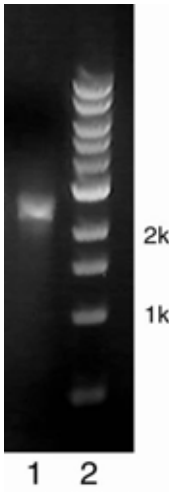

(b)

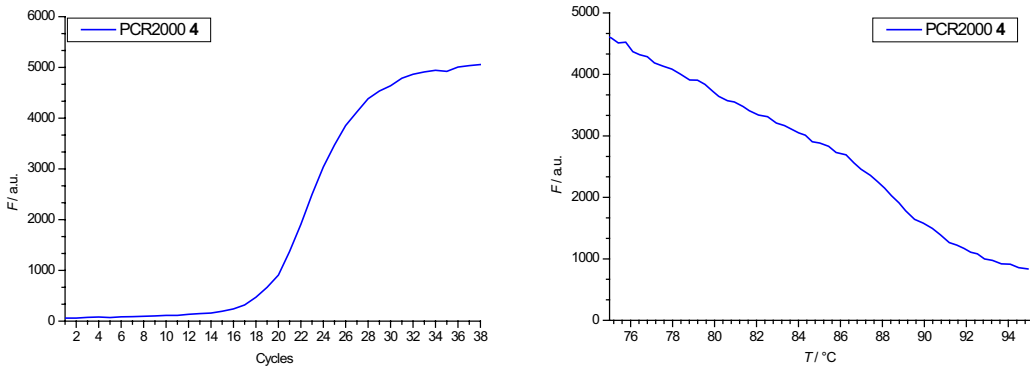

Figure 5.10 (a) Agarose gel of PCR-product. Lane 1: PCR2000•**5.4**; lane 2: DNA ladder and (b) RT-PCR profile and melting curve of PCR2000•**5.4.**

5.5.4 Sequence Analysis of the Modified PCR Products

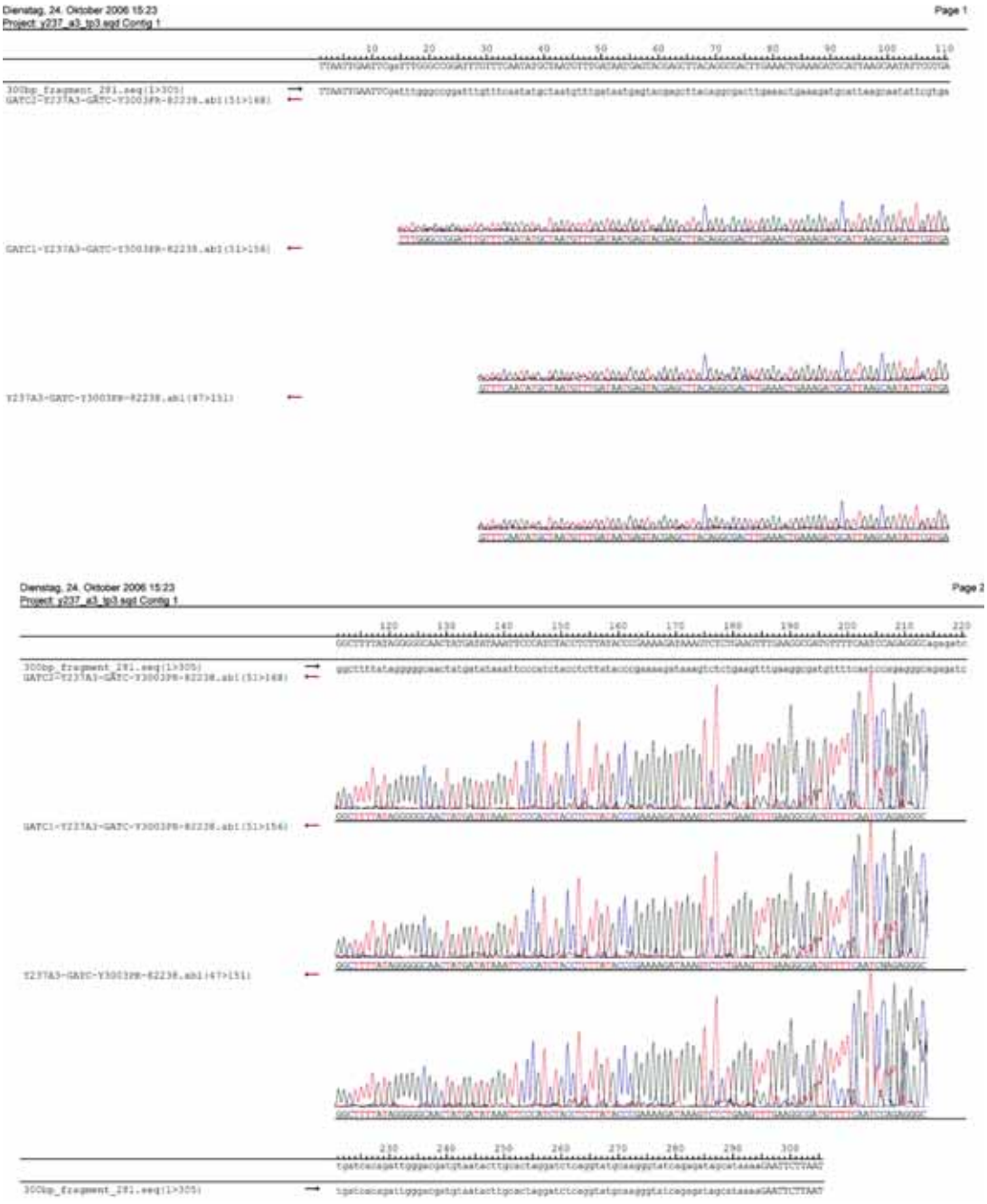

Figure 5.11 Sequencing from PCR300•**5.2**.

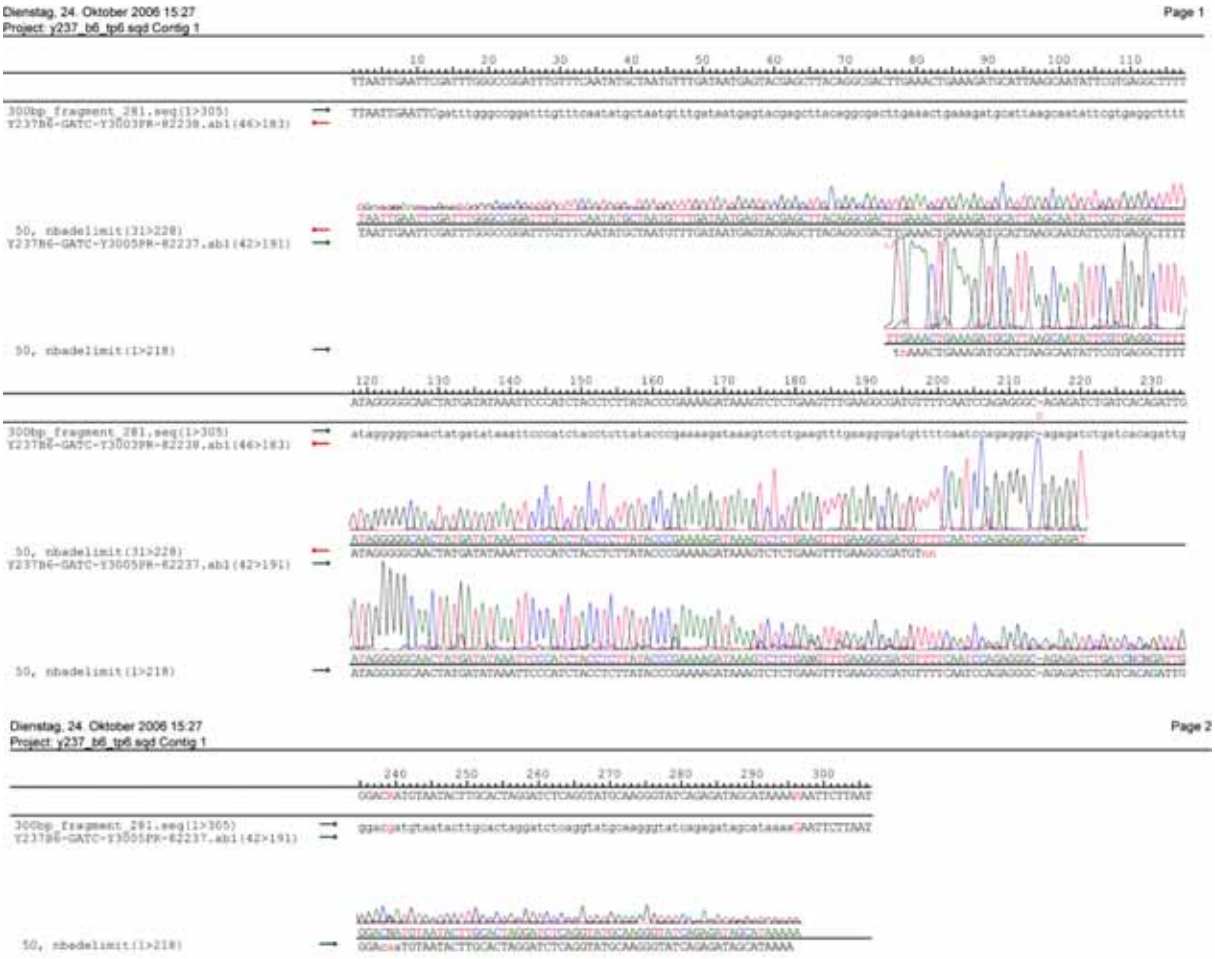

Figure 5.12 Sequencing from PCR300•**5.3**.

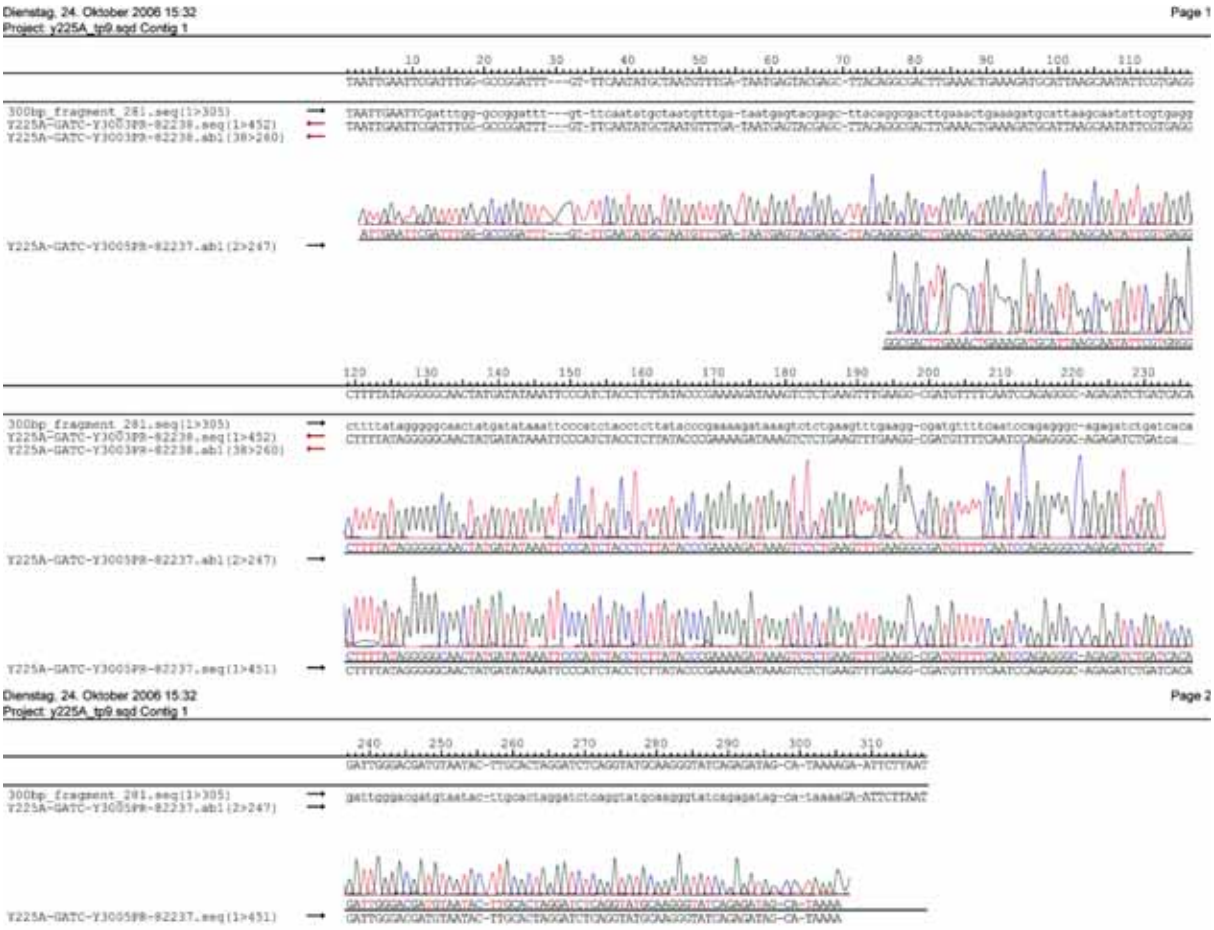

Figure 5.13 Sequencing from PCR300•**5.4**.

5.5.5 Restriction Assay

For the restriction assays 200 ng of DNA were incubated with 10 U of Bgl II or Tsp509 I (15 U for Bcl I) at the optimal temperature given by the manufacturer (New England Biolabs; Bgl II: 37 °C; Bcl I: 50 °C, Tsp509 I: 65 °C) in New England Biolabs restriction buffer 3 (50 mM Tris-HCl, 100 mM NaCl, 10 mM $MgCl_2$, 1 mM Dithiothreitol) for 1 h. The reaction mixture was purified using the PCR reaction cleanup kit (Qiagen) and analyzed by PAGE. The gel was stained with SYBR Green.

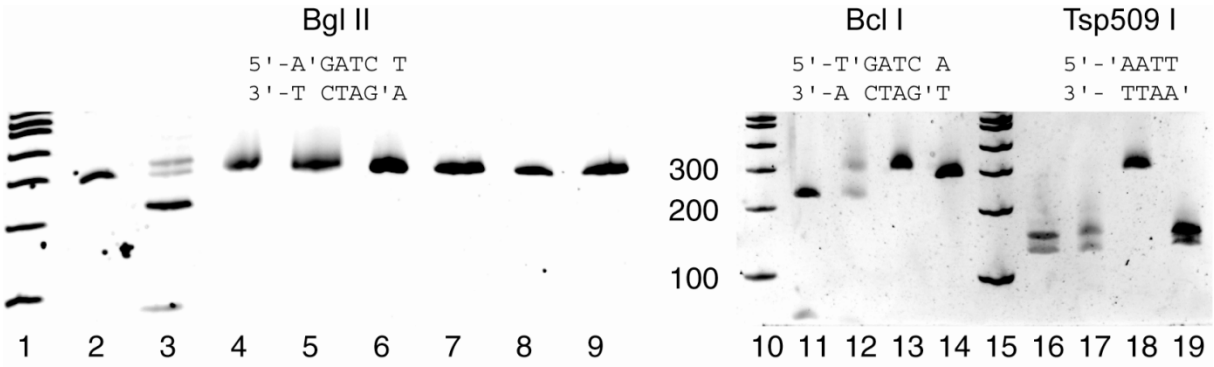

Figure 5.14 Restriction digest with the different PCR300•**N**,**5.2**,**5.3**,**5.4** products with different restriction enzymes (lanes 1,10,15: DNA ladder, lane 2: PCR300•**N**, lane 3: PCR300•**N** + Bgl II, lane 4: PCR300•**5.2**, lane 5: PCR300•**5.2** + Bgl II, lane 6: PCR300•**5.3**, lane 7: PCR300•**5.3** + Bgl II, lane 8: PCR300•**5.4**, lane 9: PCR300•**5.4** + Bgl II, lane 11: PCR300•**N** + Bcl I, lane 12: PCR300•**5.2** + Bcl I, lane 13: PCR300•**5.3** + Bcl I, lane 14: PCR300•**5.4** + Bcl I, lane 16: PCR300•**N** + Tsp509 I, lane 17: PCR300•**5.2** + Tsp509 I, lane 18: PCR300•**5.3** + Tsp509 I, lane 19: PCR300•**5.4** + Tsp509 I. The recognition sites of the enzymes are shown above.

5.5.6 UV- and CD-Spectroscopy

UV-spectra of the monomers of **5.2-5.4** (recorded during HPLC by the PDA, data normalized to **5.1**):

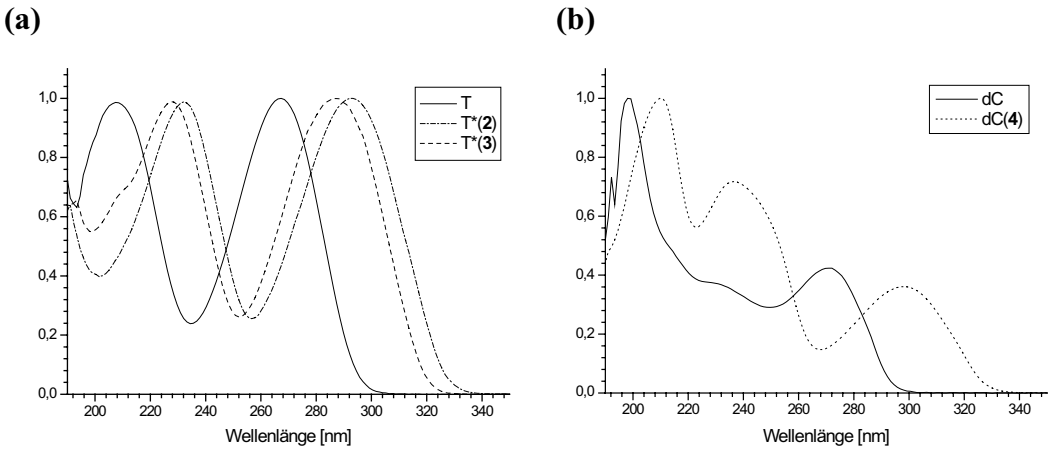

Figure 5.15 (a) UV-spectra of the modified monomers of **5.2** and **5.3**, (b) UV-spectra of the monomer of cytidine **5.4** in comparison with the natural base.

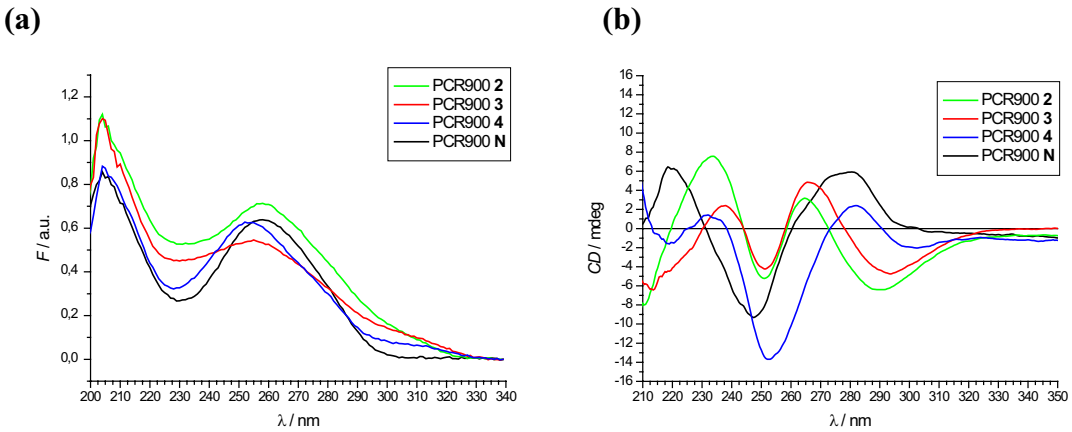

Figure 5.16 UV-spectrum (a) and CD-spectrum (b) of 900 base pair PCR product measured in 10 mM Tris/HCl. The addition of NaCl to adjust the salt concentration to 150 mM did not change the CD spectra.

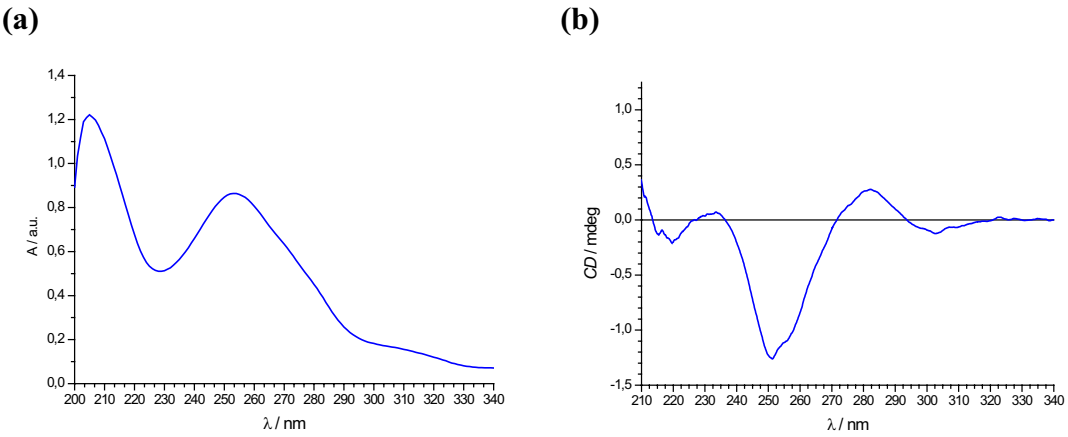

Figure 5.17 (a) UV-spectrum and (b) CD-spectrum of PCR2000•**5.4**.

5.5.7 Click on the PCR Product

General procedure

To a solution of DNA (300 µL with 80-90 ng/µL) a solution of sugar azide (300 µL, 50 mM in 10 mM Tris) and 100 µL CuBr-solution (10 mM, 1 mg CuBr (99.99%) dissolved in 700 µL 10 mM TBTA-ligand[24] in *t*BuOH/DMSO 1:3) were added and incubated for 2 h at r. t. The reactions were divided in three portions and precipitated with EtOH separately.

Purification

Ethanol precipitation can be done straight from the reaction mixture or from the carefully lyophilized sample. To the sample (example volume: ca. 50 µL) 150 µL Na^+OAc^- (0.3 M) and 900 µL EtOH were added. The mixture was vortexed and cooled down to -80 °C for 1 to 3 h. Then sample was centrifuged at 13 000 rpm for 15 min, the supernatant removed and the pellet washed with cold 70% EtOH, centrifuged again and the supernatant removed a second time. The pellet was then dissolved in pure water (50-100 µL) or buffer and digested directly as shown in the following Section.

5.5.8 Enzymatic Digest

For the enzymatic digestion the DNA (ca. 1.5 µg in 50 µL water) was incubated in 10 µL Buffer A (300 mM $NH_4^+OAc^-$, 100 mM $CaCl_2$, 1 mM $ZnSO_4$, pH 5.7), 11 U nuclease P1 (*penicilinum citrium*) and 0.05 U calf spleen phosphodiesterase II. The sample was shaken at 37 °C for 3 h. The digest was completed by adding 12 µL buffer B (500 mM Tris-HCl, 1 mM EDTA, pH 8.0), 10 U alkaline phosphatase (CIP) and 0.1 U snake venom phosphodiesterase I (*crotalus adamanteus venom*). The sample was shaken for another 3 h at 37 °C. For workup 6 L of 0.1 M HCl was added and the probes centrifuged (6000 rpm, 5 min). The digest was analyzed by HPLC (interchim Interchrom Uptisphere 3 HDO column (150 x 2.1 mm), buffer A: 2 mM TEA/HOAc in H_2O; buffer B: 2 mM TEA/HOAc H_2O/MeCN 1:4 or Buffer A: 2 M NH_4HCOO in H_2O (pH 5.5); buffer B: 2 mM NH_4HCOO in H_2O/MeCN 1:4; Gradient: 0 →

12 min: 0% → 3% B, 12 → 60 min: 3% → 60% B, 60 → 62 min: 60% → 100% B, 62 → 66 min: 100% B, 66 → 68 min: 100% → 0% B, 68 → 90 min: 0% B, flow 0.2 mL/min). The different peaks were assigned by co-injection, UV and FT-ICR-HPLC-MS-MS using the same conditions. In the MS-spectrum always adducts of the buffer anion or chloride are the most prominent ions. The molecular ions are normally only visible in the MS-MS-spectrum. The HPLC chromatograms are shown in the main text.

Table 5.6 Results of the FT-ICR-HPLC-MS-MS analysis of the 300 base pair PCR-products of the modified triphosphates before the click reaction.

PCR product	FT-ICR MS	MS-MS
PCR300•**5.2** 22.3 min	$[M+CHO_2]^-$ calcd. for $[C_{12}H_{13}N_2O_7]^-$: 297.0730, found 297.0728. $[M+Cl]^-$ calcd. for $[C_{11}H_{12}ClN_2O_5]^-$: 287.0673, found 287.0438	M^-: 251.1
PCR300•**5.3** 42.5 min	$[M+CHO_2]^-$ calcd. for $[C_{17}H_{19}N_2O_5]^-$: 377.1354, found 377.1352.	M^-: 331.2
PCR300•**5.4** 42.0 min	$[M+CHO_2]^-$ calcd. for $[C_{18}H_{22}N_3O_6]^-$: 376.1514, found 376.1512.	M^-: 330.1

Table 5.7 Masses from the HPLC-MS-analysis of the enzymatic digest of a sugar modified PCR product. The HPLC chromatograms are shown in the main text.

Click reaction	FT-ICR MS	MS-MS
2a: PCR300•**5.2** + **5.1** 23.4 and 24.0 min	$[M+OAc]^-$ calcd. for $[C_{19}H_{26}N_5O_{12}]^-$: 516.1583, found 516.1573. $[M+Cl]^-$ calcd. for $[C_{17}H_{23}ClN_5O_{10}]^-$: 492.1139, found 492.1130. $[M]^-$ calcd. for $[C_{17}H_{22}N_5O_{10}]^-$: 456.1372, found 456.1365. Starting material **2** at 21.8 min: $[M+Cl^-]^-$ calc for $[C_{11}H_{12}ClN_2O_5]^-$: 287.0440, found 287.0436.	$[M]^-$: 455.9
3a: PCR300•**5.3** + **5.1** 30.7 and 31.2 min	$[M+OAc]^-$ calcd. for $[C_{25}H_{34}N_5O_{12}]^-$: 596.2209, found 596.2197. $[M+Cl]^-$ calcd. for $[C_{23}H_{31}ClN_5O_{10}]^-$: 572.1765, found 572.1754. $[M]^-$ calcd. for $[C_{23}H_{30}N_5O_{10}]^-$: 536.1998, found 536.1987. Starting material **3** at 42 min: $[M+OAc]^-$ calcd. for $[C_{19}H_{23}N_2O_7]^-$: 391.1511, found 391.1505.	$[M]^-$: 536.2

4a: PCR300•**5.4** + **5.1** 31.6 and 32.0 min	$[M+OAc]^-$ calcd. for $[C_{25}H_{35}N_6O_{11}]^-$: 595.2369, found 595.2357. $[M+Cl]^-$ calcd. for $[C_{23}H_{32}ClN_6O_9]^-$: 571.1925, found 571.1913. $[M]^-$ calcd. for $[C_{23}H_{31}N_6O_9]^-$: 535.2158, found 535.2148.	$[M^-]$: 535.0
4a: PCR2000•**5.4** + **5.1**	$[M+OAc]^-$ calcd. for $[C_{25}H_{35}N_6O_{11}]^-$: 595.2369, found 595.2356. $[M+Cl]^-$ calcd. for $[C_{23}H_{32}ClN_6O_9]^-$: 571.1925, found 571.1912. $[M]^-$ calcd. for $[C_{23}H_{31}N_6O_9]^-$: 535.2158, found 535.2147.	$[M^-]$: 535.1

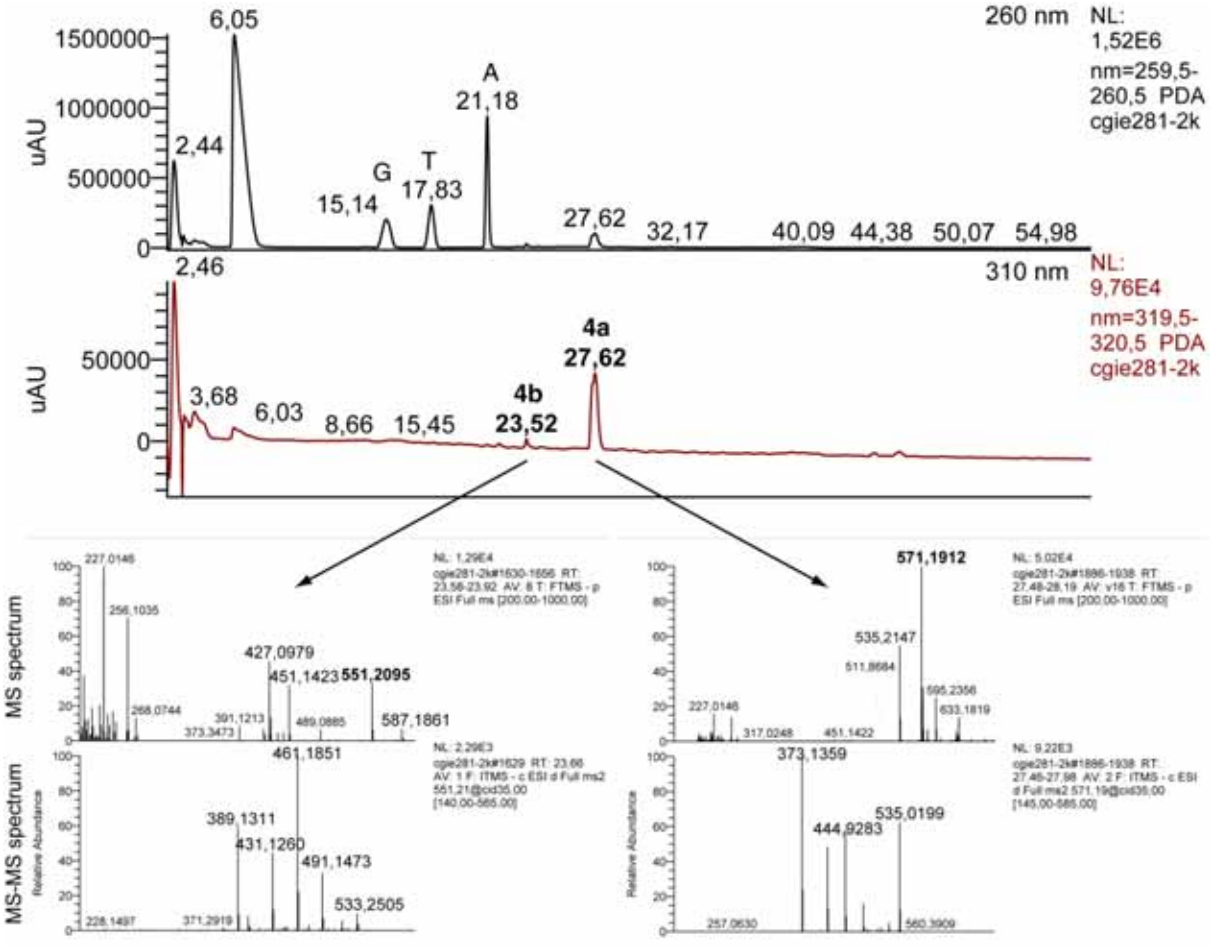

Figure 5.18 HPLC-MS-MS experiment of an enzymatic digest of a click reaction of PCR2000•**5.4** with sugar azide **5.1**, where the reaction mixture was removed in a SpeedVac at r. t. before EtOH precipitation (HPLC-MS uses a different gradient: 0 → 60 min: 0% → 60% B, 60 → 62 min: 60% → 100% B, 62 → 66 min: 100% , 66 → 68 min: 100% → 0% B, 68 → 90 min: 0% B, flow 0.2 mL/min). The upper part shows the UV traces at 260 nm and 310 nm; the lower part shows the MS spectra and MS-MS spectra of the two peaks at 23.5 min and 27.6 min. The MS-MS spectra are from the masses shown in bold in the MS spectra.

When the click reaction mixtures were treated at higher temperatures or when the solvent was removed unfrozen before ethanol precipitation, a minor side product was seen. Beside the almost complete conversion of **5.4** to the correct click product **5.4a**, a small peak at 23.5 min appeared. It has the same buffer and chloride adducts, but is exactly one oxygen heavier than **5.4a** (551.2095 vs 535.2147). In the MS-MS spectrum the fragmentation of the pyranosyl sugar part of **5.4a** to the terminal triazol (373.14) was observed. The side product **5.4b** gives identical fragmentation shifted by the mass of one oxygen (389.12). We therefore propose the following structure **5.4b** for the side product. A similar structure was already assumed by Krasinsky et al. in other click reactions.[29]

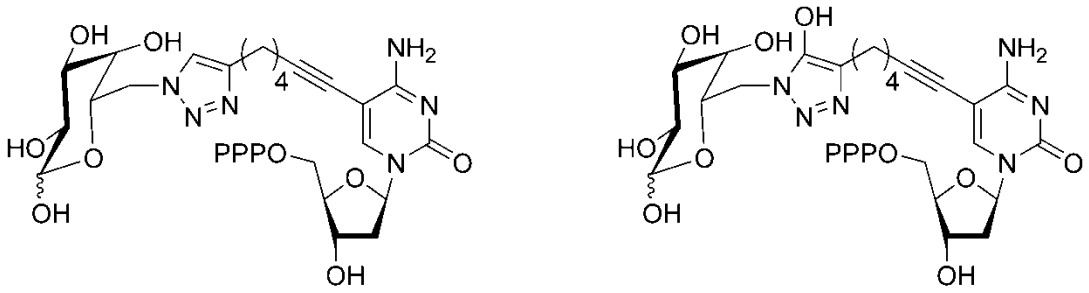

5.4a **5.4b**

Scheme 5.6 Structure of the clicked product **5.4a** and the proposed structure for the side product **5.4b**.

5.6 Author´s Contribution

*Triphosphate **5.5** was synthesized by Alexandra Schmidt, who was a bachelor student supervised by the author. Biochemical experiments on **5.5** were performed by the author.*

5.7 References

[1] U. Feldkamp, C. M. Niemeyer, *Angew. Chem. Int. Ed.* **2006**, *45*, 1856-1876; A. Condon, *Nat. Rev. Genet.* **2006**, *7*, 565-575; P. W. K. Rothemund, *Nature* **2006**, *440*, 297-302; J. J. Storhoff, C. A. Mirkin, *Chem. Rev.* **1999**, *99*, 1849-1862.

[2] Q. Gu, C. Cheng, R. Gonela, S. Suryanarayanan, S. Anabathula, K. Dai, D. T. Haynie, *Nanotech.* **2006**, *17*, R14-R25.

[3] Q. Gu, C. Cheng, S. Suryanarayanan, K. Dai, D. T. Haynie, *Physica E* **2006**, *33*, 92-98; J. M. Kinsella, A. Ivanisevic, *Langmuir* **2007**, *23*, 3886-3890.

[4] E. Braun, Y. Eichen, U. Silvan, G. Ben-Yoseph, *Nature* **1998**, *391*, 775-778; K. Keren, M. Krueger, R. Gilad, G. Ben-Yoseph, U. Sivan, E. Braun, *Science* **2002**, *297*, 72-75.

[5] G. A. Burley, J. Gierlich, M. R. Mofid, S. T. H. Nir, Y. Eichen, T. Carell, *J. Am. Chem. Soc.* **2006**, *128*, 1398-1399.

[6] T. Gourlain, A. Sidorov, N. Mignet, S. J. Thorpe, S. E. Lee, J. A. Grasby, D. M. Williams, *Nucl. Acids Res.* **2001**, *29*, 1898-1905.

[7] T. Tasara, B. Angerer, M. Damond, H. Winter, S. Dörhöfer, U. Hübscher, M. Amacker, *Nucleic Acids Res.* **2003**, *31*, 2636-2646.

[8] S. Jäger, G. Rasched, H. Kornreich-Leshem, M. Engeser, O. Thum, M. Famulok, *J. Am. Chem. Soc.* **2005**, *127*, 15071-15082.
[9] M. Kuwahara, J.-i. Nagashima, M. Hasegawa, T. Tamura, R. Kitagata, H. Kazuo, S.-i. Hososhima, T. Kasamatsu, H. Ozaki, H. Sawai, *Nucl. Acids Res.* **2006**, *34*, 5383-5394.
[10] R. Ting, J. M. Thomas, L. Lermer, D. M. Perrin, *Nucl. Acids Res.* **2004**, *32*, 6660-6672; C. G. Peng, M. J. Damha, *J. Am. Chem. Soc.* **2007**, *129*, 5310-5311.
[11] S. E. Lee, A. Sidorov, T. Gourlain, N. Mignet, S. J. Thorpe, J. A. Brazier, M. J. Dickman, D. P. Hornby, J. A. Grasby, D. M. Williams, *Nucl. Acids Res.* **2001**, *29*, 1565-1573.
[12] M. M. Masud, A. Ozaki-Nakamura, M. Kuwahara, H. Ozaki, H. Sawai, *ChemBioChem* **2003**, *4*, 584-588.
[13] R. Huisgen, *Angew. Chem. Int. Ed.* **1963**, *2*, 565-632; R. Huisgen, G. Szeimies, L. Möbius, *Chem. Ber.* **1967**, *100*, 2494-2507.
[14] H. C. Kolb, M. G. Finn, K. B. Sharpless, *Angew. Chem. Int. Ed.* **2001**, *40*, 2004-2021.
[15] C. W. Tornoe, C. Christensen, M. Meldal, *J. Org. Chem.* **2002**, *67*, 3057-3064.
[16] V. V. Rostovtsev, L. G. Green, V. V. Fokin, K. B. Sharpless, *Angew. Chem. Int. Ed.* **2002**, *41*, 2596-2599.
[17] V. D. Bock, H. Hiemstra, J. H. van Maarseveen, *Eur. J. Org. Chem.* **2006**, 51-68; G. W. Goodall, W. Hayes, *Chem. Soc. Rev.* **2006**, *35*, 280-312; J.-F. Lutz, *Angew. Int. Ed.* **2007**, *46*, 1018-1025.
[18] R. L. Weller, S. R. Rajski, *Chembiochem* **2006**, 243-245; R. L. Weller, S. R. Rajski, *Org. Lett.* **2005**, *7*, 2141-2144; N. K. Devaraj, G. P. Miller, W. Ebina, B. Kakaradov, J. P. Collman, E. T. Kool, C. E. D. Chidsey, *J. Am. Chem. Soc.* **2005**, *127*, 8600-8601; T. S. Seo, X. Bai, D. H. Kim, Q. Meng, S. Shi, H. Ruparel, Z. Li, N. J. Turro, J. Ju, *Proc. Nat. Acad. Sci. USA* **2005**, *102*, 5926-5931; T. S. Seo, Z. Li, H. Ruparel, J. Ju, *J. Org. Chem.* **2003**, *68*, 609-612.
[19] J. Gierlich, G. A. Burley, P. M. E. Gramlich, D. M. Hammond, T. Carell, *Org. Lett.* **2006**, *8*, 3639-3642.
[20] M. Fischler, U. Simon, H. Nir, Y. Eichen, G. A. Burley, J. Gierlich, P. M. E. Gramlich, T. Carell, *Small* **2007**, *3*, 1049-1055.
[21] T. Kovacs, L. Ötvös, *Tetrahedron Lett.* **1988**, *29*, 4525-4528.
[22] W. H. Pearson, S. C. Bergmeier, J. A. Chytra, *Synthesis* **1990**, 156-159.
[23] H. A. Held, S. A. Benner, *Nucleic Acids Res.* **2002**, *30*, 3857-3869.
[24] T. R. Chan, R. Hilgraf, K. B. Sharpless, V. V. Fokin, *Org. Lett.* **2004**, *6*, 2853-2855.
[25] B. M. Znosko, T. W. Barnes III, T. R. Krugh, D. H. Turner, *J. Am. Chem. Soc.* **2003**, *125*, 6090-6097.
[26] F. Seela, V. R. Sirivolu, *Chem. Biodiversity* **2006**, *3*, 509-514.
[27] J. He, F. Seela, *Nucl. Acids Res.* **2002**, *30*, 5485-5496.
[28] J. D. Kahl, M. M. Greenberg, *J. Am. Chem. Soc.* **1999**, *121*, 597-604.
[29] A. Krasinski, V. V. Fokin, K. B. Sharpless, *Org. Lett.* **2004**, *6*, 1237-1240.

6 Pronounced Effect of DNA Hybridization on Click Reaction Efficiency

This Section was published in:

C. T. Wirges, P. M. E. Gramlich, K. Gutsmiedl, J. Gierlich, G. A. Burley, T. Carell, *QSAR Comb. Sci.* **2007**, *26*, 1159-1164.

6.1 Abstract

We report about the efficiency of the click reaction directly on PCR products containing alkyne-modified uridine nucleosides. Galactose azide was clicked onto single-stranded and double-stranded 300mer DNA in order to investigate the efficiency of sugar labeling of DNA under various conditions. Single-stranded alkyne-modified DNA was prepared by selective lambda exonuclease digestion of 5'-phosphate-labeled double strands. A comparison of the click reaction efficiency on modified single and double stranded 300mers under identical conditions shows a pronounced effect of the strandedness on the yield of the click reaction.

6.2 Introduction

DNA is currently a promising candidate for the construction of nanoscale electrical circuits. Although the DNA molecule has the required extraordinary self-assembling properties to build complex structures, it lacks sufficient conductivity.[1] In order to overcome this limitation, efficient high-density functionalization of DNA is required. Furthermore, modern genomic analysis creates a growing demand for highly sensitive and specific methods of DNA detection.[2] In this area as well, efficient and biocompatible reactions for the selective functionalization of DNA are of highest importance. Among the number of methods currently available for the functionalization of DNA, the copper(I)-catalyzed variant of the 1,3-dipolar Huisgen cycloaddition[3] of azides and alkynes, developed by Meldal and coworkers[4] and Sharpless and coworkers,[5] represents the most versatile and reliable procedure.[6, 7] By virtue of its generally high yield and functional group tolerance, it has been frequently and successfully applied in materials chemistry and nanotechnology as well as in the biomolecular sciences.[8]

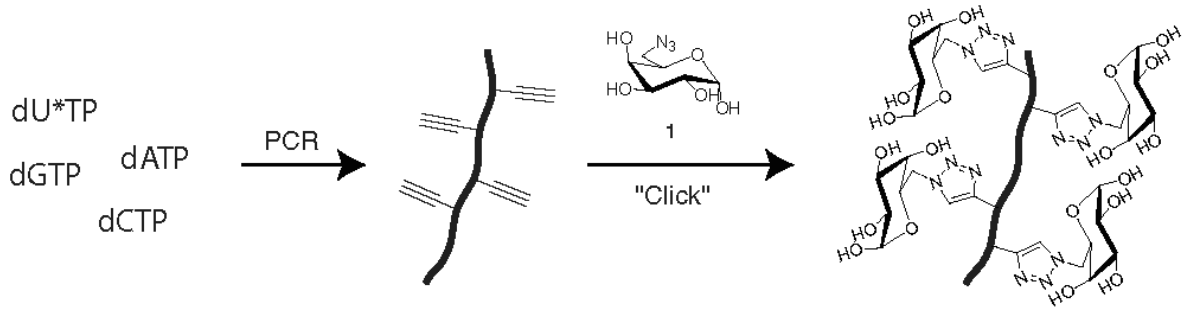

Scheme 6.1 Schematic depiction of DNA functionalization using click chemistry. dU*TP is a uridine derivative modified with a terminal alkyne functionality.

In this and in preceding studies, the reaction allowed for the selective, high-density functionalization of DNA.[7, 9] For this purpose, synthetic alkyne-modified nucleoside triphosphates (dU*TP) are incorporated into long DNA strands by a PCR reaction, as shown in Scheme 6.1. In this process, the modified base replaces one of the canonical triphosphates. The resulting high-density alkyne-modified DNA can then be further derivatized using the click reaction with various azide-bearing functional molecules.

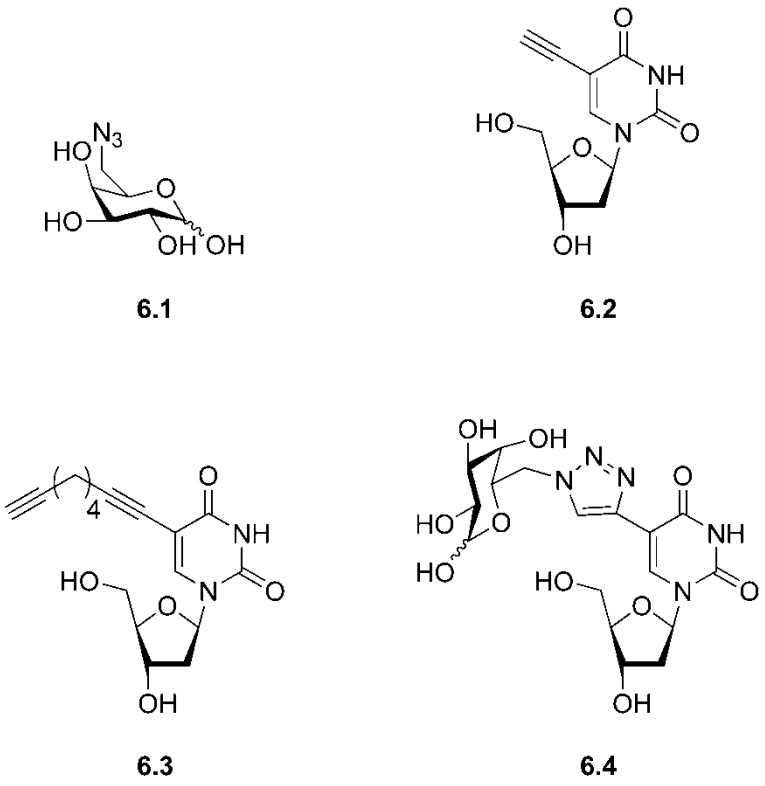

Scheme 6.2 Sugar azide **6.1**, alkyne-modified deoxyuridine **6.2**, alkyne-modified deoxyuridine **6.3** and click-product **6.4**, which is formed as a mixture of the α- and β-anomer at the galactose moiety.

In addition to the modification of DNA with fluorescent dyes such as fluorescein azide or coumarin azide,[7] we recently demonstrated the functionalization of DNA with sugars, which function as hemi-protected aldehydes. These aldehyde groups allowed sequence-selective metal deposition on DNA. After clicking galactose azide **6.1** (Scheme 6.2) onto alkyne-decorated PCR products, the resulting sugar-modified DNA could be selectively silver stained in the presence of nonstaining natural DNA.[9] For this purpose, the Tollens reaction of aldehydes with ammoniacal silver solution was exploited, leading to a highly sensitive DNA detection method. Furthermore, such DNA strands, modified with reducing sugar molecules, served as templates for the deposition of elemental metal around the DNA, resulting in exceptionally thin and homogeneous nanowires.[9, 10]

Recently, we have studied the efficiency of the click reaction between galactose azide **6.1** and alkyne-modified DNA.[7, 11] We noted a marked difference in the click reaction yield between DNA containing 5-ethynyluridine **6.2**[12] and DNA containing alkyne-modified uridine **6.3**,[9] whose alkyne function is attached to a six-carbon atoms long spacer. The latter reproducibly

gave near-quantitative yields in click reactions with various azides, whereas the former did not react to completeness in all cases. The strong reactivity differences were observed in a study with short strands, which were analyzed by MALDI-TOF MS.[7]
This interesting result prompted us to investigate in more detail the reaction between DNA, modified with ethynyluridine **2**, and galactose azide **1**, aiming at a better understanding of the click reaction on DNA, one of the most challenging biomolecular substrates.

6.3 Results and Discussion

The decreased click reaction yield for DNA modified with short-chain alkyne nucleoside **6.2** could, in principle, be caused by two different factors. One is steric shielding of the alkyne group due to the proximity of the nucleobase, the other is an electronic effect. The electron-deficient heterocyclic ring in conjugation with the terminal alkyne might change its reactivity in the Cu(I)-catalyzed cycloaddition. In order to evaluate possible steric effects, we set out to compare the click reaction efficiency of double-stranded (dsDNA·**6.2**) with single-stranded (ssDNA·**6.2**) 300-bases long DNA modified with **6.2**.
To this end, we prepared ssDNA·**6.2** by an enzymatic approach. First, dsDNA·**6.2** was produced via a PCR reaction with one of the two primers phosphorylated at the 5'-position, as shown in Figure 6.1. The resulting mono-5'-phosphorylated DNA was subsequently treated with lambda exonuclease, which digests only the phosphorylated strand, leaving the counter-strand intact.

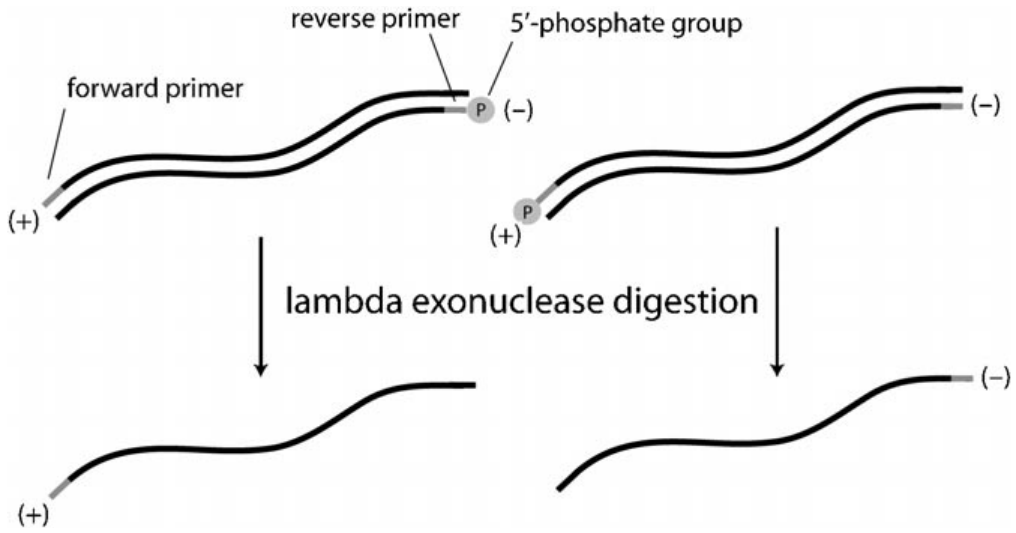

Figure 6.1 Lambda exonuclease digestion of 5'-phosphate-labeled PCR products for the preparation of single-stranded DNA.

After careful optimization of enzyme concentration and reaction time, both the plus-strand and the minus-strand of dsDNA·**6.2** (+ssDNA·**6.2** and -ssDNA·**6.2**) could be obtained as single strands in good yields and excellent purity. Figure 6.2 shows a denaturing polyacrylamide gel of the digest reactions. In lanes 2 and 3, the starting material and the product of the lambda exonuclease digest to +ssDNA·**6.2** are shown, respectively. Lanes 5 and 6 contain the

corresponding starting material (lane 5) and product (lane 6) of the digestion reaction giving -ssDNA·**6.2**.

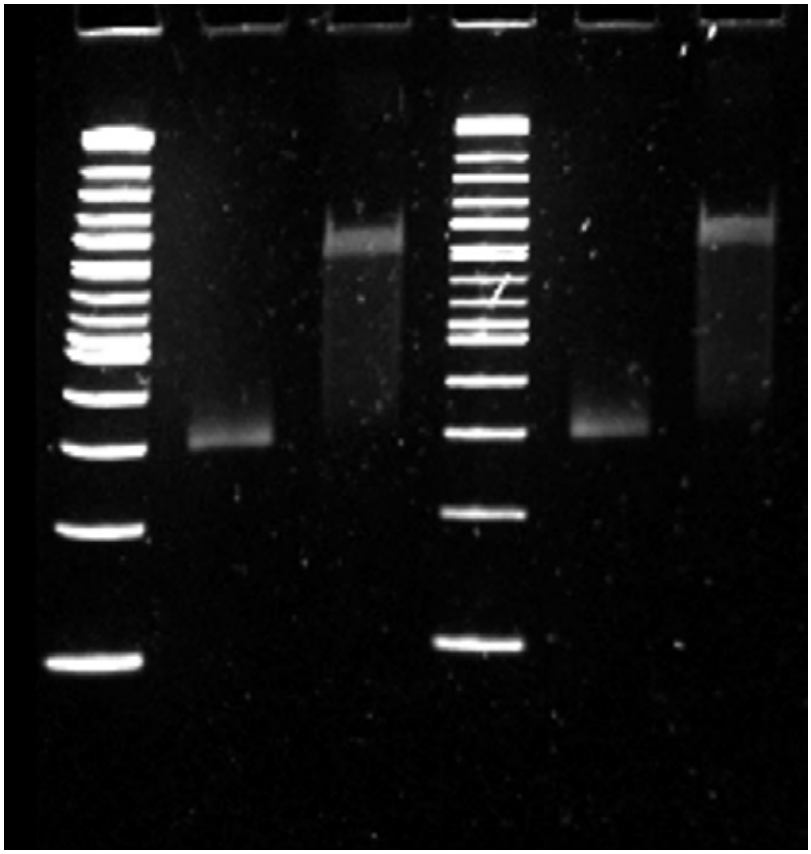

Figure 6.2 Lambda exonuclease digest of mono-5'-phosphate-modified DNA. Lane 1: 2-log DNA ladder, lane 2: dsDNA·**6.2** with reverse primer 5'-phosphate-modified, lane 3: product of digest: +ssDNA·**6.2**, lane 4: 2-log DNA ladder, lane 5: dsDNA·**6.2** with forward primer 5'-phosphate-modified, lane 6: product of digest: -ssDNA·**6.2**. The gel was stained with SYBR-Green.

All three DNA substrates (+ssDNA·**6.2**, -ssDNA·**6.2**, and dsDNA·**6.2**) possess a similar distribution of nucleotides in the sequence. In all strands, about every fourth nucleobase of the sequence is alkyne-modified and represents a site for the click reaction. Also, in both strands, the maximum number of modified bases in a row is four. If sterical reasons were to be neglected, one would expect a comparable click reaction yield for all three substrates. Table 6.1 shows a detailed analysis of the base distribution in the three DNA samples. The small amount of thymidine present in the modified DNA strands results from the unmodified primer strands used in the PCR reaction.

Table 6.1 Percentage of nucleobases in the sequence of the DNA click reaction substrates +ssDNA·**2**, -ssDNA·**6.2** and dsDNA·**6.2**.

	6.2 [%]	T [%]	G [%]	C [%]	A [%]
+ssDNA·**6.2**	23	6	23	16	32
-ssDNA·**6.2**	26	6	16	23	29
dsDNA·**6.2**	25	6	19	19	31

In order to examine the possible differences in click reaction yield between single- and double-stranded DNA, +ssDNA·**6.2** and dsDNA·**6.2** were subjected to the previously described[7, 9] click reaction with galactose azide **6.1** under identical conditions.
This model click reaction was conducted with a final concentration of 40 ng/mL of DNA substrate, 2.1 mM of a CuBr/TBTA-ligand[13] (1:1 solution), and 24.5 mM galactose azide in a total volume of 24 µL (see Section 6.5.2 for a detailed description, entry 2 in Table 6.2.). The mixtures were shaken at 37 °C for 2 h, followed by an ethanol precipitation step. The samples were then digested to the free nucleosides using a combination of DNA nucleases and phosphatases (see Section 6.5.1). The obtained mixture of the free nucleosides was finally analyzed by HPLC-MS/MS, enabling us to identify and quantify the obtained nucleoside species. Quantification was performed by integration of the chromatographic signals measured at 310 nm, a characteristic UV absorption band of alkyne-modified pyrimidine nucleosides that is not present in natural nucleosides. A correction factor determined by measuring the absorption constants of **6.2** and **6.4** was used to account for the slightly different molar absorptivities of the starting material and the click product.

Table 6.2 Yield of the click reaction of single- and double-stranded 300DNA·**6.2** at different azide reagent concentrations.

Entry	Final concentration of azide **1** [mM]	-ssDNA·**6.2** [%]	+ssDNA·**6.2** [%]	dsDNA·**6.2** [%]
1	50.0	> 95	> 95	85
2	24.5	92	92	78
3	5.4	89	90	76
4	1.2	76	75	64

Figure 6.3 shows a chromatogram of the nucleoside mixture obtained after click reaction and total enzymatic digest. The gray line represents the digest of the click reaction on +ssDNA·**6.2** and the black line the reaction on dsDNA·**6.2**. Beside the peaks of the natural nucleosides dC, dA, dG, and dT, three peaks with a characteristic absorption at 310 nm (see inset) appear in both chromatograms: they belong to unreacted modified nucleobase **6.2** (first peak) and the product of the click reaction **6.4** (second and third peaks). The sugar-modified click product **6.4** gives two peaks due to a mixture of α- and β-diastereomers at the galactose ring. Both peaks give the correct high-resolution mass spectrum in HPLC-MS/MS experiments corresponding to the click product **6.4** (Table 6.4).
As it is clearly visible from the chromatograms measured at 260 and 310 nm absorption wavelengths, the single-stranded DNA sample has reacted with significantly higher yield than the double-stranded DNA. The product peaks integrate to 92% yield for the single strand and 78% for the double strand at the diagnostic wavelength of 310 nm.
This result motivated us to further investigate the click reaction efficiency of single and double stranded 300DNA·**6.2** at different concentrations of sugar azide, keeping the catalyst and DNA concentrations constant. The minus-strand of 300DNA·**6.2** was also included in the study to rule out a possible influence of the nucleobase sequence on the click reaction efficiency.

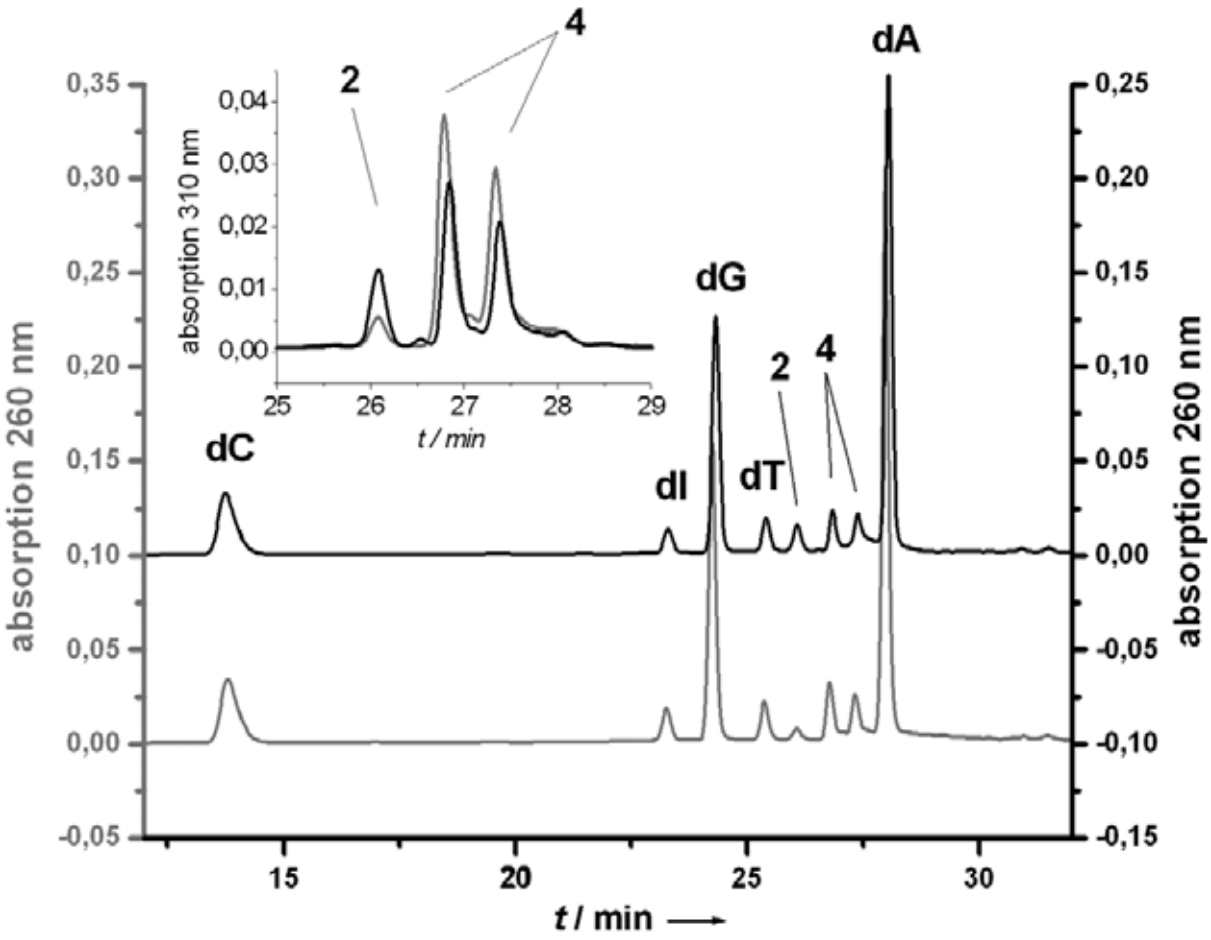

Figure 6.3 HPLC chromatogram of enzymatic digest of +ssDNA·**2** (gray) and dsDNA·**6.2** (black) after click reaction with sugar azide **6.1**. dI represents inosine, resulting from enzymatic deamination of adenosine. Inset: HPLC chromatogram with UV/Vis-monitoring at the diagnostic wavelength of 310 nm.

Our results show a considerably higher click reaction yield for single-stranded DNA compared to double-stranded DNA for all tested azide concentrations (Table 6.2). Furthermore, both single strands, the minus- and the plus-strand, give similarly high yields, confirming that the observed result is not created by nucleobase sequence effects but indeed caused by the strandedness of the DNA substrate.
We observed a pronounced effect of azide reagent concentration on the yield of the reaction, both for single- and double-stranded DNA samples, whereas a prolonged reaction time or an increase in the catalyst concentration had only a small effect on the efficiency of the reaction (data not shown).

6.4 Summary and Outlook

The comparison of single- and double-stranded DNA samples under otherwise identical reaction conditions has uncovered a surprisingly strong effect of DNA hybridization on the yield of the click reaction with short-chain alkyne substrate DNA·**6.2**. This result suggests that steric, and not electronic effects are largely responsible for the lower clicking efficiency of

DNA modified with nucleoside **6.2** compared to its long-chain alkyne analogue **6.3**. We postulate that double-stranded DNA, in which the alkyne groups of **6.2** are located within the major groove of the DNA helix, provides greater steric hindrance, making the click reaction less efficient compared to single-stranded DNA.
Our results show in addition that small variations of the azide concentration have a considerable effect on the yield of the click reaction, particularly with challenging substrates. These data suggest that in the case of difficult click reactions, increasing the azide concentration should be the first step of an optimization process.

6.5 Experimental Section

The conditions for PCR amplification were identical to the ones used in a previous publication,[9] the only difference being that 5'-phosphorylated primers were used where denoted. As template, the gateway expression vector pExp007-polη with the polymerase η gene from *Saccharomyces cerevisiae* was used. Plus-strand signifies the coding strand of the pol η gene, minus-strand denotes the complementary strand.

6.5.1 Lambda Exonuclease Digest and Gel Electrophoresis

The DNA (2.5 µg) was typically digested in a total volume of 125 µL with 1 × lambda exonuclease buffer and 10 U of enzyme. The mixture was incubated for 15 min at 37 °C, purified from nucleotides and enzyme by a spin column. The digest was checked for completeness by electrophoresis on a 5% TBE-urea-polyacrylamide gel (30 min, 12 mA constant current) and visualization of the bands with SYBR Green (Raytest LAS-3000 imager, cutoff filter 515 nm).

6.5.2 Click Reaction on the PCR Product

DNA (1 µg in a solution of about 30 ng/µL concentration) and sugar azide **6.1** (aliquots from a 100 mM stock solution according to Table 6.3) were placed in a 1.5 mL reaction tube and lyophilized. In a separate tube, CuBr was dissolved in TBTA ligand[13] solution (10 mM in DMSO/*t*BuOH 3:1) to give a 1:1 Cu(I)/ligand ratio. This solution (5 µL) was added to the lyophilisate of DNA and azide. Water (7 µL) and DMSO/*t*BuOH 3:1 (12 µL) were added to give a total volume of 24 µL. The solution was shaken at 37 °C for 2 h, then NaOAc solution (125 µL, 0.3 M) and 0.9 mL of EtOH were added, the vial was vortexed and placed in a freezer (-20 °C) over night. After centrifugation (15 min at 13000 rpm) the supernatant was carefully removed from the DNA pellet. EtOH (70%, -20 °C) was added, the vial was vortexed, centrifuged, and the supernatant was removed again. This washing step was repeated twice. After the last washing step, the pellet was dried in air and taken up in 100 µL of water.

Table 6.3 Volumes of 100 mM galactose azide used in reaction entries 1-4 from Table 6.2.

	Galactose azide **6.1** (100 mM), [µL]	Final concentration [mM]
1	12.00	50.0
2	5.90	24.5
3	1.30	5.4
4	0.28	1.2

6.5.3 Enzymatic Digest and HPLC Analysis

The DNA sample (1-1.5 µg in 100 mL water) was incubated with 10 µL buffer A (300 mM $NH_4^+OAc^-$, 100 mM $CaCl_2$, 1 mM $ZnSO_4$, pH 5.7), 11 U nuclease P1 (*Penicillinum citrinum*), and 0.05 U calf spleen phosphodiesterase II for 3 h at 37 °C. Then 12 µL of buffer B (500 mM Tris-HCl, 1 mM EDTA, pH 8.0), 10 U alkaline phosphatase (CIP), and 0.1 U snake venom phosphodiesterase I (*Crotalus adamanteus venom*) were added, followed by incubation for 3 h at 37 °C. After the digest, the samples were centrifuged (6000 rpm, 10 min) and the supernatant was analyzed by HPLC (Interchim Interchrom Uptisphere 3 HDO column, buffer A: 2 mM $NH_4^+OAc^-$ in H_2O, buffer B: 2 mM $NH_4^+OAc^-$ in H_2O/MeCN 1:4, gradient: 0-12 min: 0→3% B, 12-60 min: 3→60% B, 60-62 min: 60→100% B, 62-90 min: 100% B, 90– 95 min: 100→0% B, 95-130 min: 0% B, flow 0.15 mL/min) coupled with diode array UV-Vis detection and/or MS/MS analysis. The peaks were assigned by UV and FTICR-HPLC-MS/MS. The high-resolution masses found are shown in Table 6.4. For integration of the peaks, a correction factor was introduced to account for the slightly different molar absorptivities of the starting material **6.2** (3.41 mM^{-1} cm^{-1}) and click product **6.4** (3.80 mM^{-1} cm^{-1}) at the diagnostic wavelength of 310 nm.

Table 6.4 HPLC-MS/MS data of the total enzymatic digest.

	FTICR-MS	MS/MS
Starting material: nucleoside **6.2** at 26.1 min	$[M+HCOO]^-$: calc. 297.0728, found 297.0726	$[M]^-$: found 251.1
Click product: nucleoside **6.4** at 26.9 min	$[M+HCOO]^-$: calc. 502.1427, found 502.1419	$[M]^-$: found 455.9
Click product: nucleoside **6.4** at 27.2 min	$[M+HCOO]^-$: calc. 502.1427, found 502.1421	$[M]^-$: found 455.9

6.6 Author´s Contribution

This work was performed in collaboration with Christian Wirges. Click reactions were performed by the author, the selective enzymatic digestion to yield ssDNA was developed and performed by Christian Wirges. All other experiments were performed together with Christian Wirges.

6.7 References

[1] U. Feldkamp, C. M. Niemeyer, *Angew. Chem. Int. Ed.* **2006**, *45*, 1856-1876; E. Braun, Y. Eichen, U. Silvan, G. Ben-Yoseph, *Nature* **1998**, *391*, 775-778; Y. Eichen, E. Braun, U. Sivan, G. Ben-Yoseph, *Acta Polym.* **1998**, *49*, 663-670.

[2] N. L. Rosi, C. A. Mirkin, *Chem. Rev.* **2005**, *105*, 1547-1562; T. Niazov, V. Pavlov, Y. Xiao, R. Gill, I.Willner, *Nano Lett.* **2004**, *4*, 1683-1687; D. M. Hammond, A. Manetto, J. Gierlich, V. A. Azov, P. M. E. Gramlich, G. A. Burley, M. Maul, T. Carell, *Angew. Chem. Int. Ed.* **2007**, *46*, 4184-4187.

[3] R. Huisgen, *Angew. Chem. Int. Ed.* **1963**, *2*, 565-632.

[4] C. W. Tornoe, C. Christensen, M. Meldal, *J. Org. Chem.* **2002**, *67*, 3057-3064.

[5] V. V. Rostovtsev, L. G. Green, V. V. Fokin, K. B. Sharpless, *Angew. Chem. Int. Ed.* **2002**, *41*, 2596-2599.

[6] T. S. Seo, Z. Li, H. Ruparel, J. Ju, *J. Org. Chem.* **2003**, *68*, 609-612; R. L. Weller, S. R. Rajski, *Org. Lett.* **2005**, *7*, 2141-2144; N. K. Devaraj, G. P. Miller, W. Ebina, B. Kakaradov, J. P. Collman, E. T. Kool, C. E. D. Chidsey, *J. Am. Chem. Soc.* **2005**, *127*, 8600-8601; F. Seela, V. R. Sirivolu, *Chem. Biodiversity* **2006**, *3*, 509-514.

[7] J. Gierlich, G. A. Burley, P. M. E. Gramlich, D. M. Hammond, T. Carell, *Org. Lett.* **2006**, *8*, 3639-3642.

[8] V. D. Bock, H. Hiemstra, J. H. van Maarseveen, *Eur. J. Org. Chem.* **2006**, 51-68; J.-F. Lutz, *Angew. Chem. Int. Ed.* **2007**, *46*, 1018-1025.

[9] G. A. Burley, J. Gierlich, M. R. Mofid, S. T. H. Nir, Y. Eichen, T. Carell, *J. Am. Chem. Soc.* **2006**, *128*, 1398-1399.

[10] M. Fischler, U. Simon, H. Nir, Y. Eichen, G. A. Burley, J. Gierlich, P. M. E. Gramlich, T. Carell, *Small* **2007**, *3*, 1049-1055.

[11] J. Gierlich, K. Gutsmiedl, P. M. E. Gramlich, A. Schmidt, G. Burley, T. Carell, *Chem. Eur. J.* **2007**, *13*, 9486-9494.

[12] P. J. Barr, A. S. Jones, P. Serafinowski, R. T. Walker, *J. Chem. Soc., Perkin Trans. 1* **1978**, *10*, 1263-1267; T. Kovacs, L. Ötvös, *Tetrahedron Lett.* **1988**, *29*, 4525-4528.

[13] T. R. Chan, R. Hilgraf, K. B. Sharpless, V. V. Fokin, *Org. Lett.* **2004**, *6*, 2853-2855.

7 Synthesis of Modified DNA by PCR with Alkyne Bearing Purines Followed by a Click Reaction

This Section was published in:

P. M. E. Gramlich, C. T. Wirges, J. Gierlich, T. Carell, *Org. Lett.* **2008**, *10*, 249-251.

7.1 Abstract

Alkyne-bearing deazapurine triphosphates were prepared and successfully incorporated into DNA using the polymerase chain reaction (PCR). The obtained alkyne-labeled DNA was successfully used in a click reaction with galactose azide.

7.2 Introduction

The utilization of DNA for the assembly of functional materials has received considerable interest in recent years.[1] To this end, modified DNA was created featuring a multitude of novel functions which, for example, allows one to accelerate the detection of an analyte,[2] to sequence DNA,[3] to create DNA- and RNA-based receptors (aptamers),[4] or to assemble them into novel nanomaterials.[5] In order to introduce the modifications in a highly controllable manner in long DNA strands, the exchange of the natural triphosphates by chemically modified building blocks in enzymatic reactions such as the PCR reaction is the most common approach. This method is, however, not generally applicable because it cannot be predicted if and how a specific triphosphate is accepted by different DNA polymerases.[6, 7] We therefore decided to develop a two-step procedure in which a nucleoside precursor is incorporated into DNA by PCR, which can be subsequently converted into a variety of derivatives. For a similar approach using the Staudinger ligation, see ref.[8] For the functionalization step, we exploited the recently described Cu-catalyzed Huisgen-Meldal-Sharpless reaction,[9] termed click reaction. We already used this chemistry to efficiently modify DNA-bearing alkyne functionalities at thymidines or cytidines.[2, 10, 11] We herein wish to report the extension of the technology to the purine bases dA and dG.

7.3 Results and Discussion

In order to limit structural perturbation of the DNA duplex to a minimum, we placed the alkyne group in the major groove.[6, 12] To achieve this, we prepared the alkyne-bearing derivatives of the 7-deazapurine bases 7-deaza-dA and 7-deaza-dG (Scheme 7.1). The adenine building block was synthesized by a Sonogashira coupling on the unprotected 7-deaza-7-iodo-2′-deoxyadenosine **7.1** to give the free nucleoside **7.2**.[13-15] The synthesis of the triphosphate **7.3** was achieved by the method of Kovacs et al.[16] The corresponding 7-deaza-7-iodo-2′-deoxyguanosine **7.4** was synthesized in 10 steps according to literature procedures.[14, 15] Sonogashira coupling of **7.4** with 1-TMS-protected 1,7-octadiyne gave the key intermediate **7.5** in good yield. After deprotection of the alkyne and cleavage of the sugar protecting groups

to **7.6**, the monomer was successfully converted into triphosphate **7.7**,[16] suitable for enzymatic incorporation.

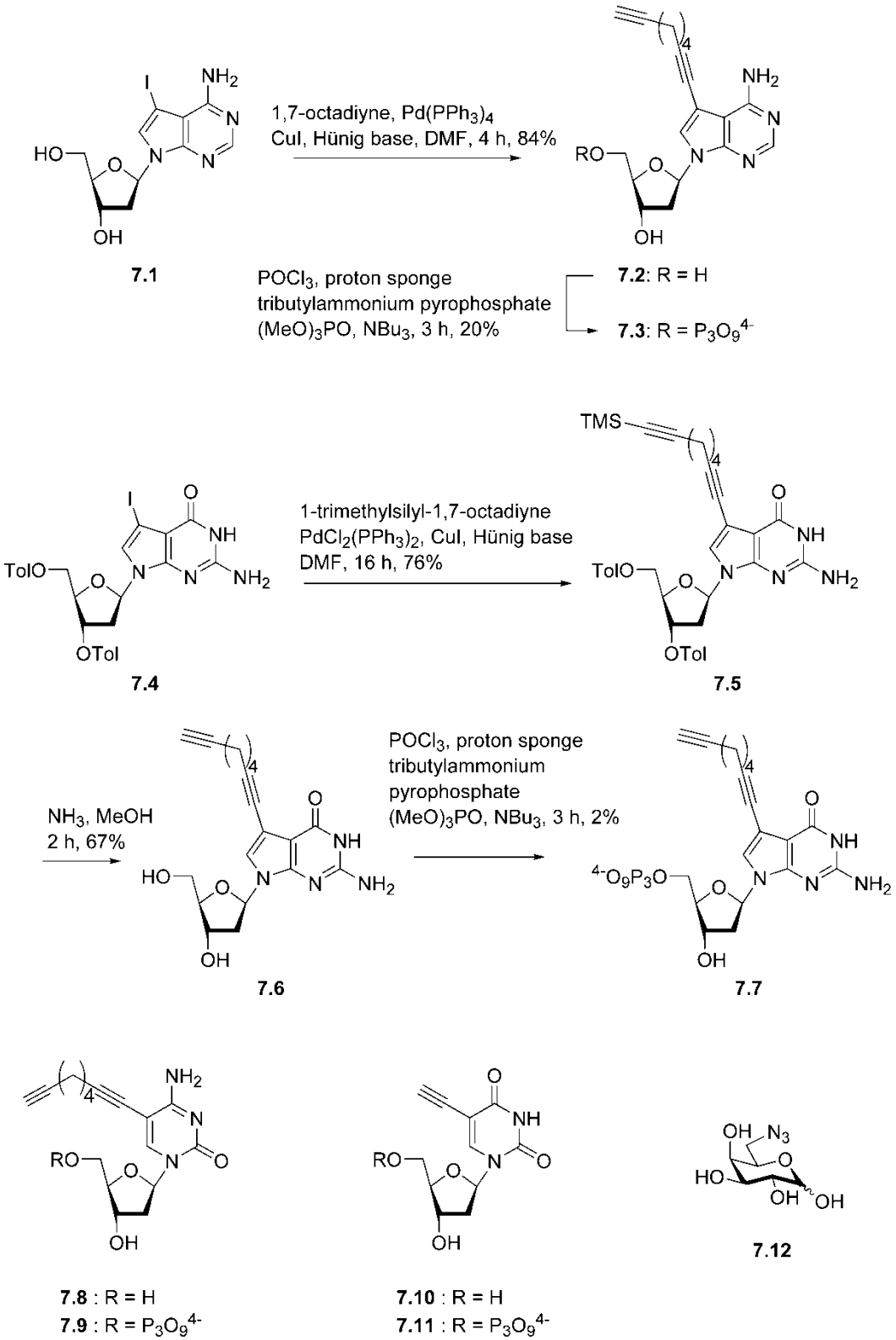

Scheme 7.1 Syntheses of the triphosphates **7.3** and **7.7**. The alkyne-bearing pyrimidine triphosphates **7.9** and **7.11** as well as the galactose azide **7.12** were reported previously.

To examine how the triphosphates **7.3** and **7.7** are accepted by polymerases, we first performed primer extension studies. To this end, a fluorescently labeled primer was hybridized to a 30mer template. The elongation of the primer was followed using PAGE. In the initial test runs, we used two different templates containing each of the canonical bases at least one time.[17]As expected from literature precedents,[6] the unnatural alkyne-bearing purines **7.3** and **7.7** were able to fully replace the canonical bases dA and dG in typical primer extension experiments. In further experiments, we could also replace the nucleobases dT and dC by the alkyne-modified bases **7.9** and **7.11**, allowing us to prepare a DNA derivative in which each nucleobase carries an alkyne-bearing functional group. In all cases, we obtained a clean, full-length product, proving that all triphosphates were efficiently incorporated (Section 7.5.3).

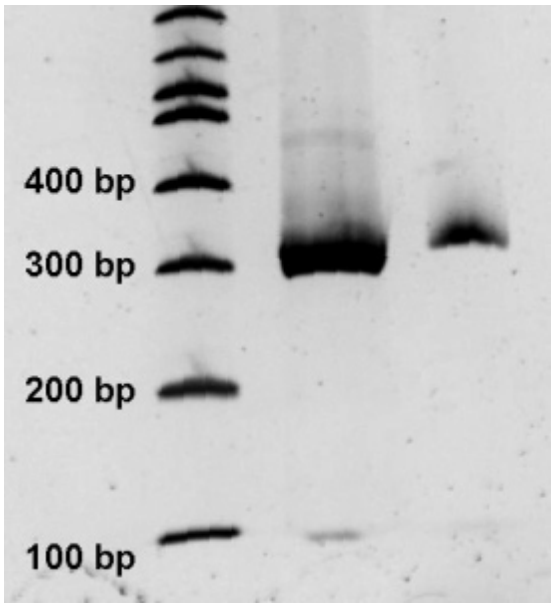

Figure 7.1 5% PAGE of the PCR amplicons 300DNA•**7.2** (lane 2) and 300DNA•**7.6 (**lane 3). Lane 1 contains a 100 bp DNA ladder.

Encouraged by this result, we started to incorporate our building blocks **7.3** and **7.7** using PCR. To this end, we used a 300mer template DNA to create two modified DNA strands, DNA300•**7.2** (dATP replaced by **7.3**) and DNA300•**7.6** (dGTP replaced by **7.7**). Detection of the PCR products obtained with the building block **7** turned out to be difficult because the ethidium bromide fluorescence is typically quenched by deazapurine derivatives.[18-20] We found that the PCR product DNA300•**7.2**, however, was stainable with ethidium bromide and also with SYBR green. Detection of DNA300•**7.6** required the use of a fluorescein-labeled primer strand. With the help of the KOD XL polymerase, we could indeed prepare DNA300•**7.2** and DNA300•**7.6** efficiently without the use of any additives (Figure 7.1). The obtained amplicons comprise 170 (DNA300•**7.2**) or 103 (DNA300•**7.6**) alkynes attached to the purine bases. Simple screenings of the different temperature steps (annealing, elongation, and denaturation) of the PCR cycle were sufficient to achieve this goal. An attempted PCR incorporation of all four alkyne-modified triphosphates into a 300mer DNA unfortunately failed. In order to investigate the structure of the modified DNA in more detail, we performed

UV and CD measurements (Section 7.5.5). Both DNA strands exhibited an additional absorption band at longer wavelengths due to conjugation of the nucleobase to the internal alkyne. This observation is in accord with previous results obtained by us.[11] This additional band is also visible in the CD spectra, which exhibit an extra minimum at 310 nm. The overall shape of the curve is similar to a typical B-form DNA, which is an indication that both DNA strands DNA300•**7.2** and DNA300•**7.6** adopt a B-type conformation as duplexes.

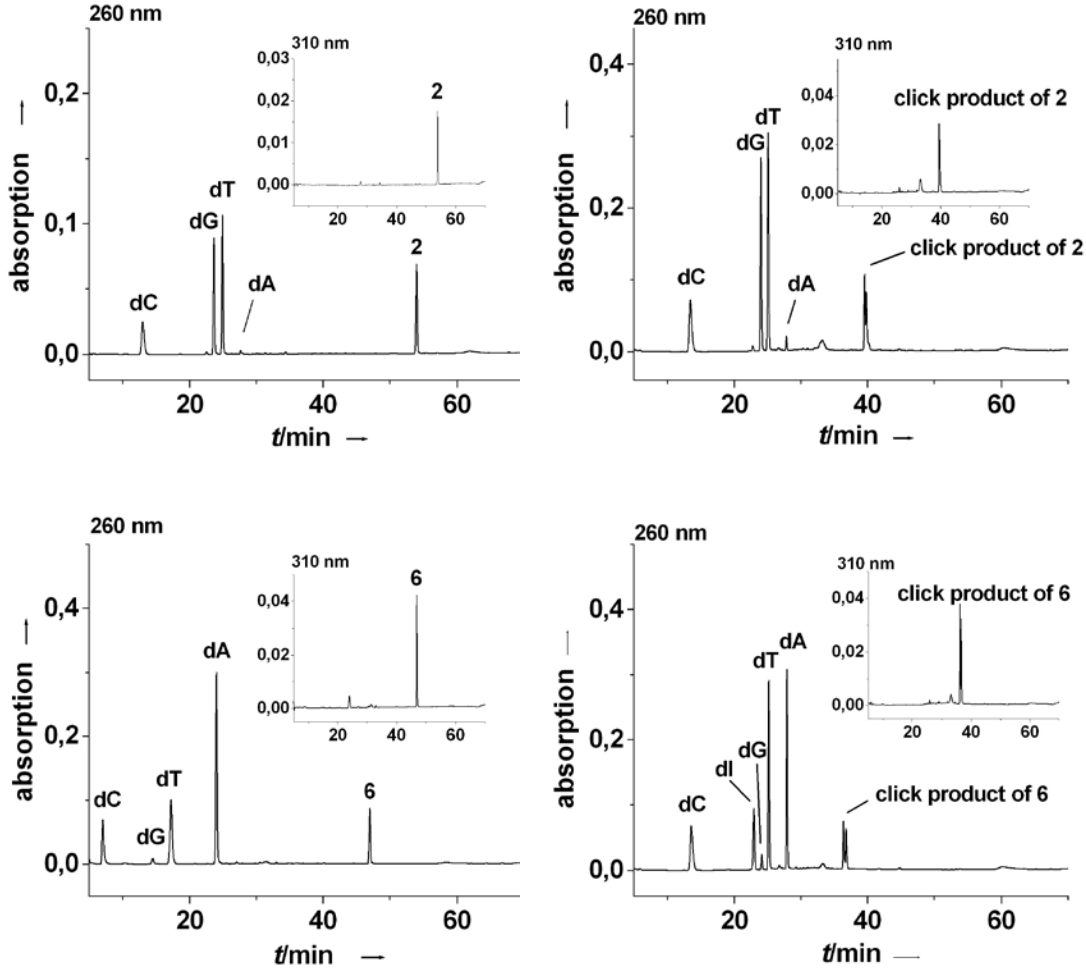

Figure 7.2 HPLC chromatograms of the enzymatic digest of DNA300•**7.2** (top) and DNA300•**7.6** (bottom) before (left) and after (right) the click reaction with galactose azide **7.12**. The inset shows the HPLC trace at 310 nm. Deoxyinosine (dI) is formed by deamination of dA during the enzymatic digest. The click products form double peaks due to anomerization of the sugar moiety.

In order to prove the presence of the modifications in the DNA strands, we performed enzymatic digests of 300DNA•**N** (unmodified), 300DNA•**7.2**, and 300DNA•**7.6** (Figure 7.2). The DNA was treated with nuclease P1, calf spleen phosphodiesterase, snake venom phosphodiesterase and alkaline phosphatase. The obtained mixture of nucleosides was separated by HPLC and the modified bases **7.2** and **7.6** were co-injected. These spectra show that the DNA indeed contains the modified purine bases **7.2** and **7.6**. Only a small amount of the unsubstituted purine nucleosides dA and dG was detected, which derive from the commercial primers that were used for the PCR reactions. This result proves that our triphosphates were efficiently

incorporated into 300DNA•**7.2** and 300DNA•**7.6**. Further proof for the presence of the modified bases was obtained from ESI-MS/MS and UV spectra of the eluting compounds.
Having achieved the successful incorporation of **7.3** and **7.7** into the PCR amplicons, we wanted to know if the modified DNA features sequence changes. To this end, we used 300DNA•**7.2** and 300DNA•**7.6** as templates for a PCR reaction with the natural dNTPs and either KOD XL or Deep Vent exo$^-$ polymerase. The resulting amplicons were sequenced (Section 7.5.6). We observed that the 300DNA•**N** strands retained the original sequence, proving that the modified bases do not reduce the polymerase fidelity in our PCR reaction but are faithfully copied.
In order to prove the proficiency of the alkyne-containing DNA in the click reaction, we used DNA•**7.2** and DNA•**7.6** as a reaction partner in the Cu(I)-catalyzed click reaction with galactose azide **7.12**. CuBr and TBTA ligand[21] were added to perform the reaction. The reaction products were purified from excess reactants by simple ethanol precipitation and were digested enzymatically. HPLC chromatography of the resulting nucleoside mixtures combined with UV and MS/MS analysis clearly showed the quantitative yield of the postsynthetic click functionalization, which proceeds without formation of any detectable side product. No traces of unreacted alkynes could be found (Figure 7.2).

7.4 Summary and Outlook

In summary, we present novel alkyne-bearing purines, which can be incorporated into DNA via a PCR reaction. These building blocks act as selective reaction partners in the click reaction with azides. Quantitative conversion of more than 100 alkynes in DNA was again observed.

7.5 Experimental Section

7.5.1 Synthesis of Modified Triphosphates

7-Deaza-7-(octa-1,7-diynyl)-2′-deoxyadenosine (**7.2**)

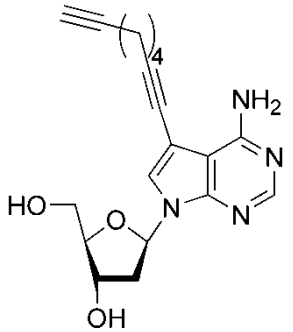

To a degassed solution of 7-deaza-7-iodo-2'-deoxyadenosine **7.1**[15] (285 mg, 0.758 mmol) and CuI (29 mg, 0.152 mmol) in dry DMF (3 mL) was added dropwise over 15 min a de-

gassed mixture of 1,7-octadiyne (805 mg, 7.58 mmol) and DIPEA (197 mg, 1.52 mmol) in dry DMF (1 mL). Then, $Pd(PPh_3)_4$ was added and the mixture was stirred at r. t. for 4 h. The mixture was concentrated *in vacuo* and chromatographed on silica ($CHCl_3$/MeOH 40:1 → 25:1) to yield the product as a complex with DIPEA. The amine was removed by dissolving the mixture in MeOH (2 mL) and adding water (20 mL) to precipitate the product. The suspension was then lyophilized and finally dried in high vacuum to yield the pure product as a light yellow powder (225 mg, 0.63 mmol, 84%).
R_f ($CHCl_3$/MeOH 6:1): 0.3. ^{1}H-NMR (400 MHz, d_6-DMSO): δ = 1.60-1.65 (m, 4H, $CH_2(CH_2)_2CH_2$), 2.15-2.25 (m, 4H, $C_{2'}H$, $H_2CC{\equiv}C$-Si), 2.45-2.55 (m, 2H, $H_2CC{\equiv}C$-Ar), 2.77 (t, 1H, *J* = 2.7 Hz, $HC{\equiv}C$), 3.50-3.60 (m, 2H, $C_{5'}H$), 3.80-3.85 (m, 1H, $C_{4'}H$), 4.30-4.35 (m, 1H, $C_{3'}H$), 5.05 (t, 1H, *J* = 5.6 Hz, $C_{5'}OH$), 5.24 (d, 1H, *J* = 4.1 Hz, $C_{3'}OH$), 6.47 (dd, 1H, *J* = 8.1, 6.0 Hz, $C_{1'}H$), 6.65 (sbr, 2H, NH_2), 7.65 (s, 1H, C_8H), 8.10 (s, 1H, C_2H). ^{13}C-NMR (100 MHz, d_6-DMSO): δ = 17.2 (CH_2), 18.4 (CH_2), 27.2 (CH_2), 27.3 (CH_2), 39.8 (CH_2), 61.9 (CH_2), 71.0, 71.4 (CH), 73.8, 83.1 (CH), 84.2, 87.5 (CH), 92.2, 95.4, 102.3, 125.5 (CH), 149.0, 152.5, 157.5. HRMS (ESI): calcd. for $C_{19}H_{23}N_4O_3^+$ $[M+H]^+$: 355.1765, found: 355.1755.

7-Deaza-7-(octa-1,7-diynyl)- 5'-*O*-triphosphate-2′-deoxyadenosine (**7.3**)

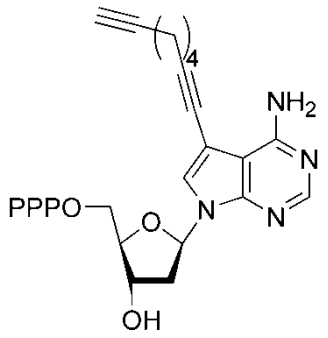

Starting material **7.2** together with 1,8-bis(dimethylamino)naphthalene (proton sponge) was dried over night under high vacuum. Trimethyl phosphate and the mixture of tributylammonium pyrophosphate and tributyl amine were stirred over night over molecular sieves.
To a cooled solution (0 °C) of **7.2** (20 mg, 0.056 mmol) and proton sponge (18 mg, 0.084 mmol) in trimethyl phosphate (1 mL) was added $POCl_3$ (6 µL, 0.07 mmol) dropwise over 5 min. The reaction mixture was then stirred for 3 h at 0 °C. A solution of tributylammonium pyrophosphate (133 mg, 0.28 mmol) in dry DMF (0.56 mL) was added to the reaction mixture which was stirred for 10 min followed by quenching with triethylammonium bicarbonate solution (1.0 M, 4 mL, pH 8.5). The mixture was stirred at r. t. for additional 3 h and then lyophilized over night. RP-HPLC purification (gradient of 0→55% B with 0.1 M triethylammonium acetate in H_2O as solvent A and 0.1 M triethylammonium acetate in H_2O/MeCN 4:1 as solvent B over 45 min at a flow rate of 5 mL min^{-1}) yielded **7.3** (22.2 min, 11.0 µmol, 20%) as the triethylammonium salt. The triphosphate was dissolved in doubly distilled, sterile water, and its molar concentration was determined by measuring its UV absorption.

^{31}P-NMR (81 MHz, D_2O): δ = -21.9 (t, 1P, *J* = 19 Hz, -β), -10.1 (d, 1P, *J* = 19 Hz, -α), -9.5 (d, 1P, *J* = 20 Hz, -γ). HRMS (ESI): calcd. for $C_{19}H_{24}N_4O_{12}P_3^-$ $[M-H]^-$: 593.0609, found: 593.0602.

7-Deaza-7-(7-trimethylsilyl-octa-1,7-diynyl)-3′,5′-*O*-(di-*p*-toluoyl)-2′-deoxyguanosine (**7.5**)

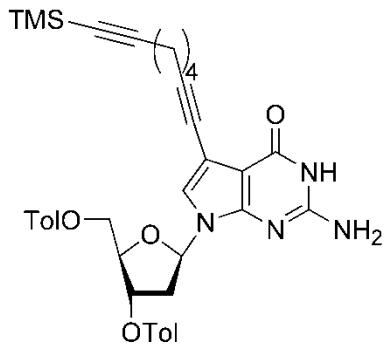

To a thoroughly degassed solution of **7.4** (130 mg, 0.207 mmol), $PdCl_2(PPh_3)_4$ (29.0 mg, 0.041 mmol) and CuI (15.7 mg, 0.082 mmol) in dry DMF (0.7 mL) was added degassed DIPEA (180 µL, 1.0 mmol) in DMF (0.4 mL) and the reaction mixture was degassed again. A degassed solution of trimethylsilyl-1,7-octadiyne (92 µL, 0.4 mmol) in DMF (0.3 mL) was added to the reaction mixture over 20 min. After complete addition, the reaction mixture was stirred at r. t. over night. The solvent was removed *in vacuo* and the residue directly applied to a flash column chromatography (DCM/MeOH 20:1). The product was obtained as a pale yellow powder (107 mg, 0.158 mmol, 76%).

R_f ($CHCl_3$/MeOH 10:1): 0.45. ^{1}H-NMR (600 MHz, $CDCl_3$): δ = 0.13 (s, 9H, $SiCH_3$), 1.63-1.73 (m, 4H, $CH_2(CH_2)_2CH_2$), 2.25 (t, 2H, *J* = 6.9 Hz, H_2C-C≡ C-Si), 2,41 (s, 3H, H_3C-Ar), 2,44 (s, 3H, H_3C-Ar), 2.45 (t, 2H, *J* = 6.6 Hz, H_2C-C≡ C-Ar), 2.62 (ddd, 1H, *J* = 2.1, 5.8, 14.1 Hz, $C_{2'}H$), 2.73-2.79 (m, 1H, $C_{2'}H$), 4.53-4.56 (m, 1H, $C_{4'}H$), 4.60 (dd, 1H, *J* = 4.3, 11.8 Hz, $C_{5'}H$), 4.69 (dd, 1H, *J* = 4.6, 11.8 Hz, $C_{5'}H$), 5.67-5.70 (m, 1H, $C_{3'}H$), 5.97 (sbr, 2H, NH_2), 6.48 (dd, 1H, *J* = 6.1, 8.2 Hz, $C_{1'}H$), 6.94 (s, 1H, C_8H), 7.25 (d, 2H, *J* = 7.8 Hz, CH_{Ar}), 7.27 (d, 2H, *J* = 7.8 Hz, CH_{Ar}), 7.94 (d, 2H, *J* = 8.4 Hz, CH_{Ar}), 7.96 (d, 2H, *J* = 8.4 Hz, CH_{Ar}), 11.17 (sbr, 1H, NH). ^{13}C-NMR (150 MHz, $CDCl_3$): δ = 0.2 (CH_3), 19.4 (CH_2), 21.7 (CH_3), 21.7 (CH_3), 27.7 (CH_2), 27.9 (CH_2), 37.5 (CH_2), 64.2 (CH_2), 73.8, 75.1 (CH), 81.9 (CH), 83.7 (CH), 84.8, 90.6, 100.5, 100.6, 107.1, 121.6 (CH), 126.5, 126.8, 129.2 (CH), 129.2 (CH), 129.7 (CH), 129.8 (CH), 143.9, 144.3, 151.1, 152.9, 160.1, 165.9, 166.3. HRMS (ESI): calcd. for $C_{38}H_{43}N_4O_6Si^+$ $[M+H]^+$: 679.2952, found: 679.2962.

7-Deaza-7-(octa-1,7-diynyl)-2′-deoxyguanosine (**7.6**)

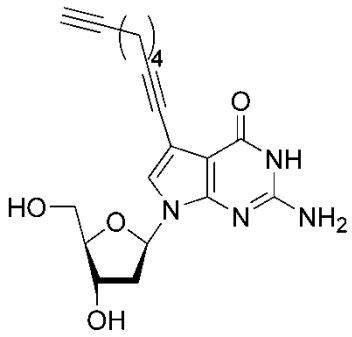

7.5 (30 mg, 0.044 mmol) was dissolved in dry MeOH (10 mL) saturated with NH_3. The solution was heated in a pressure vessel (140 °C) for 2 h. The solvent was removed *in vacuo*. The product (11 mg, 0.027 mmol, 67%) was obtained by flash column chromatography (DCM/MeOH 9:1) as a light brown solid.

R_f (DCM/MeOH 9:1): 0.16. ^{1}H-NMR (400 MHz, CD_3OD): δ = 1.63–1.74 (m, 4H, $CH_2(CH_2)_2CH_2$), 2.19 (t, 1H, *J* = 2.8 Hz, HC≡ C), 2.20–2.27 (m, 3H, H_2CC≡ C-H, $C_{2'}H$), 2.42 (t, 2H, *J* = 6.6 Hz, H_2CC≡ C-Ar), 2.49 (ddd, 1H, *J* = 6.1, 8.0, 13.8 Hz, $C_{2'}H$), 3.66-3.73 (m, 2H, $C_{5'}H$), 3.92 (dt, 1H, *J* = 2.8, 4.0 Hz, $C_{4'}H$), 4.45 (td, 1H, *J* = 2.8, 5.9 Hz, $C_{3'}H$), 6.35 (dd, 1H, *J* = 6.1, 8.0 Hz, $C_{1'}H$). 7.08 (s, 1H, C_8H). ^{13}C-NMR (CD_3OD, 100 MHz): δ = 18.6 (CH_2), 19.9 (CH_2), 28.9 (CH_2), 29.0 (CH_2), 41.3 (CH_2), 63.7 (CH_2), 69.6, 72.9, 73.6, 74.7, 84.9, 85.4, 88.7, 91.3, 101.8, 123.3 (CH), 151.9, 154.3, 161.3. HRMS (ESI): calcd. for $C_{19}H_{21}N_4O_4^-$ $[M-H]^-$: 369.1563, found: 369.1573.

7-Deaza-7-(octa-1,7-diynyl)-5′-*O*-triphosphate-2′-deoxyguanosine (**7.7**)

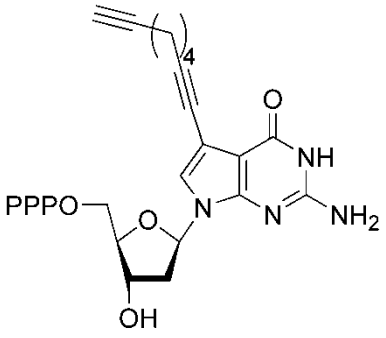

To a cooled solution (0 °C) of **7.6** (32 mg, 0.086 mmol.) and 1,8-bis(dimethylamino)naphthalene (proton sponge, 0.068 g, 0.316 mmol) in trimethyl phosphate (0.8 mL) was added $POCl_3$ (9.5 µL , 0.103 mmol) dropwise over 5 min under a nitrogen atmosphere. The reaction mixture was stirred for 3 h at 0 °C. A solution of tributylammonium pyrophosphate (0.086 g, 0.16 mmol) in dry DMF (1.0 mL) and tributyl amine (136 µL) was added to the reaction mixture and stirred for 35 min followed by quenching with triethylammonium bicarbonate (1.0 M, 12 mL, pH 8.5). The reaction mixture was stirred for 2 h and lyophilized over night. RP-HPLC purification (gradient of 0→40% B with 0.1 M triethylammonium acetate in H_2O as solvent A and 0.1 M triethylammonium acetate in H_2O/MeCN 4:1 as solvent B over 45 min at a flow rate of 15 mL min^{-1}) yielded **7.7**

(22.2 min, 1.7 μmol, 2%) as the triethylammonium salt. The triphosphate was dissolved in doubly distilled, sterile water, and its molar concentration was determined by measuring its UV absorption.
^{31}P-NMR (81 MHz, D_2O): δ = -22.3 (t, 1P, *J* = 20 Hz, -β), -10.3 (d, 1P, *J* = 20 Hz, -α), -9.9 (d, 1P, *J* = 20 Hz, -γ). MS (MALDI-TOF): 608.9 $[M-H]^-$.

7.5.2 Primer Extension Using up to Four Alkyne-Modified Triphosphates

Pr1	3′-CA TGG GCC AAG CTT CTT CGG-5′
T1	5′-TCG TCA GTC GGT ACC CGG TTC GAA GAA GCC-3′
T2	5′-TCG TAA GTC GGT ACC CGG TTC GAA GAA GCC-3′

For primer extension experiments an assay developed by Held et al. was used.[17] The primer extensions were run in a total volume of 20 μL with the final concentrations of 750 nM primer, 900 nM template, 200 μM dNTPs, 1 × KOD XL PCR buffer and 1 U polymerase. The primer and template were hybridized by heating to 95 °C and cooling to 4 °C prior to the reaction. The extension was started by adding the polymerase and incubating the entire mixture at 40 °C (temperature increment +1 °C per 120 s up to 74 °C). The extension was then quenched with 2 μL EDTA (0.1 M, pH 7.5) and 10 μL gel loading buffer. From that solution 10 μL were run on a 20% PAGE-gel.

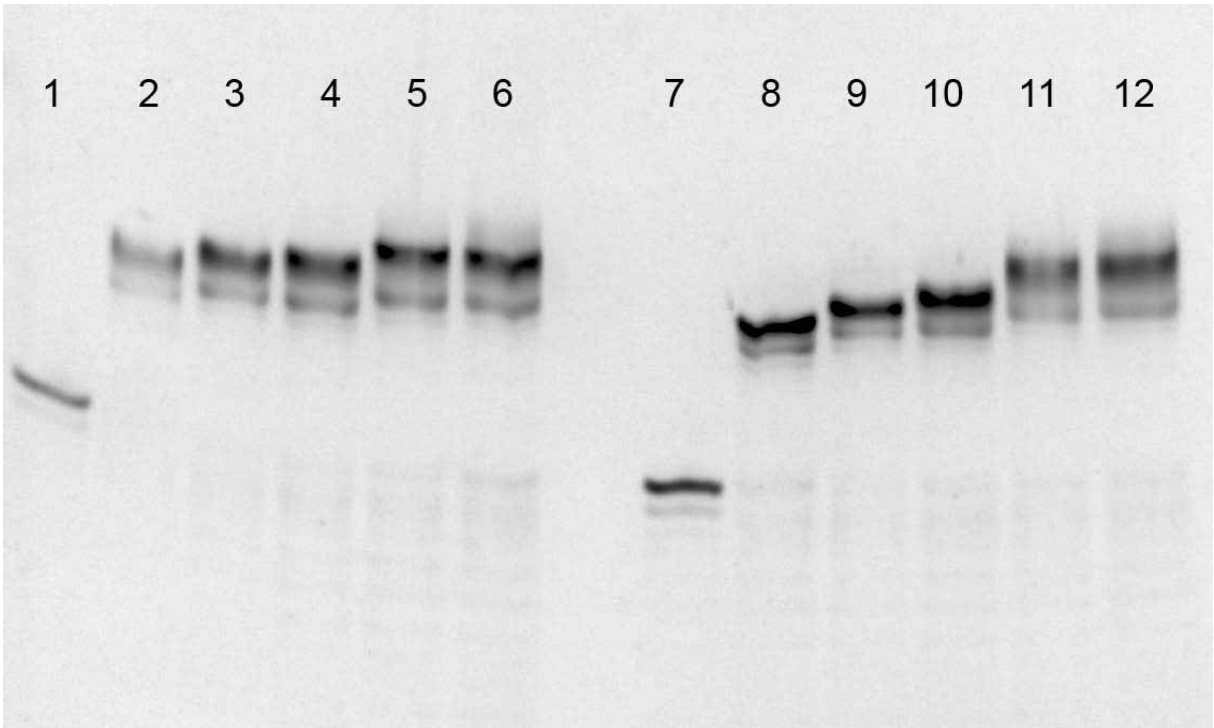

Figure 7.3 Primer extension on **T1** (lanes 1-6) and **T2** (lanes 7-12). Lanes 1 and 7: primers, lanes 2 and 8: primer extension with dNTPs, lanes 3 and 9: **7.9**, dATP, dGTP, dTTP, lanes 4 and 10: **7.9**, **7.11**, dATP, dGTP, lanes 5 and 11: **7.3**, **7.9**, **7.11**, dGTP, lanes 6 and 12: **7.3**, **7.7**, **7.9**, **7.11**.

7.5.3 Polymerase Chain Reaction with **7.3** and **7.7**

Incorporation of triphosphates **7.3** or **7.7** into a PCR amplicon

A typical PCR reaction in a total volume of 25 µL contained 0.4 µg template, 0.3 µM each of the forward and reverse primers (both fluorescein-labeled for **7.7**, both unlabeled for **7.3**), 1 U KOD XL polymerase, 10 × polymerase buffer as supplied by the manufacturer (2.5 µL) and 200 µM of each dNTP (corresponding natural dNTPs substituted by modified triphosphates **7.3** or **7.7**).

PCR program for amplification of **7.3**

Hotstart (2 min at 95 °C), 9 cycles of touchdown amplification (15 s at 95 °C, 30 s at 58 °C with temperature increment of -1 °C/cycle, 45 s at 72 °C), then 30 cyles of amplification (15 s at 95 °C, 30 s at 57 °C, 45 s at 72 °C) followed by a final incubation at 72 °C for 2 min.

PCR program for amplification of **7.7**

For amplification hotstart (2 min at 97.6 °C) was used, followed by 9 cycles of touchdown amplification (30 s at 97.6 °C, 30 s at 60.7 °C, temperature increment -1 °C per cycle, 60 s at 74 °C), 30 cycles amplification (30 s at 97.6 °C, 30 s at 59.7 °C, 60 s at 74 °C) and a final incubation for 2 min at 72 °C.

7.5.4 UV-Vis and CD Spectra of the Modified DNA Strands

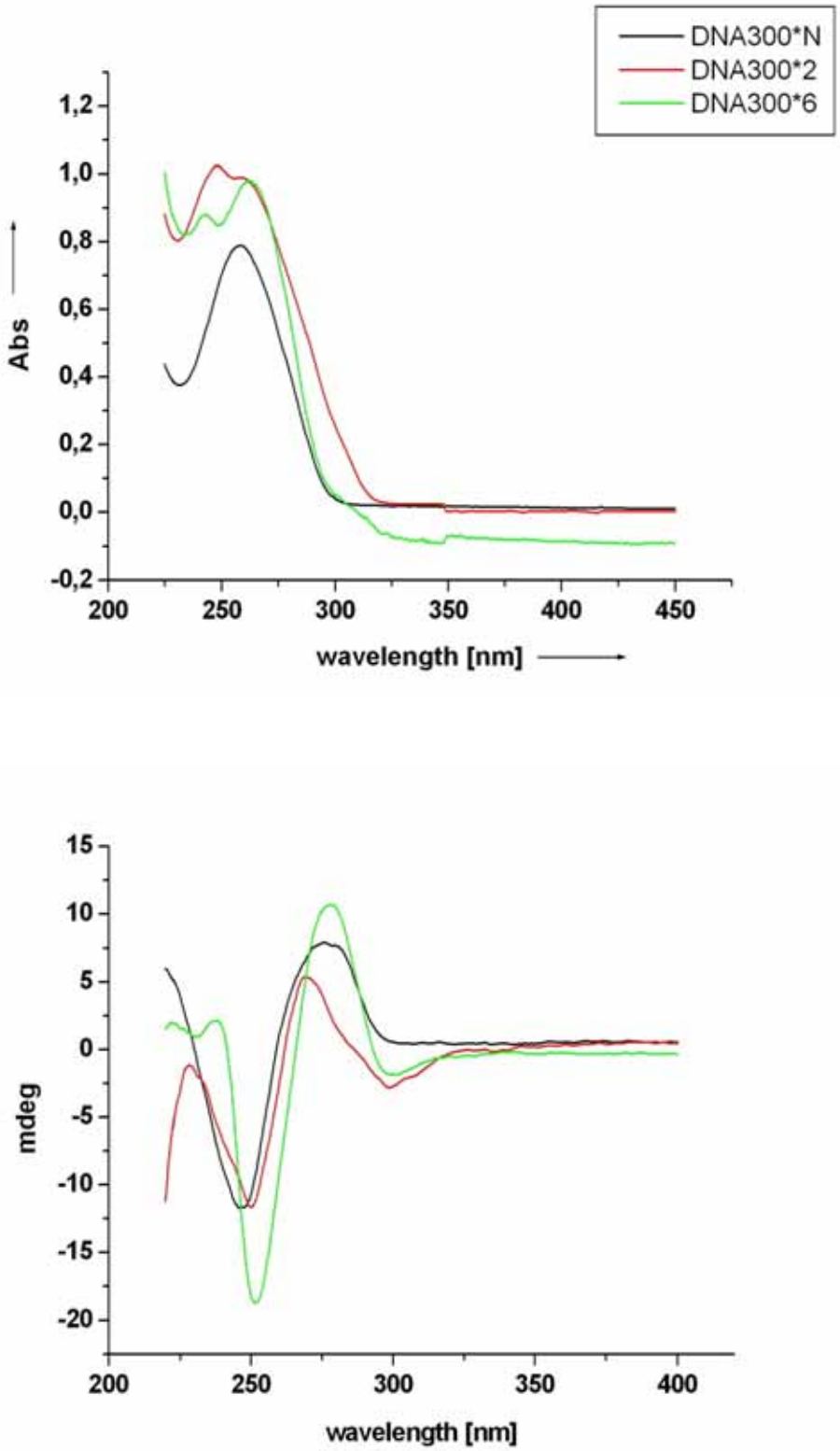

Figure 7.4 UV (top) and CD (bottom) spectra of DNA300•**N**, DNA300•**7.2** and DNA300•**7.6**.

7.5.5 Sequence Analysis

PCR conditions for amplification of modified template DNA300•**7.2** with natural dNTPs

20 ng of DNA300•**7.2** as template, 0.3 µM of both primers, 1 U Deep Vent exo$^-$ polymerase, 10× Deep Vent exo$^-$ buffer (2.5 µL) and 200 µM of each dNTP were mixed to a total volume of 25 µL with sterile, doubly distilled water.
PCR program: Hotstart (2 min at 95 °C), 9 cycles of touchdown amplification (15 s at 95 °C, 30 s at 62 °C with temperature increment of -1 °C/cycle, 45 s at 72 °C), then 30 cyles of amplification (15 s at 95 °C, 30 s at 59 °C, 45 s at 72 °C) followed by a final incubation at 72 °C for 2 min.

PCR conditions for amplification of modified template DNA300•**7.7** with natural dNTPs

10 µg DNA300•**7.6**, 0.3 mM each of the forward and reverse primers, 1 U KOD XL or Pwo polymerase, 10 × KOD or Deep Vent exo$^-$ PCR buffer (2.5 µL) and 200 µM of each dNTP were mixed to a total volume of 25 µL with sterile, doubly distilled water.
PCR program: Hotstart (2 min at 95 °C), followed by 9 cycles of touchdown amplification (15 s at 95 °C, 30 s at 60.7 °C (KOD XL) or 53.2 °C (Deep Vent exo$^-$), temperature increment -1 °C per cycle, 45 s at 72 °C), 30 cycles amplification (15 s at 95 °C, 30 s at 58.5 °C (KOD XL) or 50.2 °C (Deep Vent exo$^-$), 45 s at 72 °C) and a final incubation for 2 min at 72 °C.

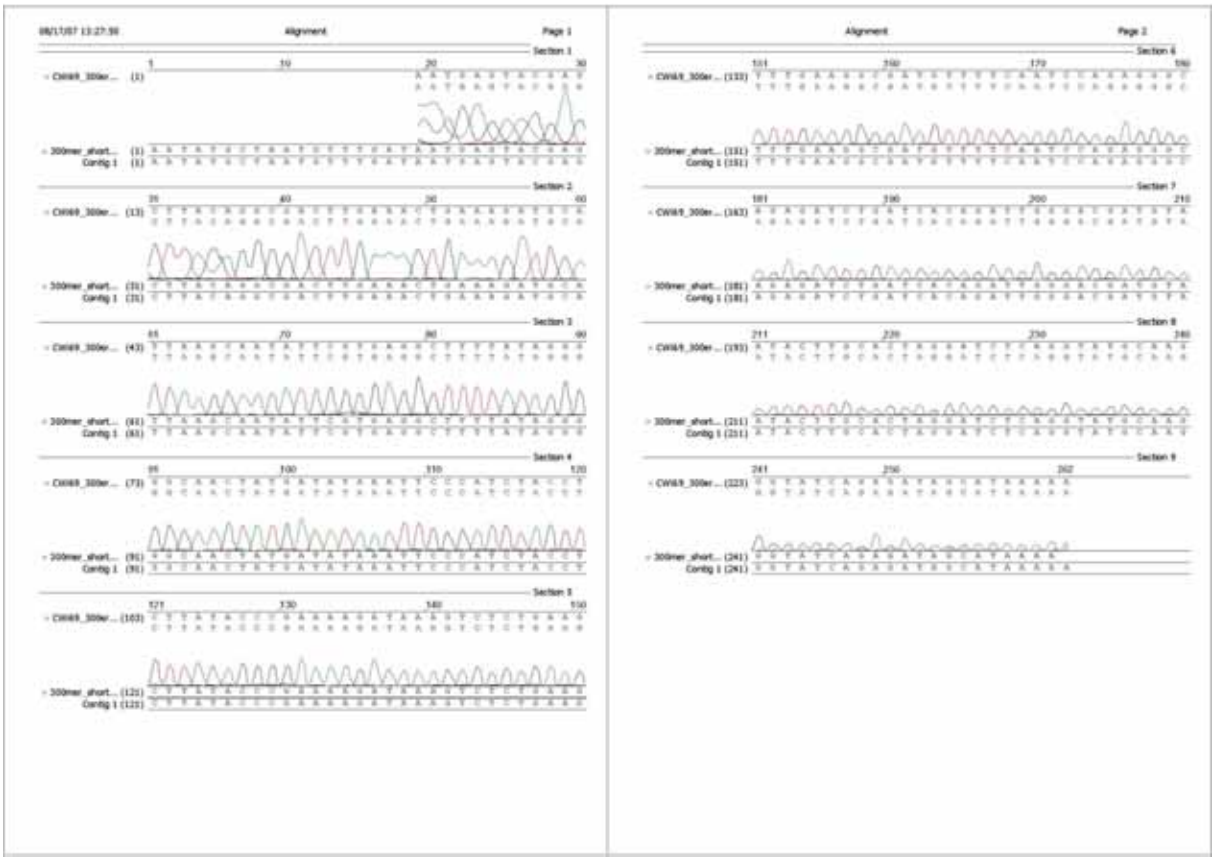

Figure 7.5 Sequence analysis for retranscription product of DNA300•**7.2** using Deep Vent exo$^-$ polymerase.

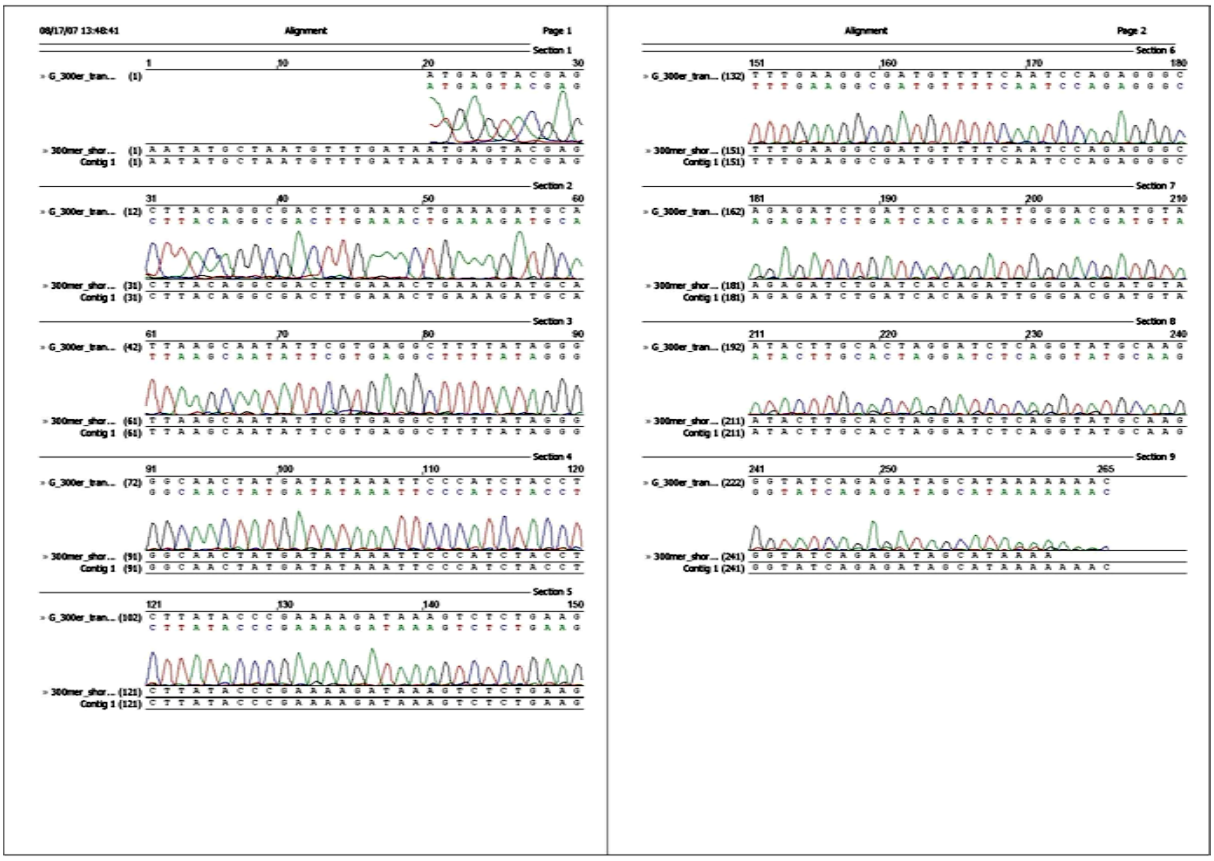

Figure 7.6 Sequence analysis for retranscription product of DNA300•**7.6** using KOD XL polymerase.

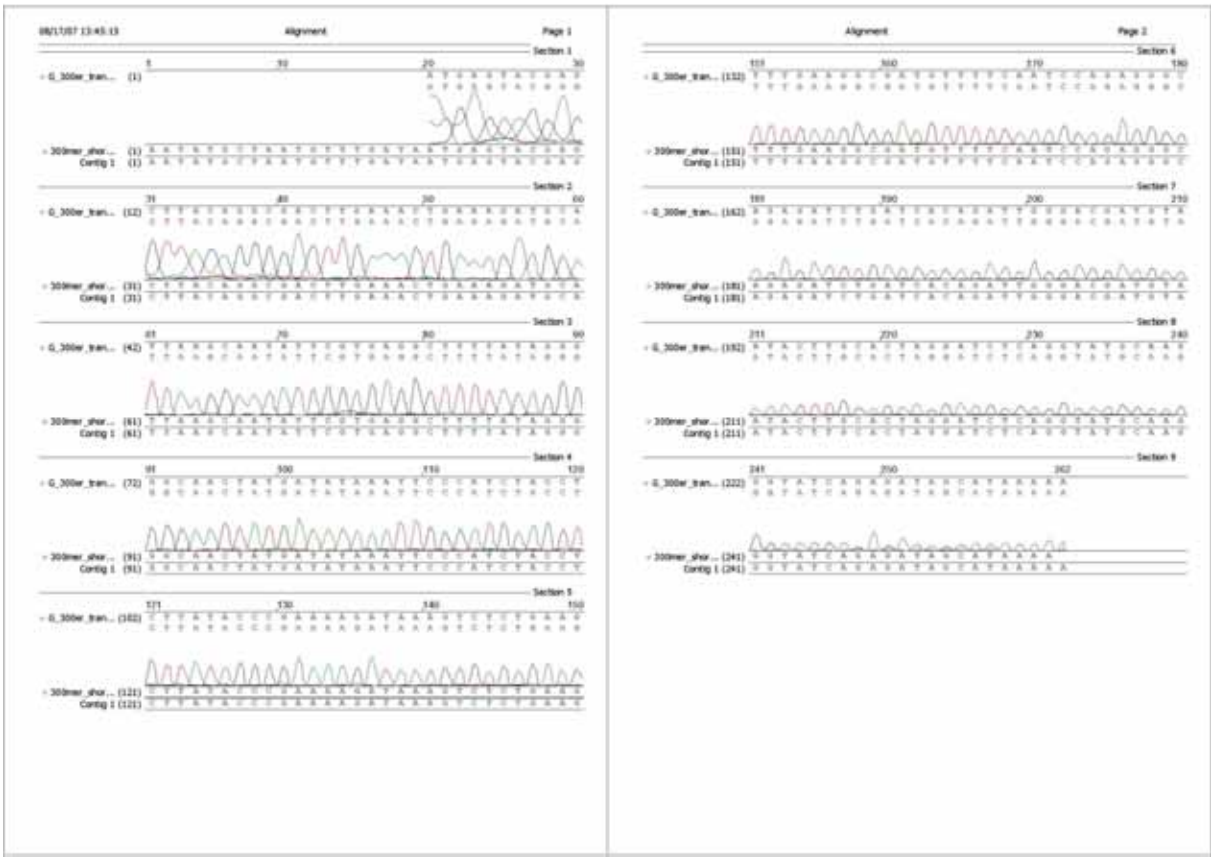

Figure 7.7 Sequence analysis for retranscription product of DNA300•**7.6** using Deep Vent exo$^-$ polymerase.

Both sequence analyses show an exact accordance with the original template sequence. This shows that both adenosine triphosphate **7.3** and guanosine triphosphate **7.7** are incorporated into DNA with high sequence-fidelity and can be retranscribed by two different polymerases.

7.5.6 Click Reaction on PCR Amplicons and Evaluation of Product Yield by Enzymatic Digestion, HPLC and MS/MS

2 µg DNA and 2 µmol **7.12** were placed in a 1.5 mL vial and lyophilized. In a separate vial, CuBr solution (10 mM in DMSO/*t*BuOH 3:1, 5 µL) and TBTA ligand[21] solution (10 mM in DMSO/*t*BuOH 3:1, 5 µL) were vortexed and added to the DNA. 10 µL H_2O were added. The solution was shaken at 37 °C for 2 h and then lyophilized to dryness. 100 µL Na^+OAc^- solution (0.3 M) was added to dissolve the DNA. 1 mL EtOH was added, the vial was vortexed and placed in a freezer (-20 °C) over night. After centrifugation (15 min at 13 000 rpm) the supernatant was carefully removed from the DNA pellet. 70% EtOH (-20 °C) was added, the vial was vortexed, centrifuged and the supernatant removed. This washing step was repeated twice. After the last washing step the pellet was left drying on air.

For the enzymatic digest the DNA (about 2 µg taken up in 100 µL water) was incubated in 10 µL buffer A (300 mM $NH_4^+OAc^-$, 100 mM $CaCl_2$, 1 mM $ZnSO_4$, pH 5.7) together with 11 U of nuclease P1 and 0.05 U of calf spleen phosphodiesterase II. The sample was shaken at

37 °C for 3 h. The digest was completed by adding 12 µL buffer B (500 mM Tris-HCl, 1 mM EDTA, pH 8.0), 10 U alkaline phosphatase (CIP) and 0.1 U snake venom phosphodiesterase I. The sample was shaken for another 3 h at 37 °C. For workup the samples were centrifuged (13 000 rpm, 5 min).
The digest solution was analyzed by HPLC, buffer A: 2 mM NH_4HCOO in H_2O (pH 5.5); buffer B: 2 mM NH_4HCOO in H_2O:MeCN 1:4; gradient: 0 → 12 min: 0% → 3% B, 12 → 60 min: 3% → 60% B, 60 → 62 min: 60% → 100% B, 62 → 90 min: 100% B, 90 → 95 min: 100% B → 0% B, 95 → 130 min: 0% B, flow 0.15 mL/min). The different peaks were assigned by co-injection, UV and FT-ICR-HPLC-MS-MS using the same conditions.

Table 7.1 ESI-MS/MS-data of the digest of DNA300•**7.2**.

	FTICR-MS	MS/MS
Starting material: nucleoside **7.2** at 54.0 min ($C_{19}H_{22}N_4O_3$)	$[M+HCOO]^-$: calc. 399.1674, found 399.1674	$[M-H]^-$: calc. 353.2, found 353.2
Click product of nucleoside **7.2** at 39.6 min and 39.9 min ($C_{25}H_{33}N_7O_8$)	$[M+HCOO]^-$: calc. 604.2373, found 604.2371	$[M-H]^-$: calc. 558.2, found 558.1

Table 7.2 ESI-MS/MS-data of the digest of DNA300•**7.6**.

	FTICR-MS	MS/MS
Starting material: nucleoside **7.6** at 47.0 min ($C_{19}H_{22}N_4O_4$)	$[M+HCOO]^-$: calc. 415.1623, found 415.1623	$[M-H]^-$: calc. 369.2, found 369.2
Click product of nucleoside **7.6** at 36.4 min and 36.8 min ($C_{25}H_{33}N_7O_9$)	$[M-H]^-$: calc. 574.2267, found 574.2265	-

7.6 Notes Added after Publication

7.6.1 Fluorescence Quenching of SYBR Green and Ethidium Bromide by DNA300•**7.2** and DNA300•**7.6**

7-Deazapurines have been described to quench the fluorescence of ethidium bromide, an intercalating dye that is frequently used for the visualization of DNA after gel electrophoresis. Quenching of the ethidium fluorescence by 7-deazaguanosines has been investigated for short synthetic oligonucleotides[18] as well as for PCR products.[19] In both cases the quenching efficiency has been shown to be very high. The quenching efficiency of 7-deazaadenines on ethidium bromide has been shown to be only 30%, exemplified again with short oligonucleotides.[20] To the best of our knowledge, there is no report on the quenching efficiency of these purine derivatives on SYBR green.
For these experiments, PCR amplicons were prepared as described in Section 7.5.3, the only exception being that the primers used for the incorporation of **7.2** were not labeled with fluorescein, so that no aberrant fluorescence would be detected. DNA strands were purified on a QIAquick PCR purification kit (Qiagen). The concentration of the resulting strands was de-

termined on a NanoDrop ND-1000 spectrophotometer from preQlab. The shift for the modified strands is a result of the increased molecular weight.

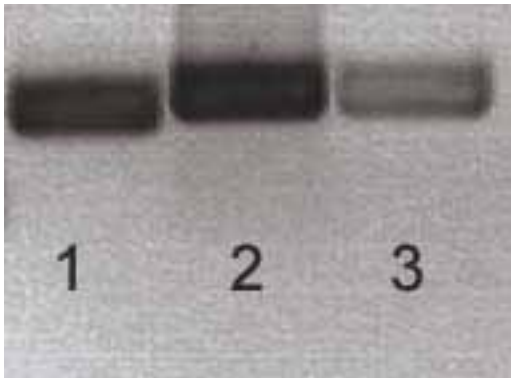

Figure 7.8 Demonstration of the quenching efficiency of DNA300•**7.2** and DNA300•**7.6**. 2% Agarose gel stained with ethidium bromide. Lane 1: DNA300•N; lane 2: DNA300•**7.2**; lane 3: DNA300•**7.6**. Each lane contains 400 ng DNA.

Quantification of the bands in Figure 7.8 (AIDA image analyzer) shows that the ethidium fluorescence is essentially the same for DNA300•N and DNA300•**7.2.** The fluorescence is quenched by 60% for DNA300•**7.6**.

Figure 7.9 Demonstration of the quenching efficiency of DNA300•**7.2** and DNA300•**7.6**. 5% PAGE gel stained with SYBR green. Lane 1: DNA300•N; lane 2: DNA300•**7.2**; lane 3: DNA300•**7.6**. Each lane contains 100 ng DNA.

Quantification of the bands in Figure 7.9 shows that the SYBR green fluorescence is essentially the same for DNA300•N and DNA300•**7.2.** For DNA300•**7.6**, the fluorescence is quenched by > 90%.

7.6.2 Simultaneous Incorporation of **7.3** and **7.13** into 100mer PCR products

Previous experiences with PCR reactions using alkyne-modified triphosphates showed that the incorporation of up to two alkyne-modified triphosphates (e. g. **7.9** and **7.13**) into 300mer PCR products was well feasible as long as the modified triphosphates were situated on different base pairs. Incorporation of all four alkyne-modified triphosphates was only possible in a

primer extension reaction, for which an unmodified template was used. Therefore it was attempted to incorporate the alkyne triphosphates **7.3** and **7.13** into a 300mer PCR product. The PCR product would contain a modified AT base pair, in which both building blocks bear alkynes. After extensive screening of reaction conditions, it became apparent that it would be literally impossible to obtain a specific reaction product. Therefore it was attempted to synthesize a simpler PCR product of only about 100 bp in length using the primers reported in Table 7.3.

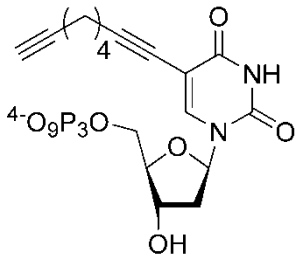

7.13

Scheme 7.2 Structure of triphosphate **7.13**.

Table 7.3 Primer sequences for the amplification of a 100 bp PCR product using the same template as for the amplification of the 300mer PCR product.

reverse primer	5'-AAT TGC TAA CGC AGT CAG GC-3'
forward primer	5'-AAG CCT ATG CCT ACA GCA TC-3'

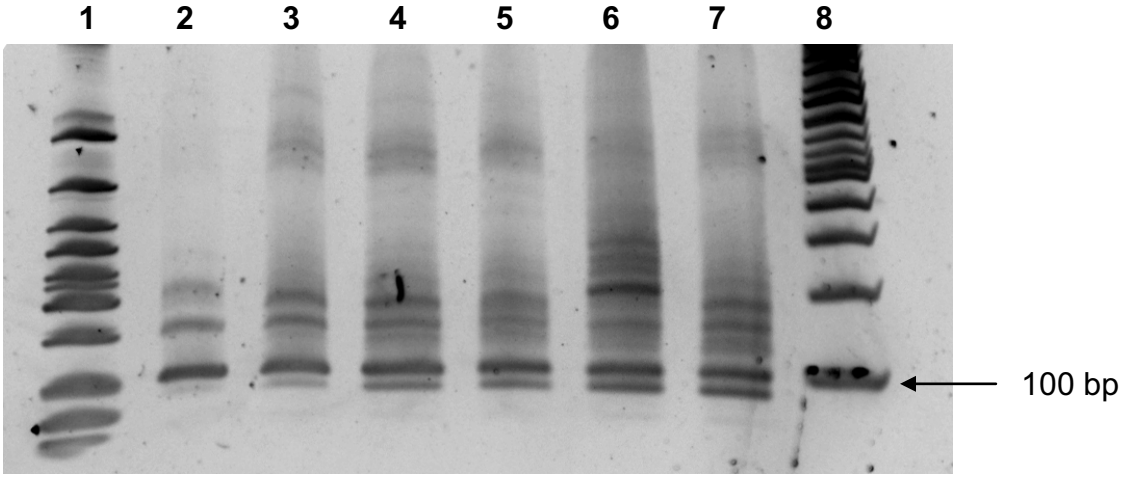

Figure 7.10 8% PAGE for the amplification of a 100mer PCR product containing the triphosphates **7.3** and **7.13**. PCR was performed using the same reagent amounts as reported for the amplification of the 300mer. Lane 1: low MW DNA ladder, lane 2: annealing at 64.8 °C, lane 3: 62.5 °C, lane 4: 58.8 °C, lane 5: 54.8 °C, lane 6: 51.5 °C, lane 7: 50.2 °C, lane 8: 100 bp DNA ladder.

Amplification of this 100mer was shown to be extremely easy with up to two modified bases which are not situated on the same base pair (data not shown). For the analogous amplifica-

tion using the modified AT base pair (**7.3** + **7.13**), extensive screening of reaction conditions was required to obtain the desired 100mer PCR product along with several different, unspecific products (Figure 7.10). It can therefore be concluded that the difficulty in producing a PCR product containing all four alkyne-modified bases stems from difficulties in placing a modified base opposite another modified one. On the other hand, the results show that it is not completely impossible to synthesize base pairs containing two alkyne modifications. Synthesis of PCR products containing two modified bases on different base pairs (e. g. cytidine and uridine) does not pose a significant challenge.

7.7 Author´s Contribution

*Syntheses of the free nucleosides were performed by Johannes Gierlich in collaboration with three bachelor students. Markus Spallek, a bachelor student supervised by the author, finished the synthesis of guanosine triphosphate **7.7**. Veronika Ehmke, a bachelor student supervised by Christian Wirges, finished the synthesis of adenosine triphosphate **7.3**. Biochemical investigations on these novel triphosphates were performed by the author in collaboration with Christian Wirges, who both contributed equally to this endeavor.*

7.8 References

[1] A. Condon, *Nat. Rev. Genet.* **2006**, *7*, 565-575; U. Feldkamp, C. M. Niemeyer, *Angew. Chem. Int. Ed.* **2006**, *45*, 1856-1876.

[2] D. M. Hammond, A. Manetto, J. Gierlich, V. A. Azov, P. M. E. Gramlich, G. A. Burley, M. Maul, T. Carell, *Angew. Chem. Int. Ed.* **2007**, *46*, 4184-4187.

[3] T. S. Seo, X. Bai, D. H. Kim, Q. Meng, S. Shi, H. Ruparel, Z. Li, N. J. Turro, J. Ju, *Proc. Nat. Acad. Sci. USA* **2005**, *102*, 5926-5931.

[4] A. Sidorov, J. A. Grasby, D. M. Williams, *Nucl. Acids Res.* **2004**, *32*, 1591-1601.

[5] E. Braun, Y. Eichen, U. Silvan, G. Ben-Yoseph, *Nature* **1998**, *391*, 775-778; K. Keren, M. Krueger, R. Gilad, G. Ben-Yoseph, U. Sivan, E. Braun, *Science* **2002**, *297*, 72-75; Q. Gu, C. Cheng, R. Gonela, S. Suryanarayanan, S. Anabathula, K. Dai, D. T. Haynie, *Nanotech.* **2006**, *17*, R14-R25.

[6] S. Jäger, G. Rasched, H. Kornreich-Leshem, M. Engeser, O. Thum, M. Famulok, *J. Am. Chem. Soc.* **2005**, *127*, 15071-15082.

[7] M. Kuwahara, J.-i. Nagashima, M. Hasegawa, T. Tamura, R. Kitagata, H. Kazuo, S.-i. Hososhima, T. Kasamatsu, H. Ozaki, H. Sawai, *Nucl. Acids Res.* **2006**, *34*, 5383-5394; T. Gourlain, A. Sidorov, N. Mignet, S. J. Thorpe, S. E. Lee, J. A. Grasby, D. M. Williams, *Nucl. Acids Res.* **2001**, *29*, 1898-1905.

[8] C. C. Y. Wang, T. S. Seo, Z. Li, H. Ruparel, J. Ju, *Bioconj. Chem.* **2003**, *14*, 607-701; S. H. Weisbrod, A. Marx, *Chem. Commun.* **2007**, 1828-1830.

[9] R. Huisgen, *Vol. 1,3-Dipolar Cycloaddition Chemistry*, Wiley, New York, **1984**, pp. 1-176; C. W. Tornoe, C. Christensen, M. Meldal, *J. Org. Chem.* **2002**, *67*, 3057-3064; H. C. Kolb, M. G. Finn, K. B. Sharpless, *Angew. Chem. Int. Ed.* **2001**, *40*, 2004-2021.

[10] J. Gierlich, G. A. Burley, P. M. E. Gramlich, D. M. Hammond, T. Carell, *Org. Lett.* **2006**, *8*, 3639-3642; G. A. Burley, J. Gierlich, M. R. Mofid, S. T. H. Nir, Y. Eichen, T. Carell, *J. Am. Chem. Soc.* **2006**, *128*, 1398-1399.

[11] J. Gierlich, K. Gutsmiedl, P. M. E. Gramlich, A. Schmidt, G. Burley, T. Carell, *Chem. Eur. J.* **2007**, *13*, 9486-9494.

[12] P. Capek, H. Cahová, R. Pohl, M. Hocek, C. Gloeckner, A. Marx, *Chem. Eur. J.* **2007**, *13*, 6196-6203.
[13] F. Seela, M. Zulauf, *Synthesis* **1996**, 726-730; F. Seela, V. R. Sirivolu, *Chem. Biodiversity* **2006**, *3*, 509-514.
[14] J. Davoll, *J. Chem. Soc.* **1960**, *1960*, 130-138.
[15] C. A. Buhr, R. W. Wagner, D. Grant, B. C. Froehler, *Nucleic Acids Res.* **1996**, *24*, 2974-2980.
[16] T. Kovacs, L. Ötvös, *Tetrahedron Lett.* **1988**, *29*, 4525-4528.
[17] H. A. Held, S. A. Benner, *Nucleic Acids Res.* **2002**, *30*, 3857-3869.
[18] H. Li, F. Seela, *Nucleosides & Nucleotides* **2005**, *24*, 865-868.
[19] J. Weiss, H.-D. Zucht, W.-G. Forssmann, *PCR Methods and Appl.* **1994**, *4*, 124-125.
[20] L. J. P. Latimer, J. S. Lee, *J. Biol. Chem* **1991**, *266*, 13849-13851.
[21] T. R. Chan, R. Hilgraf, K. B. Sharpless, V. V. Fokin, *Org. Lett.* **2004**, *6*, 2853-2855.

8 Click–Click–Click: Single to Triple Modification of DNA

This Section was published in:

P. M. E. Gramlich, S. Warncke, J. Gierlich, T. Carell, *Angew. Chem. Int. Ed.* **2008**, *47*, 3442-3444.

8.1 Introduction

The attachment of labels such as fluorescent dyes or biotin molecules to DNA is of paramount importance for DNA-based molecular diagnostics[1] and for nanotechnological applications.[2, 3] There is high demand for such modified oligonucleotides, but the chemistry behind the labeling procedures is cumbersome, and the modified oligonucleotides are frequently obtained in only low yields. Presently, the labels are incorporated as the corresponding phosphoramidites[4] during the solid-phase synthesis of oligonucleotides, which frequently reduces the coupling yield significantly. This method is restricted to labels that can withstand the harsh conditions of DNA synthesis and deprotection. Alternatively, the labels are introduced postsynthetically[5] by, for example, reaction of the corresponding activated esters with aminoalkyl-modified oligonucleotides.[6] This method suffers from inefficient coupling yields, making the purification of the labeled oligonucleotides a challenging task.
In a world in which the demand for labeled oligonucleotides is rapidly growing, new methods for the efficient incorporation of multiple different labels are required. Seela and Sirivolu[7] and our group[2, 8] have recently discovered that the copper(I)-catalyzed version of the azide-alkyne reaction to give triazoles, developed by Meldal et al.[9] and Sharpless et al.[10] can be used to functionalize alkyne-modified DNA nucleobases with extremely high efficiency. A critical point is the presence of a sufficient amount of a proper copper(I)-complexing ligand[11] to prevent the copper-catalyzed cleavage of DNA.[12] Herein we report that this chemistry can be extended to label oligonucleotides with up to three (and possibly more) different labels. These functionalizations can be achieved either directly on the resin[13] or in solution after deprotection of the oligonucleotide. The latter method can be used to incorporate extremely sensitive labels with unprecedented efficiency.

8.2 Results and Discussion

The first goal was to establish a method for the introduction of two different labels[14] during the solid-phase synthesis of oligonucleotides. We thought that the best way to achieve this goal would be to introduce one free alkyne for the first click reaction and a second TMS-protected alkyne (Scheme 8.1) for the second click process after removal of the TMS group with mild acid on the resin. To test the feasibility of a click reaction on the resin we prepared a test strand containing the base derived from alkyne **8.1** and performed the click reaction directly on the resin, followed by DNA deprotection. Comparison of the HPLC trace of the functionalized DNA strand with that of an untreated DNA strand of the same series showed virtually quantitative conversion proving that the click reaction proceeded with extremely

high efficiency directly on the controlled pore glass (CPG) support used for DNA synthesis (data not shown).

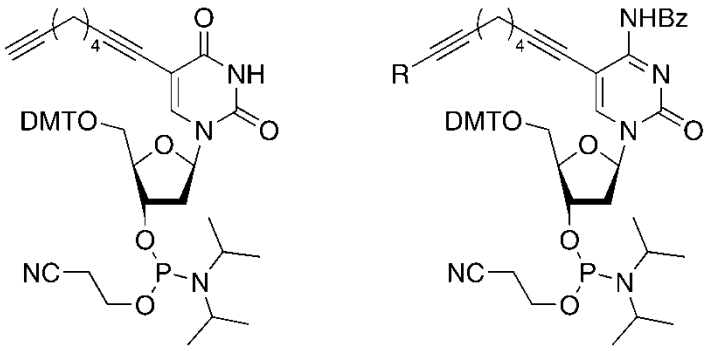

8.1

8.2a: R = TMS
8.2b: R = TIPS

Scheme 8.1 Phosphoramidites **8.1** and **8.2**. DMT = 4,4'-dimethoxytriphenylmethyl, TMS = trimethylsilyl, TIPS = triisopropylsilyl, Bz = benzoyl.

Table 8.1 ODNs employed in this study.[a]

ODN	Sequence
ODN-**8.1**	5'-GCGC**X**GTTCATT**Y**GCG-3'
ODN-**8.2**	5'-CGC**Y**ACACGAA**X**CCG-3'
ODN-**8.3**	5'-GCGC**Z**GTTCATT**X**GCG-3'
ODN-**8.4**	5'-GCGC**Y**GTT**X**ATT**Z**CGC-3'

[a] **X** = DNA nucleotide based on **8.1**, **Y** = DNA nucleotide based on **8.2a**, **Z** = DNA nucleotide based on **8.2b**.

To introduce two labels, we incorporated the thymidine and the cytidine building blocks **8.1** and **8.2a** into oligonucleotides such as ODN-**8.1** and ODN-**8.2** (Table 8.1) using standard phosphoramidite chemistry. The coupling yields of both phosphoramidites were excellent. After full assembly of the oligonucleotide on the solid support, the resin was dried and the first click reaction was performed by shaking the resin with a solution of CuBr, tris(benzyltriazolylmethyl)amine (TBTA),[11] sodium ascorbate, and benzyl azide (**8.3**, Scheme 8.2). The resin was washed and rinsed with 1% acetic acid to cleave the TMS protecting group on the second alkyne. Then the second click reaction was performed analogously to the first one using azide **8.8**. The DNA was finally cleaved from the resin, and all protecting groups were removed by exposing the resin to NH_3 in H_2O/EtOH (3:1). The MALDI-TOF spectrum obtained for the crude product was in full agreement with the expected mass of the doubly modified oligonucleotide (Table 8.2, entry 1 and Section 8.4.4), showing that two stable labels can be introduced into DNA directly on the solid support.

To test the functionalization of oligonucleotides with labels too unstable to survive the harsh cleavage conditions, we next performed the second click reaction in solution after oligonucleotide deprotection. Treatment of the singly modified ODN-**8.2** (Table 8.1) with conc. NH_3 in H_2O/EtOH cleaved the DNA from the resin. Under these conditions the base protecting groups and the TMS group on the second alkyne were removed as well. The obtained DNA,

bearing one clicked-on modification and one free alkyne, was subjected to the second click reaction in solution (CuBr, TBTA, azide **8.4**), yielding the doubly modified DNA in excellent yields and purity (Table 8.2, entry 2).

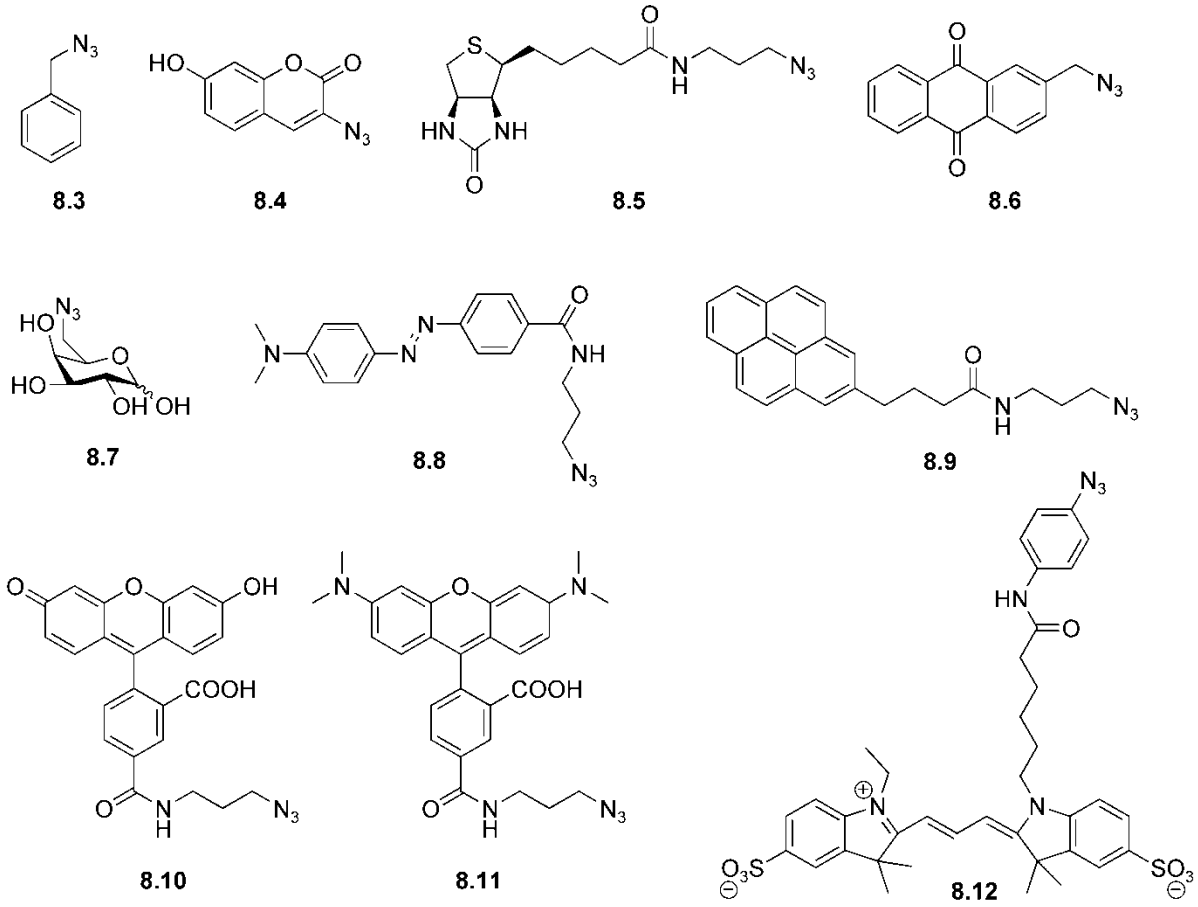

Scheme 8.2 Azide building blocks used.

The previously unmet challenge was to prepare oligonucleotides modified with two sensitive molecules. This can be readily achieved with the building blocks **8.1** and **8.2b**, which were incorporated into ODN-**8.3** (Table 8.1) using standard phosphoramidite chemistry. After deprotection and cleavage of the oligonucleotide from the resin, the first click reaction was performed (using the solution conditions reported above) yielding the singly modified oligonucleotide with the expected high yield of > 90% on average and full retention of the TIPS protecting group. For the second click step we cleaved the TIPS protecting group with a solution of tetrabutylammonium fluoride (TBAF) in MeCN/DMF (4:1 v/v) without causing any damage to the DNA. The second click reaction in solution yielded the doubly modified oligonucleotides in excellent yields (60-90% over three steps). We performed the double click with a whole series of different labels and always observed excellent yields (Table 8.2, entries 3–15). It is worth mentioning that in all cases simple precipitation of the product from ethanol after each reaction step was sufficient for purification. Figure 8.1 shows a typical HPLC chromatogram and a MALDI-TOF spectrum of the crude product obtained after a double modification of ODN-**8.3**. For very sensitive applications one final HPLC purification is recom-

mended. In rare cases, such as for Cy3 azide **8.12**, we found that the linker was cleaved to a small extent, making the development of a more stable linker necessary.

Table 8.2 Postsynthetic labeling of ODNs **8.1**-**8.4**.[d]

Entry	DNA	Label 1	Label 2	Label 3	Yield [%][a]
1	ODN-**8.1**	**8.3***	**8.8***	-	[b]
2	ODN-**8.2**	**8.3***	**8.4**	-	75[c]
3	ODN-**8.3**	**8.5**	**8.4**	-	67
4	ODN-**8.3**	**8.4**	**8.6**	-	59
5	ODN-**8.3**	**8.4**	**8.7**	-	59
6	ODN-**8.3**	**8.3**	**8.5**	-	70
7	ODN-**8.3**	**8.3**	**8.4**	-	85
8	ODN-**8.3**	**8.3**	**8.7**	-	67
9	ODN-**8.3**	**8.3**	**8.9**	-	66
10	ODN-**8.3**	**8.8**	**8.4**	-	83
11	ODN-**8.3**	**8.9**	**8.3**	-	92
12	ODN-**8.3**	**8.9**	**8.5**	-	62
13	ODN-**8.3**	**8.9**	**8.4**	-	90
14	ODN-**8.3**	**8.10**	**8.5**	-	74
15	ODN-**8.3**	**8.8**	**8.11**	-	58
16	ODN-**8.4**	**8.3***	**8.8**	**8.7**	45[c]
17	ODN-**8.4**	**8.3***	**8.7**	**8.5**	52[c]

[a] Determined by integration of the HPLC trace of the crude product at 260 nm after the last click reaction. [b] n.a. [c] HPLC purification after the click reaction on the resin. [d] Click reaction performed on resin.

Using the click reaction followed by precipitation of the product from ethanol, it was also possible to modify oligonucleotides with three different labels. To this end, we introduced the building blocks **8.1**, **8.2a**, and **8.2b** into oligonucleotides such as ODN-**8.4** (Table 8.1). The first click reaction was performed directly on the resin. The singly modified oligonucleotide was subsequently cleaved from the support under concomitant cleavage of the TMS group and then purified by HPLC. The second click reaction was performed in solution with the expected high yield. Precipitation of the doubly modified oligonucleotide from ethanol, cleavage of the TIPS group with TBAF, and a subsequent third click reaction in solution furnished the desired triply modified oligonucleotides after a final precipitation in yields of about 50% (Table 8.2, entries 16 and 17).

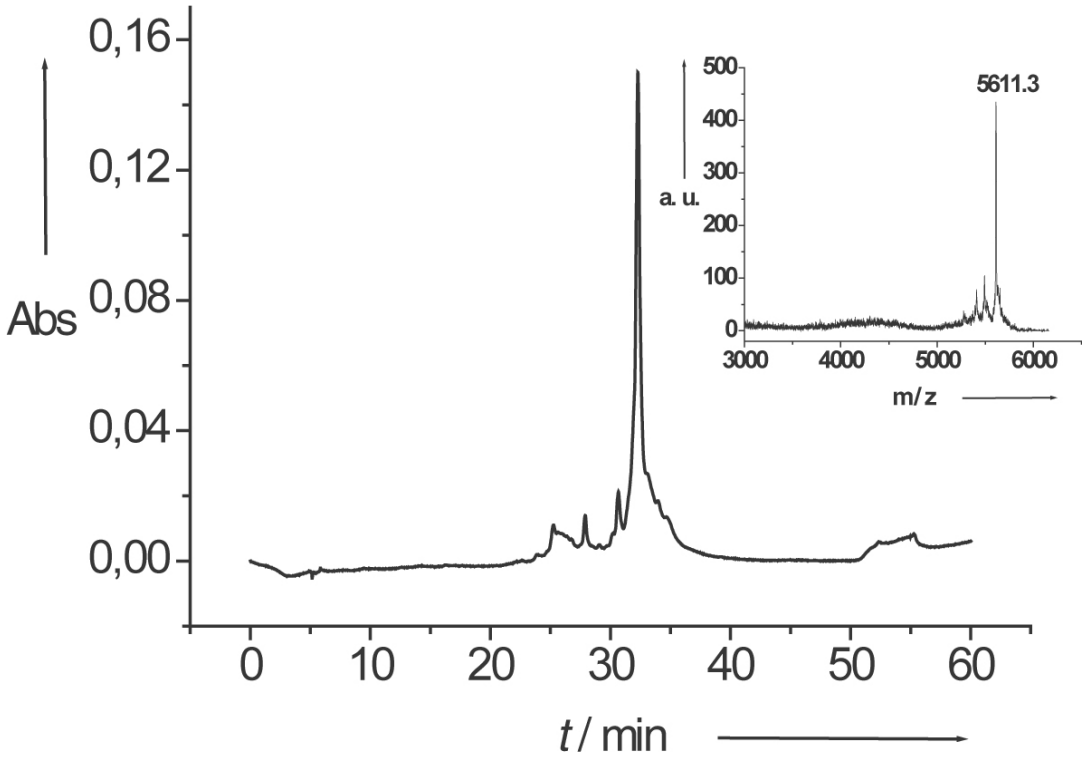

Figure 8.1 HPLC trace (260 nm) of the crude product ODN-**8.3** modified with **8.8** and **8.4** (Table 8.2, entry 10) and the corresponding MALDI-TOF spectrum (inset).

Labeling of oligonucleotides directly at certain bases (here dC and dT) is highly desirable, but the introduction of labels outside the nucleobases, for example, on the phosphates or the sugars is also frequently needed. For this, we prepared the alkyne-bearing nonnucleoside DNA modifiers **8.13** and **8.14** (Scheme 8.3). Click reactions using these building blocks in DNA worked just as efficiently.[15]

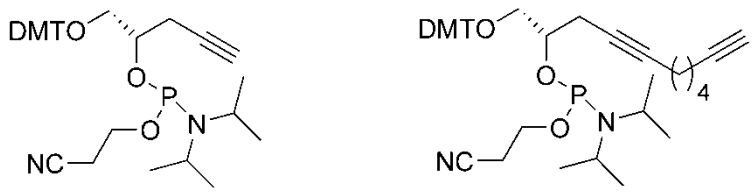

8.13 **8.14**

Scheme 8.3 Nonnucleoside DNA modifiers **8.13** and **8.14**.

8.3 Summary and Outlook

In summary, we have developed a highly efficient, modular, and robust multiple functionalization protocol for DNA. The efficiency of the method is based on three observations: 1. The TMS protecting group is quantitatively removed with ammonia during DNA deprotection. 2. The TIPS-protected alkyne is quantitatively retained during this ammonia treatment. 3. The TIPS protecting group can be removed efficiently and mildly. We believe that the chemistry presented here can change the way in which modified oligonucleotides are prepared.

8.4 Experimental Section

8.4.1 Synthesis

Phosphoramidite building blocks

The syntheses of **8.1**,[8] **8.16a**[8, 16] and **8.17**[17] were reported previously. The synthesis of **8.16b** was reported previously,[18] but without any analytical data given.

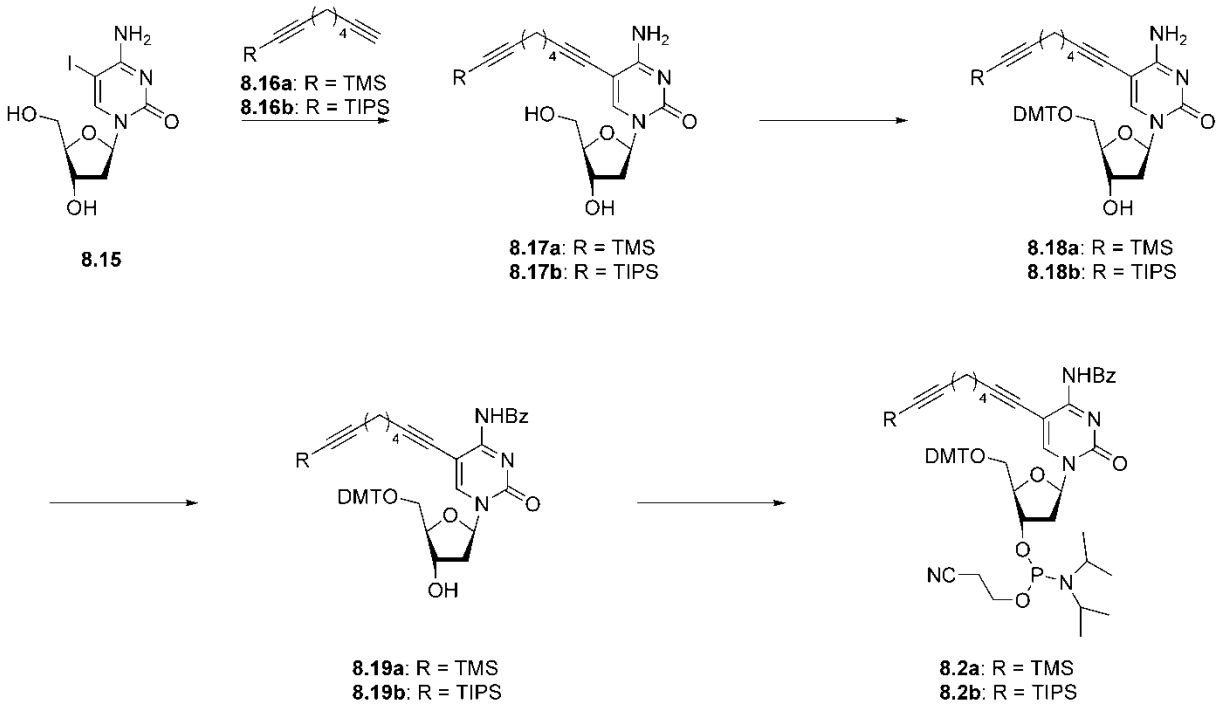

Scheme 8.4 Syntheses of building blocks **8.2a** and **8.2b**.

1-Triisopropylsilyl-octa-1,7-diyne (**8.16b**)

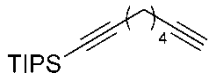

To a solution of 1,7-octadiyne (3.10 mL, 23.3 mmol) in dry THF (50 mL) at -78 °C was added LiHMDS (1.0 M in THF, 23.3 mL). The solution was stirred for 30 min, then TIPS-Cl (4.95 mL, 23.3 mmol) was added over 1 h. The solution was warmed to r. t. and stirred for 2.5 h, quenched with water (100 mL), extracted with Et_2O and washed with 1 M HCl. The organic layer was dried over Na_2SO_4 and the solvent was removed *in vacuo*. The crude product was distilled (bath temp = 115-135 °C, HV pump) to give 2.82 g (10.8 mmol, 46%) of **8.16b** as a colorless liquid.

^{1}H-NMR (600 MHz, $CDCl_3$): δ = 1,04-1,08 (m, 21H, *i*Pr), 1.63-1.70 (m, 4H, 2 × CH_2), 1.94 (t, 1H, *J* = 2.6 Hz, HC≡ C), 2.23 (dt, 2H, *J* = 2.6, 6.6 Hz, H_2CC≡ CH), 2.29 (t, 1H, *J* = 6.6 Hz, H_2CC≡ CSi). ^{13}C-NMR (75 MHz, $CDCl_3$): δ = 11.3 (CH), 17.9 (CH_2), 18.6 (CH_3), 19.3

(CH_2), 27.4 (CH_2), 27.7 (CH_2), 68.4, 80.5, 84.1, 108.5. HRMS (EI): calcd. for $C_{10}H_{17}Si^+$ $[M]^+$: 262.2117, found: 262.2131.

5-(8-Triisopropylsilyl-octa-1,7-diynyl)-2'-deoxycytidine (**8.17b**)

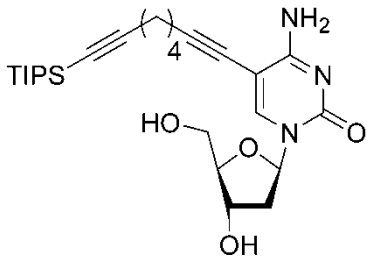

To a solution of **8.15** (2.00 g, 5.66 mmol), $Pd(PPh_3)_4$ (870 mg, 0.750 mmol) and CuI (280 mg, 1.47 mmol) in DMF (40 mL) was added triethylamine (2.10 mL, 15.0 mmol). **8.16b** (3.00 g, 11.45 mmol) was added to the reaction mixture over 5 min. After complete addition, the reaction mixture was stirred at r. t. over night. The solvent was removed *in vacuo* and the residue was directly applied to a flash column chromatography (DCM/MeOH 12:1). The product was obtained as a pale yellow powder (2.09 g, 4.28 mmol, 76%).
^{1}H-NMR (400 MHz, CD_3OD): δ = 1.05-1.10 (m, 21H, *i*Pr), 1.63-1.72 (m, 2H, CH_2), 1.73-1.81 (m, 2H, CH_2), 2.13 (td, 1H, J = 6.5, 13.3 Hz, $C_{2'}H$), 2.30-2.42 (m, 3H, CH_2, $C_{2'}H$,), 2.49 (t, 2H, J = 6.9 Hz, CH_2), 3.73 (dd, 1H, J = 3.7, 12.0 Hz, $C_{5'}H$), 3.82 (dd, 1H, J = 3.2, 12.0 Hz, $C_{5'}H$), 3.94 (q, 1H, J = 3.5 Hz, $C_{4'}H$), 4.36 (td, 1H, J = 3.8, 6.4 Hz, $C_{3'}H$), 6.21 (t, 1H, J = 6.4 Hz, $C_{1'}H$), 8.23 (s, 1H, NH). ^{13}C-NMR (100 MHz, CD_3OD): δ = 12.5 (CH), 19.1 (CH_3), 19.7 (CH_2), 20.0 (CH_2), 28.7 (CH_2), 29.1 (CH_2), 42.4 (CH_2), 62.6 (CH_2), 71.8 (CH), 72.3, 81.3, 87.9 (CH), 89.1 (CH), 93.6, 97.1, 110.2, 145.0 (CH), 156.8, 166.6. HRMS (ESI): calcd. for $C_{26}H_{42}N_3O_4Si^+$ $[M+H]^+$: 488.2939, found: 488.2936.

5-(8-Trimethylsilyl-octa-1,7-diynyl)-5′-*O*-(4,4′-dimethoxytrityl)-2'-deoxycytidine (**8.18a**)

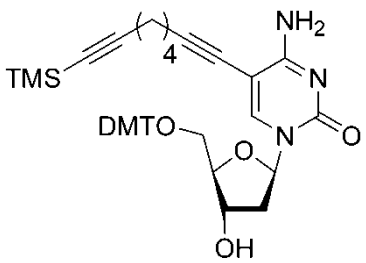

8.17a (1.00 g, 2.48 mmol) was co-evaporated twice with pyridine and dissolved in dry pyridine (14 mL). The solution was cooled to 0 °C. DMAP (60 mg, 0.49 mmol), 4,4′-dimethoxytrityl chloride (1.09 g, 3.22 mmol) and triethylamine (0.69 mL, 5.0 mmol) were added and the solution stirred for 15 min at 0 °C. The solution was allowed to warm to

r. t. and stirred for 5 h. The reaction mixture was quenched with MeOH (30 mL) and the solvent evaporated. The residue was extracted with DCM, washed with aqueous $NaHCO_3$ solution and dried over $NaSO_4$. The residue was purified by flash column chromatography (DCM/MeOH/NEt_3 200:7:1) to give **8.18a** (1.12 g, 1.69 mmol, 68%) as a white powder.
^{1}H-NMR (200 MHz, d_6-acetone): $\delta = 0.10$ (s, 9H, $SiCH_3$), 1.45-1.52 (m, 4H, $2 \times CH_2$), 2.11-2.16 (m, 2H, CH_2), 2.18-2.29 (m, 3H, CH_2, $C_{2'}H$), 2.47 (ddd, 1H, $J = 2.7, 5.9, 13.7$ Hz, $C_{2'}H$), 3.32 (dd, 1H, $J = 3.0, 10.5$ Hz, $C_{5'}H$), 3.36 (dd, 1H, $J = 4.3, 10.5$ Hz, $C_{5'}H$), 3.80 (s, 6H, OCH_3), 4.09-4.13 (m, 1H, $C_{4'}H$), 4.52-4.57 (m, 1H, $C_{3'}H$), 6.27 (dd, 1H, $J = 6.0, 7.2$ Hz, $C_{1'}H$), 6.35 (s, 1H, NH/OH), 6.90 (dd, 4H, $J = 1.6, 8.9$ Hz, ArH), 7.08 (s, 1H, OH/NH), 7.22-7.27 (m, 1H, ArH), 7.31-7.36 (m, 2H, ArH), 7.39-7.44 (m, 4H, ArH), 7.51-7.55 (m, 2H, ArH), 8.09 (s, 1H, C_6H). ^{13}C-NMR (100 MHz, d_6-acetone): $\delta = 0.3$ (CH_3), 19.8 (CH_2), 19.9 (CH_2), 28.5 (CH_2), 28.9 (CH_2), 43.1 (CH_2), 55.8 (CH_3), 64.6 (CH_2), 71.9, 72.5 (CH), 85.2, 88.2, 88.3 (CH), 93.7, 97.5, 108.3, 114.3 (CH), 128.0 (CH), 129.0 (CH), 129.3 (CH), 131.3 (CH), 131.3 (CH), 137.1, 137.2, 144.3 (CH), 146.2, 156.7, 160.2, 160.2, 166.6. HRMS (ESI): calcd. for $C_{41}H_{48}N_3O_6Si^+$ $[M+H]^+$: 706.3307, found: 706.3297.

5-(8-Triisopropylsilyl-octa-1,7-diynyl)-5′-*O*-(4,4′-dimethoxytrityl)-2'-deoxycytidine (**8.18b**)

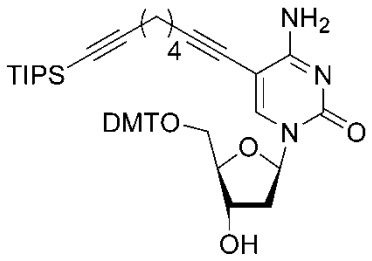

8.17b (1.95 g, 4.00 mmol) was co-evaporated twice with pyridine and dissolved in dry pyridine (20 mL). The solution was cooled to 0 °C. DMAP (100 mg, 0.82 mmol), 4,4′-dimethoxytrityl chloride (2.03 g, 5.23 mmol) und triethylamine (1.11 mL, 7.98 mmol) were added and the solution stirred for 45 min at 0 °C. The solution was allowed to warm to r. t. and stirred for 4 h. The reaction mixture was quenched with MeOH (40 mL) and the solvent evaporated. The residue was extracted with DCM, washed with aqueous $NaHCO_3$ solution and dried over $NaSO_4$. The residue was purified by flash column chromatography ($CHCl_3$/MeOH/NEt_3 200:5:1) to give **8.18b** (2.59 g, 3.28 mmol, 82%) as a white powder.
^{1}H-NMR (400 MHz, d_6-acetone): $\delta = 1.03$-1.09 (m, 21H, *i*Pr), 1.47-1.60 (m, 4H, $2 \times CH_2$), 2.16-2.32 (m, 5H, $2 \times CH_2$, $C_{2'}H$), 2.46 (ddd, 1H, $J = 2.8, 5.9, 13.4$ Hz, $C_{2'}H$), 3.32 (dd, 1H, $J = 3.0, 10.5$ Hz, $C_{5'}H$), 3.36 (dd, 1H, $J = 4.3, 10.5$ Hz, $C_{5'}H$), 3.79 (s, 6H, OCH_3), 4.08-4.13 (m, 1H, $C_{4'}H$), 4.50-4.56 (m, 1H, $C_{3'}H$), 6.26 (dd, 1H, $J = 6.1, 7.1$ Hz, $C_{1'}H$), 6.90 (dd, 4H, $J = 1.6, 8.9$ Hz, ArH), 7.21-7.54 (m, 9H, ArH), 8.08 (s, 1H, C_6H). ^{13}C-NMR (100 MHz, d_6-acetone): $\delta = 13.0$ (CH), 20.0 (CH_3), 20.4 (CH_2), 20.6 (CH_2), 29.2 (CH_2), 29.7 (CH_2), 43.6 (CH_2), 56.5 (CH_3), 65.6 (CH_2), 73.2 (CH), 73.3 (CH), 73.6, 81.6, 88.1 (CH), 88.4 (CH), 88.4, 97.1, 110.0, 115.0 (CH), 115.0 (CH), 128.6 (CH), 129.7 (CH), 130.0 (CH), 131.9 (CH), 132.0 (CH), 137.8, 137.9, 145.0 (CH), 147.0, 155.5, 160.6. HRMS (ESI): calcd. for $C_{47}H_{60}N_3O_6Si^+$ $[M+H]^+$: 790.4246, found: 790.4283.

4-*N*-Benzoyl-5-(8-trimethylsilyl-octa-1,7-diynyl)-5′-*O*-(4,4′-dimethoxytrityl)-2'-deoxycytidine (**8.19a**)

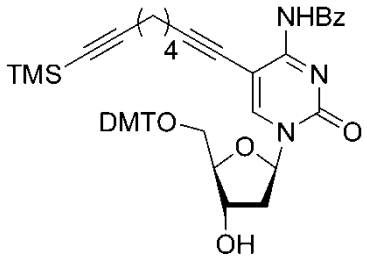

8.18a (555 mg, 0.786 mmol) was co-evaporated twice with pyridine and dissolved in dry pyridine (3 mL). Trimethylsilyl chloride (357 µL, 2.80 mmol) was added and the solution stirred for 2.5 h at r. t. The reaction mixture was cooled on an ice-water bath while benzoyl chloride (143 µL, 1.23 mmol) was added dropwise. The solution was stirred for 2.5 h at r. t.. The reaction was quenched by addition of MeOH (1 mL) and all the solvent removed *in vacuo*. Purification by silica gel chromatography ($CHCl_3$/MeOH/pyridine 200:4:1) gave **8.19a** (639 mg, 0.788 mmol, 100%) as pale yellow solid.
^{1}H-NMR (400 MHz, d_6-acetone): δ = 0.08 (s, 9H, $SiCH_3$), 1.50-1.66 (m, 4H, 2 × CH_2), 2.17-2.30 (m, 5H, 2 × CH_2, $C_{2'}H$), 2.41-2.58 (m, 1H, $C_{2'}H$), 3.36 (dd, 1H, *J* = 2.7, 10.7 Hz, $C_{5'}H$), 3.41 (dd, 1H, *J* = 4.2, 10.7 Hz, $C_{5'}H$), 3.79 (s, 6H, OCH_3), 4.17 (q, 1H, *J* = 3.3 Hz, $C_{4'}H$), 4.60-4.65 (m, 1H, $C_{3'}H$), 6.28 (t, 1H, *J* = 6.6 Hz, $C_{1'}H$), 6.91 (dd, 1H, *J* = 1.6, 8.7 Hz, ArH), 7.22-7.64 (m, 12H, ArH), 8.26 (s, 1H, C_6H), 8.55-8.63 (m, 2H, ArH). ^{13}C-NMR (100 MHz, CD_3OD): δ = 1.3 (CH_3), 20.5 (CH_2), 20.8 (CH_2), 29.3 (CH_2), 29.5 (CH_2), 43.1 (CH_2), 55.5 (CH_3), 65.4 (CH_2), 70.2 (CH), 70.3, 73.0 (CH), 73.8, 85.8, 88.3, 88.5 (CH), 88.9, 109.0, 115.0 (CH), 115.0 (CH), 128.6 (CH), 129.7 (CH), 129.9 (CH), 130.1 (CH), 130.8 (CH), 131.1 (CH), 131.9 (CH), 131.9 (CH), 134.3 (CH), 137.8, 146.9, 160.6, 160.6, 210.9. HRMS (ESI): calcd. for $C_{48}H_{52}N_3O_7Si^+$ $[M+H]^+$: 810.3569, found: 810.3547.

4-*N*-Benzoyl-5-(8-triisopropylsilyl-octa-1,7-diynyl)-5′-*O*-(4,4′-dimethoxytrityl)-2'-deoxycytidine (**8.19b**)

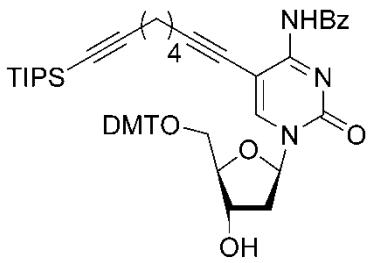

8.18b (3.00 g, 3.79 mmol) was co-evaporated twice with pyridine and dissolved in dry pyridine (12 mL). Trimethylsilyl chloride (1.46 mL, 11.5 mmol) was added and the solution stirred for 2.5 h at r. t. The reaction mixture was cooled on an ice-water bath while benzoyl

chloride (580 µL, 5.00 mmol) was added dropwise. The solution was stirred for 2.5 h at ambient temperature. The reaction was quenched by addition of MeOH (10 mL) and all the solvent removed *in vacuo*. Purification by column chromatography (DCM/pyridine 200:1 → DCM/MeOH/pyridine 200:8:1) gave **8.19b** (1.68 g, 1.88 mmol, 49%) as pale yellow solid.
^{1}H-NMR (400 MHz, d_6-acetone): δ = 1.01-1.07 (m, 21H, *i*Pr), 1.57-1.71 (m, 4H, 2 × CH_2), 2.23-2.29 (m, 4H, 2 × CH_2), 2.41-2.50 (m, 1H, $C_{2'}H$), 2.51 (ddd, 1H, *J* = 3.5, 6.1, 13.5 Hz, $C_{2'}H$), 3.36 (dd, 1H, *J* = 2.9, 10.7 Hz, $C_{5'}H$), 3.36 (dd, 1H, *J* = 4.2, 10.7 Hz, $C_{5'}H$), 3.79 (s, 3H, OCH_3), 3.79 (s, 3H, OCH_3), 4.15-4.18 (m, 1H, $C_{4'}H$), 4.60-4.66 (m, 1H, $C_{3'}H$), 6.28 (t, 1H, *J* = 6.6 Hz, $C_{1'}H$), 6.91 (dd, 4H, *J* = 1.4, 8.9 Hz, ArH), 7.22-7.61 (m, 12H, ArH), 8.26 (s, 1H, C_6H), 8.32 (d, 2H, *J* = 7.2 Hz, ArH). ^{13}C-NMR (100 MHz, d_6-acetone): δ = 13.0 (CH), 20.0 (CH_3), 20.4 (CH_2), 20.7 (CH_2), 29.2 (CH_2), 29.7 (CH_2), 43.2 (CH_2), 56.5 (CH_3), 65.5 (CH_2), 73.2 (CH), 73.9, 81.7, 88.4 (CH), 88.6, 89.0, 110.9, 115.0 (CH), 115.0 (CH), 128.6 (CH), 129.8 (CH), 129.9 (CH), 130.2 (CH), 131.6 (CH), 131.9 (CH), 132.0 (CH), 134.4 (CH), 137.7, 137.8, 147.0, 160.7. HRMS (ESI): calcd. for $C_{54}H_{64}N_3O_7Si^+$ $[M+H]^+$: 894.4508, found: 894.4503.

4-*N*-Benzoyl-5-(8-trimethylsilyl-octa-1,7-diynyl)-3′-*O*-[(2-(cyanoethoxy)(diisopropylamino)-phosphono)]-5′-*O*-(4,4′-dimethoxytrityl)-2'-deoxycytidine (**8.2a**)

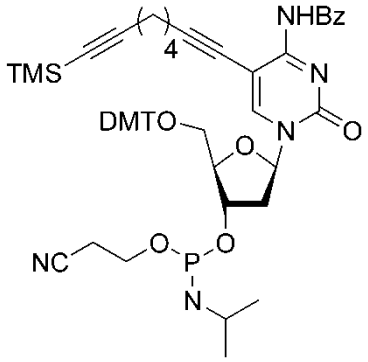

8.19a (920 mg, 1.14 mmol) and diisopropylammonium tetrazolide (93 mg, 0.55 mmol) were co-evaporated twice with pyridine and dissolved in dry DCM (57 mL). 2-cyanoethyl tetraisopropyl phosphoramidite (400 µL, 1.26 mmol) was added and the solution stirred for 3 h at r. t. The reaction mixture was concentrated *in vacuo* to 1/4 of the original volume. The residue was purified by flash chromatography on passivated silica gel ($CHCl_3$/MeOH/NEt_3 200:4:1). **8.2a** was obtained as a yellow solid (1.03 g, 1.02 mmol, 90%).
^{1}H-NMR (200 MHz, d_6-acetone): δ = 0.08-0.10 (2 × s, 9H, $SiCH_3$), 1.50-1.65 (m, 4H, 2 × CH_2), 2.15-2.27 (m, 5H, 2 × CH_2, $C_{2'}H$), 2.54-2.70 (m, 3H, H_2CCN, $C_{2'}H$), 2.73-2.82 (m, 2H, H_2COP), 3.41-3.48 (m, 2H, $C_{5'}H$), 3.80 (2 × s, 6H, OCH_3), 4.22-4.34 (m, 1H, $C_{4'}H$), 4.70-4.84 (m, 1H, $C_{3'}H$), 6.22-6.32 (m, 1H, $C_{1'}H$), 6.88-6.97 (m, 4H, ArH), 7.24-7.60 (m, 12H, ArH), 8.24-8.35 (m, 3H, C_6H, ArH). ^{31}P-NMR (81 MHz, d_6-acetone): δ = 149.2, 149.5.

4-*N*-Benzoyl-5-(8-triisopropylsilyl-octa-1,7-diynyl)-3′-*O*-[(2-(cyanoethoxy)(diisopropylamino)-phosphono)]-5′-*O*-(4,4′-dimethoxytrityl)-2'-deoxycytidine (**8.2b**)

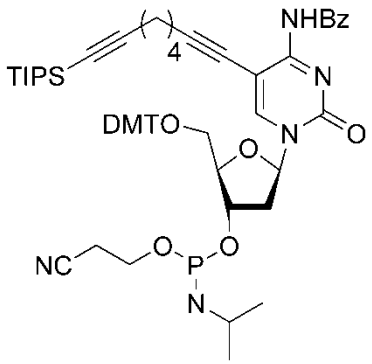

8.19b (134 mg, 0.149 mmol) and diisopropylammonium tetrazolide (15 mg, 88 µmol) were co-evaporated twice with pyridine and dissolved in dry DCM (10 mL). 2-cyanoethyl tetraisopropyl phosphoramidite (60 µL, 0.19 mmol) was added and the solution stirred for 3 h at r. t. The reaction mixture was concentrated *in vacuo* to 1/4 of the original volume. The residue was purified by flash chromatography on passivated silica gel ($CHCl_3$/MeOH/NEt_3 200:4:1). **8.2b** was obtained as a yellow solid (104 mg, 95 µmol, 63%).
^{1}H-NMR (200 MHz, d_6-acetone): δ = 1.02-1.07 (m, 21H, *i*Pr), 1.57-1.68 (m, 4H, 2 × CH_2), 2.20-2.30 (m, 5H, 2 × CH_2, $C_{2'}H$), 2.57-2.69 (m, 3H, H_2CCN, $C_{2'}H$), 2.73-2.82 (m, 2H, H_2COP), 3.41-3.48 (m, 2H, $C_{5'}H$), 3.80 (s, 6H, OCH_3), 4.23-4.33 (m, 1H, $C_{4'}H$), 4.69-4.84 (m, 1H, $C_{3'}H$), 6.22-6.33 (m, 1H, $C_{1'}H$), 6.87-6.98 (m, 4H, ArH), 7.21-7.62 (m, 12H, ArH), 8.25 (s, 1H, C_6H), 8.27-8.36 (m, 2H, ArH). ^{31}P-NMR (81 MHz, d_6-acetone): δ = 149.2, 149.5.

Syntheses of azide building blocks

8.3[19], **8.4**[20], **8.5**[21], **8.6**[22], **8.7**[23], **8.10**[24] and **8.11**[25] were prepared according to literature procedures.

Dabcyl azide (**8.8**)

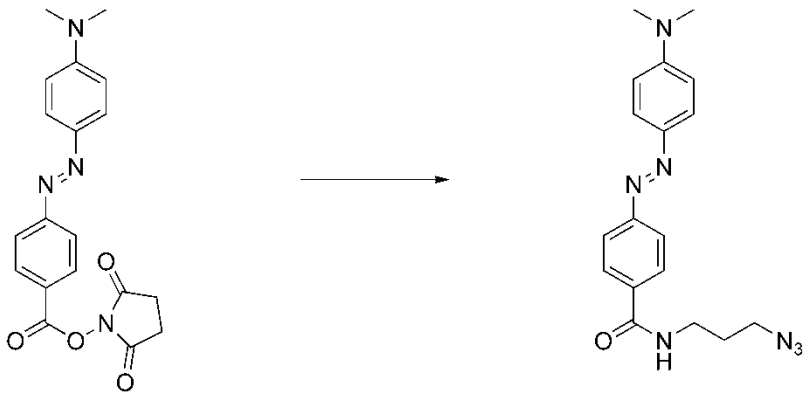

8.8

Scheme 8.5 Synthesis of Dabcyl azide **8.8**

Dabcyl-*N*-hydroxysuccinimide ester (29 mg, 79 µmol) and DMAP (9.5 mg, 78 µmol) were dissolved in dry pyridine (2 mL). A solution of 3-azido-propylamine (1.3 M in toluene, 95 µL, 124 µmol) was added dropwise and the solution stirred for 1 d at r. t. The solvent was removed and the raw product purified by column chromatography (*i*Hex/EtOAc 3:1) to give 28 mg **8.8** (79 µmol, 100%) as a red powder.

^{1}H-NMR (600 MHz, $CDCl_3$): δ = 1.93 (quin, 2H, *J* = 6.6 Hz, CH_2), 3.10 (s, 6H, CH_3), 3.46 (t, 2H, *J* = 6.5 Hz, H_2C-N_3), 3.57 (q, 2H, *J* = 6.5 Hz, H_2C-NH), 6.48 (t, 1H, *J* = 5.0 Hz, NH), 6.75 (d, 2H, *J* = 9.1 Hz, ArH), 7.86-7.91 (m, 6H, ArH). ^{13}C-NMR (150 MHz, $CDCl_3$): δ = 28.8 (CH_2), 37.9 (CH_2), 40.3 (CH_3), 49.6 (CH_2), 111.4 (CH), 122.2 (CH), 125.4 (CH), 127.7 (CH), 134.3, 143.6, 152.8, 155.1, 167.2. HRMS (EI) calcd. for $C_{18}H_{21}N_7O^+$ $[M]^+$: 351.1802, found: 351.1815.

Pyrene azide (**8.9**)

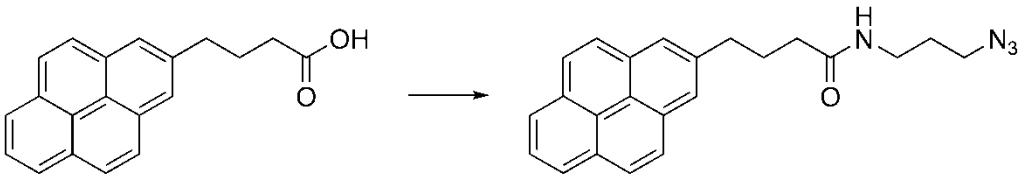

8.9

Scheme 8.2 Synthesis of pyrene azide **8.9**.

4-Pyren-2-yl-butyric acid (288 mg, 1.00 mmol), HOBt (162 mg, 1.20 mmol) and DCI (176 µL, 1.14 mmol) were dissolved in DMF (5 mL) and stirred for 24 h at r. t. A solution of 3-azido-propylamine (1.3 M in toluene, 1.15 mL, 1.50 mmol) was added dropwise and the reaction mixture stirred for an additional 48 h. Water (100 mL) was added and the reaction mixture extracted with EtOAc (2 × 100 mL). The combined organic phases were washed with water and dried over Na_2SO_4. **8.9** was obtained as light yellow solid (110 mg, 0.296 mmol, 30%) after column chromatography ($CHCl_3$/MeOH 20:1).

^{1}H-NMR (400 MHz, $CDCl_3$): δ = 1.62 (quin, 2H, *J* = 6.7 Hz, CH_2), 2.10-2.16 (m, 4H, 2 × CH_2), 3.15-3.24 (m, 4H, 2 × CH_2), 3.28 (t, 2H, *J* = 7.3 Hz, CH_2), 5.72 (t, 1H, *J* = 5.6 Hz, NH), 7.77 (d, 1H, *J* = 7.8 Hz, ArH), 7.94-8.00 (m, 3H, ArH), 8.03-8.08 (m, 2H, ArH), 8.13 (d, 2H, *J* = 7.7 Hz, ArH), 8.22 (d, 1H, *J* = 9.3 Hz, ArH). ^{13}C-NMR (75 MHz, $CDCl_3$): δ = 27.2 (CH_2), 28.7 (CH_2), 32.6 (CH_2), 35.8 (CH_2), 36.9 (CH_2), 49.2 (CH_2), 123.2 (CH), 124.7 (CH), 124.8 (CH), 125.8 (CH), 126.6 (CH), 127.2 (CH), 127.3 (CH), 127.4 (CH), 128.6, 129.8, 130.8, 131.3, 135.7, 172.7. HRMS (EI) calcd. for $C_{23}H_{22}N_4O^+$ $[M]^+$: 370.1788, found: 370.1775.

Cy3-azide (**8.12**)

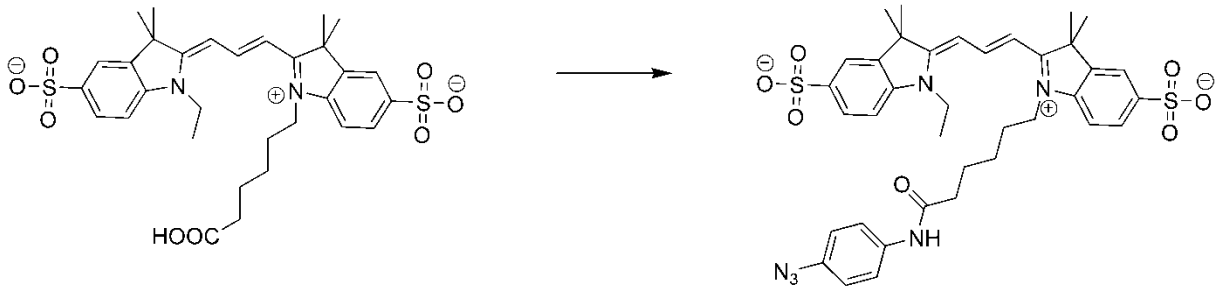

8.20 **8.12**

Scheme 8.7 Synthesis of Cy3 azide **8.12**.

8.20 was prepared according to literature procedures.[26]

8.20 (325 mg, 0.516 mmol), 4-azidoaniline hydrochloride (352 mg, 2.06 mmol) and HATU (785 mg, 2.06 mmol) were dissolved in dry DMF (10 mL) and DIPEA (0.5 mL). The solution was stirred at r. t. over night. The raw product was precipitated with dry EtOAc (50 mL) and separated by RP-HPLC. The separation was performed using 0.1 M $HNEt_3$/OAc buffers (buffer A: H_2O, buffer B: MeCN/H_2O 4:1). The flow rate was 5 mL with a linear gradient from 100% A to 60% A in 45 min. **8.12** (0.31 mmol, 60%) was eluted at 45.0 min as its bis-triethylammonium salt.
^{1}H-NMR (600 MHz, D_2O): δ = 1.00-1.03 (m, 2H, CH_2), 1.14 (t, 21H, *J* = 7.2 Hz, CH_3, 2 × 3 CH_3 (TEA)), 1.33 (s, 12H, 4 × CH_3), 1.50-1.55 (m, 2H, CH_2), 2.00-2.08 (m, 2H, CH_2), 3.06 (q, 14H, *J* = 7.2 Hz, H_2CCONHAr, 2 × 3 CH_2 (TEA)), 3.75-3.90 (m, 4H, CH_2), 6.08 (d, 1H, *J* = 13.8 Hz, C*H*CHCH), 6.14 (d, 1H, *J* = 13.8 Hz, C*H*CHCH), 6.42-6.47 (m, 2H, ArH), 7.04-7.16 (m, 4H, ArH), 7.66-7.73 (m, 4H, ArH), 8.08 (t, 1H, *J* = 13.8 Hz, CHC*H*CH). ^{13}C-NMR (150 MHz, $CDCl_3$): δ = 11.7, 24.9, 25.5, 26.7, 27.1, 27.2, 36.3, 39.6, 42.4, 44.2, 49.2, 59.1, 103.2, 103.6, 105.0, 111.2, 111.6, 118.7, 119.1 , 120.0, 121.6, 126.9, 134.9, 140.3, 141.3, 141.4, 143.4, 143.9, 151.5, 175.0, 175.7, 181.6. HRMS (ESI) calc. for $C_{37}H_{41}N_6O_7S_2^+$ $[M]^-$: 745.2489, found: 745.2496.

8.4.2 Click-Deprotect-Click Procedure

Click reaction on the resin[a]

Approx. 0.02 µmol DNA on CPG resin was dried under high vacuum after DNA synthesis and placed in a 1.5 mL vial together with 20 µL benzyl azide **8.3**. In a separate vial, 40 µL CuBr solution (10 mM in DMSO/*t*BuOH 3:1), 10 µL sodium ascorbate (100 mM in water) and 80 µL ligand[11] solution (10 mM in DMSO/*t*BuOH 3:1) were vortexed and added to the DNA.

[a] The following procedures describe click reactions on ODNs bearing one alkyne. For DNA with more than one alkyne the amounts of reagents have to be adjusted accordingly.

The reaction vial was gently rotated over night,[b] centrifuged and the solution carefully removed and discarded. The resin was washed repeatedly (2 × DMSO, 2 × H_2O, 2 × EtOH) by adding the solvent, vortexing, centrifuging and discarding the supernatant. The DNA was subsequently deprotected as described above.

Click reaction in solution

DNA (0.38 mM, 200 µL) and azide[c] (10 mM, 114 µL) were placed in a 1.5 mL vial. In a separate vial, 17 µL CuBr solution (100 mM in DMSO/*t*BuOH 3:1) and 34 µL ligand[11] solution (100 mM in DMSO/*t*BuOH 3:1) were vortexed and added to the DNA.[d] The solution was shaken at 25 °C for 4 h[e] and evaporated to near-dryness in a SpeedVac. Na^+OAc^- solution (0.3 M, 100 µL) was added and the suspension left standing for 1 h with occasional vortexing.[f] 1 mL EtOH was added, the vial vortexed and placed in a freezer (-20 °C) over night. After centrifugation (15 min at 13 000 rpm) the supernatant was carefully removed from the DNA pellet. 70% EtOH (-20 °C) was added, the vial vortexed, centrifuged and the supernatant removed. This washing step was repeated twice. After the last washing step the pellet was left drying on air and taken up in water or buffer, as preferred.

Deprotection of the TIPS-alkyne

Lyophilized DNA was dissolved in dry MeCN (400 µL) and dry DMF (100 µL). Two drops of TBAF (1.0 M in THF) were added and the solution shaken at 45 °C for 2 h. Excess fluoride ions were quenched with MeOTMS (10 µL). If an additional click reaction is to be performed on the DNA strand, the organic solvents should be exchanged to water as follows: the reaction solution was evaporated to near-dryness in a SpeedVac. Water (1 mL) was added, the solution frozen, lyophilized to dryness and taken up in an appropriate amount of water.

[b] This can conveniently be achieved by attaching the vial onto a rotary evaporator with sticky tape.
[c] Azide solutions should be as concentrated as possible. The azides reported here were all soluble in water, DMSO or DMSO/*t*BuOH (3:1).
[d] No additional solvent was added to achieve complete dissolution of all components.
[e] In order to check the progress of the Click reaction, 1.5 µL of the reaction solution can be removed during the reaction, spotted on a desalting membrane and analyzed by MALDI-TOF MS (HPA matrix).
[f] At this point it is not necessary to obtain a clear solution, the precipitation is performed from the suspension.

8.4.3 MALDI-TOF Analyses of Entries 1-17 of Table 8.2

Table 8.3 Exact and average masses of the functionalized strands.

Entry	exact parent mass	average mass	mass found
1	5540.1808	5542.9746	5539.0
2	5035.0095	5037.5220	5034.2
3	5585.1217	5587.9905	5582.5
4	5522.0386	5524.8236	5523.9
5	5464.0390	5466.7413	5465.5
6	5515.1526	5517.9868	5515.1
7	5392.0332	5394.7233	5396.7
8	5394.0699	5396.7376	5394.0
9	5559.1794	5562.0160	5560.3
10	5610.1499	5612.9783	5607.8
11	5559.1794	5562.0160	5562.5
12	5752.2679	5755.2832	5756.9
13	5629.1485	5632.0197	5631.0
14	5840.2112	5843.2591	5844.9
15	5921.3497	5924.3996	5921.7
16	5849.3133	5852.2924	5849.5
17	5824.2850	5827.2850	5826.0

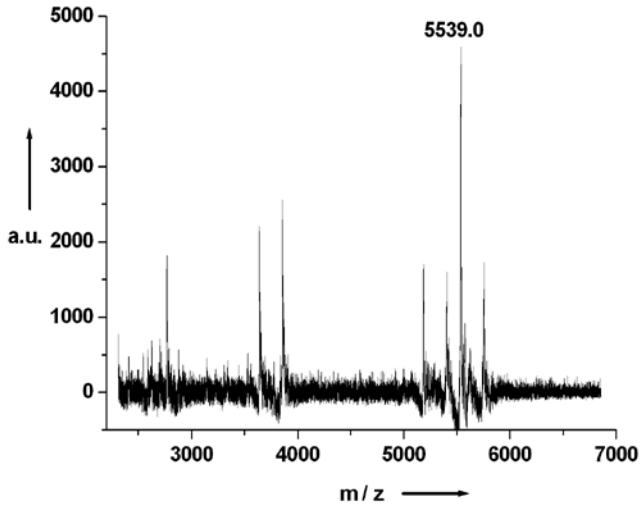

Figure 8.2 MALDI-TOF analysis of entry 1 (Tables 8.2 and 8.3).

8.5 Notes Added after Publication

8.5.1 Improved Protocol for TIPS Deprotection[27]

Lyophilized DNA was dissolved in a 100 µL TBAF solution (1.0 M in dry THF) and shaken at 25 °C for 1 d. For workup, 100 µL tris-HCl (1 M, pH 7.5) were added and the resulting

solution was evaporated to near-dryness in a SpeedVac. Precipitation of the DNA was performed as described in Section 8.4.2.

8.5.2 Design for a Quadruple DNA Modification

Christian Wirges works on the synthesis of aldehyde-modified DNA in order to deposit silver nanowires on the DNA backbone via a Tollens reaction. To this end he synthesized nucleotides containing diols (**8.21** in Scheme 8.8). This functional group can be used for a postsynthetic cleavage reaction using $NaIO_4$ which is both mild and nearly quantitative in yield. The resulting aldehydes can be used for a postsynthetic modification reaction using amines or hydroxylamines to yield imines or oximes, respectively.

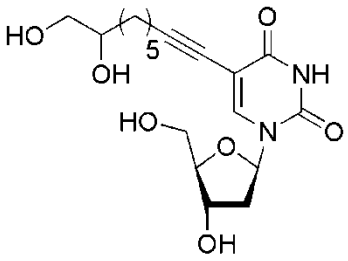

8.21

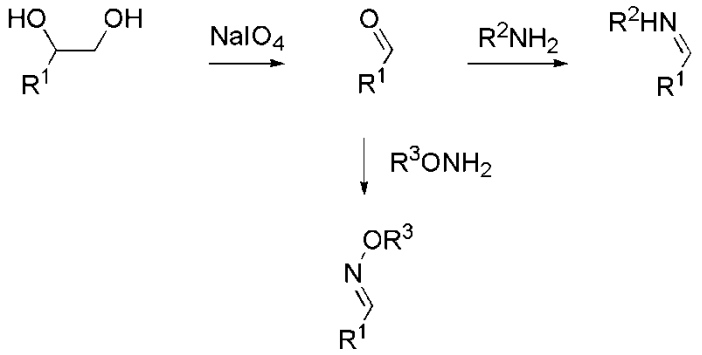

Scheme 8.8 Structure of diol-containing nucleoside **8.21** (top) and postsynthetic functionalization of the diols to give imines or oximes (bottom).

A DNA strand (5′- G**W**GC**X**GTT**Y**ATT**Z**GCG-3′, **W** = **8.2a**, **X** = **8.1**, **Y** = **8.2b**, **Z** = **8.21**) bearing a free alkyne group (on **8.1**) and both TMS and TIPS-protected alkynes (on **8.2a** and **8.2b**, respectively) as well as the diol stemming from **8.21**. Both chemistries, the click reaction and the formation of imines and oximes appeared to be orthogonal to us. The experiments to achieve a quadruple DNA modification have not been performed to date.

8.5.3 Attempts to Improve the Yield of the Click Reaction on the Resin

The yield of the click reaction directly on the resin was found to be rather low and only badly reproducible for many azide substrates. Intrinsically, the click reaction on the resin is performed before the ammonia deprotection of the DNA strand so that sensitive functionalities suffer damage. Still, even azides showing no susceptibility to alkaline treatment, like benzyl azide **8.3**, did not yield a quantitative conversion in every case. In order to address this issue, different test strands have been synthesized (Table 8.4) in which two questions were to be answered concerning the click reaction on the resin: Does the distance of the alkyne group to the solid-phase resin influence the yield of the click reaction? Does the kind of resin material used influence the yield?

Table 8.4 ODN sequences used in optimization studies for the click reaction on the resin.

ODN	Sequence
ODN-**8.5**	5′-CAT **X**G-3′
ODN-**8.6**	5′-GCG CTG T**X**C ATT CGC G-3′
ODN-**8.7**	5′-**X**TT GCC CTT GAG GCG TGG CTG CAG CGG-3′

The first question concerning the dependence of the click reaction yield on the distance of the alkyne to the resin was answered by synthesizing ODN-**8.5**-**8.7** on CPG resin. These ODNs were subjected to a click reaction with **8.3**, following the procedure described in Section 8.4.2. It was found that both ODN-**8.6** and ODN-**8.7** (8 and 20 bases distance to the resin, respectively) showed the same click reaction efficiency, whereas ODN-**8.5** (1 base distance) showed a significantly decreased yield. It can be concluded that a very short distance of the alkyne group to the resin somewhat hampers the click reaction, whereas already 8 bases seem to be enough to safeguard the expected click yield. To address the question of whether the material of the resin would influence the click reaction yield, ODN-**8.6** was synthesized on polystyrene resin in addition to the CPG-bound ODN-**8.6**. Both types of resins were shown to give the same results in a click reaction performed as described above.
Although these optimization experiments did not give a breakthrough in finding out about the reduced click reaction yield on the resin, further experiments should not be discouraged by this account, as a highly reliable click reaction on the resin would be very desirable due to its applicability in automated synthesis systems.

8.6 Author´s Contribution

*This is the author´s work, except for two parts: Simon Warncke synthesized and clicked Cy3 azide **8.12**, Johannes Gierlich performed the work on the nonnucleosidic DNA modifiers **8.13** and **8.14**.*

8.7 References

[1] D. M. Hammond, A. Manetto, J. Gierlich, V. A. Azov, P. M. E. Gramlich, G. A. Burley, M. Maul, T. Carell, *Angew. Chem. Int. Ed.* **2007**, *46*, 4184-4187.

[2] G. A. Burley, J. Gierlich, M. R. Mofid, S. T. H. Nir, Y. Eichen, T. Carell, *J. Am. Chem. Soc.* **2006**, *128*, 1398-1399.

[3] Q. Gu, C. Cheng, R. Gonela, S. Suryanarayanan, S. Anabathula, K. Dai, D. T. Haynie, *Nanotech.* **2006**, *17*, R14-R25.

[4] C. Wagner, H.-A. Wagenknecht, *Chem.--Eur. J.* **2005**, *11*, 1871-1876.

[5] J. A. Prescher, C. R. Bertozzi, *Nat. Chem. Biol.* **2005**, *1*, 13-21.

[6] L. M. Smith, S. Fung, M. W. Hunkapiller, T. J. Hunkapiller, L. E. Hood, *Nucleic Acids Res.* **1985**, *13*, 2399-2412.

[7] F. Seela, V. R. Sirivolu, *Chem. Biodiversity* **2006**, *3*, 509-514.

[8] J. Gierlich, G. A. Burley, P. M. E. Gramlich, D. M. Hammond, T. Carell, *Org. Lett.* **2006**, *8*, 3639-3642.

[9] C. W. Tornoe, C. Christensen, M. Meldal, *J. Org. Chem.* **2002**, *67*, 3057-3064.

[10] V. V. Rostovtsev, L. G. Green, V. V. Fokin, K. B. Sharpless, *Angew. Chem. Int. Ed.* **2002**, *41*, 2596-2599.

[11] T. R. Chan, R. Hilgraf, K. B. Sharpless, V. V. Fokin, *Org. Lett.* **2004**, *6*, 2853-2855.

[12] C. J. Burrows, J. G. Muller, *Chem. Rev.* **1998**, *98*, 1109-1151; S. Thyagarajan, N. N. Murthy, A. A. N. Sarjeant, K. D. Karlin, S. E. Rokita, *J. Am. Chem. Soc.* **2006**, *128*, 7003-7008.

[13] F. Seela, V. R. Sirivolu, *Helv. Chim. Acta* **2007**, *90*, 535-552; C. Bouillon, A. Meyer, S. Vidal, A. Jochum, Y. Chevolot, J.-P. Cloarec, J.-P. Praly, J.-J. Vasseur, F. Morvan, *J. Org. Chem.* **2006**, *71*, 4700-4701.

[14] V. Aucagne, D. A. Leigh, *Org. Lett.* **2006**, *8*, 4505-4507.

[15] D. I. Rozkiewicz, J. Gierlich, G. A. Burley, K. Gutsmiedl, T. Carell, B. J. Ravoo, D. N. Reinhoudt, *ChemBioChem* **2007**, *8*, 1997-2002.

[16] B. M. Trost, M. T. Rudd, *Org. Lett.* **2003**, *5*, 4599 - 4602.

[17] M. Fischler, U. Simon, H. Nir, Y. Eichen, G. A. Burley, J. Gierlich, P. M. E. Gramlich, T. Carell, *Small* **2007**, *3*, 1049-1055.

[18] J. Xiang, W. Jiang, P. L. Fuchs, *Tetrahedron Lett.* **1997**, *38*, 6635-6638; A. Orsini, A. Viterisi, A. Bodlenner, J.-M. Weibel, P. Pale, *Tetrahedron Lett.* **2005**, *46*, 2259-2262.

[19] J. L. Johnson, S. Hamm-Alvarez, G. Payne, G. B. Sancar, K. V. Rajagopalan, A. Sancar, *Proc. Nat. Acad. Sci. USA* **1988**, *85*, 2046-2050.

[20] K. Sivakumar, F. Xie, B. M. Cash, S. Long, H. N. Barnhill, Q. Wang, *Org. Lett.* **2004**, *6*, 4603-4606.

[21] P.-C. Lin, S.-H. Ueng, M.-C. Tseng, J.-L. Ko, K.-T. Huang, S.-C. Yu, A. K. Adak, Y.-J. Chen, C.-C. Lin, *Angew. Chem. Int. Ed.* **2006**, *45*, 4286-4290.

[22] L. V. Lee, M. L. Mitchell, S.-J. Huang, V. V. Fokin, K. B. Sharpless, C.-H. Wong, *J. Am. Chem. Soc.* **2003**, *125*, 9588-9589; T. Furuta, H. Torigai, M. Sugimoto, M. Iwamura, *J. Org. Chem.* **1995**, *60*, 3953-3956.

[23] F. Moris-Varas, X.-H. Qian, C.-H. Wong, *J. Am. Chem. Soc.* **1996**, *118*, 7647-7652.

[24] Q. Wang, T. R. Chan, R. Hilgraf, V. V. Fokin, K. B. Sharpless, M. G. Finn, *J. Am. Chem. Soc.* **2003**, *125*, 3192-3193; M. Adamczyk, J. R. Fishpaugh, K. J. Heuser, *Bioconjugate Chem.* **1997**, *8*, 253-255.

[25] A. E. Speers, B. F. Cravett, *Chem. Biol.* **2004**, *11*, 535-546.

[26] R. B. Mujumdar, L. A. Ernst, S. R. Mujumdar, C. J. Lewis, A. S. Waggoner, *Bioconjugate Chem.* **1993**, *4*, 105-111.

[27] R. Micura, *Chem. Eur. J.* **1999**, *5*, 2077-2082.

9 Sequential Click Chemistry on PCR Products

9.1 Introduction

The enzymatic synthesis of long, alkyne-decorated DNA strands of up to 2000 bps has been elaborated in Section 5 and in a pioneering work by Gierlich and Carell.[1] The utility of these macromolecular scaffolds for the preparation of metallized nanowires was demonstrated for silver nanowires,[1] gold nanoparticles[2] and bimetallic silver-gold nanowires (Section 4).[3] All these examples exhibit highly uniform metal deposition on the DNA backbone, possibly furnishing electrically conductive nanomaterials (measurements in progress).
There is currently no strategy for the site-selective immobilization of two different labels onto the DNA scaffold. The simplest strategy to achieve this would be to perform the click reaction with a mixture of azides. In this case a uniform distribution of labels on the DNA can not be warranted as: 1) different azides exhibit different efficiencies and kinetics in the click reaction; 2) azides could potentially be clustered by cooperative effects, thereby further diminishing the uniformity of label distribution. An exact placement or a defined patterning of the different labels would be completely impossible using these alkyne-modified strands. Therefore we sought to apply the sequential click chemistry outlined in Section 8 to PCR products. This technique allows for the stepwise labeling of DNA with different sets of azides by additionally introducing silyl-protected alkynes, which do not react under click reaction conditions and can subsequently be deprotected under mild conditions. In the case of PCR products and assuming that the reaction yield will be nearly quantitative in every case, a uniform distribution of the labels could be warranted by the sequence of the template. By using periodic sequences on the template strand, which can for example be synthesized by rolling circle amplification,[4] one could even produce DNA with a repetitive pattern of labels or segregated segments of different labels without using ligation techniques.

9.2 Results and Discussion

9.2.1 Synthesis of TMS-Protected **9.2**

Previous experiences with different silyl protecting groups (TMS and TIPS) on the terminal alkynes (Section 8) were used to decide for an appropriate protecting group for use in a PCR-based system. Silyl groups greatly enhance the hydrophobicity of the DNA, as exemplified by a drastic shift in retention time for TIPS-protected DNA strands on a reverse phase HPLC. In order to limit the degree of hydrophobicity and to allow for a mild deprotection reaction, the sterically least hindered silyl protecting group (TMS) seemed appropriate. The main limitation for the use of this protecting group in phosphoramidite chemistry (Section 8) is its lability in the deprotection step (conc. NH_3), which is not required after the PCR reaction. The only potential problem seemed to be the alkaline pH at high temperatures of typical PCR programs (95-98 °C during denaturation at pH 8.5 to 9.0, depending on the DNA polymerase used). As a preliminary experiment to address this issue, **9.1** (Scheme 9.1) was subjected to 95 °C in typical PCR buffers. No degradation was observable after prolonged time (30 min), leading to the conclusion that the TMS protecting group would be adequate for the desired purpose.

Pyrimidine nucleotides are more easily prepared than the corresponding purines. Therefore the nucleosides 5-iodo-2′-deoxycytidine and 5-iodo-2′-deoxyuridine seemed to be appropriate candidates as starting materials for the synthesis of silyl-protected alkynyl triphosphates. Nucleotide triphosphate **9.2**, based on 2′-deoxycytidine, seemed to be most facile to prepare as the purification after the Sonogashira cross-coupling with 1-trimethylsilyl-1,7-octadiyne to yield **9.1** can be easily performed, particularly when unprotected 5-iodo-2′-deoxycytidine is used. Performing the synthesis on the unprotected nucleoside is essential, as otherwise the TMS group could not be retained. Phosphorylation of **9.1** was achieved by using the Ludwig-Eckstein procedure.[5] The acetyl protection of the 3′-OH, which is typically performed before applying the Ludwig-Eckstein procedure, needs to be omitted as this group can not be selectively cleaved in the presence of the TMS alkyne. Still, the Ludwig-Eckstein procedure gave a far better yield (7%) than the Yoshikawa procedure ($POCl_3$, Me_3PO, $(HNBu_3)_2P_2O_7$),[6] which is typically used for unprotected nucleosides (< 1%).

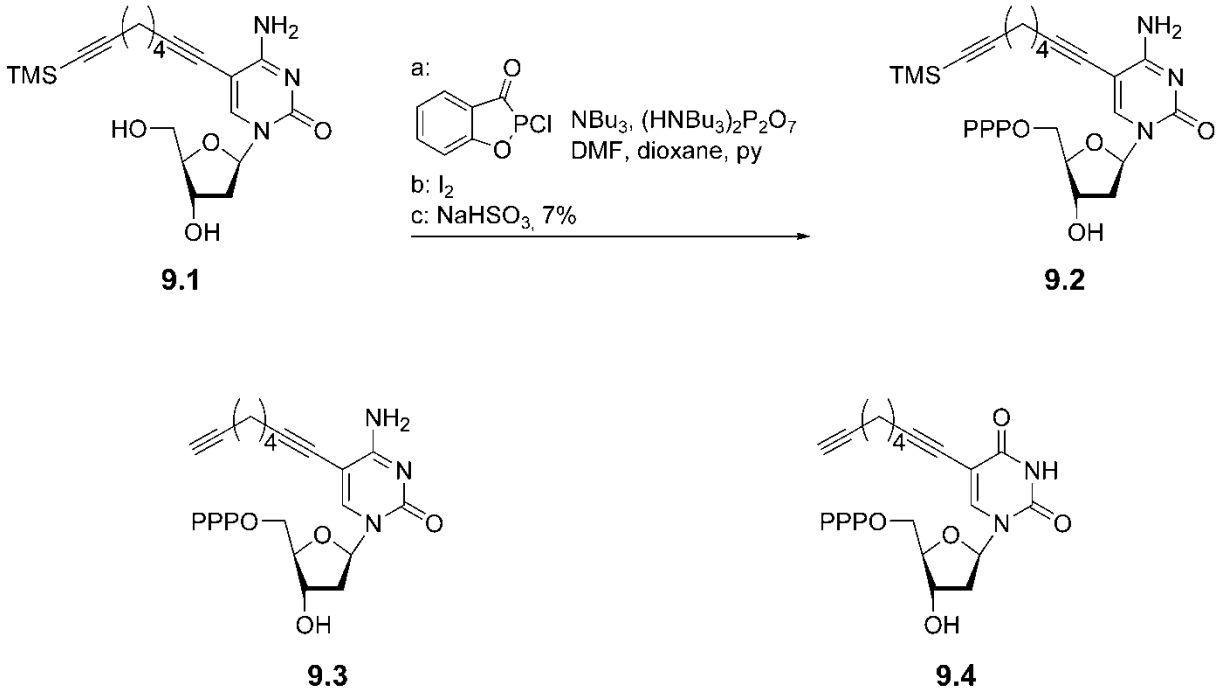

Scheme 9.1 Synthesis of triphosphate **9.2** by the Ludwig-Eckstein procedure and the structures of **9.3** and **9.4** used in this study.

9.2.2 Incorporation of **9.2** and **9.4** into PCR Products 300DNA(**9.2**/**9.4** 100%)[a]

In previous experiments, triphosphates **9.3** and **9.4** could simultaneously be incorporated into 300mer PCR products (data not shown). These highly modified DNA strands carry one modified building block in every base pair (dC replaced by **9.3** and dT replaced by **9.4**). Therefore, it seemed feasible to incorporate both **9.2** and **9.4** into the same DNA strand by fully replacing the natural nucleotides. Using KOD XL polymerase with some additives (4% DMSO, 0.4 mM

[a] The following nomenclature is used for the PCR products: (length of the PCR product) "DNA" (incorporated modified nucleotides)(percentage replacement of modified nucleotides in the triphosphate mixture).

Mg^{2+}, 0.08 U pyrophosphatase) in a touchdown PCR program, the desired DNA product 300DNA(**9.2**/**9.4** 100%) could indeed be obtained. Although several parameters have been thoroughly screened to yield this protocol, it is not a very reliable one and therefore about half the PCR reactions do not yield any of the desired product.
The high density of alkyne functions and silyl groups on the PCR products greatly complicated further manipulations with this material. As can be seen in Figure 9.1, lane 2, 300DNA(**9.2**/**9.4** 100%) gave a rather strong smear on a PAGE gel. Attempts to extract the DNA from the PCR reaction mixture gave poor results with all methods tested (chloroform/phenol extraction, ethanol precipitation, gel filtration spin columns from different providers, QIAquick PCR purification kit, C18 Sep-Pak cartridges). Performing the click reaction without prior purification gave low yields. Thus, two strategies have been devised to lower the density of the alkyne substituents on the DNA scaffold, as will be described in Sections 9.2.3 and 9.2.4.
Interestingly, the morphology of the PCR product lyophilisate (300DNA(**9.2**/**9.4** 100%)) strongly differs from natural DNA and also from DNA modified with free alkyne groups. It forms an elastic foam of extremely low density, which can be readily dissolved in aqueous solutions. These resulting solutions are much more viscous than comparable DNA solutions devoid of the TMS groups. It can be hypothesized that some sort of nano-detergent has been formed. The backbone of the DNA is highly polar due to the anionic phosphate groups and the major groove is functionalized with hydrophobic side chains. Unconventional secondary structures or micelles could potentially be formed from this material in aqueous solution. In order to elucidate, if these anomalous macroscopic properties also correspond to microscopically abnormal structures, electron microscopy is currently being performed in cooperation with the group of Prof. Bein.

9.2.3 Incorporation of **9.2** and **9.3** into PCR Products 300DNA(**9.2**/**9.3** 50%)

In order to lower the density of functionalization of the PCR products, thus allowing for easier manipulations and handling, **9.2** and **9.3** were used in equal amounts to replace dCTP in the PCR reaction. These modified triphosphates were both incorporated at comparable rates (28% **9.2**, 72% **9.3**, see also Section 9.2.4) by KOD XL polymerase and yielded the desired product 300DNA(**9.2**/**9.3** 50%) in a highly reliable manner. These DNA strands presumably exhibit a random arrangement of **9.1** and **9.3** on every position for dC. The handling of this material indeed turned out to be much easier than with 300DNA(**9.2**/**9.4** 100%), as can be seen from the much sharper band in the PAGE gel (Figure 9.1, lane 4) compared to 300DNA(**9.2**/**9.4** 100%) (lane 2). The proof of concept experiments for the click-deprotect-click reaction sequence was performed with the DNA described in the next Section, as it outperforms 300DNA(**9.2**/**9.3** 50%) in terms of versatility and handling.

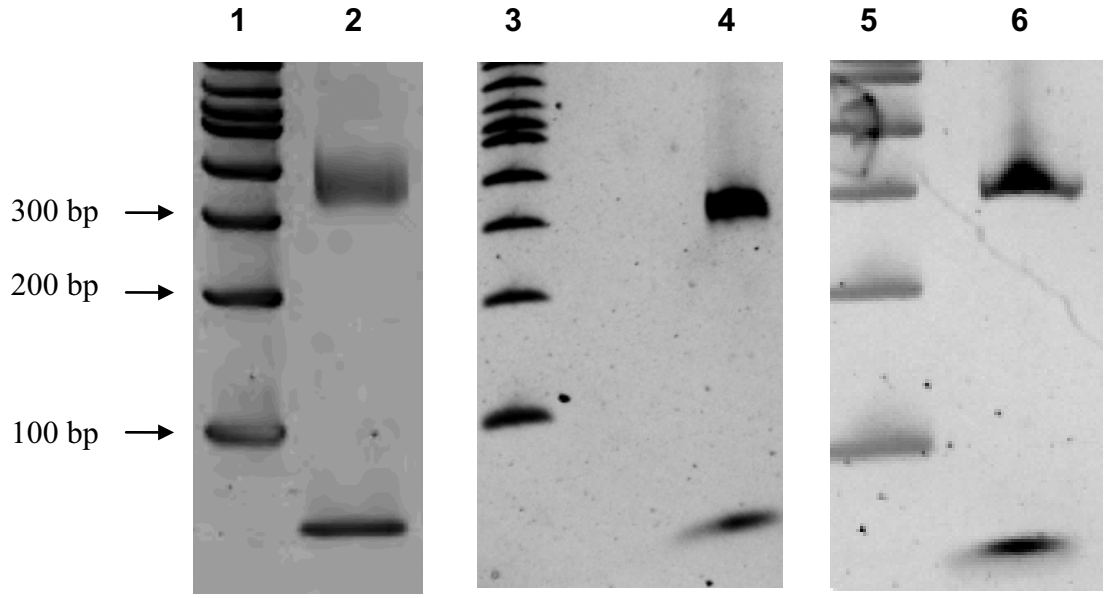

Figure 9.1 PAGE gels following PCR amplification without prior purification. Lanes 1, 3, 5: 100 bp DNA marker, lane 2: 300DNA(**9.2**/**9.4** 100%), lane 4: 300DNA(**9.2**/**9.3** 50%), lane 6: 300DNA(**9.2**/**9.4** 50%).

9.2.4 Incorporation of **9.2**/dCTP and **9.4**/dTTP into PCR Products 300DNA(**9.2**/**9.4** 50%) and Subsequent Click-Deprotect-Click Functionalization

300DNA(**9.2**/**9.4** 100%) offers the advantage of enabling the separate functionalization of two different nucleobases with two different labels: dUTP derivative **9.4**, which carries the free, terminal alkyne, can be labeled with the first azide and the dCTP derivative **9.2** can be labeled with the second azide after the deprotection step. The high density of labeling in 300DNA(**9.2**/**9.4** 100%) foreclosed the development of a simple protocol for the double modification of these PCR products. In the case of 300DNA(**9.2**/**9.3** 50%) the density of functionalization is decreased by 50%, as only the natural dCTPs are replaced by alkyne-bearing triphosphates **9.2** and **9.3**. The complete randomness of the distribution of these two modifications at each dC site prevents the utilization of base sequence for programming defined functionality onto the DNA template. Therefore a doping strategy was envisioned: 50% of the amounts of both dCTP and dTTP were replaced by **9.2** and **9.4**, respectively. The modified building blocks were expected to be incorporated at a lower rate compared to the natural triphosphates, whereas this difference was not expected to be large as such alkyne-modified triphosphates have already been used for the synthesis of a 2000mer PCR product (Section 5).[7] The protocol for the PCR reaction to give 300DNA(**9.2**/**9.4** 50%) could be established by varying the conditions for the previously discussed constructs 300DNA(**9.2**/**9.4** 100%) and 300DNA(**9.2**/**9.3** 50%) to yield a robust protocol. An enzymatic digestion of 300DNA(**9.2**/**9.4** 50%), followed by HPLC/UV and HPLC/MS-MS analyses, indeed showed a surprisingly high incorporation rate of the modified triphosphates[b] (32% at

[b] The diagnostic wavelength in these experiments was 260 nm. The alkyne substituent on the 5-position of the pyrimidine nucleobases in **9.1**-**9.4** leads to a shift in the absorption maximum. Therefore the extinction coefficients at 260 nm are not exactly equal when comparing dCTP with **9.2** or **9.3** and dTTP with **9.4**. This deviation has been shown to be of minor importance when quantifying these HPLC traces (Section 6).

each dC position and 19% at each dT position, average of three independent experiments)[8] The density of modified nucleotides is thus even lower than in the previously reported cases (50% for 300DNA(**9.2**/**9.4** 100%), 25% for 300DNA(**9.2**/**9.4** 50%) and 13% for 300DNA(**9.2**/**9.4** 50%)). These findings are a very strong proof of the proficiency of alkyne-modified nucleotide triphosphates like **9.2** and **9.4** to be accepted by DNA polymerases as substrates in a PCR reaction. By varying the percentage of modified triphosphates in the triphosphate mixtures one can probably fine-tune the density of functionalization.

In the most comprehensive methodological publication on the incorporation of alkyne-modified triphosphates into PCR products, the question was raised whether **9.3** or **9.4** are better substrates for the polymerases (Section 5).[7] In this study it was found that DNA strands containing **9.3** were more easily assembled than in the case of **9.4**. With this set of experiments it could not be concluded if this observed effect was due to a higher incorporation efficiency of **9.3**, because the density of alkyne labeling is 49% higher in the case of **9.4** compared to **9.3** due to the rather low GC content of the template strand. The doping experiment described above does in contrast allow for a more precise comparison of the incorporation rates. It in fact appears that the modified cytidine derivatives are better substrates for polymerases than the corresponding uridines.

HPLC analyses of the enzymatic digestions of 300DNA(**9.2**/**9.4** 50%) showed that the TMS group was partially cleaved off (38% **9.2**, 62% **9.3** as percentages of all detected modified dCTP derivatives). TMS protecting groups can in principle be cleaved by acidic and alkaline conditions. The deprotection reaction could occur at three instances: 1) during storage of the triphosphate solution; 2) during PCR amplification (95-98 °C at pH 8.5-9.0); 3) during enzymatic digestion (37 °C at pH 5.7, then pH 8.0). Integrity of the triphosphate solution of **9.2** was proven by a MALDI-TOF analysis, which showed no sign of decomposition of **9.2**. In order to test, whether the cleavage occurs during the PCR amplification, modified protocols were tested, in which different parameters were changed with the aim of avoiding a potential deprotection at high temperature and pH. The denaturation step was performed at lower temperatures for shortened time intervals (94 °C, 15 s), the reaction buffer was modified (addition of NaH_2PO_4 pH 5.2, HCl, citric acid, neutral buffers, phosphoric acid; replacing the KOD XL buffer by Pwo or Vent exo$^-$ buffers) and several enzymes were tested (KOD XL, Pwo or Vent exo$^-$). All these modified protocols furnished essentially the same amounts of cleavage product in the HPLC analyses. Some degree of improvement could be found in the case of adding NaH_2PO_4 buffer (pH 5.2, 40 mM final concentration, 44% **9.2** as percentage of all detected modified dCTP derivatives), HCl (8 mM, 41%) or H_3PO_4 (30 mM, 42%). Finally, the buffers for the enzymatic digestion were modified by running different experiments in which each of the buffer components was omitted one at a time. Again, the cleavage reaction could not be prevented in any of these cases. Remarkably, almost all of these modified protocols furnished good yields of the desired PCR product, although some of the conditions strongly differ from the optimized conditions reported in Table 9.2. Even completely changing the reaction buffer or lowering the pH can still lead to product formation. At this point, it can not be concluded at which step the cleavage reaction of the TMS group on **9.2** occurs. Changing to the hydrolytically more stable TES protecting group could potentially solve the problem.

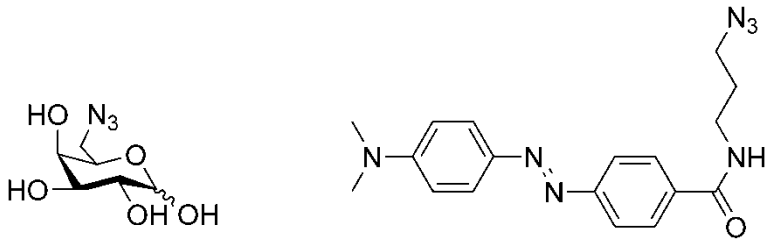

9.5 **9.6**

Scheme 9.2 Galactose azide **9.5** and dabcyl azide **9.6**.

In case the cleavage occurs during the enzymatic digestion, the click-deprotect-click reaction sequence could still be performed in a selective manner because then intact material would be obtainable after PCR amplification. To this end, 300DNA(**9.2**/**9.4** 50%) was subjected to a click reaction with galactose azide **9.5** (Scheme 9.2), followed by a mild TBAF deprotection and a second click reaction with dabcyl azide **9.6**. The HPLC peaks of the enzymatic digestion of the reaction product could not be unambiguously assigned, but relative intensities of the peaks in the ESI-MS spectrum are reported in Table 9.1. These values can not be used for an exact quantification of the product ratios, but do give an insight as to whether the desired products **9.4•9.5** and **9.2•9.6** are formed preferentially. The selectivity that can be estimated from Table 9.1 appears to be somewhat higher (2.5-3:1) than might be expected by the ratio of deprotected **9.3** to intact **9.2** in the enzymatic digestion of the unfunctionalized strands (28% intact **9.2** for 300DNA(**9.2**/**9.3** 50%)[c] and 38% for 300DNA(**9.2**/**9.4** 50%)). This result indicates that the cleavage of the TMS group occurs at least partially during the enzymatic digestion. If this can be proven by further experiments it would mean that TMS might indeed be a sufficiently stable protecting group for the assembly PCR products that are modified with two different azides in a selective manner.

Table 9.1 ESI-MS data of the sequential click reaction on 300DNA(**9.2**/**9.4** 50%) followed by enzymatic digestion.

click reaction product	relative intensity (ESI-MS signal)	calculated mass* [m/z]	found mass [m/z]
9.2•9.5	200	581.2213	581.2201
9.4•9.5**	500	582.2053	582,2042
9.2•9.6**	1500	727.3322	727.3304
9.4•9.6	500	728.3162	728.3147
9.2	0	448.1909	-
9.3	400	376.1514	376.1510
9.4	150	377.1354	377.1350

* formiate adducts.
** desired products.

[c] Maximum expected value: 50%.

9.3 Summary and Outlook

In this Section the synthesis of three different PCR products containing free and TMS-protected alkynes is reported. Doping experiments have hinted at modified cytidine triphosphates being better substrates for polymerases than the corresponding uridine derivatives. Enzymatic digestion of these 300mer DNA strands indicates that some of the TMS protecting groups are cleaved off. The exact point at which this cleavage occurs could not be located. Applying a click-deprotect-click reaction sequence to the doubly-labeled DNA scaffolds yields a product, in which the desired selectivity (first azide conjugated to **9.4**, second azide conjugated to **9.2**) could at least be partially achieved. Future experiments should therefore be focused on either finding the exact instant the TMS group is removed or repeating the experiments with a hydrolytically more stable silyl protecting group like TES. Additionally, it was found that silyl-protected PCR products display unusual macroscopic characteristics. Electron microscopy is currently being performed to elucidate whether these findings correlate to unusual microscopic structures.

9.4 Experimental Section

9.4.1 Synthesis

5-(8-Trimethylsilyl-octa-1,7-diynyl)-5´-*O*-triphosphate-2´deoxycytidine (**9.2**)[5]

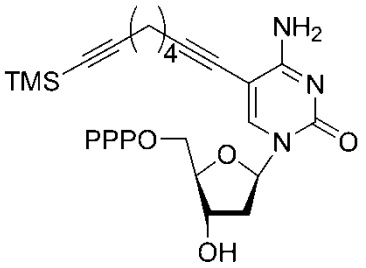

5-(8-Trimethylsilyl-octa-1,7-diynyl)-2´deoxycytidine **9.1** (80 mg, 0.22 mmol) was dissolved in dry pyridine and co-evaporated to dryness three times. Molecular sieves (4 Å), dry pyridine (0.4 mL) and dry DMF (1.7 mL) were added. The solution was left standing over night. A 1 M solution of 2-chloro-4*H*-1,2,3-dioxaphosphorin-4-one in dry dioxane (220 µL, left standing over night over molecular sieves, 4 Å) was injected into the well-stirred solution of the nucleoside. After 10 min a 0.5 M solution of bis(tri-*N*-butylammonium) pyrophosphate in anhydrous DMF (0.62 mL) and tri-*n*-butylamine (0.21 mL, left standing over night over molecular sieves, 4 Å) was quickly injected. A solution of 1% iodine in pyridine/water (98:2 v/v, 5 mL, 0.39 mmol) was then added. After 15 min excess iodine was destroyed by adding a few drops of a 5% aqueous solution of $NaHSO_3$ and the reaction solution evaporated to dryness. The residue was dissolved in water (30 mL) and left standing at room temperature for 30 min. The solution was evaporated to dryness, the residue dissolved in water and purified by RP-HPLC. The separation was performed using 0.1 M $HNEt_3$/OAc buffers (buffer A: H_2O, buffer B: MeCN/H_2O 4:1). The flow rate was 15 mL/min with a linear gradient from 100% A to 50% A in 45 min. The product **9.2** was eluted at 20.4 min (16 µmol, 7%).

^{31}P NMR (D_2O, 81 MHz): δ -22.4 (t, 1P, J = 20.4 Hz, β), -10.5 (d, 1P, J = 20.2 Hz, α), -10.0 (d, 1P, J = 19.4 Hz, γ). MS (MALDI-TOF): 641.9 $[M-H]^-$.

9.4.2 PCR

Table 9.2 Conditions for the PCR reactions for 300DNA(**9.2**/**9.4** 100%), 300DNA(**9.2**/**9.3** 50%) and 300DNA(**9.2**/**9.4** 50%).*

	300DNA(**9.2**/**9.4** 100%)	300DNA(**9.2**/**9.3** 50%)	300DNA(**9.2**/**9.4** 50%)
Annealing**	63.0 °C, 30 s	68.0 °C, 30 s	65.5 °C, 30 s
Denaturation	98.0 °C, 30 s	98.0 °C, 30 s	98.0 °C, 30 s
Elongation	74.0 °C, 60 s	74.0 °C, 40 s	74.0 °C, 30 s
Primer, 10 mM [µL]***	0.75	0.75	0.75
Buffer 10x [µL]	2.5	2.5	2.5
Template, 165 ng/µL [µL]***	2	2	2
DMSO [µL]	1	0.6	0.6
KOD XL, 2.5 U/µL [µL]	0.4	0.3	0.25
$MgSO_4$, 25 mM [µL]	0.4	-	-
Pyrophosphatase 0.2 U/µL [µL]	0.2	0.2	-
Formamide [µL]	-	1	-

* All reactions were run in a total volume of 25 µL.
** All protocols use a touchdown PCR program, which starts with the given annealing temperature +1 °C, then 9 cycles with an annealing temperature increment of -1 °C, followed by 30 cycles at the given annealing temperature.
*** Sequences are the same as reported in the literature.[1]

Purification of the PCR products

PCR products containing silyl protecting groups are intrinsically difficult to purify due to the high hydrophobicity of the silyl groups. Of the many methods tested, only two can be recommended here.

Sep-Pak: The pre-packed Sep-Pak column was conditioned by first rinsing with MeCN and then water (10 mL each). The PCR solution was directly applied to the top of the column and washed with water (5 mL). The product was eluted with MeCN/H_2O 1:1. After 3-4 mL of this solvent mixture no more product eluted.

Gel filtration: The PCR reaction solution can be directly applied to a HiLoad 16/60 Superdex 30 column. 5 mM tris buffer, pH 7.5, was used at a flow rate of 1 mL/min. The PCR product eluted between 40-50 mL.

9.4.3 Click-Deprotect-Click Procedure

Click Reaction

Purified PCR product (100 µL, 110 ng/µL[d]) was lyophilized together with the azide (1 µmol). 3 µL CuBr solution (0.1 M in DMSO/*t*BuOH 3:1) and 6 µL TBTA ligand[9] solution (0.1 M in DMSO/*t*BuOH 3:1) were combined, vortexed and immediately added to the lyophilisate. 5 µL water were added and the resulting solution degassed by bubbling argon through it for some seconds. The vial was firmly closed and shaken at 30 °C for 2 h. The desired DNA was precipitated directly from the reaction solution as described below.[e]

Deprotection of the TMS-alkyne

Lyophilized DNA was dissolved in 200 µL dry THF. 20 µL TBAF (1 M in dry THF) was added and the solution was shaken at 25 °C for 70 min. 100 µL tris-HCl (1 M) was added and the resulting solution evaporated to near-dryness in a SpeedVac and precipitated as described below.

Ethanol precipitation

100 µL NaOAc solution (0.3 M) and 1 mL ethanol were added to the DNA from the click or deprotection reactions and left over night at -20 °C. The suspension was centrifuged (10 min at 13 000 rpm) and the supernatant carefully removed. Ethanol (1 mL) was added, the suspension vortexed, centrifuged and the supernatant removed. This washing step was performed twice. The resulting pellet was left drying on air.

9.4.4 Enzymatic Digestion

For the enzymatic digestion the DNA (1-10 µg in 100 µL water) was incubated in 10 µL buffer A (300 mM NH_4OAc, 100 mM $CaCl_2$, 1 mM $ZnSO_4$, pH 5.7), 22 U nuclease P1 (*penicilinum citrium*) and 0.05 U calf spleen phosphodiesterase II. The sample was incubated at 37 °C for 3 h. The digestion was completed by adding 12 µL buffer B (500 mM tris-HCl, 1 mM EDTA, pH 8.0), 5 U antarctic phosphatase and 0.1 U snake venom phosphodiesterase I (*crotalus adamanteus venom*). The sample was incubated for another 3 h at 37 °C. For workup the samples were centrifuged (13 000 rpm, 5 min). The resulting nucleoside mixture was analyzed by HPLC (Interchim Interchrom Uptisphere 3 HDO column (150 x 2.1 mm)), buffer A: 2 mM TEA/HOAc in H_2O; buffer B: 2 mM TEA/HOAc H_2O:MeCN 1:4; 0 → 12 min: 0% → 3% B; 12 → 60 min: 3% → 60 % B; 60 → 62 min: 60% → 100 %; 62 → 90 min: 100% B; 90 → 95 min: 100% → 0% B; 95 → 130 min: 0% B; flow rate

[d] UV spectroscopy of these DNAs frequently yields inconclusive data both on a conventional UV spectrometer and on a Nanodrop UV spectrometer. The given concentrations therefore do not represent an exact value.
[e] In case of larger reaction volumes (> 20 µL DMSO in total) the reaction mixture should either be split into smaller aliquots prior to precipitation or evaporated to near-dryness in a SpeedVac.

0.15 mL/min. The different peaks were assigned by co-injection, UV and FT-ICR-HPLC/MS-MS using the same conditions.

9.4.5 HPLC Analyses of the Enzymatic Digestions

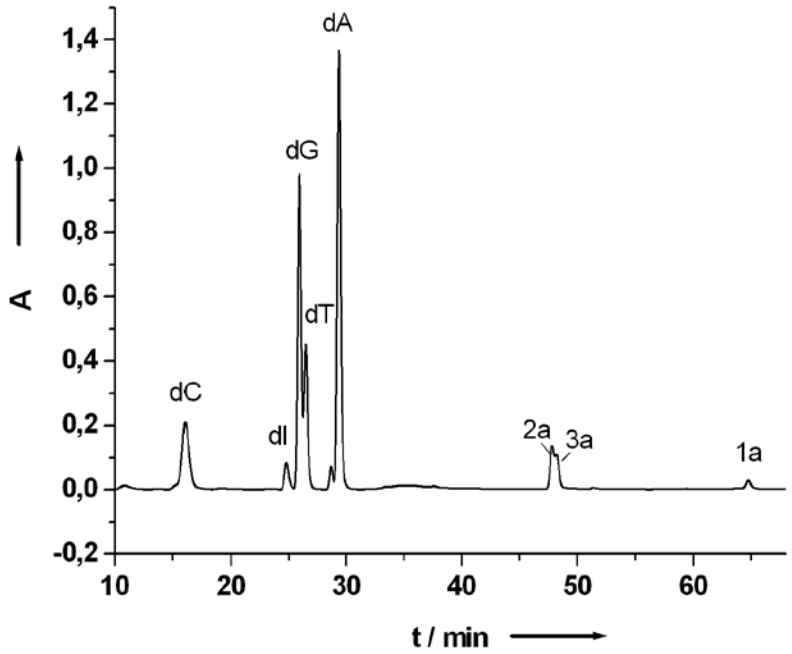

Figure 9.2 HPLC of 300DNA(**9.2**/**9.4** 50%).

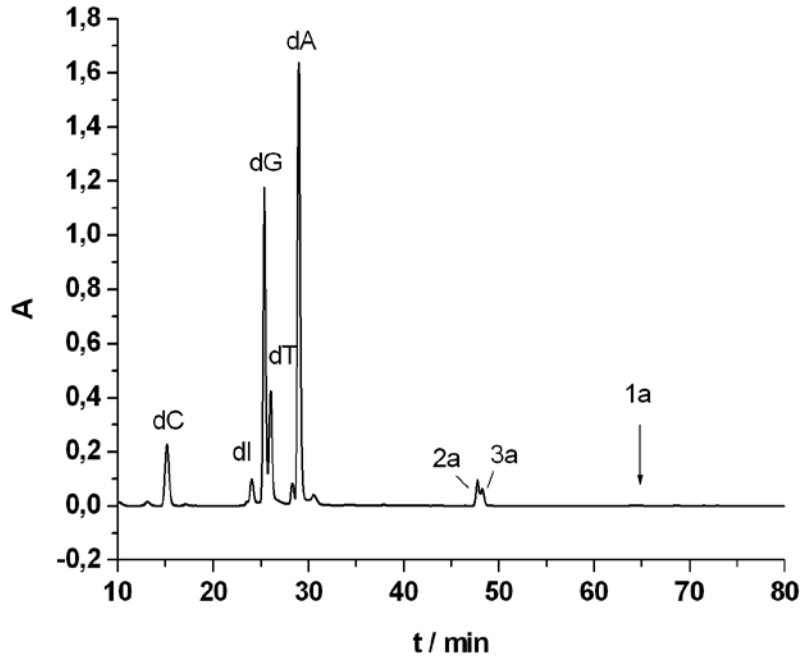

Figure 9.3 HPLC of 300DNA(**9.2**/**9.4** 50%) after deprotection.

Table 9.3 Absorption maxima of the nucleosides.

nucleoside	**Absorption maximum [nm]**
deoxycytidine	271
deoxyinosine	249
deoxyguanosine	253 + shoulder
deoxythymidine	267
deoxyadenosine	260
9.2	298
9.3	298
9.4	292

9.5 References

[1] G. A. Burley, J. Gierlich, M. R. Mofid, S. T. H. Nir, Y. Eichen, T. Carell, *J. Am. Chem. Soc.* **2006**, *128*, 1398-1399.

[2] M. Fischler, A. Sologubenko, J. Mayer, G. Clever, G. Burley, J. Gierlich, T. Carell, U. Simon, *Chem. Commun* **2008**, 169-171.

[3] M. Fischler, U. Simon, H. Nir, Y. Eichen, G. A. Burley, J. Gierlich, P. M. E. Gramlich, T. Carell, *Small* **2007**, *3*, 1049-1055.

[4] S. Beyer, P. Nickels, F. C. Simmel, *Nano Lett.* **2005**, *5*, 719-722.

[5] J. Ludwig, F. Eckstein, *J. Org. Chem.* **1989**, *54*, 631-635.

[6] M. Yoshikawa, T. Kato, T. Takenishi, *Tetrahedron Lett.* **1967**, *8*, 5065-5068.

[7] J. Gierlich, K. Gutsmiedl, P. M. E. Gramlich, A. Schmidt, G. Burley, T. Carell, *Chem. Eur. J.* **2007**, *13*, 9486-9494.

[8] C. T. Wirges, P. M. E. Gramlich, K. Gutsmiedl, J. Gierlich, T. Carell, *QSAR Comb. Sci.* **2007**, *26*, 1159-1164.

[9] T. R. Chan, R. Hilgraf, K. B. Sharpless, V. V. Fokin, *Org. Lett.* **2004**, *6*, 2853-2855.

10 Sequential Click Chemistry for the Attachment of DNA onto Colloidal Mesoporous Silica (Cooperation with Prof. Bein)

10.1 Introduction

The following Section describes a cooperation project with Axel Schlossbauer[1] from the group of Prof. Bein (LMU München). The project is dedicated to utilizing modified DNAs to attach selectively addressable lids to the pores of a colloidal mesoporous silica (CMS) nanoparticle in order to release drug molecules or other useful agents in a defined biological context. Successful proof-of-concept experiments have been performed and the work is currently being continued by Simon Warncke.

10.1.1 Selectively Functionalized CMS

Mesoporous silica materials attracted great interest in the last decade due to their various applications in affinity chromatography,[2] chemical sensing[3] or as carrier of catalysts[4] and biomolecules.[5] In particular, the high surface areas (700-1500 m^2/g), tunable pore sizes and morphologies are characteristic and useful properties of this class of materials. The high chemical and thermal stability, together with the simple functionalization chemistry of silica, further promote its use.[6] CMS does not exhibit cytotoxic effects on mammalian cells, a particularly important property in the context of a drug release system.[7] Some mammalian cells have been shown to be able to actively internalize CMS by endocytosis and the nanoparticles are released from endosomes to reach the cytosol.[8]

The first mesoporous silica material with defined, large pores (> 1 nm), was introduced in 1992 by researchers at the Mobil Corporation (MCM-41) by heating a mixture of certain surfactants with aluminas and orthosilicates.[9] This synthetic strategy was based on the formation of liquid-crystalline mesophases of surfactants that serve as templates for the in-situ polymerization of the orthosilicates.[6] The templating surfactants were subsequently removed by calcination at 540 °C. Already at this point it was possible to fine-tune the pore size in a defined way by varying the surfactants as well as the ratio of surfactant to silicate. The particles were obtained in the size range of several μm, the pore sizes were in the range between 2 and 30 nm.

In order to obtain smaller particles of a narrow size distribution, three approaches have been developed to date. The growth reaction can be interrupted after seconds to minutes by dilution followed by pH neutralization.[10] Another approach uses a second surfactant, which can block the access of the growth species to the surface.[11] The third procedure, which is followed in the present work, is to add triethanolamine (TEAH) as base and complexing agent.[12]

To enhance the properties of these materials, organic moieties can be introduced at different stages of the synthesis. In a grafting method, nanoparticles are first synthesized without the organic moieties and subsequently reacted with organotrialkoxysilanes or organotrichlorosilanes, which are thus attached to the silica surfaces postsynthetically.[13] Another approach, which is utilized in this work, is the co-condensation.[14] Functionalization with organic moieties is achieved by copolymerization of an organosilane with a silica precursor in the presence of the templating surfactant. This method implies the removal of the template by extraction

methods, since calcination at high temperature (> 400 °C), as in the case of MCM-41,[9] would destroy most organic functionalities.

Selective functionalization of the outer surface of a CMS material can be achieved by a novel variation of the co-condensation process, introduced by Bein et al.[15] To this end, the functionalized organosilanes are added at later stages of the polymerization process (Figure 10.1). The interior of the nanoparticle thus remains unfunctionalized and only the external segments, which are formed after the addition of the organosilane, display the desired functionality.

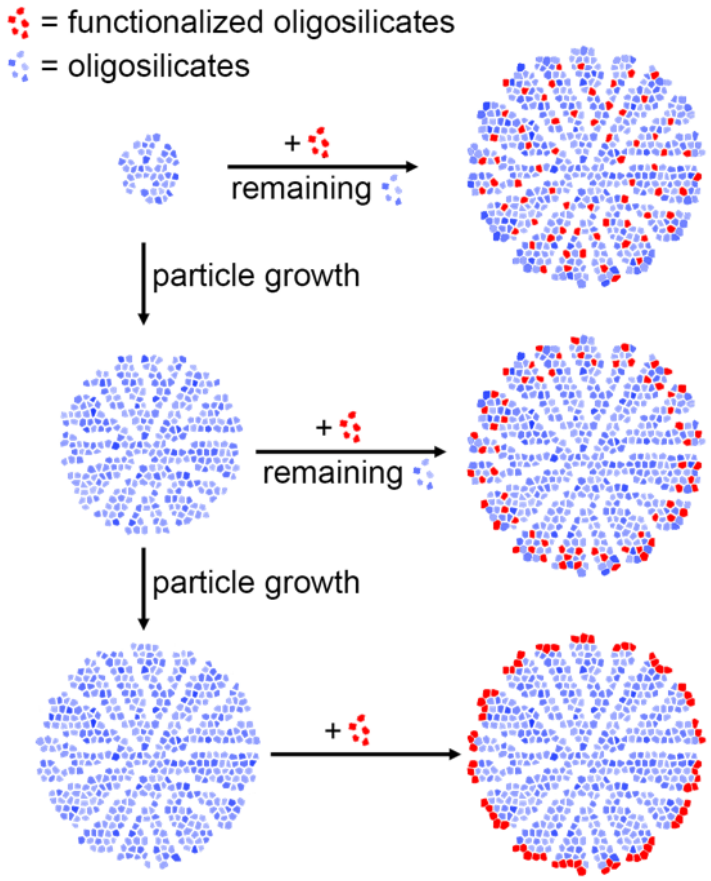

Figure 10.1 Strategy for the selective functionalization of CMS surfaces. Reproduced from Bein et al.[15]

As significant progress has been made in the selective preparation and functionalization of these materials, complex tasks like controlled drug release are presently being tackled.[16] In a publication by Lin et al., a selective drug-release system was introduced (Figure 10.2).[17] The nanoparticles were soaked in a solution of the drug molecule (ATP or vancomycin). The nanopores bore linkers with an internal disulfide bridge and an amine group, which could be used for the attachment of the carboxylic acid functionalized CdS nanoparticles. The CdS nanoparticles were thus used to close the pores, preventing a premature leaching of the drug molecules. The CdS caps could be conveniently removed by reduction of the disulfide bonds with thiols like mercaptoethanol or dithiothreitol, thereby liberating the drug molecules. This

removal was thus triggered by a distinct chemical stimulus. A more general approach will be elaborated in the next Section, in which DNA is used to close the nanopores.

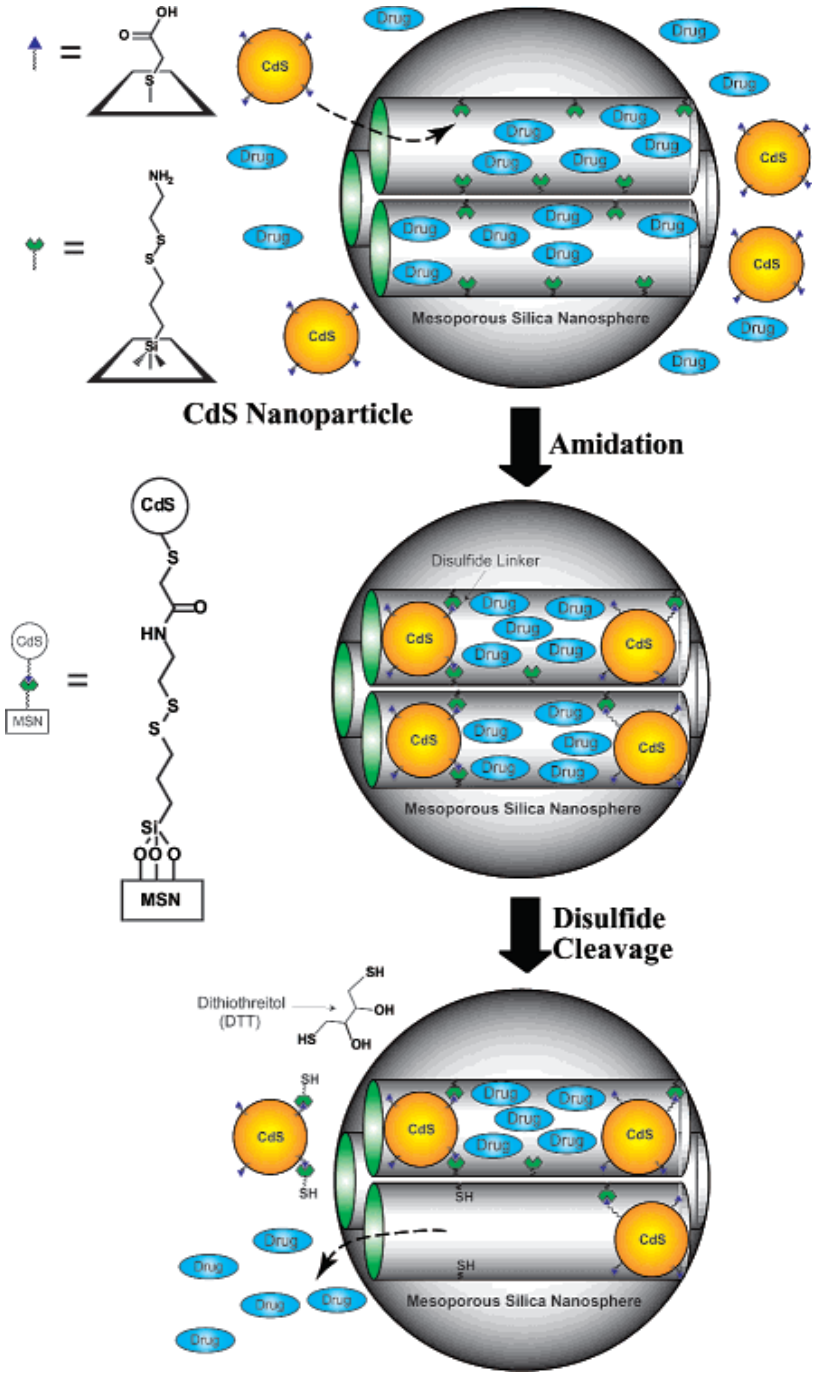

Figure 10.2 CdS nanoparticles for the reversible closing of nanoparticle pores. Reproduced from Lin et al.[17]

10.1.2 Selectively Modified DNA for Nanotechnology Applications

The strategy discussed above relies on the breakage of a chemical bond to liberate the drug molecules from the CMS. The design of a DNA-based lid for the nanopores, on the other

hand, would only require the separation of two complementary DNA strands, which can be brought forth by a multitude of stimuli. A first catcher oligodeoxynucleotide (ODN) has to be designed with a free alkyne for attachment to the CMS surface. As second modification, this ODN needs to bear a dye/quencher in order to be able to follow its attachment via confocal microscopy. The strategy for the attachment of up to three different labels onto DNA using click chemistry, which is being followed in this Section, has been elaborated in Section 8. To this end, one free alkyne and one TIPS-protected alkyne is introduced into the ODN. The free alkyne is used for the attachment of the dye/quencher. Then the TIPS protecting group on the second alkyne can be removed under mild conditions with TBAF to give a free alkyne for the attachment to the CMS surface. This ODN is now used as a catcher for the lid-ODN with complementary sequence, which needs to carry the nanopore lid and a dye/quencher compatible to the dye/quencher on the first ODN. The dye/quencher couple can be used to follow the hybridization on the nanoparticle surface by confocal microscopy. The event, which will trigger the release of the encapsulated drug molecules, will thus be the removal of the second ODN, which can be effected by a multitude of effects. Temperature, pH, buffer concentration and the presence of complementary DNA or RNA strands can lead to a dehybridization of the DNA double helix. With this approach, a multitude of targets could, in principle, be targeted by a smart design of the DNA sequence.

10.2 Results and Discussion

10.2.1 Synthesis of the Catcher ODN

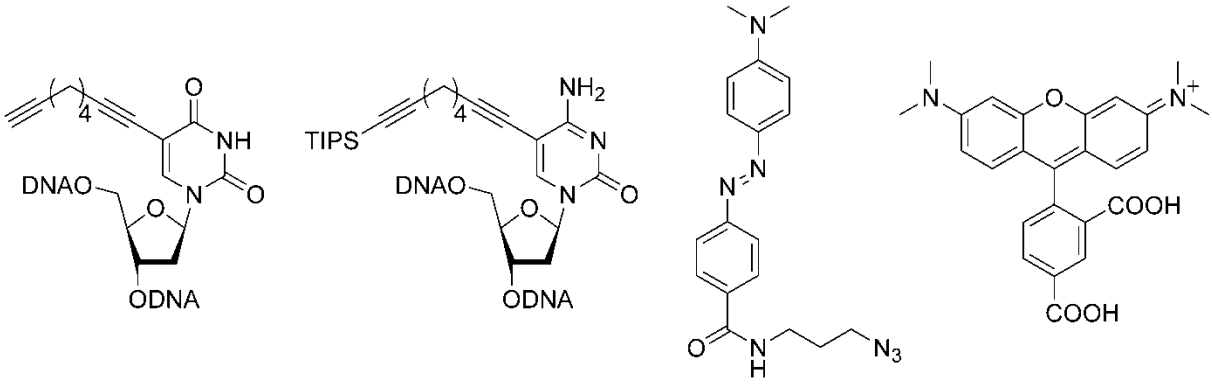

10.1 **10.2** **10.3** **10.4**

Scheme 10.1 Alkyne-bearing nucleotides **10.1** and **10.2**, Dabcyl azide **10.3** and TAMRA **10.4**.

The first set of proof-of-concept experiments was dedicated to the following questions: Is it possible to immobilize a DNA strand onto CMS via click chemistry? Can the catcher ODN sequence still be addressed by a second ODN? Can the second ODN be removed under mild conditions? ODN-**10.1** (Table 10.1), bearing one free and one TIPS-protected alkyne, was used for these preliminary experiments (see also Section 8). The free alkyne was reacted with

Dabcyl azide **10.3** (Scheme 10.1), then the TIPS protecting group on **10.2** was removed with TBAF, thereby generating another free alkyne for CMS functionalization. ODN-**10.2** was obtained from a commercial supplier.

Table 10.1 ODN sequences.

ODN-**10.1**	5′-GCGCYGTTCATTXGCG-3′	X: Dabcyl-labeled dT (**10.1** in Scheme 10.1) Y: alkyne-labeled dC (**10.2** in Scheme 10.1) for nanoparticle immobilization
ODN-**10.2**	5′-CGCAAAXGAACGGCGC-3′	X: TAMRA (**10.4**)-labeled dT

10.2.2 Synthesis of Azide-Functionalized, Mesoporous Silica Nanoparticles

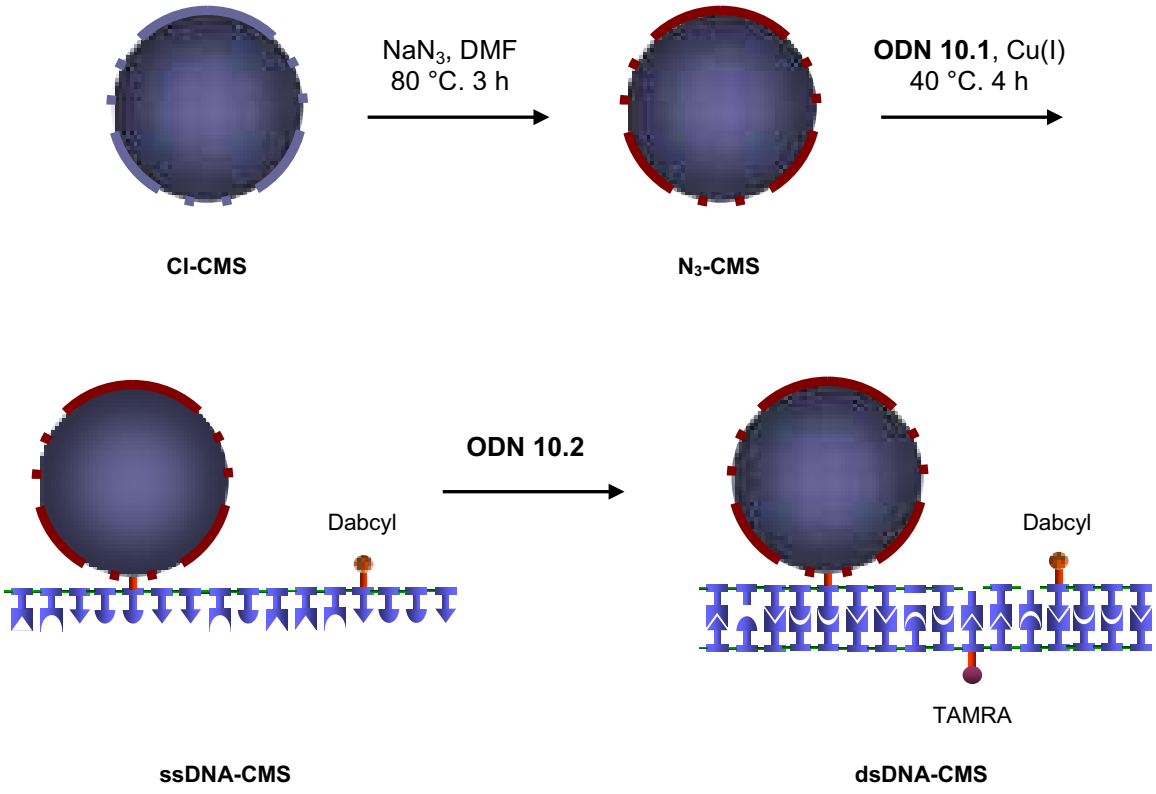

Figure 10.3 Reaction pathway for the functionalization of CMS with dsDNA.

The CMS material employed in this work was synthesized by adding triethanolamine (TEAH) to the reaction mixture to limit the particle growth. After initial particle growth without organosilanes, CMS was selectively functionalized in situ on the outer surface with a 3-chloropropyltrimethoxysilane (CTMS)/tetraethoxyorthosilicate (TEOS) mixture of the molar ratio 1:3 to yield CMS with a pore size of 3.8 nm. Subsequently, the chloro-functionalized CMS (**Cl-CMS**) was treated with NaN_3 in order to obtain a surface displaying propylazido groups (**N_3-CMS**). The resulting material was reacted with ODN-**10.1** in a click reaction

(**ssDNA-CMS**) before being hybridized with the complementary ssDNA carrying a TAMRA modification **10.4**, leading to double stranded DNA bound to the CMS surface (**dsDNS-CMS**, Figure 10.3). After synthesis, the sample was washed with water multiple times in order to remove unbound DNA.

The obtained sample was investigated with confocal microscopy to visualize the (de)hybridization of the DNA duplex on the CMS. **DsDNA-CMS** was fixed on a glass slide by spin coating. The sample was investigated three times at exactly the same position: Directly after hybridization, after 15 min at 60 °C and after 14 h at 60 °C (Figure 10.4). The obtained pictures show agglomerates of the synthesized **dsDNA-CMS**, which were generated during the spin coating process. As can be seen, the fluorescence intensity increased with the heating time. This effect presumably occured due to the heat-induced melting of the dsDNA, which is just one representative of a whole range of dehybridization methods. The Dabcyl quencher and the TAMRA dye (**10.4**) were no longer in close contact to each other, therefore the fluorescence intensity of the TAMRA dye increased. We take this observation to imply that the Dabcyl label on ODN-**10.1** was still intact after the click reaction to **N_3-CMS**.

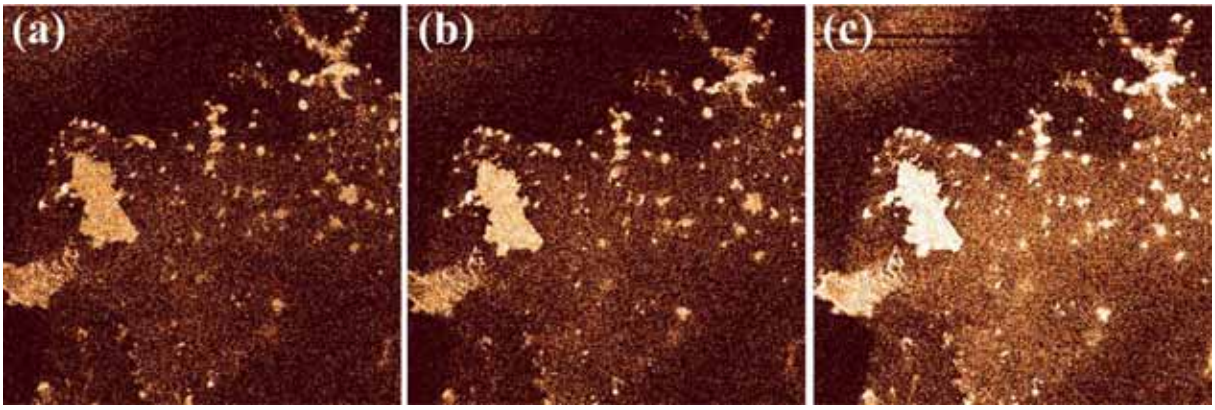

Figure 10.4 Confocal microscopy of **dsDNS-CMS** after hybridization (a), after 15 min at 60 °C (b), and after 14 h at 60 °C (c). One pixel corresponds to 300 nm.

For further characterization, IR spectroscopy of the samples **N_3-CMS** and **dsDNA-CMS** was performed (Figure 10.5). Bands corresponding to DNA are marked with asterisks.

The progress of the click reaction is shown by a decrease of the azide stretch band at 2108 cm^{-1}. It should be noted that the recorded IR spectra do not contain exact quantitative information due to the applied DRIFT mode. DNA exhibits two characteristic bands, the aromatic C=C stretch and the C=O stretch of the nucleobases (Figure 10.5b). **N_3-CMS** contains adsorbed water, indicated by a band at 1660 cm^{-1} (Figure 10.5a). The dashed line in Figure 10.5 allows an easy differentiation of the described water band and the aromatic C=C stretch of the bound DNA.

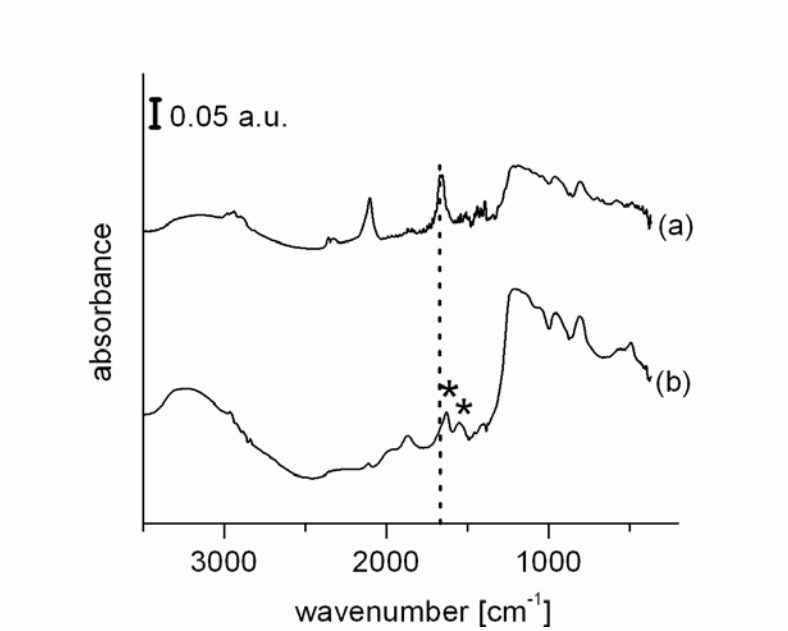

Figure 10.5 IR-measurements of samples **N_3-CMS** (a) and **dsDNA-CMS** (b).

Table 10.2 Assignment of the bands in Figure 10.5.

group	**wavenumber [cm^{-1}]**	**assignment**
azide	2108	asymmetric azide stretch
DNA	1633	C=O stretch
	1551	aromatic C=C stretch
adsorbed water	1660	

It should be noted that while the obtained results qualitatively prove the hybridization and subsequent melting of the DNA strands, they do not contain any quantitative information. The efficiency of the hybridization and number of incorporated DNA strands before and after melting remains unknown.

10.3 Summary and Outlook

The work presented here constitutes some proof-of-concept experiments for a novel drug delivery system based on CMS. It was shown that a DNA strand bearing one Dabcyl label, attached via click chemistry, could be immobilized onto the CMS surface via a second alkyne group on the DNA. This represents the first application of the sequential click chemistry strategy described in Section 8. A second DNA strand, bearing a TAMRA label, could be hybridized to the first ODN, which was proven by a quenching of the TAMRA fluorescence by the Dabcyl label (confocal microscopy). Once the construct was heated, the second strand was removed, as evidenced by an increased fluorescence of the TAMRA dyes. To gain precise information about the amount of attached ds-DNA, further FRET experiments in more sophisticated systems are necessary. Two more milestones will have to be reached in order to establish a functional drug delivery system. The second DNA strand needs to bear a lid moiety for

the nanopores. To this end, leaching experiments with encapsulated drug molecules will have to be performed to prove that the lid can actually restrain molecules inside the CMS. Secondly, the DNA duplex needs to be designed in a way that it can be selectively opened inside a specific biological environment. DNA duplexes can be opened by a wide variety of events, like temperature increase, presence of a DNA or RNA strand with a complementary sequence or a change in buffer concentration or pH. In addition to the immobilized DNA, labels that improve the cell permeability or selective targeting could be attached to the CMS. Due to the tunability of the CMS structure and the selective addressability of DNA, the approach outlined here offers great promise as a future drug delivery vehicle.

10.4 Experimental Section

ODN-**10.1** was synthesized as described in Section 8.

ODN-**10.2.** was purchased from Metabion.

Synthesis of **10.1-10.3** was described in Section 8.

10.4.1 Preparation of Cl-CMS

Mesoporous silica nanoparticles were prepared according to literature from reaction mixtures with a molar composition of 1 TEOS: 0.20 CTAC: 10.37 TEAH: 130.15 H_2O.[19] The combined TEOS (1.92 g, 9.22 mmol) and TEAH (14.3 g, 95.6 mmol) were heated for 20 min at 90 °C without stirring in a 100 mL polypropylene reactor. A solution of CTAC (25% in water, 2.41 mL, 1.83 mmol) and water (21.7 g, 1.21 mol) preheated to 60 °C was added. CTMS/TEOS 1:3 (molar ratio) was added to the reaction mixture after 30 min. The combined amount of both silanes was 185 µmol in all samples, i.e. 2% of the total amount of "Si" in the initial CMS synthesis. The resulting mixture was stirred at r. t. for 12 h. After addition of 100 mL EtOH, the **Cl-CMS** was separated by centrifugation, redispersed in EtOH and extracted according to the procedure described below.

10.4.2 Extraction of Cl-CMS

Extraction of the organic template from the **Cl-CMS** material was performed by heating of 250 mg of **Cl-CMS** for 30 min under reflux at 90 °C for two times in a solution containing 2 g $NH_4^+NO_3^-$ in 100 mL ethanol, followed by 30 min under reflux in a solution of 4 g conc. HCl in 100 mL EtOH. The **Cl-CMS** nanoparticles were separated by centrifugation. The obtained material was washed with EtOH after each extraction step. **Cl-CMS** was obtained as clear ethanolic suspension.

10.4.3 Synthesis of N_3-CMS

After extraction, the as-synthesized **Cl-CMS** was subsequently redispersed in a saturated solution of NaN_3 in DMF. The mixture was allowed to stir for 4 h at 80 °C. 10 mL of water

were added before centrifugation. The product **N_3-CMS** was washed with water and EtOH before being redispersed in water.

10.4.4 Synthesis of ssDNA-CMS

A solution of 0.05 µmol ODN-**10.1** in water (2 mL) was added to **N_3-CMS** (25 mg). Then, TBTA ligand (20 µl, 0.1 M in DMSO/*t*BuOH 3:1 v/v)[20] and CuBr (10 µl, 0.1 M in DMSO/*t*BuOH 3:1 v/v) were premixed and quickly added. The reaction mixture was allowed to stir for 4 h at 35 °C before centrifugation and redispersion in water. The product was washed two times with 10 mL of water followed by centrifugation and redispersion in 10 mL of water.

10.4.5 Synthesis of dsDNA-CMS

A suspension of 25 mg of DNA-functionalized **ssDNA-CMS** in water was heated to 50 °C in a water bath. A solution of 0.04 µmol of ODN-**10.2** in water (500 µl) was added to the solution. The resulting mixture was cooled to room temperature followed by centrifugation and redispersion in water.

10.5 Author´s Contribution

The DNA strand has been synthesized by the author. All click reactions on the DNA and on the CMS material have been performed by the author as well.

10.6 References

[1] A. Schloßbauer, Diploma thesis, LMU München (München), **2007**.
[2] H. Lakhiari, E. Legendre, D. Muller, J. Jozefonvicz, *J. Chromatogr., B.* **1995**, *664*, 163-173; J. E. Schiel, R. Mallik, S. Soman, K. S. Joseph, D. S. Hage, *J. Sep. Sci.* **2006**, *29*, 719-737.
[3] D. R. Radu, C.-Y. Lai, J. W. Wiench, M. Pruski, V. S.-Y. Lin, *J. Am. Chem. Soc.* **2004**, *126*, 1640-1641.
[4] G. A. Ozin, C. Gil, *Chem. Rev.* **1989**, *89*, 1749 - 1764.
[5] J. Suna, H. Zhanga, R. Tianb, D. Ma, X. Bao, D. S. Suc, H. Zou, *Chem. Commun.* **2006**, 1322-1324.
[6] B. G. Trewyn, I. I. Slowing, S. Giri, H.-T. Chen, V. S.-Y. Lin, *Acc. Chem. Res.* **2007**, *40*, 846-853.
[7] D. R. Radu, C.-Y. Lai, K. Jeftinija, E. W. Rowe, S. Jeftinija, V. S.-Y. Lin, *J. Am. Chem. Soc.* **2004**, *126*, 13216 - 13217.
[8] I. Slowing, B. G. Trewyn, V. S.-Y. Lin, *J. Am. Chem. Soc.* **2006**, *128*, 14792 - 14793; Y.-S. Lin, C.-P. Tsai, H.-Y. Huang, C.-T. Kuo, Y. Hung, D.-M. Huang, Y.-C. Chen, C.-Y. Mou, *Chem. Mater.* **2005**, *17*, 4570 - 4573.
[9] C. T. Kresge, M. E. Leonowicz, W. J. Roth, J. C. Vartuli, J. S. Beck, *Nature* **1992**, *359*, 710-712.
[10] C. E. Fowler, D. Khushalani, B. Lebeau, S. Mann, *Adv. Mater.* **2001**, *13*, 649-652.
[11] K. Suzuki, K. Ikari, H. Imai, *J. Am. Chem. Soc.* **2004**, *126*, 462 - 463.

[12] J. E. Haskouri, D. O. d. Zárate, C. Guillem, A. Beltrán-Porter, M. Caldés, M. D. Marcos, D. Beltrán-Porter, J. Latorre, P. Amorós, *Chem. Mater.* **2002**, *14*, 4502 - 4504.
[13] M. H. Lim, A. Stein, *Chem. Mater.* **1999**, *11*, 3285 - 3295.
[14] T. Yokoi, H. Yoshitake, T. Tatsumi, *J. Mater. Chem.* **2004**, *14*, 951-957.
[15] J. Kecht, A. Schloßbauer, T. Bein, *manuscript in preparation*.
[16] I. I. Slowing, B. G. Trewyn, S. Giri, V. S.-Y. Lin, *Adv. Funct. Mater.* **2007**, *17*, 1225-1236; B. G. Trewyn, S.Giri, I. I. Slowing, V. S.-Y. Lin, *Chem. Commun.* **2007**, 3236–3245.
[17] C.-Y. Lai, B. G. Trewyn, D. M. Jeftinija, K. Jeftinija, S. Xu, S. Jeftinija, V. S.-Y. Lin, *J. Am. Chem. Soc.* **2003**, *125*, 4451-4459.
[18] H. Robson, *Microporous Mesoporous Mater.* **1998**, *22*, 495-666.
[19] K. Möller, J. Kobler, T. Bein, *Adv. Funct. Mater.* **2007**, *17*, 605–612.
[20] T. R. Chan, R. Hilgraf, K. B. Sharpless, V. V. Fokin, *Org. Lett.* **2004**, *6*, 2853-2855.

11 Tetrathiafulvalene (TTF)-DNA Conjugates

11.1 Introduction

Tetrathiafulvalene (TTF, **11.3** in Scheme 11.2) is a nonaromatic 14π electron system in which oxidation to the cation radical and dication occurs sequentially and reversibly at low potentials ($E^1_{1/2}$ = 0.37 V and $E^2_{1/2}$ = 0.67 V in DCM vs. SCE).[1] TTF thus acts as a very strong electron donor because oxidation to the cation (13π electrons) and dication (12π electrons) is favored due to the resulting aromaticity. The first studies on TTF were concentrated on the crystallization of donor-acceptor charge-transfer (CT) crystals. High electric conductivity of 10 500 S cm^{-1} (Cu: 650 000 S cm^{-1}) was observed for co-crystals with the strong π electron acceptor tetracyanoquinodimethane (TCNQ).[2] These crystals show metallic behavior and are therefore sometimes called organic metals.[3] It was found that two different morphologies are formed preferentially: as segregated stacks of donor and acceptor molecules or as alternate stacks with mixed donor/acceptor arrays. Segregated stacks of donors and acceptors display an electric conductivity several orders of magnitude higher than the corresponding alternate stacks.[4]

TTF has found numerous applications in macromolecular systems,[5] supramolecular chemistry,[6] inorganic/organic hybrid materials[7] and nonlinear optical (NLO) materials.[8] This multitude of potential applications prompted us to undertake a program to covalently immobilize TTF on a DNA scaffold. The electron acceptors (I_2, TCNQ, tetracyanoethylene TCNE) could either be added as non-covalent modifications or site-selectively immobilized onto DNA using sequential click chemistry approaches (Sections 8 and 9). Using a sequential click chemistry approach, one could even mimic the segregated and alternate stacking arrangements found in crystals, in order to further elucidate the different charge-transfer mechanisms. Electrically conductive nanomaterials are the ultimate goal of this project. The DNA sequence would still be addressable in these constructs, in contrast to metallized DNA.[9] The resulting TTF-DNA hybrid materials could also outperform metallized DNA in terms of uniformity and thinness.

In private communications with several other groups it was found out that their respective attempts to attach TTF onto DNA failed. This was presumably because presynthetic strategies have been followed, for which TTF is too sensitive and reactive to withstand the harsh conditions of DNA synthesis and deprotection. Our experiences with the postsynthetic DNA functionalization using click chemistry, with which we have succeeded in the attachment of many structurally different labels (Section 8), suggested that TTF immobilization might indeed be possible.

11.2 Results and Discussion

The first question to be solved was if a TTF azide would be stable. Azide groups can be reduced efficiently by e. g. P(III) in a Staudinger reduction and could, in principle, also be reduced by the strong electron donor TTF. An extensive literature screening furnished only two examples of a molecule containing both an azide group and a TTF moiety.[10] It was therefore necessary to synthesize a TTF azide test molecule to clarify this stability issue. **11.3** could be readily synthesized starting from TTF (**11.1**) via 4-carboxytetrathiafulvalene (**11.2**), followed

by an amide coupling with 4-azidoaniline in just two steps overall. **11.3** showed no signs of instability of the azide group and was used in a click reaction with test substrates (data not shown). Click reaction efficiency and solubility of **11.3** were not satisfactory. Certain aromatic azides exhibit a decreased click reaction efficiency, the phenyl ring furthermore hampers the solubility of **11.3**.

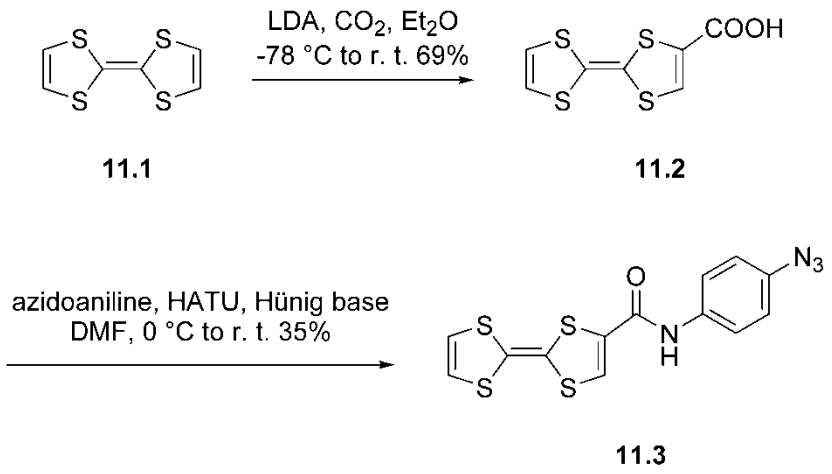

Scheme 11.1 Synthesis of TTF azide **11.3**.

In order to address these problems, TTF azide **11.6** was synthesized, which is devoid of the phenyl ring of **11.3**. The synthesis started with TTF **11.1**, which is deprotonated with LDA and formylated with *N*-methyl-*N*-phenylformamide to give **11.4**. Reduction of the aldehyde to an alcohol using $NaBH_4$, followed by azidonation with DPPA, gave the desired TTF azide **11.6** in a facile three-step synthesis.

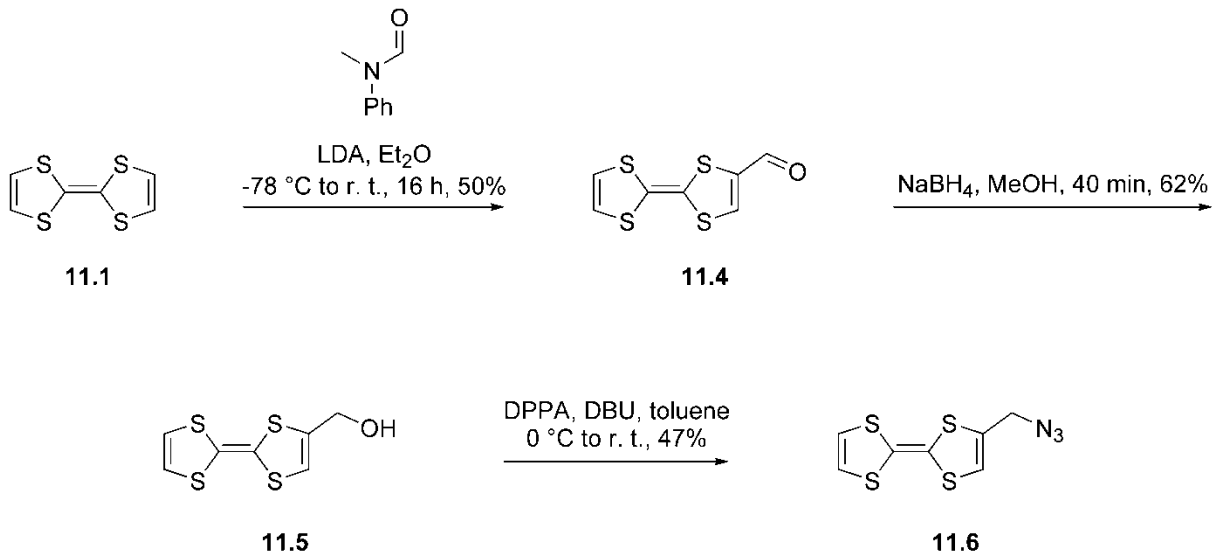

Scheme 11.2 Synthesis of TTF azide **11.6**.

In order to immobilize several TTF moieties on a simple DNA scaffold, three different oligodeoxynucleotides (ODN-**11.1** - ODN-**11.3**, Table 11.1), bearing four to six alkyne uridines **11.7** (Scheme 11.3) in variable arrangements, were synthesized as described in Section 2. The solubility and also the click reaction efficiency of **11.6** were shown to be strongly enhanced in comparison to **11.3**. The click reaction was tested on ODN-**11.1**, which bears six consecutive alkyne groups, showing that even sterically hindered substrates can be functionalized with TTF. To the best of our knowledge this constitutes the world record for the bioconjugation of TTF, outperforming the immobilization of four TTF molecules on a peptidic scaffold.[11] This proves that high-density labeling of DNA with TTF can be achieved. The work is currently being continued by Dr. Aline Gegout.

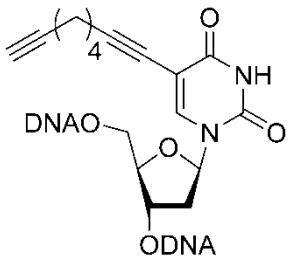

11.7

Scheme 11.3 Alkyne uridine used for the DNA strands in Table 11.1.

Table 11.1 DNA sequences. X = **11.7**.

ODN-**11.1**	5′-GCGCXXXXXXGTCGCG-3′
ODN-**11.2**	5′-GCGCXGXCXAXTCGCG-3′
ODN-**11.3**	5′-GCGXCGXGAXGTXGCG-3′

11.3 Summary and Outlook

Two different TTF azides **11.3** and **11.6** were prepared using robust syntheses. The azide group is not degraded by the presence of the TTF moiety within the same molecule. A successful click reaction on ODN-**11.1** has been performed in collaboration with Dr. Aline Gegout, showing that six consecutive alkyne groups can be labeled with TTF azide **11.6**. To the best of our knowledge, this constitutes the first example of a DNA-TTF conjugate and also the world record for TTF bioconjugation. Several applications can be envisioned with TTF-DNA hybrid materials. The most challenging and obvious one is the construction of electrically conductive nanowires, in which the DNA sequence can still be addressed. Using ethynyl-2′-deoxyuridine **11.9** in a click reaction with the aromatic TTF azide **11.3**, a DNA-based material (**11.10**) with nonlinear optical (NLO) properties could result. **11.10** constitutes a Donor-π-Acceptor push-pull system with uridine, the most electron-poor nucleobase, as acceptor. Such Donor-π-Acceptor push-pull systems are known to exhibit NLO properties.[12] Another application would be to use the distinct spectral changes, which occur in TTF-based

materials upon oxidation, as a detector system for electron transfer studies on DNA. Dr. Aline Gegout is currently continuing the work presented here.

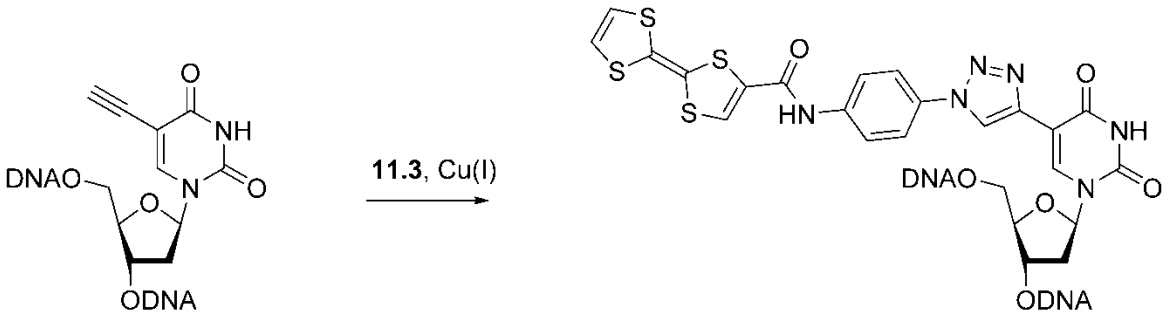

Scheme 11.4 A potential DNA-based NLO material **11.10**.

11.4 Experimental Section

ODN-**11.1** - ODN-**11.3** were synthesized as described in Section 2.

Click reactions were performed as described in Section 8.

For the assignment of the spectra the following numbering was used:

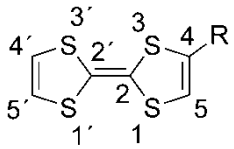

11.4.1 Synthesis

4-Carboxytetrathiafulvalene (**11.2**)[13]

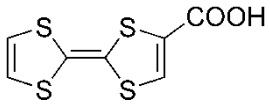

Into a stirred solution of tetrathiafulvalene **11.1** (888 mg, 4.35 mmol) in dry Et_2O (53 mL) at -78 °C, a solution of LDA (2.0 M, 2.44 mL, 4.88 mmol) was added over a period of 5 min. At this time, a thick, yellow precipitate of monolithio-TTF began to form and stirring was continued for further 90 min at -78 °C. Dry CO_2 gas was bubbled through the stirred suspension for 1 h at -78 °C to form a slurry of the lithium salt of the TTF-carboxylate. The mixture was

then slowly allowed to warm to r. t. over 16 h. The mixture was filtered and the solid washed with Et_2O to remove unreacted TTF to give **11.2** (750 mg, 3.02 mmol, 69%) as a red powder. R_f ($CHCl_3$/MeOH 2:1): 0.55. ^{1}H-NMR (200 MHz, d_6-DMSO): δ = 6.65 (s, 2H, $C_{4'}H$, $C_{5'}H$), 6.99 (s, 1H, C_5H). HRMS (ESI): calcd. for $C_7H_3O_2S_4^-$ [M - H]$^-$: 246.9032, found: 246.9020.

4-[Carboxylic acid (4-azidophenyl)-amide]-tetrathiafulvalene (**11.3**)[14]

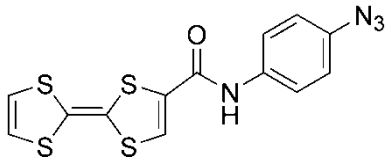

11.2 (100 mg, 0.40 mmol), 4-azidoaniline (69 mg, 0.51 mmol), HATU (184 mg, 0.48 mmol), DIPEA (0.17 mL, 0.97 mmol) and dry DMF (3 mL) were stirred at 0 °C for 10 min and another 90 min at r. t. The solvent was evaporated, the residue taken up in DCM and washed with HCl (1 M), water and brine. The organic phase was dried over Na_2SO_4 and adsorbed onto silica gel. Purification by column chromatography (DCM/*i*Hex 1:1) yielded **11.3** as a red solid (51 mg, 0.14 mmol, 35%).
R_f ($CHCl_3$/MeOH 50:1): 0.64. ^{1}H-NMR (200 MHz, d_6-acetone): δ = 6.66 (s, 2H, $C_{4'}H$, $C_{5'}H$), 7.03-7.12 (m, 2H, CH_{Ar}), 7.57 (s, 1H, C_5H), 7.68-7.78 (m, 2H, CH_{Ar}), 9.54 (sbr, 1H, NH). HRMS (ESI): calcd. for $C_{13}H_7N_4OS_4^-$ [M - H]$^-$: 362.9508, found: 362.9512.

4-Formyltetrathiafulvalene (**11.4**)[13]

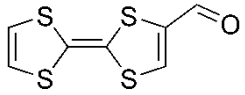

Into a stirred solution of tetrathiafulvalene **11.1** (100 mg, 0.49 mmol) in dry Et_2O (6 mL) at -78 °C, a solution of freshly prepared LDA (0.84 M, 0.64 mL, 0.54 mmol) was added over a period of 5 min. At this time, a thick, yellow precipitate of monolithio-TTF began to form and stirring was continued for further 75 min at -78 °C. A solution of *N*-methyl-*N*-phenylformamide (120 µL, 0.98 mmol, in 1 mL dry Et_2O) was added and stirring continued at -78 °C for 2 h and slowly warmed to r. t. over 14 h. Water (3 mL) was added and the mixture acidified with 2 N HCl (1 mL), turning the mixture deep red. The organic layer was separated and the aqueous layer extracted with DCM. The combined organic layers were washed with water twice, dried over $MgSO_4$ and directly adsorbed onto silica gel. Column chromatography (toluene/*i*Hex 1:1) gave **11.4** as a deep red powder (57 mg, 0.25 mmol, 50%).
R_f ($CHCl_3$/MeOH 50:1): 0.81. ^{1}H-NMR (200 MHz, $CDCl_3$): δ = 6.32 (d, 1H, J = 6.4 Hz), 6.36 (d, 1H, J = 6.6 Hz), 7.43 (s, 1H, C_5H), 9.47 (s, 1H, CHO). HRMS (EI): calcd. for $C_7H_4OS_4^+$ [M$^+$]: 231.9139, found: 231.9141.

4-(Hydroxymethyl)tetrathiafulvalene (**11.5**)[13]

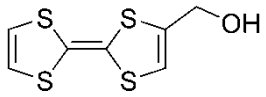

To a stirred solution of **11.4** (373 mg, 1.59 mmol) in dry MeOH (20 mL) was added $NaBH_4$ (65 mg, 1.72 mmol). The mixture was stirred at r. t. for 40 min, at which time it turned yellow. DCM (100 mL) was added and the organic phases were washed with brine (50 mL). The combined organic phases were dried over $MgSO_4$ and directly adsorbed onto silica gel. Column chromatography (DCM) gave **11.5** as a yellow solid (235 mg, 1.00 mmol, 62%).
R_f (*i*Hex/EtOAc 1:1): 0.59. ^{1}H-NMR (200 MHz, $CDCl_3$): δ = 1.90 (sbr, 1H, OH), 4.40 (s, 2H, CH_2), 6.22 (s, 1H, C_5H), 6.31 (s, 2H). HRMS (EI): calcd. for $C_7H_6OS_4^+$ [M^+]: 233.9296, found: 233.9303.

4-(Azidomethyl)tetrathiafulvalene (**11.6**)[15]

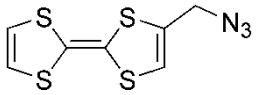

A mixture of **11.5** (109 mg, 0.465 mmol) and diphenyl phosphorazidate (DPPA, 121 µL, 0.558 mmol) was dissolved in dry toluene (6 mL). The mixture was cooled to 0 °C and neat DBU (83 µL, 0.558 mmol) was added. The mixture was stirred at 0 °C for 2 h and then at r. t. for 16 h. DPPA (60 µL, 0.277 mmol) and DBU (40 µL, 0.269 mmol) were added and the resulting mixture stirred for another 5 h. EtOAc (50 mL) was added and the organic phases washed with brine (50 mL) and 2 N HCl (50 mL). The combined aqueous phases were extracted with DCM. The combined organic phases were dried over $MgSO_4$ and directly adsorbed onto silica gel. Column chromatography (*i*Hex/EtOAc 10:1) gave **11.6** as a red-brown solid (57 mg, 0.22 mmol, 47%).
R_f ($CHCl_3$/MeOH 50:1): 0.88. ^{1}H-NMR (600 MHz, $CDCl_3$): δ = 4.07 (s, 2H, CH_2), 6.26 (s, 1H, C_5H), 6.31 (s, 2H). HRMS (EI): calcd. for $C_7H_5N_3S_4^+$ [M^+]: 258.9361, found: 258.9360.

11.4.2 MALDI-TOF Analysis of **11.6** Conjugated to ODN-**11.1**

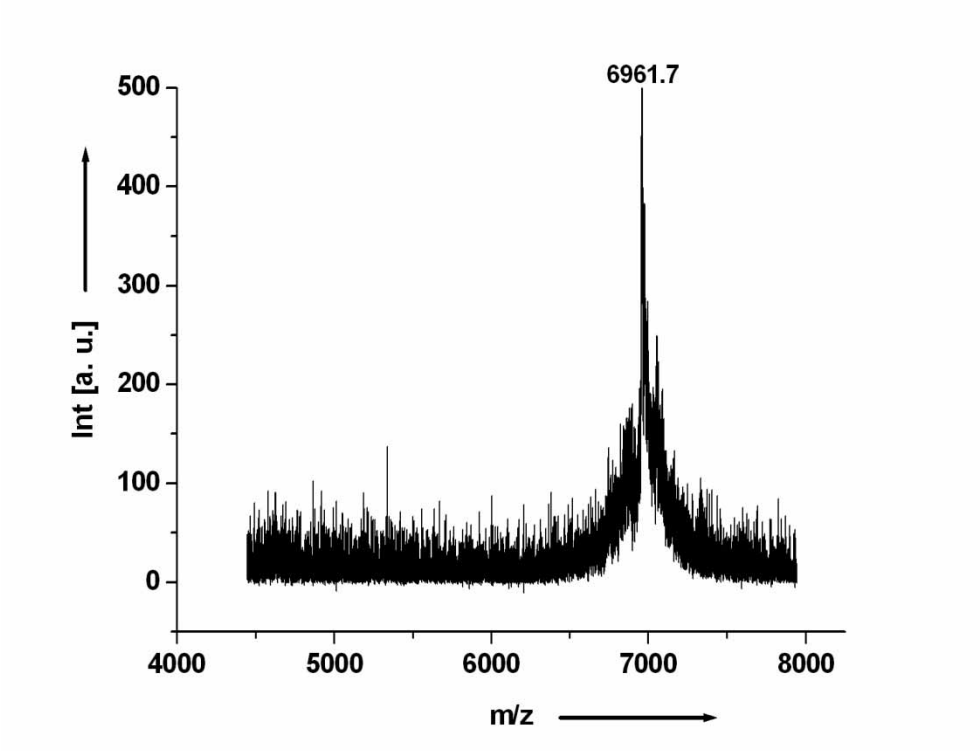

Figure 11.1 MALDI-TOF of **11.6** conjugated to ODN-**11.1**. Mass calcd.: 6967.2..

11.5 References

[1] J. L. Segura, N. Martin, *Angew. Chem. Int. Ed.* **2001**, *40*, 1372-1409.

[2] A. Aumüller, P. Erk, S. Hünig, H. Meixner, J.-U. v. Schütz, H.-P. Werner, *Liebigs Ann. Chem.* **1987**, *11*, 997-1006.

[3] J. H. Perlstein, J. P. Ferraris, V. V. Walatka, D. O. Cowan, G. A. Candela, *AIP Conference Proceedings* **1973**, *10*, 1494-1498.

[4] J.-S. Lee, K.-C. Huang, W.-J. Wang, J.-L. Wang, *Synth. Met.* **1995**, *70*, 1227-1228.

[5] M. R. Bryce, W. Devonport, L. M. Goldenberg, C. Wang, *Chem. Commun.* **1998**, 945 - 952.

[6] T. Jørgensen, T. K. Hansen, J. Becher, *Chem. Soc. Rev.* **1994**, *23*, 41-51; M. B. Nielsen, C. Lomholt, J. Becher, *Chem. Soc. Rev.* **2000**, *29*, 153-164.

[7] E. Coronado, C. J. Gómez-García, *Chem. Rev.* **1998**, *98*, 273 - 296.

[8] M. González, J. L. Segura, C. Seoane, N. Martín, J. Garín, J. Orduna, R. Alcalá, B. Villacampa, V. Hernández, J. T. L. Navarrete, *J. Org. Chem.* **2001**, *66*, 8872-8882; J. Garin, J. Orduna, R. Andreu, *Recent Res. Devel. Org. Chem.* **2001**, *5*, 77-87.

[9] G. A. Burley, J. Gierlich, M. R. Mofid, S. T. H. Nir, Y. Eichen, T. Carell, *J. Am. Chem. Soc.* **2006**, *128*, 1398-1399; E. Braun, Y. Eichen, U. Silvan, G. Ben-Yoseph, *Nature* **1998**, *391*, 775-778.

[10] L. Binet, J.-M. Fabre, *Synthesis* **1997**, 1179-1184; G. Cooke, *Synth. Commun.* **1996**, *26*, 2917-2923.

[11] S. Booth, E. N. K. Wallace, K. Singhal, P. N. Bartlett, J. D. Kilburn, *J. Chem. Soc., Perkin Trans. 1* **1998**, 1467-1474.

[12] S. R. Marder, B. Kippelen, A. K.-Y. Jen, N. Peyghambarian, *Nature* **1997**, *388*, 845-851.
[13] J. Garin, J. Orduna, S. Uriel, A. J. Moore, M. R. Bryce, S. Wegener, D. S. Yufit, A. K. Howard, *Synthesis* **1994**, 489-493.
[14] B. Anichini, R. Ricci, G. Fabbri, G. Balacco, S. Mauro, A. Triolo, M. Altamura, C. A. Maggi, L. Quartara, *J. Pept. Sci.* **2000**, *6*.
[15] A. S. Thompson, G. R. Humphrey, A. M. DeMarco, D. J. Mathre, E. J. J. Grabowski, *J. Org. Chem.* **1993**, *58*, 5886-5888.

12 Conjugation of Fluorescent Dyes to DNA for the Construction of DNA Nanotags (Cooperation with Prof. Armitage)

12.1 Introduction

The following Section describes a cooperation project with Andrea Benvin from the group of Prof. Armitage (Carnegie Mellon University, Pittsburgh). Successful proof-of-concept experiments have been performed and the work is currently being continued by Christian Wirges. The project deals with the covalent immobilization of intercalating benzothiazole azide dyes onto alkyne functionalized DNA for applications like fluorescent biomolecular probes. The following work stems from the PhD thesis of Andrea Benvin[1] while the DNA synthesis and bioconjugation have been performed in our laboratories.

The asymmetric cyanine dyes like **TO-PRO-3** and **YO-PRO-1** (Figure 12.1, left) are an important class of probes for the detection and study of DNA and are attractive because of their favorable photophysical properties.[2] This class of dyes is readily synthesized from *N*-quaternized heterocycles linked by methine or polymethine bridges. The absorption and emission maximum of the asymmetric cyanine dyes is determined by the heterocycles and the length of the methine bridge. As a result, the absorptive and emissive wavelengths of these dyes span the optical spectrum.[3, 4] Classified as monointercalators, **YO-PRO-1** and **TO-PRO-1** exhibit high binding affinities for DNA (10^5-10^7 M^{-1} monointercalation[5]) and have large molar absorptivities > 50 000 cm^{-1} M^{-1} in DNA.[3, 6]) These dyes have little to no intrinsic fluorescence when free in solution but show large enhancements in fluorescence when bound to DNA.[7, 8] The fluorogenic nature of these dyes arises from the fact that in solution, excitation energy is readily lost through nonradiative pathways due to the rapid rotation around the bonds bridging the heterocycles.[7] When intercalated into DNA, this motion is restricted and radiative decay, such as fluorescence, becomes an efficient pathway to the ground state.[5, 7, 9]

Our understanding of complex biological events is dependent upon our ability to visualize and detect biomolecular interactions. Fluorescence imaging has become one of the most powerful tools to investigate and probe cellular processes.[11] The use of single molecule spectroscopy has revolutionized our understanding of how biomolecules work, elucidating a range of information about conformational changes to single enzyme reaction kinetics. As single molecule applications continue to gain in importance, there is an increasing need for the design of adequate fluorophores to provide better resolution in microscope images and for more sensitive detection systems.[12]

In a study by Armitage et al. it was demonstrated that DNA nanotechnology can be used to meet this challenge.[10] A DNA three-way junction (3WJ, Figure 12.1, right) was successfully used as a nano-host matrix for non-covalently organizing and concentrating multiple fluorescent intercalating dyes (Figure 12.1, left). The structural regularity of the DNA double helix allowed the group to achieve unprecedented densities of fluorescent dyes in a compact nanostructure. The dyes are also prevented from self-quenching one another, as they are each separated by at least two base pairs (7 Å) due to the fact that only every other intercalation site inside DNA can be used. The DNA-templated intercalator dye structures (i.e. nanotags) offer (1) ease of assembly, (2) flexibility in the choice of excitation and emission wavelengths, (3)

intense brightness and (4) functional nanomaterials that can be readily adapted to current fluorescent applications.[10] Although the ease of assembly for these supramolecular fluorophores is appealing, the development of covalently attached analogues is desired to prevent dissociation of these dyes from DNA and thereby allowing one to use lower concentrations of functionalized nanotags. This should pave the way to fully exploit the potential of these fluorescent labels for single-molecule and bioimaging applications.

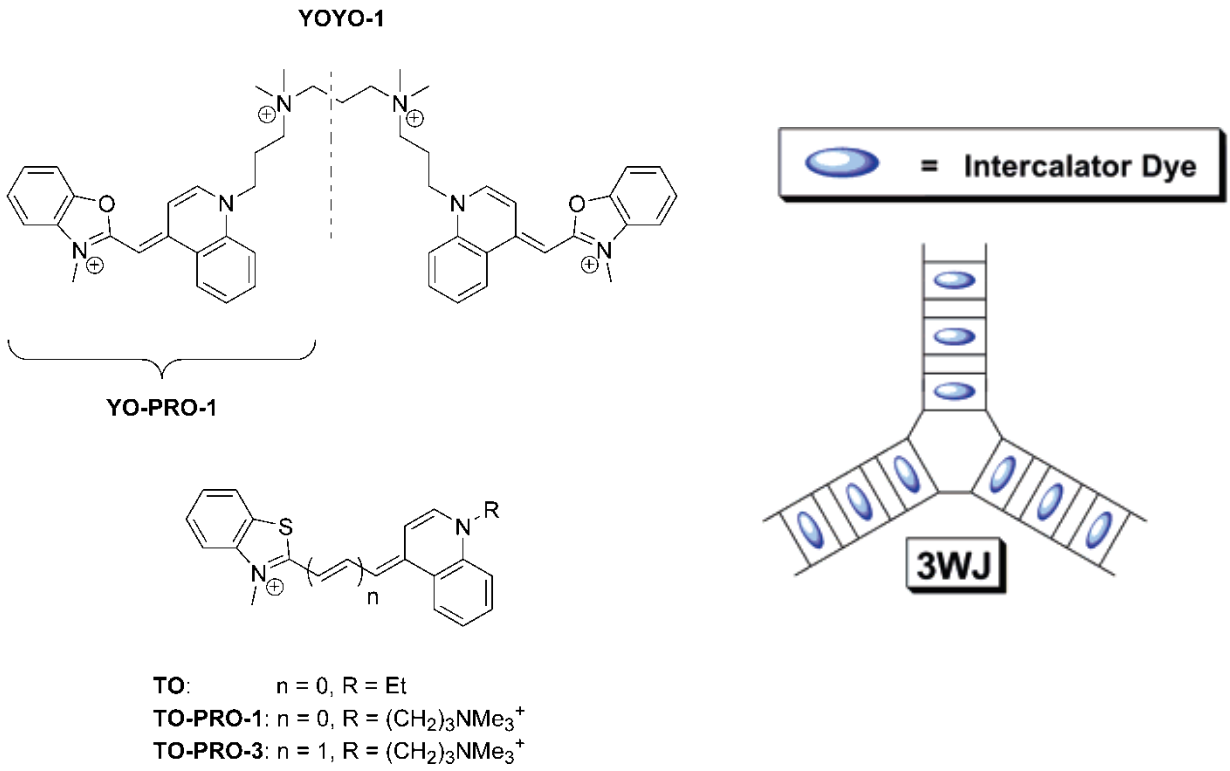

Figure 12.1 Structures of fluorescent dyes (left) and schematic representation of a 3WJ (right) used by Armitage et al.[10]

A primary advantage of using a DNA scaffold is the fact that it is easily functionalized with recognition elements and fluorophores. The click chemistry approach, outlined in Sections 1 to 9, seemed to meet the requirements for the multiple attachment of these fluorescent dyes onto DNA. It has been shown that a wide variety of different azides, including highly hydrophobic moieties like a pyrene azide (**8.9** in Section 8), can be used in this functionalization methodology.

12.2 Results and Discussion

12.2.1 Synthesis of DNA Conjugated to **Click** Dyes

In the set of preliminary experiments reported in this Section, four different benzothiazole azide dyes (**Click 1** - **Click 4**, Scheme 12.1), derived from **TO-PRO-3** (Figure 12.1), were prepared by Andrea Benvin. Two parameters were to be tested with this set of dyes: The linker length and the position of the linker, either on the benzothiazole or on the quinoline ring system. As these dyes only fluoresce when intercalated into DNA,[7, 8] the linker should be long enough to allow for the dye to fold back towards the DNA bases, thereby allowing for an intercalation into the nucleobase stack and preventing self-quenching outside the DNA helix.

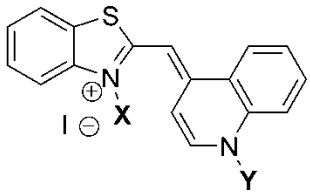

Click 1: X = CH_3
Y = $(CH_2)_2O(CH_2)_2N_3$
Click 2: X = CH_3
Y = $(CH_2CH_2O)_2(CH_2)_2N_3$
Click 3: X = $(CH_2)_2O(CH_2)_2N_3$
Y = CH_3
Click 4: X = $(CH_2CH_2O)_2(CH_2)_2N_3$
Y = CH_3

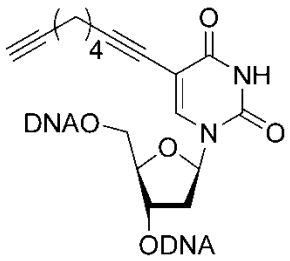

12.1

Scheme 12.1 Structures of the four different benzothiazole azide dyes **Click 1** - **Click 4** (left) and alkynyl deoxyuridine 12.**1** (right).

DNA modified with one alkyne modification (sequence: 5′-GCGCTGT**X**CATTCGCG-3′, X = **12.1**) was synthesized as a test substrate. To this strand, the dyes **Click 1**, **Click 2** and **Click 4** were conjugated in a click reaction using a standard protocol and purified by HPLC. These ODNs will be referred to as ODN-**1**, ODN-**2** and ODN-**4**, respectively. The conversions were found to be good to near-quantitative in all cases, despite the poor water solubility of the dyes.

12.2.2 Melting Temperature Analyses

UV/Vis thermal analysis was used to examine the effects of dye-functionalization on the stability of the duplex (Table 12.1). The unmodified duplex displays a cooperative melting transition at 49 °C. The presence of a single **Click** dye modification results in an increase in the melting temperature for all three functionalized duplexes. The increased stability arises from the increase in π-stacking interactions between the incteracalated dyes and the DNA bases. While ODN-**1** and ODN-**2** exhibit an increased melting temperature (51 °C), the slope of the melting transition is reduced compared to the unmodified duplex. This change in shape of the UV/Vis melting curve indicates that the cooperativity of melting for ODN-**1** and ODN-**2** du-

plexes is reduced, and thus the duplex structure is distorted upon intercalation of these covalently attached dyes.[13] This effect on duplex stability is not observed for the ODN-**4** duplex, where the azide is attached to the benzothiazole ring. The melting transition for this modified duplex increases to 56 °C, and the shape of the transition is similar to the unmodified duplex. When covalently linked to DNA, **Click-4** intercalates without disrupting the integrity of the duplex. The "half-intercalation" model, introduced by Yarmoluk et al., can be used to describe this binding mode.[4] This model predicts that the heterocyclic component, which carries less of the positive charge (quinoline) is intercalated into DNA and the heterocycle that bears more of the positive charge is positioned in the minor groove. The high melting point of ODN-**4** indicates that the geometry of the linker allows for an efficient intercalation of the quinoline into the DNA duplex.

Table 12.1 Melting temperature of ODN-**1**, ODN-**2** and ODN-**4**.

DNA	T_m [°C]*
unmodified control ODN	49
ODN-**1**	51
ODN-**2**	51
ODN-**4**	56

* in 10 mM sodium phosphate buffer, pH 7.0.

12.2.3 UV/Vis Spectroscopy

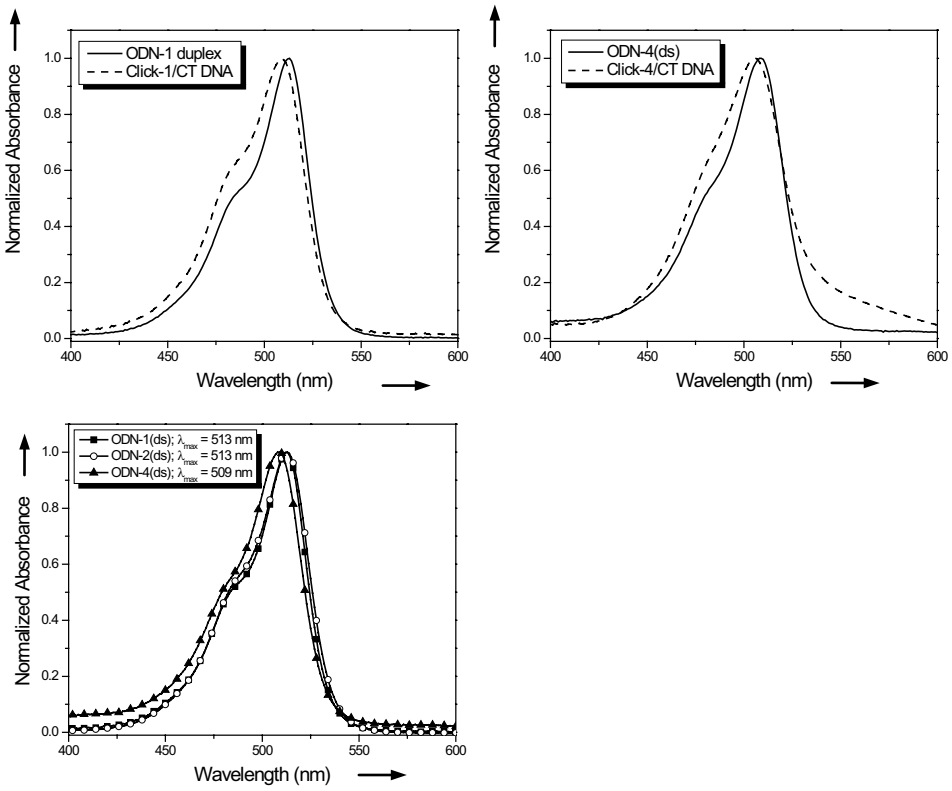

Figure 12.2 UV/Vis absorption spectra of **Click** dyes, which are covalently or non-covalently bound to DNA (in 10 mM sodium phosphate buffer, pH 7.0).

The absorption spectra for the **Click** dyes conjugated to dsDNA are shown in Figure 12.2. The shape of the absorbance spectrum for the ODN-**1** duplex is similar in shape to the spectrum shown for non-covalently linked **Click 1** bound to calf thymus (CT) DNA (**Click 1/CT**). When **Click 4** is conjugated to DNA and hybridized to its complementary strand, a shorter wavelength shoulder emerges compared to **Click 4/CT**. The absorption maxima for both ODN-**1** and ODN-**4** duplexes are shifted bathochromically compared to **Click 1/CT** and **Click 4/CT**. In addition, the spectra for ODN-**1** and ODN-**4** duplexes are narrower compared to free **Click**-dyes bound to CT DNA.

12.2.4 Fluorescence Spectroscopy

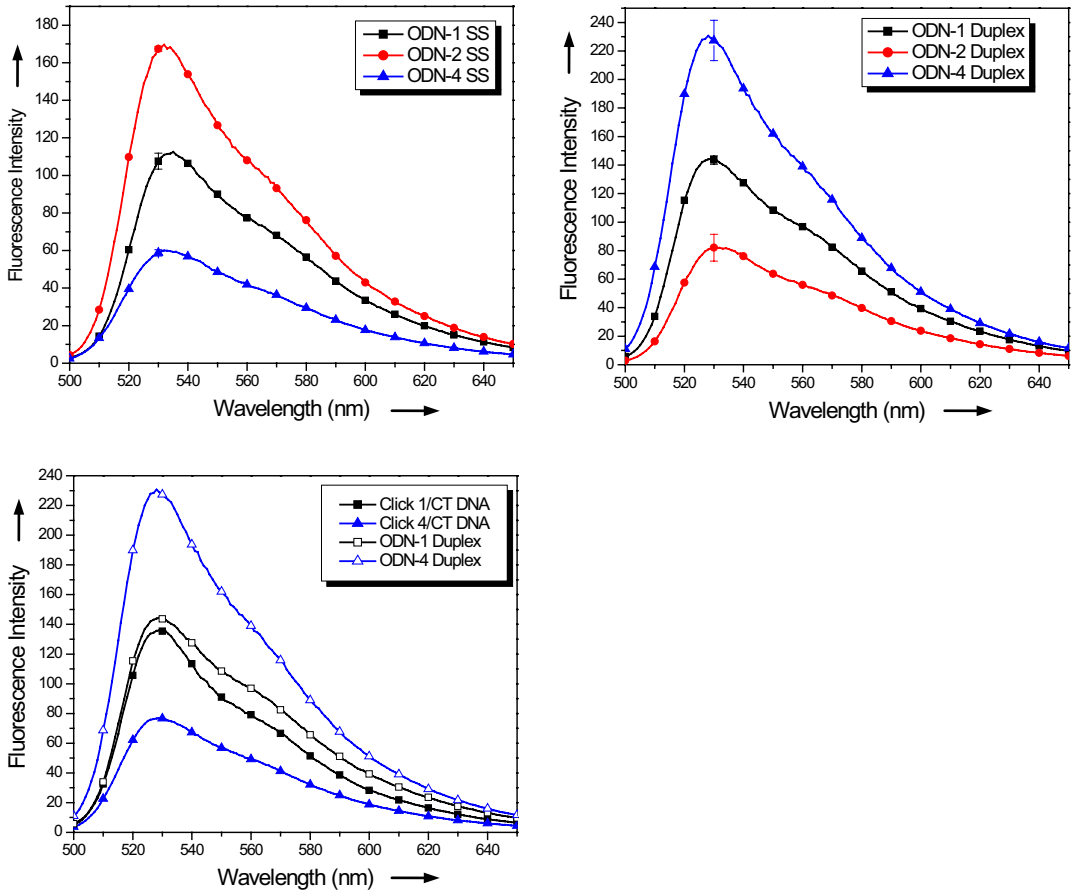

Figure 12.3 Fluorescence spectra for ODN-**1**, ODN-**2** and ODN-**4** as single strands (top left) and double strands (top right). Bottom: Fluorescence spectra of ODN-**1** and ODN-**4** compared to the non-covalent analogues **Click 1/CT** and **Click 4/CT**. Dye/DNA concentrations were 1.0 μM in 10 mM sodium phosphate buffer, pH 7.0, excitation: 450 nm.

It is important that once covalently attached, the dyes maintain their ability to intercalate and an enhancement in fluorescence in duplex DNA is observed. The fluorescence of dye-modified single strands and dye-modified duplexes (Figure 12.3) was examined. All three dyes show an enhancement in the fluorescence yield when the dyes are conjugated to single-

stranded DNA. The wavelength of maximum emission is similar to that observed for the free **Click** dyes in the presence of DNA. When single-stranded, the fluorescence intensity is greatest for ODN-**2**, followed by ODN-**1**, and finally ODN-**4**. Upon hybridization to the complementary strand, a dramatic change in the fluorescence enhancement is observed. ODN-**4** duplexes are the brightest, showing almost a four-fold increase in the amplitude of the fluorescence signal. A small enhancement in the fluorescence of ODN-**1** duplexes is observed compared to ODN-**1** single-strands. On the other hand, an almost 2-fold decrease is observed in the fluorescence signal for ODN-**2**-duplexes compared to ODN-**2** single-strands. The position of the linker affects the fluorescence of the dyes when they are covalently conjugated to DNA. The least distorting intercalation is indicated by the strongest fluorescence, which in this case hints at **Click 4** having the optimal linker geometry.

12.2.5 Energy Transfer

The next step was to determine if the covalently linked intercalating dyes were capable of efficiently transferring energy through the DNA duplex to a terminal acceptor dye. The energy transfer from either ODN-**4** or the non-covalently linked intercalator thiazole orange (**TO**, Figure 12.1) as donors to a 5'-linked Texas Red (**TR)** acceptor on the counter strand was compared. Donor emission was quenched by 77% in ODN-**4** duplexes whereas only by 62% in the case **TO** donors. Förster resonance energy transfer (FRET) experiments were performed using concentrations that were below the dissociation constant for **TO** ($K_d \sim 10^6$ M^{-1}).[5] The covalently attached donor in ODN-**4** allows to use low concentrations of DNA and still observe efficient FRET.

Table 12.2 Thermodynamic parameters extracted from fluorescence and UV/Vis thermal melting experiments.[14]

	ΔG [kcal/mol]	ΔH [kcal/mol]	T × ΔS [kcal/mol]	ΔS [kcal/mol × K]
fluorescence	-16.8	-70.2	-53.4	-0.18
UV/Vis	-15.8	-66.0	-50.2	-0.17

FRET is a sensitive technique that can be used to monitor the hybridization of a nucleic acid probe to its target molecule. Hybridization probes serve as fundamental tools in molecular genetics and are used in nucleic acid amplification assays, gene detection[15] and as antisense agents.[16] Thermodynamic data, extracted from thermal denaturation of hybridization probes and their targets are useful in optimizing probe design for these applications. Absorption techniques, such as UV/Vis melting analysis (Section 12.2.2), can be used. However, rather large amounts of sample are required. Here the energy transfer between **Click 4** and **TR** was used to monitor DNA hybridization by fluorescence melting. When hybridized, **TR** fluorescence is maximized because of energy transfer from the covalently linked intercalator **Click 4**. As the duplex melts, the bases unzip and a decrease in **TR** fluorescence is observed. First derivative analysis of the melting curve shows that the melting temperature of the duplex is similar to that obtained from UV/Vis melting experiments (Figure 12.4). In addition, extraction of the thermodynamic parameters from both fluorescence and UV/Vis melting curves are

in experimental agreement (Table 12.2). Using one-tenth the concentration of DNA compared to UV/Vis absorption methods, it was possible to achieve sensitive detection of DNA hybridization using FRET.

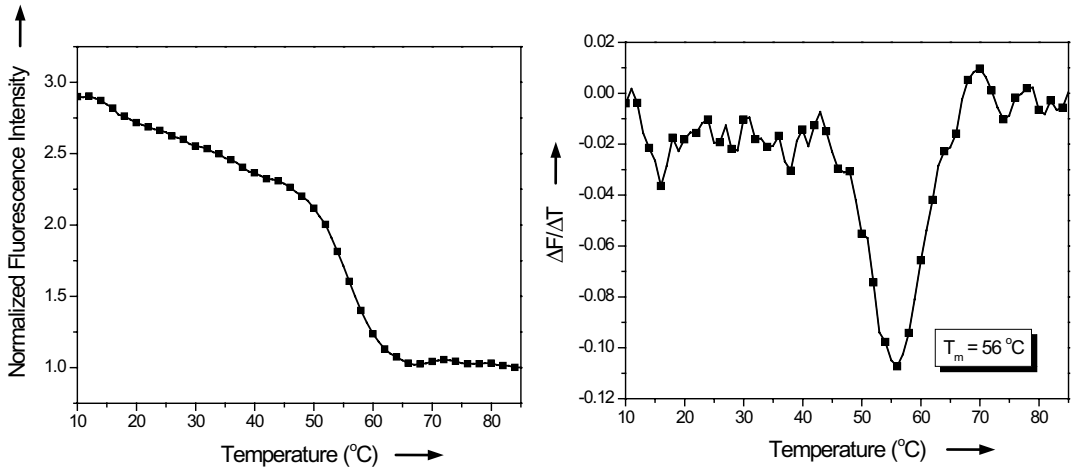

Figure 12.4 Fluorescence melting curve for ODN-**4** duplex with a **TR** acceptor fluorophore (left) and the first derivative thereof (right). Measurements were performed in 10 mM sodium phosphate buffer, pH 7.0, excitation: 450 nm.

12.2.6 Nuclease Stability

In order to determine the range of conditions, in which covalently labeled **Click**-DNA structures could be used as fluorescent labels, their biochemical stability was investigated. Previous studies have shown that bisintercalating dyes improve the stability of a DNA duplex against endonuclease degradation presumably because of lengthening and unwinding of the duplex.[17] The nuclease stability of labeled duplexes was investigated by monitoring the decrease in energy transfer from **Click 4** to Cy5 upon treatment with DNAse I. In the absence of the Cy5 acceptor, the fluorescence of **Click 4** decreases significantly after being treated with DNAse I, which is indicative of the DNA being digested (Figure 12.5A). A decrease in the fluorescence intensity of the Cy5 is also observed upon nuclease treatment (Figure 12.5B). Prior to enzymatic cleavage of duplexes labeled with both donor and acceptor fluorophores, the Cy5 acceptor quenches **Click 4** donor emission by 74% (Figure 12.5C and D).
A comparison of the fluorescence spectra for ODN-**4**/Cy5 and **TO-PRO-1**/Cy5 labeled duplexes treated with DNAse I is shown in Figure 12.6. After 30 minutes, the donor emission for **Click 4**/Cy5 labeled duplexes is quenched by 53%, whereas quenching of **TO-PRO-1** fluorescence is no longer observed. These results suggest that **Click 4** may improve nuclease stability compared to unlabeled duplexes. An unexpected enhancement in the acceptor fluorescence is observed for **TO-PRO-1**/Cy5 duplexes. **TO-PRO-1** is not covalently bound to DNA, and rapidly dissociates and binds the duplex. As the duplex is digested, **TO-PRO-1** can bind to base pairs that may be attached close to Cy5 thereby enhancing its fluorescence compared to **Click 4.**

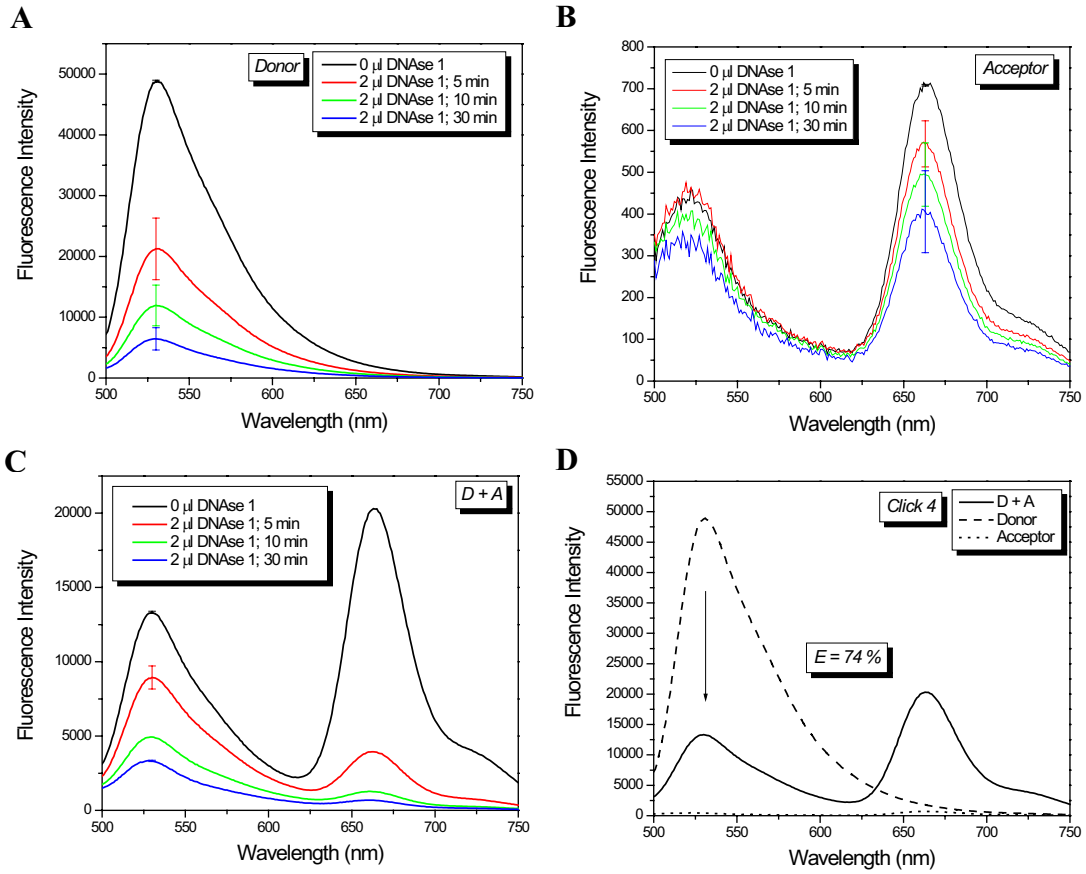

Figure 12.5 (A) Fluorescence emission of ODN-**4**, (B) Cy5 (acceptor) labeled duplex, (C) ODN-**4**/Cy5 labeled duplex upon treatment with DNAse I, (D) Energy transfer between ODN-**4**/Cy5 prior to enzymatic cleavage with DNAse I. Excitation: 450 nm.

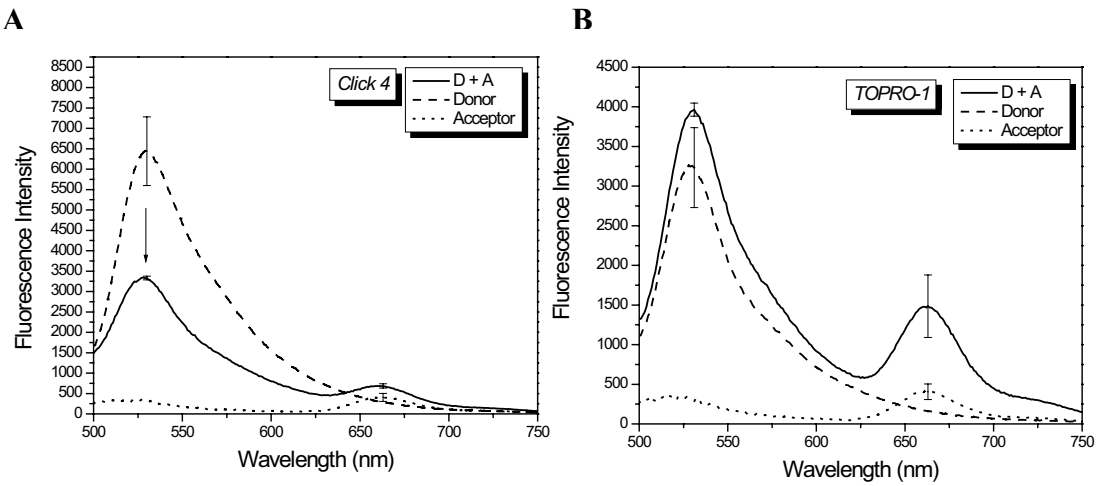

Figure 12.6 Fluorescence emission spectrum for ODN-**4** (A) and **TO-PRO-1** labeled duplexes after 30 minutes of treatment with DNAse I. [**Click 4**/DNA] = 0.1 µM, [DNA] = 0.1 µM, [**TO-PRO-1**] = 0.1 µM. The emission of the **Click 4** donor is quenched by 53%. Excitation: 450 nm.

12.2.7 Dye-DNA Duplexes as Nanotags

Fluorescent polymer and silica nanoparticles have been developed for multicolor assays and imaging. By varying the ratio of dyes encapsulated in silica nanoparticles, Wang et al. used FRET to tune the emission properties of the nanospheres so that multiple colors could be emitted using a single excitation source.[18] In the present study using the singly-modified duplexes, three distinctly colored bead populations were imaged by employing a single excitation source (Figure 12.7). Streptavidin-functionalized polystyrene beads were coated with ODN-**4** duplexes via a 5'-biotin on the complementary strand. The duplex nanotags were also modified with either a 3'-Cy3 or a 3′-Cy5 acceptor. Green (ODN-**4** labeled duplex), orange (ODN-**4**/Cy3 labeled duplex) and red (ODN-**4**/Cy5 duplex) beads were readily visualized with confocal microscopy by excitation with a single blue laser.

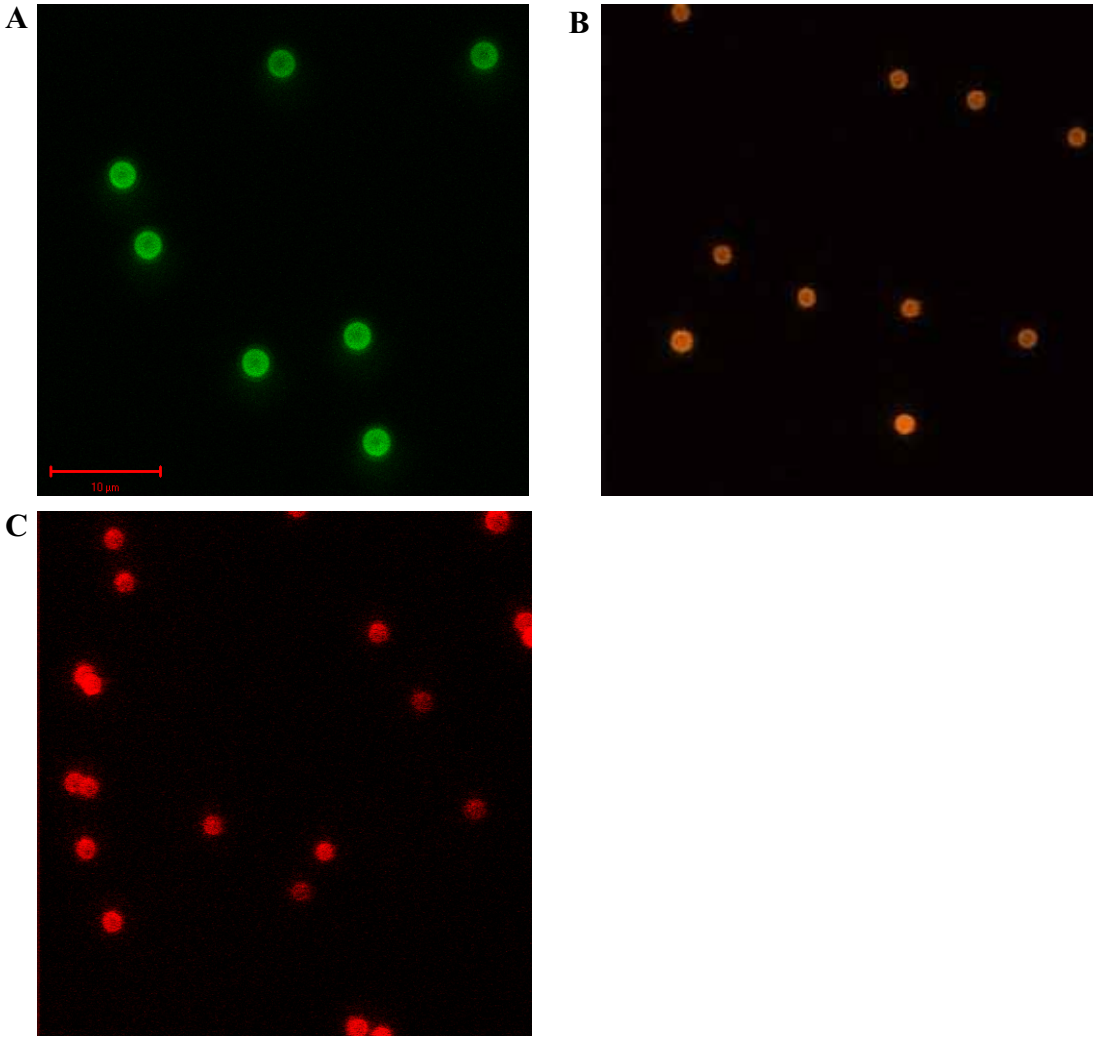

Figure 12.7 Confocal microscopy image of 2.0 µm streptavidin polystyrene beads labeled with (A) ODN-**4** duplex (green), (B) ODN-**4**/Cy3 nanotags (orange), and (C) ODN-**4**/Cy5 nanotags (red) in 10 mM sodium phosphate buffer, pH 7.

12.3 Summary and Outlook

Efficient nanotags, employing non-covalently intercalated DNA, were introduced by Armitage et al.[10] In order to prevent dissociation of dyes from the DNA nanotag, a covalent attachment was performed using click chemistry. Four benzothiazole azide dyes were prepared by Andrea Benvin from the group of Prof. Armitage. Synthesis of test strands bearing one alkyne and subsequent functionalization with three of these dye azides was accomplished in the group of Prof. Carell. **Click 4** was found to have the optimal linker geometry for efficient intercalation into DNA duplexes. The long linker allows for an efficient back-folding of the dye into the DNA helix. Attachment of the linker to the benzothiazole heterocycle was found to be optimal for the intercalation of the quinoline ring. The resulting covalently modified DNA nanotags were investigated by Andrea Benvin using various methods. Promising properties like enhanced fluorescence and an efficient FRET to an energy acceptor on a hybridized counter strand encouraged us to start synthesizing fully covalently decorated three-way junctions (3WJ), as described by Armitage et al. for the analogous, non-covalent nanotags.[10]
Three possible architectures have been elaborated in order to decorate the 3WJ with 15 **Click 4** dyes (Figure 12.8). Options A and B both require each of the three strands **S1**-**S3** to bear five click sites, while in Option C only two of the strands (**S1** and **S2**) are modified (seven and eight click sites, respectively), while the third strand (**S3**) remains unfunctionalized. This latter Option C would be desirable in order to attach a biotin label or a fluorescent energy acceptor dye for FRET experiments onto **S3**. Christian Wirges from the group of Prof. Carell is currently continuing the project by the synthesis of a fully modified 3WJ, which will be used by Andrea Benvin for further characterization.

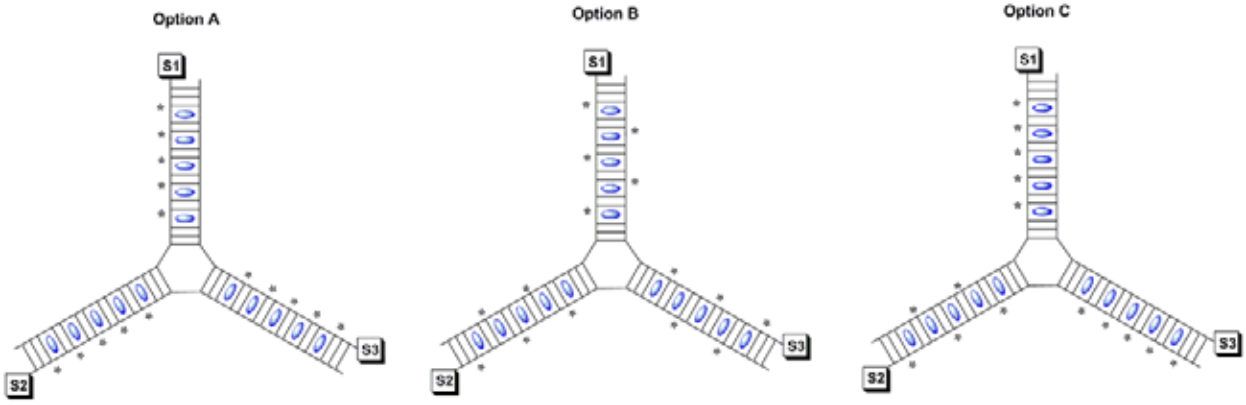

Figure 12.8 Three possible 3WJ structures each bearing a total of 15 **Click 4** dyes. Asterisks indicate click sites.

12.4 Experimental Section

For the preparation of the **Click** dyes and the exact parameters of the analytical methods, see lit.[1] Synthesis of **12.1** and DNA synthesis are described in Section 2.

General Procedure for the Click Reaction

Lyophilized alkyne DNA (0.70 μmol) and dye azide (0.2 M in DMSO, 50 μL) were placed in a 1.5 mL vial. In a separate vial, 40 μL CuBr solution (100 mM in DMSO/*t*BuOH 3:1) and 80 μL TBTA ligand[19] solution (100 mM in DMSO/*t*BuOH 3:1) were vortexed and immediately added to the DNA. The solution was shaken at 25 °C for 3 h and evaporated to near-dryness in a SpeedVac. NaOAc solution (0.3 M, 100 μL) and 1 mL EtOH were added, the vial vortexed and placed in a freezer (-20 °C) over night. After centrifugation (15 min at 13 000 rpm) the supernatant was carefully removed from the DNA pellet. 70% EtOH (-20 °C) was added, the vial vortexed, centrifuged and the supernatant removed. This washing step was repeated twice. After the last washing step the pellet was left drying on air and taken up in water or buffer, as preferred.

12.5. Author's Contribution

The DNA was synthesized and functionalized by the author with the dyes described herein. Characterization of the resulting constructs was performed by Andrea Benvin.

12.6 References

[1] A. L. Benvin, PhD thesis, Carnegie Mellon University (Pittsburgh), **2008**.

[2] B. A. Armitage, in *DNA Binders and Related Subjects, Vol. 253* (Eds.: M. J. C. Waring, B. Jonathan), Springer, Netherlands, **2005**.

[3] H. S. Rye, S. Yue, D. E. Wemmer, M. A. Quesada, R. P. Haugland, R. A. Mathies, A. N. Glazer, *Nucl. Acids Res.* **1992**, *20*, 2803-2812.

[4] S. M. Yarmoluk, S. S. Lukashov, T. Y. Ogul'Chansky, M. Y. Losytskyy, O. S. Kornyushyna, *Biopolymers* **2001**, *62*, 219-227.

[5] J. T. Petty, J. A. Bordelon, M. E. Robertson, *J. Phys. Chem. B* **2000**, *104*, 7221 - 7227.

[6] R. P. Haugland, in *Handbook of Fluorescent Probes and Research Products, Vol. 9th Edition* (Ed.: M. Probes), **2002**.

[7] T. L. Netzel, K. Nafisi, M. Zhao, J. R. Lenhard, I. Johnson, *J. Phys. Chem.* **1995**, *99*, 17936 - 17947.

[8] A. Larsson, C. Carlsson, M. Jonsson, B. Albinsson, *J. Am. Chem. Soc.* **1994**, *116*, 8459 - 8465.

[9] J. A. Bradford, G. Buller, M. Suter, M. Ignatius, J. M. Beechem, *Cytometry* **2004**, *61A*, 142-152.

[10] A. L. Benvin, Y. Creeger, G. W. Fisher, B. Ballou, A. S. Waggoner, B. A. Armitage, *J. Am. Chem. Soc.* **2007**, *129*, 2025-2034.

[11] R. M. Hoffman, *Nat. Rev. Cancer* **2005**, *5*, 796-806; B. N. G. Giepmans, S. R. Adams, M. H. Ellisman, R. Y. Tsien, *Science* **2006**, *312*, 217-224.

[12] A. Waggoner, *Curr. Opin. Chem. Biol.* **2006**, *10*, 62-66.

[13] G. M. G. Blackburn, J. Michael, in *Nucleic Acids in Chemistry and Biology*, 2nd ed., Oxford University Press, New York, **1996**.

[14] L. A. Marky, K. J. Breslauer, *Biopolymers* **1987**, *26*, 1601-1620.

[15] D. M. Hammond, A. Manetto, J. Gierlich, V. A. Azov, P. M. E. Gramlich, G. A. Burley, M. Maul, T. Carell, *Angew. Chem. Int. Ed.* **2007**, *46*, 4184-4187.

[16] V. V. Didenko, *BioTechniques* **2001**, *31*, 1106-1121.

[17] X. Meng, W. Cai, D. C. Schwartz, *J. Biomol. Struct. Dynam.* **1996**, *13*, 945-951.

[18] L. Wang, W. Tan, *Nano Lett.* **2006**, *6*, 84-88.
[19] T. R. Chan, R. Hilgraf, K. B. Sharpless, V. V. Fokin, *Org. Lett.* **2004**, *6*, 2853-2855.

13 Synthesis and Structural Studies on DNA Containing a Tryptophan-Mimetic Nucleoside (Cooperation with Prof. Riedle)

13.1 Introduction

13.1.1 Biological Background

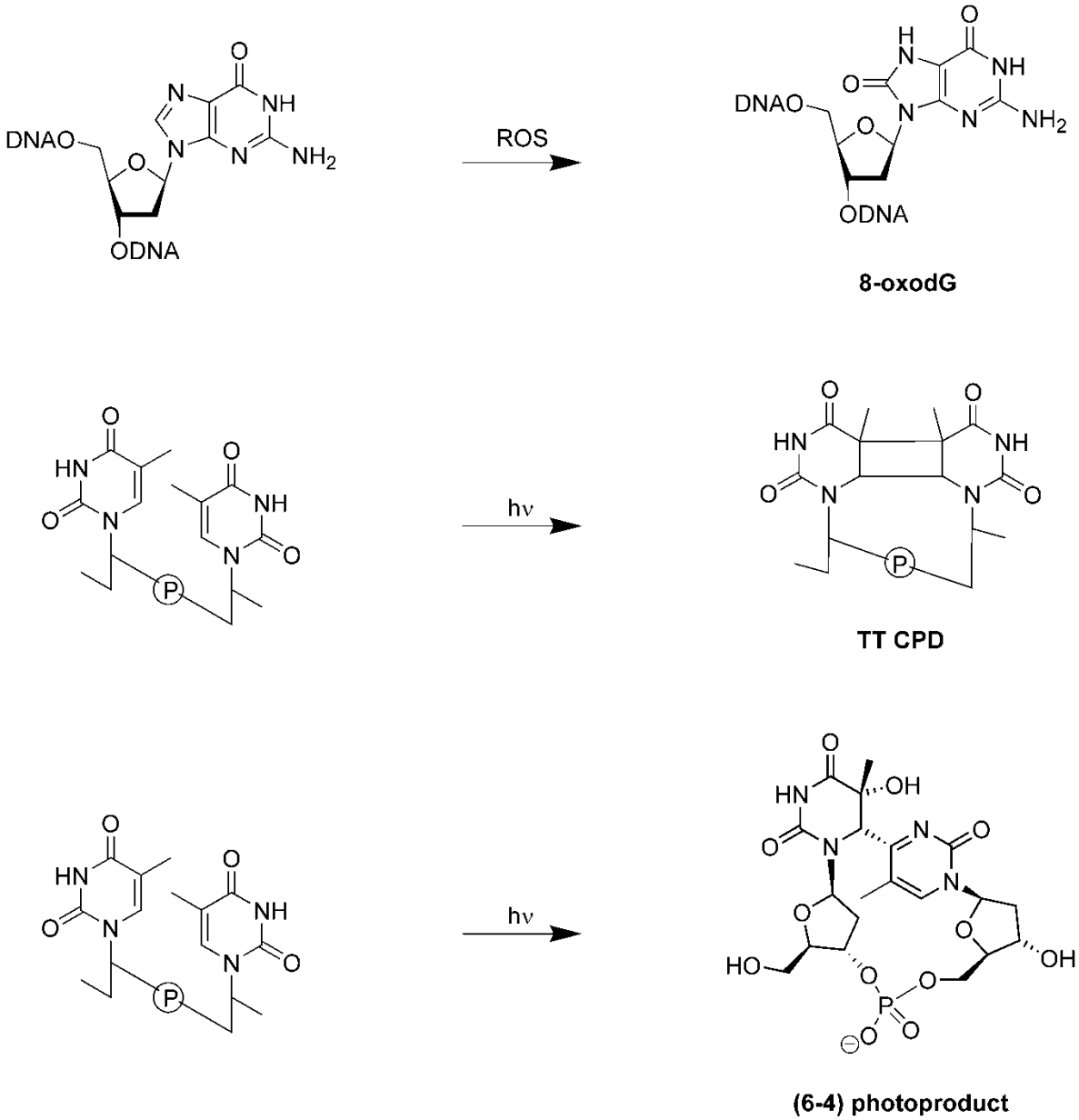

Scheme 13.1 Formation of 8-oxodG by ROS (top) and UV-light-induced cyclization of adjacent thymidines to give a TT CPD (middle) or a (6-4) photoproduct (bottom).

In 2005, more than a quarter of all deaths in Germany were caused by cancer,[1] which is brought forth by mutations of genes. The protein resulting from a mutated gene can be rendered dysfunctional, in the worst case leading to uncontrolled cell division and tumor development. Mutations can be a consequence of DNA damage, as modified DNA bases can e. g.

mispair leading to inheritable DNA sequence alterations. Two prominent classes of such damaged DNA are oxidative lesions, e. g. 8-oxoguanine (8-oxodG, Scheme 13.1 top) and photolesions like cyclobutane pyrimidine dimers (CPD) (Scheme 13.1, middle) and the (6-4)-photoproduct (Scheme 13.1, bottom). 8-OxodG can, among others, be formed by reactive oxygen species (ROS) like $OH^{\bullet}$, $^1O_2$ or O_2^{-}, which are permanently formed in the mitochondria,[2] by Fenton-type reactions[3] or stem from exogenous sources. Photolesions are formed via [2 + 2] cycloaddition by irradiation with UV light.[4]

During evolution certain organisms have developed efficient mechanisms for the repair of such damages. 8-OxodG can be excised from the DNA (base excision repair),[5] whereas CPD photolesions and (6-4) photoproducts can be repaired by a light-induced cycloreversion (photoreactivation).[4] The following Section exclusively deals with the repair of CPD lesions by photolyases. The numbering of the enzyme residues mentioned below always refers to the *Escherichia coli* (*E. coli*) photolyase.

The photoreactivation is performed by photolyases in certain representatives of all three domains of life. Photolyases are monomeric enzymes of 55-60 kDa.[4] Each investigated photolyase contains a flavin adenine dinucleotide derivative (FAD)[6] and a second cofactor, which can either be an 8-HDF[7] or a 5,10-MTHF, which mostly contains three to six, sometimes eight glutamate residues (Scheme 13.2).[8] The fact that either 8-HDF or 5,10-MTHF are acting as cofactors justifies the classification into deaza- and folate-photolyases.

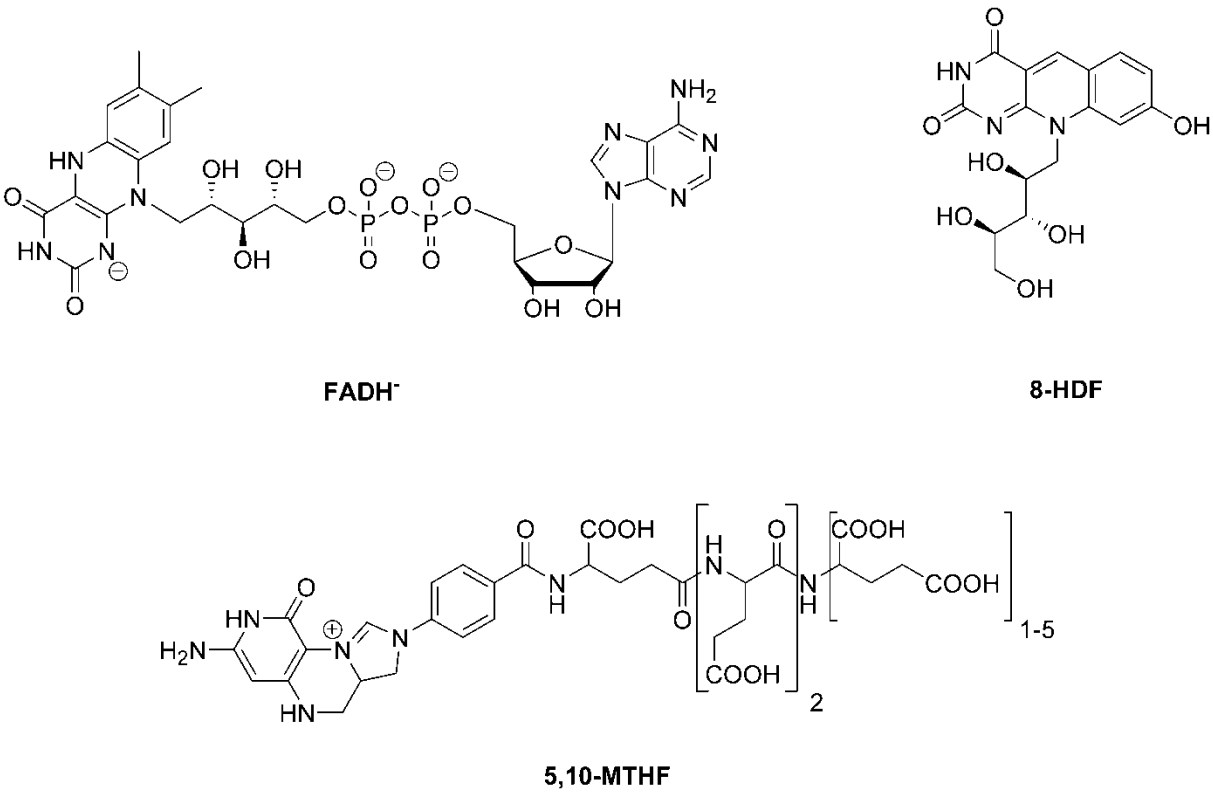

Scheme 13.2 Photolyase cofactors.

8-HDF and 5,10-MTHF absorb light between 300 and 500 nm. The absorbed energy is transferred to the flavin adenine dinucleotide, which is in its semireduced state ($FADH^{\bullet}$),[9] via a

Förster dipole-dipole interaction. The FAD unit can subsequently be reduced to $FADH^-$. The electron for this reduction stems from tryptophan W306 (in *E. coli* photolyase) and is transferred to the flavin derivative via an electron cascade over W359 and W382 (Figure 13.1). The direction of the electron transfer could be dictated by the different environments of the three tryptophan residues.[9] While W382 is predominantly surrounded by hydrophobic amino acids, W359 has a mixed hydrophobic/hydrophilic environment and W306 is surrounded by polar amino acids. This can influence the potentials of the tryptophan residues in a way to direct the electron transfer from W306 (most negative potential) via W359 to W382 (most positive potential).

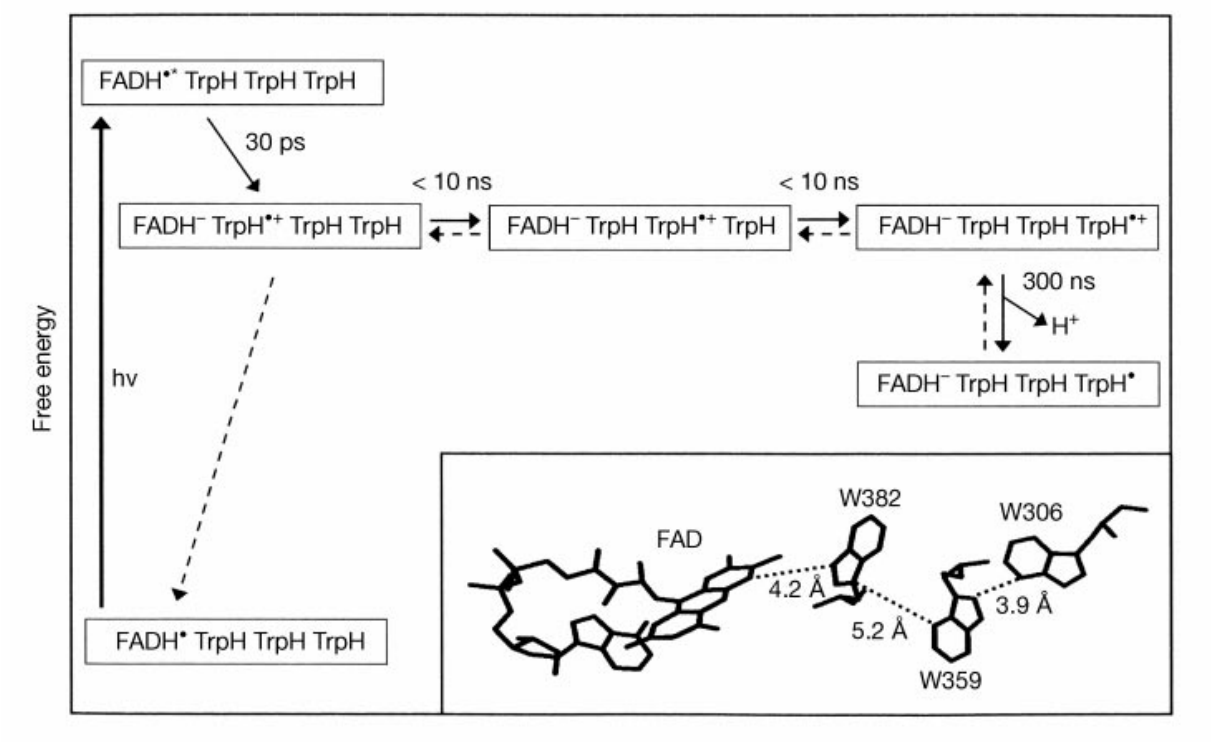

Figure 13.1 Schematic representation of the electron transfer reactions in E. coli photolyase. Reproduced from Aubert et al.[9]

In order to repair the DNA damage, the holoenzyme binds specifically to the CPD photoproduct and flips it out of the DNA helix (flipping-out-mechanism).[10] After irradiation with light, the excited cofactor $FADH^-$* can reduce the CPD photoproduct and subsequently lead to a cycloreversion, forming a thymine and a thymine radical (Scheme 13.3). The latter is oxidized by $FADH^•$ to the natural thymidine, the damage is repaired. An immediate transfer of the electron from the CPD photoproduct back to the $FADH^•$ without concomitant cycloreversion is unlikely due to the hydrophobic environment of the CPD-$FADH^-$-complex.[11]

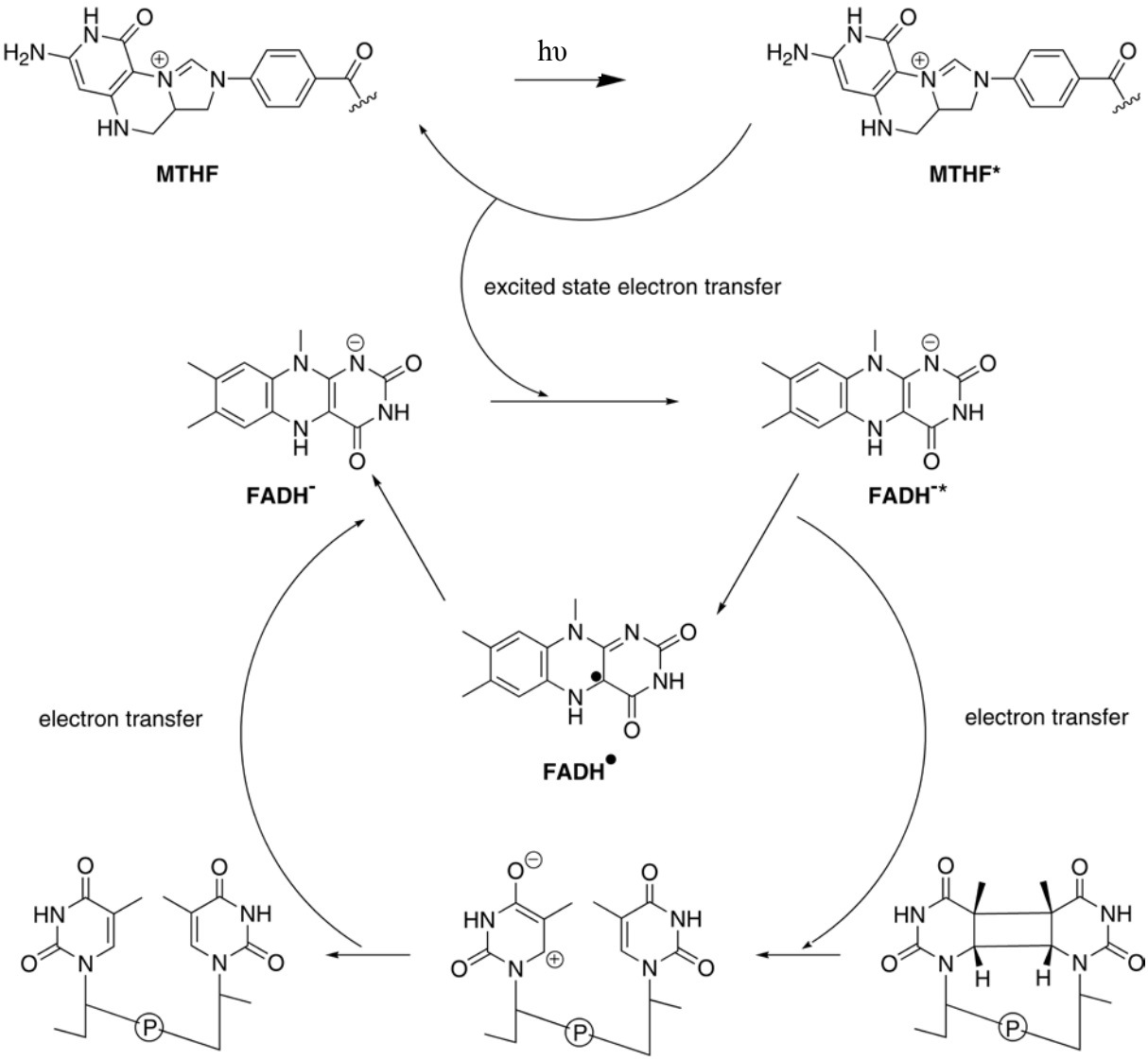

Scheme 13.3 Repair mechanism of a CPD photoproduct by *E. coli* photolyase. Reproduced from Carell.[4]

The electron transfer between the tryptophans and the flavin residue is of crucial interest for the entire repair mechanism and can be investigated by time-resolved laser spectroscopy.[12] Performing these measurements with the entire photolyase enzymes can cause several problems. Isolation and purification of large amounts of enzyme is required for the time-resolved measurements. Large parts of the enzyme do not participate in the repair reaction, their UV absorption can therefore hamper the electron transfer measurements. Therefore a simplified model system for a distance-dependent electron transfer measurement was sought after, which would allow for the placement of the tryptophan at exactly defined and variable distances to the flavin.

13.1.2 Design Rationale for a Photolyase Model System

B-form DNA has a neatly defined 3D structure. The nucleobases are separated by a stacking distance of 3.4 Å. In previous works, flavin has been incorporated into DNA as a hairpin cap for electron transfer measurements.[13] A similar approach can be envisaged for this work as well. Again the flavin acts as a hairpin cap (Figure 13.2, synthesized by Dr. Antonio Manetto), whereas the indole needs to be incorporated as a pseudo-nucleoside. The indole moiety can then be placed at different distances to the flavin, with each nucleobase constituting a 3.4 Å spacer.

Many studies have been performed on electron transfer through DNA.[14] Due to the low intrinsic conductivity of natural DNA it can be expected that it indeed will act as a passive spacer with only a minor effect on the electron transfer reaction. Experiences from previous electron transfer experiments hint at AT base pairs being the best choice for the tracts between the flavin and the indole due to the reduced risk of side reactions. The rest of the hairpin stem should bear a rather high CG content to prevent dangling ends. This model system should allow for distance dependent measurements of the electron transfer using laser flash photolysis experiments. In these experiments, the flavin needs to be in the oxidized form in its resting state in order to accept an electron from the tryptophan after excitation with laser light. The resulting, reduced flavin can e. g. transfer the electron back to the indole moiety. The timescales of these processes can be probed by the distinct changes in the fluorescence properties of the different species in the system and should yield information about the electron transfer reactions in the native enzymes. The following Section will cover the synthesis of a tryptophan-mimetic pseudo-nucleoside, its incorporation into DNA strands and some investigations on the structure of the resulting DNAs.

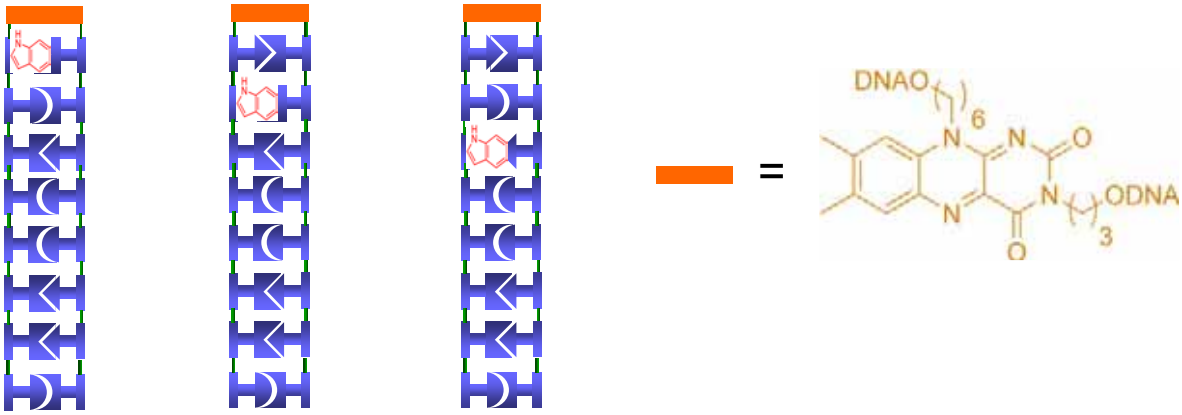

Figure 13.2 Schematic representation of a series of DNA hairpins containing a flavin cap and an indole nucleoside at variable distances to the flavin.

13.1.3 Design of a Pseudo-Nucleoside as Tryptophan Mimic

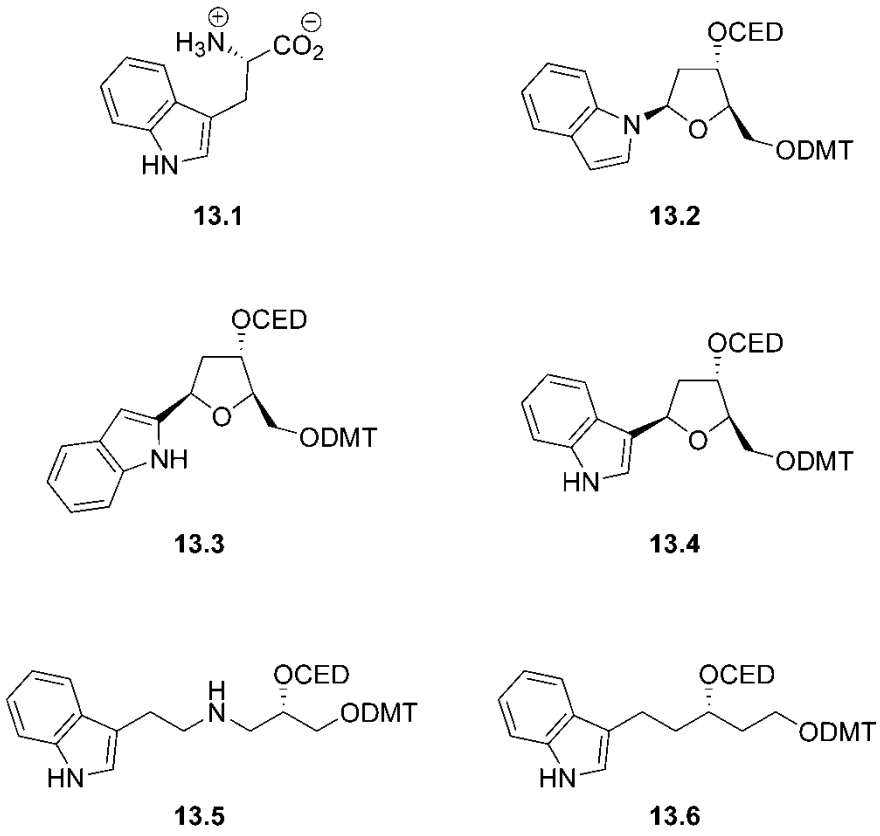

Scheme 13.4 Tryptphan **13.1** and possible pseudo-nucleosidic mimics.

The synthesis of a tryptophan-mimetic and its incorporation into DNA hairpins for femtosecond laser spectroscopy poses several challenges. The multi-milligram amounts of each hairpin of a distance-dependent series required for the spectroscopic studies call for a short, high-yielding and robust synthesis. The tryptophan-mimetic nucleoside should be structurally and electronically similar to the natural tryptophan **13.1**. On the other hand the structure of the DNA should be distorted as little as possible by the incorporation of the modified building block since this could lead to the indole moiety having an undefined distance to the flavin hairpin cap. Precedents form the literature were analyzed for their aptitude to act as tryptophan mimetics in the present study. Nucleoside **13.2**, in which the N1 nitrogen is glycosylated with deoxyribose, would only cause minimal disruption to the DNA double helix, as it closely resembles the natural purine nucleosides geometrically.[15] The electronic structure of the indole moiety would be severely blurred as compared to tryptophan **13.1**, because the sugar moiety would inductively withdraw electron density from the aromatic ring. Additionally, the deoxyribose unit is attached to the N1 position, which removes an exchangeable proton and leads to a hydrolytically labile nucleoside. Synthetic complications could arise from the requirement of a stereoselective glycosylation reaction between the indole and sugar parts of the molecule. In the cases of **13.3**[16] and **13.4**,[17] some of the critical points mentioned above can

be addressed. C-nucleosides are hydrolytically stable, whereas their stereoselective synthesis is even more challenging than in the case of N-nucleosides like **13.2**. In **13.4**, the attachment of the sugar is at the 3-position of the indole as is the case for tryptophan **13.1**. The electron-withdrawing effect of the bridging oxygen atom of the sugar, together with the expected synthetic difficulties, foreclosed the synthesis of nucleosides like **13.3** and **13.4**. The use of acyclic deoxyribose mimetics as linkers can overcome some of the aforementioned problems. By binding a methylene group to the 3-position of indole, one can very closely mimic the electronic structure of the natural tryptophan **13.1**. The glycosylation step is avoided, leading to short and practical syntheses. Wagenknecht et al. have synthesized **13.5**, which bears an acyclic linker and can be synthesized in only four steps from commercially available staring materials.[18] **13.5** does not constitute an ideal mimic for deoxyribose as it carries a 6-atom linker (deoxyribose: 5 carbon atoms) with the two OH groups on positions 5 and 6 (deoxyribose: positions 3 and 5). The NH group in the linker can further distort the B-DNA duplex. Acyclic nucleosides in general lower the melting point of DNA by 10-15 °C, which can be attributed to an entropic effect.[19] The acyclic backbone exhibits a high degree of conformational freedom, particularly in ssDNA. When hybridized to the counter strand to form dsDNAs, the nucleosides are forced into fixed conformations, which is entropically unfavorable, particularly for acyclic nucleosides. Despite this decreased duplex stability, the synthesis of an acyclic nucleoside seemed to be the best choice for this project, as the two major challenges- a very simple synthesis and a good electronic mimic for tryptophan- can be addressed. **13.6** seemed to be the best synthetic target, as it resembles natural both deoxyribose and natural tryptophan **13.1** well. The linker constitutes deoxyribose without the bridging oxygen atom. The electronic structure of natural tryptophan is mimicked well as both **13.1** and **13.6** bear a methylene group at the 3-position of the indole ring.

13.2 Results and Discussion

13.2.1 Synthesis of Acyclic Phosphoramidite **13.6**

The synthesis of phosphoramidite **13.6** can conveniently be started with the commercially available 3-(indol-3-yl)-propionic acid **13.7**.[20] The acyclic five-carbon linker can be readily built up by a Claisen-type condensation with potassium monoethyl malonate to furnish **13.8**. Enantioselective hydrogenation of the keto group in **13.8** using a Ru-BINAP complex (20 bar H_2) gave enantiopure **13.9** in excellent yield and enantiomeric excess (89%, > 99% ee). The absolute configuration of **13.9** could not be unambiguously determined in the course of the work presented here. Using a quadrants diagram,[21] the enantiomer of BINAP was determined which should lead to the desired (*S*)-enantiomer of **13.9**. The optical rotation was found to be $[\alpha]_D = -14°$. Comparison with values of similar compounds from the literature[22] does hint at (*R*)-**13.9**[a] being formed. In order to find unambiguous proof for the obtained stereochemistry, single crystals were grown by slow evaporation of a saturated of solution of **13. 10**

[a] Nomenclature in this section: **13.X** is used for enantiopure substances generated by reduction with (*S*)-BINAP or substances without stereocenters. **13.Xr** is used for racemic compounds. ODN-**13.1** refers to enantiopure **13.6** in the DNA synthesis**,** ODN-**13.1r** to the racemic **13.6r**. ODN-**13.1CS (dA)** denotes the counter strand of ODN-**13.1** with dA (Y in Table 9.1) in the position opposite the indole nucleoside.

in EtOAc and DCM. Stefan Schießer could in the following show that the desired stereoisomer has indeed been obtained.

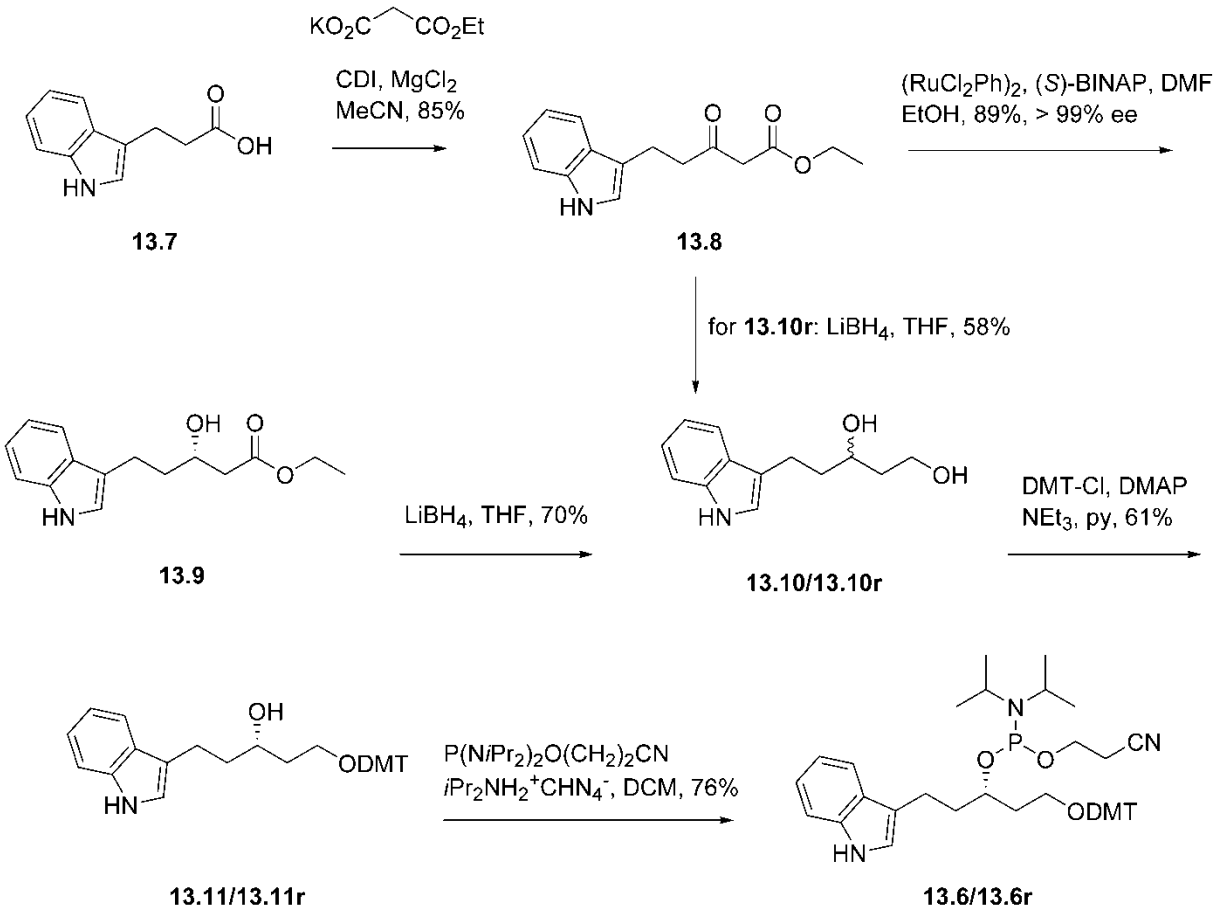

Scheme 13.5 Synthesis of nucleoside phosphoramidite **13.6**.

The ester group in **13.9** was reduced with $LiBH_4$ to give the free pseudo-nucleoside **13.10**. Selective DMT protection of the primary alcohol to give **13.11**, followed by phosphorylation of the secondary alcohol gave the desired phosphoramidite **13.6** in a high overall yield of 25% over five steps. Chiral HPLC analysis of **13.11** showed that the high ee value is retained during the synthesis. The synthesis thus meets the requirement of being short, efficient and robust. Even the high pressure hydrogenation to give **13.9** can be scaled up as it is performed in a highly concentrated solution.
For the synthesis of **13.10r**, the separate reductions of the keto- and ester groups can be conveniently performed in one step using $LiBH_4$. Phosphoramidite **13.6r** is thus available in only four steps in an overall yield of 23%. It should be noted that both syntheses do not require a protecting group for the indole-NH.

13.2.2 Structural Studies on DNAs Containing Indole Nucleosides

Phosphoramidites **13.6** and **13.6r** were incorporated into ODN-**13.1** and ODN-**13.1r**, respectively, for melting point analysis and CD spectroscopy. DNA solid phase synthesis could be

performed using standard conditions for coupling (elongated recycling time of 10 min for **13.6**) and DNA deprotection (NH_3 in H_2O/EtOH 3:1). In both cases, HPLC and MALDI-TOF showed that the desired oligonucleotides were formed. ODN-**13.1** and ODN-**13.1r** were subsequently hybridized to their counter strands ODN-**13.1CS**, in which the four canonical nucleobases as well as an abasic site were placed opposite to the indole nucleoside. CD spectroscopy of these dsODNs showed that in all cases a B-form DNA was formed, as evidenced by a negative signal at 250 nm and a positive signal at 280 nm. In the racemic series ODN-**13.1r**, the amplitudes of the CD signals were markedly higher than in the enantiopure series or the unmodified control strand. The amplitudes of the enantiopure series were very similar to those of the unmodified control strand. The data suggests that incorporation of the enantiopure indole nucleoside allows for the formation of an intact B-form DNA. An induced CD effect on the indole moiety could not be observed with this measurement, as the absorption of the indole (280 nm) was overlaid by the DNA absorption.

Table 13.1 Sequences for ODN-**13.1** and ODN-**13.2**.

ODN-**13.1 (r)**	5′-GCGCTGTXCATTCGCG-3′
ODN-**13.1CS**	3′-CGCGACAYGTAAGCGC-5′
ODN-**13.2**	5′-GCGCTTGXGATTCGCG-3′
ODN-**13.2CS**	3′-CGCGAACYCTAAGCGC-5′

X = nucleoside based on phosphoramidite **13.6** or **13.6r**. Y = dA, dC, dG, dT or an abasic site.

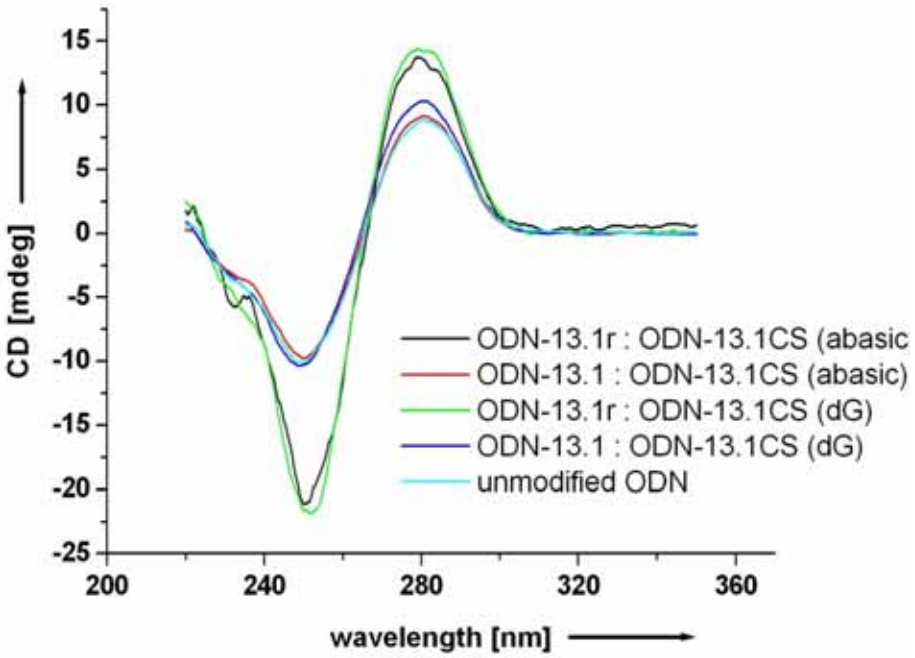

Figure 13.3 Selection of CD spectra of ODN-**13.1** and ODN-**13.1r** hybridized to different counter strands.

This series of ODNs was next used to determine the ideal counter base for indole, showing the least perturbation of the DNA double helix (highest melting temperature, Table 13.2). Melting point analyses showed a decreased melting point for the indole-bearing strand in contrast to the control ODN with an AT base pair instead of X and Y (ca. 10 °C decrease in melting temperature). This decrease is among the lowest of all acyclic nucleosides reported so far,[19, 23] probably due to the close geometric resemblance of the acyclic linker to the natural deoxyribose. The melting temperature was found to be neither dependent on the counter base nor on whether **13.6** or **13.6r** was incorporated. Two explanations can be given for this finding. Wagenknecht et al., who found the same indiscriminate pairing for **13.5**,[18] observed that their pseudo-nucleoside can act as a universal base surrogate. This was explained by the absence of hydrogen bonds to the opposite nucleobase. A second explanation for the indiscriminate pairing is that the indole, which is linked to the DNA via a flexible, acyclic linker, could be turned outside of the double helix. This is rather unlikely due to the hydrophobic nature of indole and the favorable π-stacking interaction with the nucleobases once the indole is situated inside the duplex DNA. Nonetheless, it was essential to know at this point if the indole was situated inside the DNA double helix or not, as only this could warrant a defined, distance dependent electron transfer measurement.

Table 13.2 Melting temperature analysis of ODN-**13.1** and ODN-**13.1r** hybridized to ODN-**13.1CS**. Control (AT base pair instead of XY (Table 13.1)): 71.0 °C.

counterbase Y	ODN-**13.1r**	ODN-**13.1**
dA	61.8 °C	61.6 °C
dC	58.4 °C	58.7 °C
dG	62.4 °C	61.4 °C
dT	61.3 °C	61.2 °C
abasic	60.3 °C	60.1 °C

In order to proof, whether the indole is situated inside the DNA double helix, fluorescence measurements were performed, following the approach by Wagenknecht et al.[18] Indole can be excited at 290 nm. The resulting fluorescence wavelength is strongly dependent on the nucleobases adjacent to the indole on the same strand. The typical maximum of the emission of an indole can be found at 350 nm, with adjacent guanines it shifts to 360 nm, while adjacent pyrimidines shift it to 405 nm. ODN-**13.1**, bearing two flanking pyrimidines alongside the indole, was hybridized to ODN-**13.1CS (dT)**. A second strand (ODN-**13.2**) with flanking guanines was synthesized and hybridized to its counter strand ODN-**13.2CS (dT)**. Fluorescence spectroscopy on these dsODNs neatly reproduced the findings of Wagenknecht et al. (Figure 13.4), thereby proving that the indole is indeed situated inside the DNA double helix.

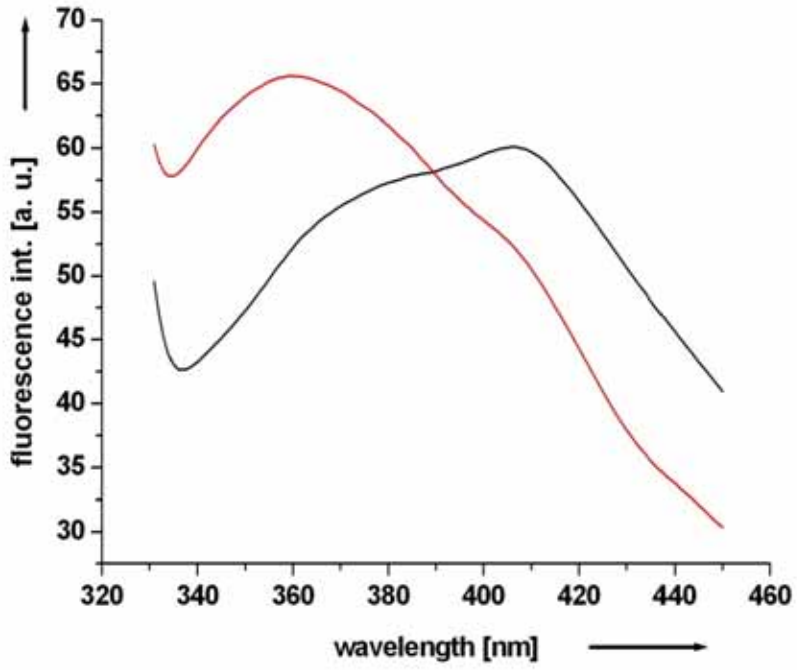

Figure 13.4 Fluorescence emission spectra of ODN-**13.1** : ODN-**13.1CS** (λ_{max} = 405 nm, black line) and ODN-**13.2** : ODN-**13.2CS** (λ_{max} = 360 nm, red line). Irradiation at 290 nm.[18]

13.3 Summary and Outlook

Robust and efficient synthetic routes have been found for both **13.6** and **13.6r**. The absolute stereochemistry of the OH group, which is formed during the chiral hydrogenation to give **13.9**, is currently being determined by X-ray crystal structure analysis. These phosphoramidites can be incorporated into DNA via standard solid-phase synthesis protocols without protection of the indole NH. CD spectroscopy showed that the enantiopure compound can be incorporated into B-form DNA without any significant disruption of the double helical structure. Melting point analyses showed that the indole nucleoside acts as a universal base surrogate with a melting temperature which is independent of the counter base. Fluorescence spectroscopy proved that the indole is situated inside the DNA duplex. As soon as the stereochemistry of **13.6** is unambiguously assigned, Stefan Schießer will continue the project by reproducing the synthesis of **13.6** on a large scale and incorporation into the hairpins outlined in Figure 13.2 together with the flavin cap (synthesized by Dr. Antonio Manetto). Femtosecond laser spectroscopy using these hairpin structures will be performed in the group of Prof. to elucidate the distance-dependence of the electron transfer between flavin and tryptophan in photolyases.

13.4 Experimental Section

For the assignment of the spectra the following numbering was used:

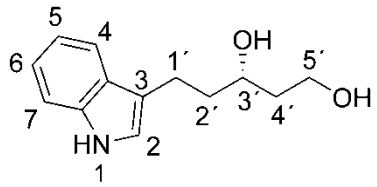

All described syntheses except for the synthesis of **13.8** can be performed on the racemic as well as on the enantiopure starting materials unless stated otherwise. Due to the free rotation of the side chain, the spectral data are alike for the racemic and enantiopure compounds and therefore reported only once.

13.4.1 Synthesis

5-(1*H*-Indol-3-yl)-3-oxopentanoic acid ethyl ester (**13.8**)[20, 24]

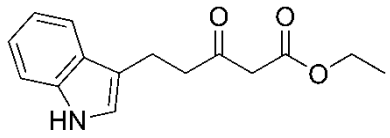

1,1´-Carbonyldiimidazole (14.3 g, 88.3 mmol) was added to 3-(indol-3-yl)-propionic acid **13.7** (15.3 g, 80.9 mmol) in 400 mL MeCN (HPLC grade) and stirred for 5 h at r. t. under inert atmosphere (Suspension A). Suspension B was prepared by adding dry NEt_3 (36.0 mL, 259 mmol) and $MgCl_2$ (19.2 g, 202 mmol) to potassium monoethyl malonate (29.0 g, 170 mmol) in MeCN (HPLC grade, 450 mL). Suspension B was stirred for 3 h at r. t. under inert atmosphere. Suspension A was quickly poured onto Suspension B and the resulting suspension was stirred for 17 h at r. t. under inert atmosphere. 100 mL HCl (13%) were added, resulting in dissolution of the suspension. Copious amounts of brine and EtOAc (> 500 mL each) were added to allow for an extraction. The aqueous phase was extracted twice more with EtOAc. The combined organic phases were washed with sat. Na_2CO_3 solution and brine and dried over $MgSO_4$. Silica gel was added to the resulting solution and the solvent evaporated to dryness to adsorb the product mixture on the silica gel. Column chromatography (*i*Hex/EtOAc 5:1) was performed to give **13.8** (17.8 g, 68.6 mmol, 85%) as a white powder.
R_f (*i*Hex/EtOAc 3:1): 0.31. ^{1}H-NMR (600 MHz, $CDCl_3$): δ = 1.25 (t, 3H, *J* = 7.1 Hz, CH_3), 2.96 (t, 2H, *J* = 7.3 Hz, $C_{2'}H$), 3.07-3.10 (m, 2H, $C_{1'}H$), 3.43 (s, 2H, $C_{4'}H$), 4.17 (q, 2H, *J* = 7.1 Hz, OCH_2), 6.98-6.99 (m, 1H, C_2H), 7.13 (ddd, 1H, *J* = 0.9, 7.1, 7.8 Hz, C_5H), 7.20 (ddd, 1H, *J* = 1.1, 7.1, 8.1 Hz, C_6H), 7.35 (td, 1H, *J* = 0.8, 8.1 Hz, C_7H), 7.56-7.59 (m, 1H, C_4H), 8.02 (sbr, 1H, NH). ^{13}C-NMR (150 MHz, $CDCl_3$): δ = 14.1 (CH_3), 19.1 (CH_2), 43.4 (CH_2), 49.4 (CH_2), 61.3 (CH_2), 111.2 (CH), 114.7, 118.6 (CH), 119.3 (CH), 121.6 (CH),

122.0 (CH), 127.2, 136.3, 167.2, 202.7. HRMS (EI): calcd. for $C_{15}H_{17}NO_3^+$ [M^+]: 259.1208, found: 259.1200.

3-Hydroxy-5-(1*H*-indol-3-yl)-pentanoic acid ethyl ester (**13.9**)[20, 25]

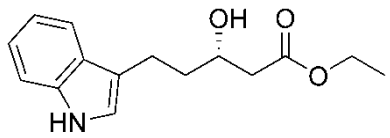

Enantiopure

(*S*)-2,2′-Bis(diphenylphosphino)-1,1′-binaphthyl (188 mg, 0.302 mmol) and benzeneruthenium(II) chloride dimer (150 mg, 0.300 mmol) were added to dry DMF (3 mL) (Solution A), which was degassed by two freeze-pump-thaw cycles prior to use. A solution of **13.8** (1.00 g, 3.86 mmol) in dry EtOH (1 mL) and dry DMF (3 mL) was degassed by two freeze-pump-thaw cycles (Solution B). Dark green Solution A and Solution B were quickly transferred to a high pressure autoclave, which was flushed with H_2 three times, and stirred at r. t. for 7 d at 20 bar H_2 pressure. The reaction solution was directly adsorbed onto silica (see synthesis of **13.8**) and purified by silica gel column chromatography (DCM) to give **13.9** (900 mg, 3.44 mmol, 89%, > 99% ee as determined by chiral HPLC) as a green oil due to minor catalyst impurities.

Racemic

13.8 (1.15 g, 4.44 mmol) was dissolved in a mixture of dry MeCN (5 mL) and dry MeOH (11 mL). The solution was cooled on an ice-bath and $NaBH_4$ (168 mg, 4.44 mmol) was added. The ice-bath was removed and the solution stirred for 20 min. The reaction solution was directly adsorbed onto silica (see synthesis of **13.8**) and purified by silica gel column chromatography (*i*Hex/EtOAc 3:1) to give **13.9r** (1.04 g, 3.99 mmol, 90%) as a white powder. R_f (*i*Hex/EtOAc 3:1): 0.13. ^{1}H-NMR (600 MHz, $CDCl_3$): δ = 1.27 (t, 3H, *J* = 7.1 Hz, CH_3), 1.60 (sbr, 1H, OH), 1.83-1.89 (m, 1H, $C_{2'}H$), 1.91-1.97 (m, 1H, $C_{2'}H$), 2.45-2.55 (m, 2H, $C_{4'}H$), 2.85-2.90 (m, 1H, $C_{1'}H$), 2.94-2-98 (m, 1H, $C_{1'}H$), 4.07-4.11 (m, 1H, $C_{3'}H$), 4.17 (q, 2H, *J* = 7.1 Hz, OCH_2), 7.01 (m, 1H, C_2H), 7.12 (ddd, 1H, *J* = 0.9, 7.0, 7.9 Hz, C_5H), 7.20 (ddd, 1H, *J* = 1.1, 7.1, 8.1 Hz, C_6H), 7.36 (dt, 1H, *J* = 0.8, 8.1 Hz, C_7H), 7.62 (d, 1H, *J* = 7.9 Hz, C_4H), 7.97 (sbr, 1H, NH). ^{13}C-NMR (150 MHz, $CDCl_3$): δ = 14.2 (CH_3), 21.1 (CH_2), 36.7 (CH_2), 41.3 (CH_2), 60.7 (CH_2), 67.5 (CH), 111.1 (CH), 115.9, 118.9 (CH), 119.2 (CH), 121.3 (CH), 122.0 (CH), 127.4, 136.4, 173.1. HRMS (ESI): calcd. for $C_{15}H_{20}NO_3^+$ $[M+H]^+$: 262.1443, found: 262.1439.

5-(1*H*-Indol-3-yl)-pentane-1,3-diol (**13.10**)

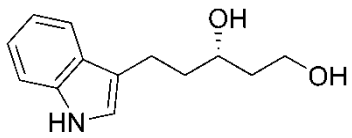

Method A: **13.9** as starting material

13.9 (5.00 g, 19.1 mmol) was dissolved in dry THF (200 mL) and heated to reflux. $LiBH_4$ (2 M in dry THF, 14.4 mL, 28.7 mmol) was slowly added over 30 min with a syringe pump. Refluxing was continued for 3 h, followed by slow addition of acetone (6 mL) and stirring at r. t. for 30 min. Sat. NH_4Cl was added and the product extracted twice with EtOAc. The combined organic phases were dried over $MgSO_4$ and purified by silica gel column chromatography (*i*Hex/EtOAc 1:2) to give **13.10** (2.96 g, 13.5 mmol, 70%) as a colorless oil.

Method B: **13.8** as starting material

13.8 (500 mg, 1.93 mmol) was dissolved in dry THF (5 mL) and heated to reflux. $LiBH_4$ (2 M in dry THF, 2.41 mL, 4.83 mmol) was slowly added over 30 min with a syringe pump. Refluxing was continued for 4 h, then the reaction solution was stirred for another 16 h at r. t. Acetone (1 mL) was slowly added and stirring continued for 30 min. Sat. NH_4Cl was added and the product extracted twice with EtOAc. The combined organic phases were dried over $MgSO_4$ and purified by silica gel column chromatography (*i*Hex/EtOAc 1:2) to give **13.10r** (245 mg, 1.12 mmol, 58%) as a colorless oil.
R_f (*i*Hex/EtOAc 1:1): 0.11. ^{1}H-NMR (300 MHz, $CDCl_3$): δ = 1.69-1.78 (m, 2H, $C_{4'}H$), 1.86-1.97 (m, 2H, $C_{2'}H$), 2.50 (sbr, 2H, OH), 2.82-2.94 (m, 2H, $C_{1'}H$), 3.78-3.83 (m, 1H, $C_{5'}H$), 3.88 (td, 1H, J = 5.2, 10.4 Hz, $C_{5'}H$), 3.92-3.97 (m, 1H, $C_{3'}H$), 6.98 (s, 1H, C_2H), 7.12 (ddd, 1H, J = 1.0, 7.1, 7.9 Hz, C_5H), 7.19 (ddd, 1H, J = 1.0, 7.2, 8.1 Hz, C_6H), 7.33-7.36 (m, 1H, C_7H), 7.60-7.63 (m, 1H, C_4H), 8.04 (sbr, 1H, NH). ^{13}C-NMR (150 MHz, $CDCl_3$): δ = 21.2 (CH_2), 37.8 (CH_2), 38.3 (CH_2), 61.7 (CH_2), 71.8 (CH), 111.1 (CH), 115.9, 118.8 (CH), 119.2 (CH), 121.3 (CH), 122.0 (CH), 127.3, 136.4. HRMS (EI): calcd. for $C_{13}H_{17}NO_2^+$ [M^+]: 219.1254, found: 219.1250.

1-(4,4′-Dimethoxytrityl)- 5-(1*H*-indol-3-yl)-pentane-1,3-diol (**13.11**)

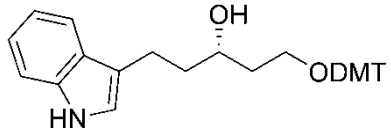

13.10 (55 mg, 0.25 mmol) and DMAP (10 mg, 0.08 mmol) were dissolved in dry pyridine and co-evaporated to dryness twice. NEt_3 (70 µL, 0.50 mmol), dry pyridine (1 mL) and DMT-Cl (119 mg, 0.35 mmol) were added at 0 °C and the solution was stirred for 4.5 h at r. t. MeOH

(0.5 mL) was added and the resulting solution stirred for 5 min. Extraction was carried out with sat. NaCl, sat. $NaHCO_3$ and EtOAc. The combined organic phases were dried over $MgSO_4$ and purified by silica gel column chromatography (*i*Hex/EtOAc/py 200:70:1) to give **13.11** as pale yellow solid (80 mg, 0.15 mmol, 61%).
R_f (*i*Hex/EtOAc 1:1): 0.54. ^{1}H-NMR (300 MHz, d_6-acetone): δ = 1.74-1.90 (m, 4H, $C_{2'}H$, $C_{4'}H$), 2.77-2.96 (m, 2H, $C_{1'}H$), 3.17-3.29 (m, 2H, $C_{5'}H$), 3.77 (s, 6H, OCH_3), 3.82-3.91 (m, 1H, $C_{3'}H$), 6.83-6.87 (m, 4H, ArH), 6.98 (ddd, 1H, *J* = 1.0, 7.0, 8.0 Hz, ArH), 7.05-7.11 (m, 2H, ArH), 7.20 (ddd, 1H, *J* = 1.3, 6.4, 8.6 Hz, ArH), 7.26-7.38 (m, 7H, ArH), 7.41-7.47 (m, 2H, ArH), 7.54-7.58 (m, 1H, ArH), 9.92 (sbr, 1H, NH). ^{13}C-NMR (100 MHz, d_6-acetone): δ = 23.0 (CH_2), 39.6 (CH_2), 40.3 (CH_2), 56.5 (CH_3), 62.9 (CH_2), 70.2 (CH), 87.8, 113.0 (CH), 114.8 (CH), 117.5, 120.2 (CH), 120.4 (CH), 122.9 (CH), 123.6 (CH), 128.4 (CH), 129.5 (CH), 130.0 (CH), 131.8 (CH), 131.8 (CH), 138.3, 138.4, 147.6, 160.5. HRMS (ESI): calcd. for $C_{34}H_{35}NNaO_4^+$ $[M+Na]^+$: 544.2458, found: 544.2458.

1-(4,4′-Dimethoxytrityl)-3-[(cyanoethoxy)(diisopropylamino)-phosphono)]-5-(1*H*-indol-3-yl)-pentane-1,3-diol (**13.6**)

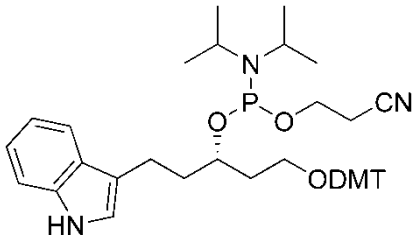

13.11 (260 mg, 0.498 mmol) and diisopropylammonium tetrazolide (48 mg, 0.28 mmol) were co-evaporated twice with dry pyridine and dissolved in dry, degassed DCM (5 mL). 2-Cyanoethyl-N,N′-diisopropylchlorophosphoramidite (0.20 mL, 0.63 mmol) was added and the solution stirred for 3.5 h at room temperature. The reaction mixture was concentrated *in vacuo* to 1/4 of the original volume. The residue was purified by flash chromatography on passivated silica gel with degassed solvents (DCM/MeOH/py 200:2:1). **13.6** was obtained as a pale yellow solid (274 mg, 0.38 mmol, 76%).
^{1}H-NMR (200 MHz, d_6-acetone): δ = 1.07-1.23 (m, 14H, *i*Pr), 1.89-2.09 (m, 4H, $C_{2'}H$, $C_{4'}H$), 2.52-4.25 (m, 8H), 3.77 (s, 6H, OCH_3), 4.05-4.24 (m, 1H, $C_{3'}H$), 6.82-7.60 (m, 18H, ArH), 9.92 (sbr, 1H, NH). ^{31}P-NMR (d_6-acetone, 81 MHz): δ = 147.9, 148.0.

13.4.2 MALDI-TOF data

	mass calcd. [Da]	mass found [m/z]
ODN-**13.1**	4841.2	4838.7
ODN-**13.1r**	4841.2	4838.2
ODN-**13.2**	4881.2	4881.2

13.4.3 HPLC of the oligonucleotides

For the following HPLC analyses a gradient was used (0.1 M $HNEt_3^+OAc^-$. Buffer A: in H_2O, Buffer B: in H_2O/MeCN 1:4. Linear gradient from 0% B to 50% B in 45 min).

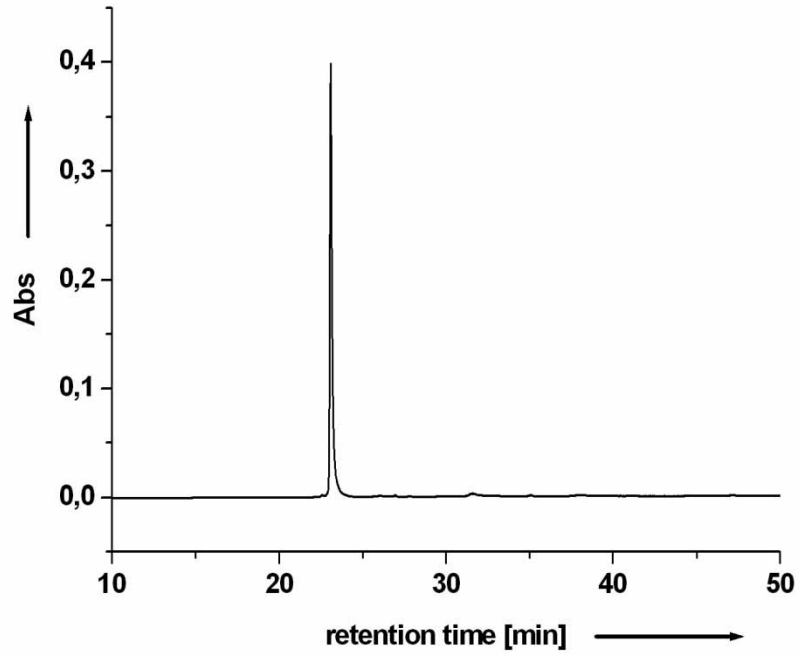

Figure 13.5 HPLC of ODN-**13.1**.

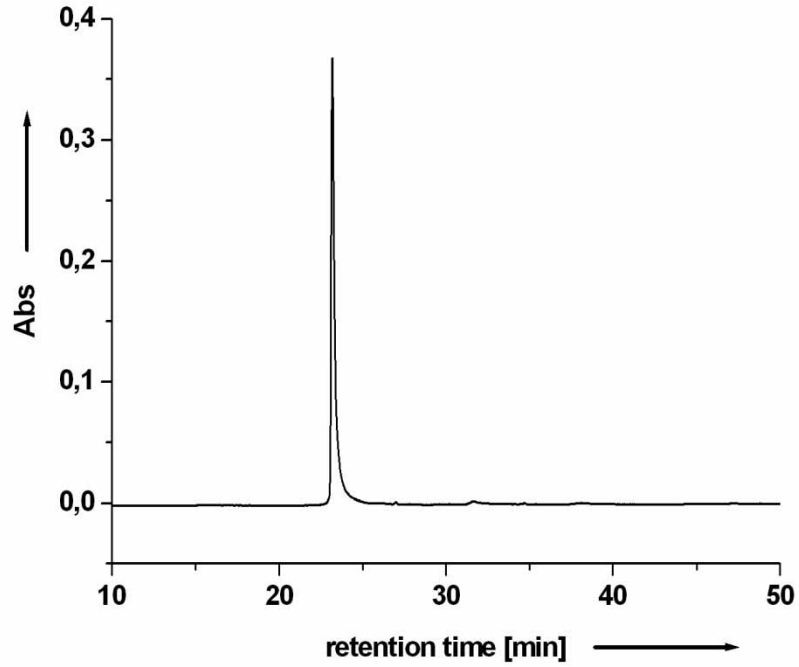

Figure 13.6 HPLC of ODN-**13.1r**.

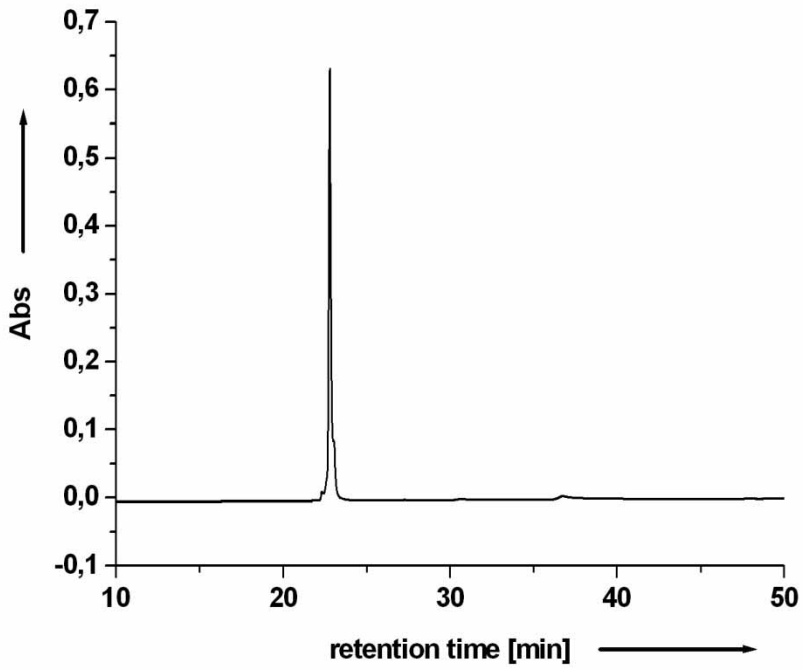

Figure 13.7 HPLC of ODN-**13.2**.

9.5 Author´s Contribution

The work presented her is the author´s in collaboration with Stefan Schießer, whose bachelor thesis was supervised by the author (synthesis of the free nucleoside).

9.6 References

[1] in *Statistisches Bundesamt Deutschland* (Ed.: R. Fachserie 12, p. 4), **2005**.
[2] M. Dizdaroglu, P. Jaruga, M. Birincioglu, H. Rodriguez, *Free Radical Biol. Med.* **2002**, *32*, 1102-1115.
[3] C. J. Burrows, J. G. Muller, *Chem. Rev.* **1998**, *98*, 1109-1151.
[4] T. Carell, *Angew. Chem. Int. Ed.* **1995**, *34*, 2491-2494.
[5] S. S. David, V. L. O'Shea, S. Kundu, *Nature* **2007**, *447*, 941-950.
[6] H. W. Park, S.-T. Kim, A. Sancar, J. Deisenhofer, *Science* **1995**, *268*, 1866-1872.
[7] A. P. M. Eker, J. K. C. Hessels, J. v. d. Velde, *Biochemistry* **1988**, *27*, 1758 - 1765.
[8] J. L. Johnson, S. Hamm-Alvarez, G. Payne, G. B. Sancar, K. V. Rajagopalan, A. Sancar, *Proc. Nat. Acad. Sci. USA* **1988**, *85*, 2046-2050.
[9] C. Aubert, M. H. Vos, P. Mathis, A. P. M. Eker, K. Brettel, *Nature* **2000**, *405*, 586-590.
[10] A. Mees, T. Klar, P. Gnau, U. Hennecke, A. P. M. Eker, T. Carell, *Science* **2004**, *306*, 1789-1793.

[11] S.-T. Kim, R. F. Hartman, S. D. Rose, *Photochem. Photobiol.* **1990**, *52*, 789-794.
[12] J. Broos, K. Tveen-Jensen, E. d. Waal, B. H. Hesp, J. B. Jackson, G. W. Canters, P. R. Callis, *Angew. Chem. Int. Ed.* **2007**, *46*, 5137-5139; A. Lukacs, A. P. M. Eker, M. Byrdin, S. Villette, J. Pan, K. Brettel, M. H. Vos, *J. Phys. Chem. B* **2006**, *110*, 15654-15658; F. Tanaka, H. Chosrowjan, S. Taniguchi, N. Mataga, K. Sato, Y. Nishina, K. Shiga, *J. Phys. Chem. B* **2007**, *111*, 5694-5699; C. Aubert, P. Mathis, A. P. M. Eker, K. Brettel, *Proc. Natl. Acad. Sci. U. S. A.* **1999**, *96*, 5423-5427; K. Bobrowski, J. Poznanski, J. Holcman, K. L. Wierzchowski, *J. Phys. Chem. B* **1999**, *103*, 10316-10324.
[13] C. Behrens, L. T. Burgdorf, A. Schwögler, T. Carell, *Angew. Chem. Int. Ed.* **2002**, *41*, 1763-1766.
[14] A. Manetto, S. Breeger, C. Chatgilialoglu, T. Carell, *Angew. Chem. Int. Ed.* **2005**, *45*, 318-321.
[15] J. S. Lai, E. T. Kool, *J. Am. Chem. Soc.* **2004**, *126*, 3040-3041.
[16] S. Matsuda, A. A. Henry, P. G. Schultz, F. E. Romesberg, *J. Am. Chem. Soc.* **2003**, *125*, 6134-6139.
[17] T. N. Sokolova, I. V. Yartseva, M. N. Preobrazhenskaya, *Carbohydrate Res.* **1981**, *93*, 19-34; W. He, H. Togo, Y. Waki, M. Yokoyama, *J. Chem. Soc., Perkin Trans. 1* **1998**, 2425-2433; M. Yokoyama, M. Nomura, H. Togo, H. Seki, *J. Chem. Soc., Perkin Trans. 1* **1996**, 2145-2149.
[18] C. Wanninger, H.-A. Wagenknecht, *Synlett* **2006**, *13*, 2051-2054.
[19] K. C. Schneider, S. A. Benner, *J. Am. Chem. Soc.* **1990**, *112*, 453-455.
[20] S. Schießer, Bachelor thesis, LMU München (München), **2007**.
[21] S. D. d. Paule, S. Jeulin, V. Ratovelomanana-Vidal, J.-P. Genêt, N. Champion, P. Dellis, *Eur. J. Org. Chem* **2003**, *2003*, 1931-1941.
[22] S. E. Denmark, T. Wynn, G. L. Beutner, *J. Am. Chem. Soc.* **2002**, *125*, 13405 - 13407; E. M. Carreira, W. Lee, R. A. Singer, *J. Am. Chem. Soc.* **1995**, *117*, 3649 - 3650.
[23] L. Kvaerno, R. Kumar, B. M. Dahl, C. E. Olsen, J. Wengel, *J. Org. Chem.* **2000**, *65*, 5167-5176; C.-H. Tsai, J. Chen, J. W. Szostak, *Proc. Nat. Acad. Sci. USA* **2007**, *104*, 14598-14603.
[24] A. Mai, D. Rotili, D. Tarantino, P. Ornaghi, F. Tosi, C. Vicidomini, G. Sbardella, A. Nebbioso, M. Miceli, L. Altucci, P. Filetici, *J. Med. Chem.* **2006**, *49*, 6897 - 6907.
[25] M. Georgy, P. Lesot, J.-M. Campagne, *J. Org. Chem.* **2007**, *72*, 3543 - 3549.

List of Abbreviations

A	adenine (adenosine)
Å	Angström, 10^{-10} m
Abs	absorption
Ac	acetyl
AFM	atomic force microscopy
bp	base pair
br	broad
Bu	butyl
C	cytosine (cytidine)
calcd.	calculated
cat.	catalytic
CD	circular dichroism
CMS	colloidal mesoporous silica
conc.	concentrated
CPD	cyclobutane-pyrimidine dimer
CPG	controlled pore glass
CT	charge transfer
CTMS	3-chloropropyltrimethoxysilane
d	day(s)
d	dublett (NMR spectroscopy)
dA	2′-deoxyadenosine
Da	Dalton
dATP	2′-deoxyadenosine 5′-triphosphate
dC	2′-deoxycytidine
dCTP	2′-deoxycytidine 5′-triphosphate
DCM	dichloromethane
dG	2′-deoxyguanosine
dGTP	2′-deoxyguanosine 5′-triphosphate
DIPEA	diisopropylethylamine (Hünig base)
DMAP	4-(dimethylamino)pyridine
DMF	*N*,*N*-dimethylformamide
DMSO	dimethyl sulfoxide
DMT	4,4′-dimethoxytrityl
DNA	deoxyribonucleic acid
dNTP	2′-deoxyribonucleotide 5′-triphosphate
ds	double stranded
dT	2′-deoxythymidine
dTTP	2′-deoxythymidine 5′-triphosphate
dU	2′-deoxyuridine
dUTP	2′-deoxyuridine 5′-triphosphate
EI	electron impact
eq.	equivalents
ESI	electrospray ionization
Et	ethyl
et al.	et alii (and others)
EtOAc	ethyl acetate
eV	electronvolt
FAD	flavin adenine dinucleotide
FRET	fluorescent resonance energy transfer

FT	Fourier transformation
G	guanine (guanosine)
h	hour(s)
HDF	8-hydroxy-5-deazaflavin
HPLC	high performance liquid chromatography
HRMS	high resolution mass spectrometry
I	intensity
i	*iso*
IR	infrared (spectroscopy)
J	coupling constant
M	molar
m	multiplett (NMR spectroscopy)
MALDI	matrix assisted laser desorption ionisation
MB	molecular beacon
mdeg	milli degree (ellipticity)
Me	methyl
MeCN	acetonitrile
MeOH	methanol
min	minute(s)
MS	mass spectrometry
mV	millivolt
NMR	nuclear magnetic resonance
ODN	oligodeoxynucleotide
PCR	polymerase chain reaction
Ph	phenyl
Pol	polymerase
ppm	parts per million
Pr	propyl
q	quartett (NMR spectroscopy)
quin	quintett (NMR spectroscopy)
R	residue
r. t.	room temperature
R_f	ratio of fronts (retention factor, TLC)
RNA	ribonucleic acid
rpm	rounds per minute
ROS	reactive oxygen species
RP	reverse phase
s	strong (IR spectroscopy)
s	second(s)
s	singlet (NMR spectroscopy)
sat.	saturated
ss	single stranded
T	thymine (thymidine)
t	triplett (NMR spectroscopy)
t	tertiary
TBAF	tetrabutylammonium fluoride
TBS/TBDMS	*tert*-butyldimethylsilyl
TBTA	tris(benzyltriazolylmethyl)amine
TEAH	triethanolamine
TEOS	tetraethoxyorthosilicate
THF	tetrahydrofuran

TIPS	triisopropylsilyl
TLC	thin layer chromatography
TMS	trimethylsilyl
TOF	time of flight (MALDI-MS)
Tris	tris(hydroxymethyl)aminomethane
TTF	tetrathiafulvalene
U	uracil, uridine
U	unit (for enzyme activity)
UV	ultraviolet
V	Volt
Vis	visible
δ	chemical shift (NMR spectroscopy)

Materials and Methods

Chemicals and solvents were, unless stated otherwise, purchased from ABCR, Alfa Aesar, Acros, Fluka, Sigma-Aldrich or TCI in the qualitites puriss., p.a. or purum. Dry solvents (< 50 ppm H_2O) were obtained from Fluka. All reactions employing dry solvents were performed under inert atmosphere (N_2). Technical grade solvents were distilled prior to use for column chromatography and liquid-liquid extractions on a rotary evaporator (Büchi Rotavapor RE-111 or Heidolph Laborota 4000). Reaction products were dried over night at high vacuum (10^{-2} mbar). Aqueous solutions were dried on a SpeedVac plus CS110A or SPD 111V from Savant or lyophilized (Christ ALPHA 2-4).

Column chromatography was performed with silica gel 60 from Merck. A gradient towards more polar solvent mixtures was always used. Passivated silica for chromatography of phosphoramidites was prepared by suspending the required amount of silica gel in a solvent mixture containing 2% pyridine. The solvent was evaporated until the silica gel was a fine powder.

DNA solid-phase synthesis: ODNs were prepared by the DMT- and β-(cyanoethyl) phosphoramidite method on CPG supports (500 Å, Glen Research) with an Äkta Oligopilot from Amersham Biosciences or an Expedite DNA synthesizer (Applied Biosystems) with a coupling time of 4 min (10 eq.) for all natural phosphoramidites (Glen Research or Samchully Pharma). Coupling time for modified bases was elongated to 10 min (10 eq.). As activator, benzylthiotetrazole (BTT) was used. Dry MeCN (< 10 ppm H_2O) was obtained from Riedel de Haen and used to dissolve all phosphoramidites and BTT. After automated synthesis, ODNs were cleaved from the solid support by soaking in NH_3 (in H_2O/EtOH 3:1) for 24 h at 25 ºC. NH_3 and EtOH were removed in a SpeedVac and the crude ODN was purified by RP-HPLC. Long DNA strands (e. g. ODN-**9** in Section 2) was synthesized with the last DMT-group on, cleaved off the solid support as mentioned above and purified by HPLC. Then the DMT-group was cleaved by absorbing the DNA on a SePac-cartridge (Waters) and treating with 2% TFA before eluting. The DNA from the column was re-purified by HPLC. UV/Vis spectroscopy (Nanodrop ND-1000, PreQlab) and MALDI-TOF mass spectrometry were used to characterize the ODNs.

Enzymes: Nuclease P1 (*penicillium citrinum*) was obtained from Sigma, calf spleen phosphodiesterase II from Calbiochem, alkaline phosphatase (CIP) from New England Biolabs and snake venom phosphodiesterase I (*crotalus adamanteus venom*) from USB corporation. Pyrophosphatase was obtained form Roche. Antarctic phosphatase was obtained from New England Biolabs. Lambda exonuclease was purchased from New England Biolabs Inc.

Polymerase	Supplier	PCR buffer
Pwo	Roche Diagnostics	100 mM Tris/HCl, 250 mM KCl, 50 mM $(NH_4)_2SO_4$, 20 mM $MgSO_4$ (pH 8.85)
Deep Vent exo$^-$	New England Biolabs	200 mM Tris/HCl, 100 mM KCl, 100 mM $(NH_4)_2SO_4$, 20 mM $MgSO_4$ 1% Triton X-100 (pH 8.8)
KOD XL	Novagen (Merck Biosciences)	200 mM Tris/HCl, 80 mM $MgCl_2$, 5mM DTT, 500 µg/mL BSA (pH 7.5)
Taq	Standard Taq, purified by Claudia Gräf	100 mM Tris/HCl, 15 mM $MgCl_2$, 500 mM KCl, 1% Triton X-100 (pH 9.0)

Fluorescence spectroscopy was performed on a FP-750 spectrofluorometer from Jasco equipped with a peltier element. Measurements were conducted in a NaH_2PO_4 buffer (10 mM, pH 5.2) with a DNA concentration of 2.5 µM for each single strand.

Gel electrophoresis: For primer extension experiments and click reactions on short strands, DNA oligomers were analyzed by 22.5% TBE-urea-PAGE using the Protean-II gel system (Bio-Rad) with a gel length of 20 cm. The gels were run at 40 °C at a constant current of 30 mA. 1% agarose gels were run with a horizontal cell (Sub-Cell Bio-Rad) at 110 V. The DNA was stained with ethidium bromide. The bands were visualized using a Raytest LAS-3000 Imager with appropriate cut-off filters (515 nm for SYBR Green, 605 nm for ethidium bromide). As light source 312 nm UV or 460 nm epi-illumination was used. To wash off the excess fluorescein azide the gels were shaken in 1:1 water/MeOH for 1 h and then in pure water for another hour before taking the image. Polyacrylamide gel electrophoresis was performed in a Mini-Protean 3-Chamber from Biorad. Gel thickness was 0.75 mm. The gels were run at 12 mA constant current with a maximum voltage of 300 V. The PAGE gels (typically 5% for a 300mer PCR product) were stained by agitating them in SYBR Green solution (1:10000 dilution) for 20-30 min. Quantification of gel bands was performed with AIDA image analyzer software.

Gel filtration: The PCR reaction solution can be directly applied to a HiLoad 16/60 Superdex 30 column. 5 mM tris buffer (pH 7.5) was used at a flow rate of 1 mL/min. The PCR product eluted between 40-50 mL.

High-pressure autoclave was used for reactions with > 1 bar pressure and obtained from Carl Roth (Roth Hochdruck Laborautoklav Model 1).

HPLC was performed on a Merck-Hitachi system (L-7400 UV detector, L-7480 fluorescence detector, L-7100 pump) or on a Waters system (alliance 2695 with PDA 2996 or 996 and fluorescence detector 2475; preparative HPLC: 1525EF with 2484 UV detector). As columns VP 250/10 Nucleosil 100-7-C18 or CC 250/4 Nucleosil 120-3-C18 from Macherey-Nagel were used. Chiral HPLC was performed with a column from Daicel.

Mass spectrometry: For EI-MS a MAT CH 7A from Varian was used. ESI-MS was performed on a Finnigan LTQ FTICR. MALDI-TOF was performed on a Bruker Autoflex II spectrometer with hydroxypicolinic acid as matrix (25 mg 3-hydroxypicolinic acid, 5 mg ammonium citrate, 5 μL 15-crown-5 in 0.5 mL H_2O). Prior to MALDI analysis, the samples were desalted on a dialysis membrane (Millipore).

Melting temperature analyses were performed on a Cary 100 Bio spectrophotometer with a Cary temperature controller, sample transport accessory and a multi cell block from Varian. The measurements were conducted in a buffer containing NaCl (150 mM) and tris-HCl (10 mM) with a DNA concentration of 3 μM for each single strand. Two different wavelengths (260 and 320 nm) were measured while the temperature was varied between 4-95 °C (five times in total to allow for an averaged value). The temperature gradient was 0.5 °C/min, the temperature measurement was performed in a reference cuvette. The spectrometer was flushed with N_2 during the measurement and the samples were covered with a layer of dimethylpolysiloxane. Interpretation of the data was performed with Origin (Microcal). To this end, the obtained melting curves were averaged and baseline corrected by the measurement at 320 nm. The curve obtained in this way was subjected to an approximation by a ninth order polynomial. The zero point of the second derivative of this polynomial was used as the melting point.

NMR spectra were recorded at r. t. on a Bruker AMX 200 (^{1}H and ^{31}P-NMR), a Varian Mercury 200VX (^{1}H and ^{31}P-NMR), a Bruker ARX 300 (^{1}H and ^{13}C-NMR), a Varian Inova 400 (^{1}H and ^{13}C-NMR) or a Bruker ARX 600 (^{1}H and ^{13}C-NMR). Chemical shifts δ are given in ppm relative to TMS, whereupon the solvent signal was used as an internal standard. Signal multiplicities are abbreviated as follows: s (singlet), d (doublet), t (triplet), q (quartet), quin (quintett), m (multiplet), br (broad) and combinations thereof. ^{13}C-NMR spectra were recorded in a ^{1}H-decoupled mode.

PCR reactions were performed on an Eppendorf Mastercycler personal or on an Eppendorf Mastercycler S ep realplex^4. Initial temperature screenings were performed on the Eppendorf Mastercycler S ep realplex^4 with a temperature gradient program. Hybridization of primer template complexes for the primer extension were run on an eppendorf personal thermocycler. The RT-PCR assays were run on an eppendorf realplex^4 thermocycler. Natural triphosphates were obtained from New England Biolabs. Gel loading buffer was obtained from Biorad.
Template and primers were the same as those mentioned in a previous study.[1] The 294 bp template contains 61.2% (180 each) [A+T] and 38.8% (114 each) [C+G]. For reasons of simplicity it is referred to as 300mer. The oligonucleotide primers for PCR were purchased from Metabion in HPLC purified form and had the following sequence:
primer 1: 5′-TTA ATT GAA TTC GAT TTG GGC CGG ATT TGT TTC-3′
primer 2: 3’-T TTT ATG CTA TCT CTG ATA CCC TTG-3’
PCR products used for click reactions were purified on a QIAquick PCR purification kit (Qiagen). DNA extraction from gels was done with a Qiagen gel extraction kit.

Sep-Pak: The pre-packed Sep-Pak column (Waters) was conditioned by first rinsing with MeCN and then water (10 mL each). The PCR solution was directly applied to the top of the column and washed with water (5 mL). The product was eluted with MeCN/H_2O 1:1. After 3-4 mL of this solvent mixture no more product eluted.

Sequence analysis: To verify the sequence-fidelity of the PCR-reaction with our modified triphosphates, the alkyne-modified PCR products (ca. 500 ng) were first purified by agarose gel electrophoresis followed by isolation of the desired band and gel elution (Qiaquick Gel Extraction Kit). The pure alkyne-modified DNA was then used as a template in a second PCR reaction, this time with native dNTPs. The unmodified DNA product of this PCR was purified by gel extraction as described above and the sequence analyzed (GATC, Konstanz).

UV- and CD-spectroscopy: UV spectra were recorded in 10 mM Tris/HCl (pH 8.4) on a Varian Cary 100 Bio spectrometer at 25 °C using a 100 µL quartz cuvette. The OD(260 nm) of the DNA solution was adjusted to 0.9-1.1 without blank substraction. From the measured spectrum a blank measurement with 10 mM Tris/HCl was subtracted.
The CD spectra were recorded in 10 mM Tris/HCl (pH: 8.4) on a Jasco J-810 spectrometer at 25 °C. The OD(260 nm) of the DNA solution was adjusted to 0.9-1.1 without blank substraction. The spectra shown are the same probes as in the UV-spectra. Before or directly after the measurement a blank measurement with 10 mM Tris/HCl was recorded and subtracted from the sample spectrum.

Thin layer chromatography (TLC) was performed with aluminum plates (silica gel 60 F_{254}, 10 × 5 cm). Substances were visualized by immersing into a solution of 10% H_2SO_4, 120 g $(NH_4)_6Mo_7O_{24} \cdot 24\ H_2O$ and 5 g $(NH_4)_2Ce(NO_3)_6$ in 800 mL H_2O and subsequent heating to 100 °C.

[1] J. Gierlich, K. Gutsmiedl, P. M. E. Gramlich, A. Schmidt, G. Burley, T. Carell, *Chem. Eur. J.* **2007**, *13*, 9486-9494.

Curriculum Vitae

Name	Philipp Mathias Edwin Gramlich
Nationality	German
Birth	12/13/1977 in München-Pasing
Martial status	unmarried, no children

09/84-07/88	Elementary school Gilching
09/88-01/92	High school Gilching
01/92-06/97	Carl-Spitzweg high school Germering
10/97-10/98	Civilian service at the social station Gilching
11/98-02/02	Chemistry at the TU München
03/02-11/04	Chemistry at the LMU München
04/04-11/04	Diploma thesis (*Versuche zur Inkorporation von charge-transfer-Komplexen in DNA*- Towards the incorporation of charge-transfer complexes into DNA) with Prof. *Carell*
since 03/05	PhD thesis with Prof. *Carell*

Marks

06/97	A-levels	1,2
10/00	Pre-diploma	1,5
11/04	Diploma	1,1
	Diploma thesis	1,0

Languages

German	mother tongue
English	fluent
Spanish	medium skills
Latin	kleines Latinum
French	basic skills

Scholarships and Prizes

06/97	Karl-von-Frisch-Prize for biology
05/00-09/04	Scholarship from Cusanuswerk
07/02-09/04	Online-scholarship from e-fellows.net
11/04	Lily Diploma Thesis Award 2004
06/05-05/07	PhD scholarship from Cusanuswerk

External projects and studies

02/01-12/02	Chemistry and Indigenous Australia Studies at the University of Sydney, Australia. Inorganic chemistry research project with Prof. *Hambley*
04/03-06/03	Physical-chemistry project with Prof. *Fuchs* at the WWU Münster